THE UNIVERSITY
of EDINBURGH

Ring-Opening Polymerisation of 1,3-Dioxolan-4-ones

Stefan Cairns

A thesis submitted at the University of Edinburgh for the Degree of Doctor of Philosophy 2018

Abstract

Polyesters have been realised as a viable replacement for slow or non-degrading petroleum derived polymers. A variety of aliphatic polyesters, e.g. poly(lactic acid), have received a lot of attention because they are produced from renewable feedstocks and have the ability to biodegrade and bioassimilate. Poly(lactic acid)'s broader family, poly(α-hydroxy acid)s, have been produced with a wide variety of properties, that has given polyesters the potential for a more diverse range of applications. However, their synthesis has proven difficult. This thesis investigates a family of 1,3-dioxolan-4-ones as a monomer source to ease difficulties in current synthetic routes.

Polymerisation of the parent 1,3-dixoxolan-4-one was tested. The copolymerisation of L-lactide and 1,3-dioxolan-4-one was conducted with various monomer feedstocks. Ring-opening polymerisation of 1,3-dioxolan-4-one led to the formation of paraformaldehyde as a polymerisation by-product. The copolymerisation was found to be best controlled when using a coordination-insertion type catalyst. 1,3-dioxolan-4-one was also copolymerised with ε-caprolactone and β-butyrolactone to produce copolymers with various compositions.

The formation of poly(lactic acid) and poly(mandelic acid) from 5-methyl-1,3-dioxolan-4-one and 5-phenyl-1,3-dioxolan-4-one was investigated. Poly(lactic acid) and poly(mandelic acid) were synthesised with either isotactic or atactic tacticities. Molecular weights were found to be lower than the expected values. A variety of MeAl(salen) catalysts were explored for the polymerisation of 5-methyl-1,3-dioxolan-4-one and catalysts ligated with tertiary-butyl substituted salens were found to have higher rates of polymerisation and reached high conversions. Altering the diimine bridge in the ligand led to variations in rates of polymerisation and molecular weights. The cause of the decrease in molecular weight was found to be caused by a side reaction. The side reaction was bypassed by polymerising 2,2,5-trimethyl-1,3-dioxolan-4-one and 2,2-dimethyl-5-phenyl-1,3-dioxolan-4-one to form poly(lactic acid) and poly(mandelic acid), respectively, with the expulsion of acetone.

The scope of 1,3-dioxolan-4-ones capable of being polymerised to form poly(α-hydroxy acid)s was expanded to include iso-propyl, cyclohexyl, normal-butyl, iso-butyl, propargyl, chloromethyl and benzyloxymethyl substituents at the five position. The glass transition temperatures accessible from this synthetic route was expanded (22-105 °C). Kinetic experiments revealed the impact of the substituents steric bulk on the rate of polymerisation and points toward a coordination-insertion mechanism. Poly(lactic acid-co-glycolic acid) was

copolymerised with 5-propargyl-1,3-dioxolan-4-one to incorporate alkynyl functionality and hence Raman spectroscopy showed the polymer had a distinct peak at 2128 cm^{-1}. Following post-polymerisation modification of poly(lactic acid-co-3-chloro-2-hydroxypropanoic acid) copolymers, acrylate functionalised polymers were produced. The copolymers were shown to be capable of crosslinking poly(α-hydroxy acid) and poly(methyl methacrylate).

Lay Summary

Polyesters have been realised as a viable replacement for slow or non-degrading petroleum derived polymers. A variety of aliphatic polyesters, e.g. poly(lactic acid), have received a lot of attention because they are produced from renewable feedstocks and have the ability to biodegrade and be broken down inside the body. Poly(lactic acid)'s broader family, poly(α-hydroxy acid)s, have been produced with a wide variety of properties, that has given polyesters the potential for a more diverse range of applications. However, their synthesis has been difficult. This thesis investigates a family of 1,3-dioxolan-4-ones as a monomer source to ease difficulties in current synthetic routes.

1,3-Dioxolan-4-one was used to make copolymers with common cyclic esters: lactide, caprolactone and butyrolactone. The copolymers' composition was changed by having different ratios of monomers at the beginning of the reaction. The type of catalyst used gave an insight into how the polymerisation occurs. This route of making polymers was explored by testing different substituted 1,3-dioxolan-4-ones. It was found to be able to make various polyesters with an array of properties and thus impacting upon how they may be used in the future.

Declaration

The work described in this thesis is of my own, unless I have acknowledged help from a named person or referenced a published source. This thesis has not been submitted, in whole or in part, for any other degree.

Signature:

Date:

12/07/2018

Acknowledgments

I am indebted to many people for the support that they have given me during my time as a PhD student at the University of Edinburgh, my research would not have taken place without you all. Firstly, I would like to thank my supervisor Prof. Michael Shaver for taking me on to be a part of his research group in the Green Materials Laboratory. He provided the mentoring, the tools and the challenges I needed to succeed and develop into the chemist I am today. I would like to thank the School of Chemistry and a Marie Curie Career Grant for funding my research.

The environment in which this research took place was truly inspiring and it was my colleagues primarily in the Green Materials Laboratory and those throughout the School of Chemistry that provided it. Thanks to all the members of lab, past and present, for the good and bad times we shared; Postdocs Ben, Vincent, Jaclyn, Mitch, and Yuechao. PhD students Jarmy, Emily, Ferny, Kevin, Genny, Jakey aka Dr. Ass, Dan, Meng the merciless, Gerry, Mo, James, Eszter, Yaz, Vishal, Joanne, Laura, Panos and Utku. Other members including Chris, Derek, Amelie, Lorna, Zoe, Francesca, Rebecca and all other undergraduate students. Special thanks to: Jarmy, Emily and Ferny for teaching me the ropes both in the lab and the group. Ben whom I constantly learned from in my three years with, and was always there in case of an emergency hospital visit, fire or in need of lab banter. Meng for never showing any mercy. Mitch for advice in the final stages of my PhD and extensive input into this thesis. Gerry and Dan for providing support in preparing this thesis. Thanks to the members of Prof. Alison Hulme's group for being there when a secondary opinion, organic expertise, or cake was needed.

Thanks are also given to the many people who helped with analytical support, namely; Dr Lorna Murray and Mr Juraj Bella with NMR spectroscopy, Dr. Logan Mackay with Mass Spectrometry, and Dr. Gary Nichol for DSC.

A huge thank you to my friends and family. The members of TS5 Rossy, Kim-Sue, Shakey and Emily, thank you for making my time during my PhD such an incredible period of my life so full of laugher, wild times and love. To my Mum and Dad thank you for giving me your all, and more. Thank you for making sacrifices so that I could go out and get my undergraduate degree and encouraging me to pursue my PhD, even when it meant moving to Scotland. Thank you for supporting and pathing the way for me to achieve some of my ultimate life goals. I love you both so much.

Last of all the person to whom I have the most to thank for, my dearest girlfriend Alisia. Wednesday used to be our day, but soon it became every day and it has been every day that you've been there to support me. You've held my hand through some of the darker times that comes with PhD life and celebrated with me the victories that came after they were conquered. Thank you for all of our incredible journeys that we've shared together and have made this time an unforgettable one. I thank you for being my rock, for pushing me when I saw no way forward, I would have never been able to do this without you. I love you.

Table of Contents

List of Figures

List of Schemes

List of Tables

Chapter 1. Introduction

1.1 The Synthesis of Polymers

Monomers are small molecules polymerised to form macromolecules. Polymers may be classed by the functional group repeated though the structure, for example polyester. However, it is not the only classification, another example is polymerisation type, for example polycondensation. In this text both classification by structure and polymerisation type will be discussed, as both provided key differences in how the polymers are synthesised and the resulting properties of the polymers.

1.2 Polycondensation

Polycondensation is a general term for a polymerisation which occurs with the elimination of a part or parts of the monomer(s). The eliminated portion, water, causes condensation to form on the inside of the reaction vessel and hence the name polycondensation was given. The monomers determine the functional group encompassed in the polymer backbone and the eliminated by-product. Polycondensation is commonly conducted using a monomer or monomers containing two functional groups, one being a nucleophile (amine, thiol, alcohol, etc.) and the other being an electrophile (acid halide, carboxylic acid, ester, etc.) (Figure 1.1).

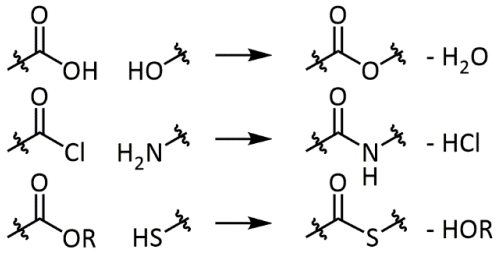

Figure 1.1. Example reactions that could be used in polycondensation. Reaction occurs leading to the formation of a polymer and a reaction by-product

Polycondensation is a subcategory of step growth polymerisation. In step growth polymer chemistry monomer design can be done in either of two ways; selecting and reacting a difunctional monomer containing both potential reaction components in a single molecule or by reacting equimolar equivalents of two distinct difunctional monomers each containing either the electrophilic or the nucleophilic components (Figure 1.2 (i)). These monomers undergo stepwise growth where monomers react with one another to form dimers, and dimers may then react with another dimer to form tetramers or react with unreacted monomers to form

trimers (Figure 1.2 (ii)), the stepwise growth continues, unselectively, to form oligomers and polymers.

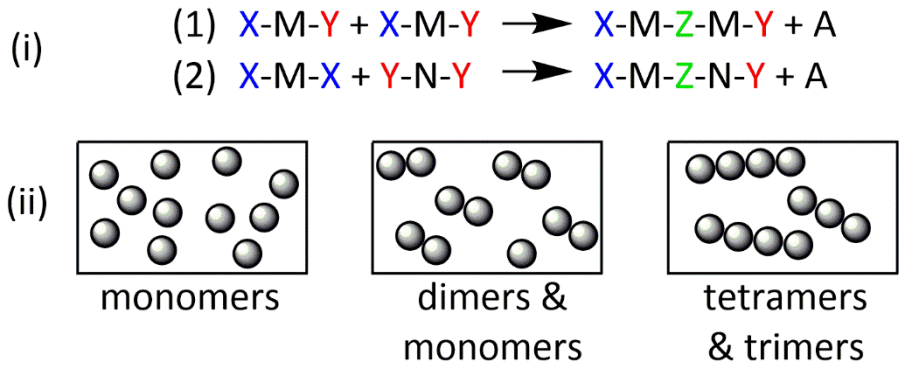

Figure 1.2. Step growth polymerisation. (i) Monomer types and their products. (ii) Stepwise growth reactants and products adding together at random

1.2.1 Polycondensation for Polyesters

During Carother's time at DuPont in the 1920-30s his group focused on synthesising polyesters from aliphatic dicarboxylic acids and aliphatic diols.[1–3] Using an understanding of reaction equilibrium and the need to drive it forward by eliminating water from the reaction mixture, they used forcing reaction conditions to do so. The reaction was completed in a Claisen flask under vacuum to distil the water and remove it from the equilibrium. It was observed that the production of water is completed after one hour and after further heating for two hours the reactions were determined to be complete. However, the molecular weights of the resultant polyesters, ranging from 800 to 5,000 and averaged 3,000 g/mol, deviate from the theoretically calculated weights by 60-90%. The lack of higher molecular weights was attributed to several factors including; the low concentration of reactive terminals groups, the high viscosity of the polyesters, and the polyester's exaggerated "molecular cohesions". Later in their work they achieved higher molecular weights and "superpolyesters", with an apparent molecular weight of about 12,000 g/mol, by completing reactions using still heads pioneered by Washburn for the separation of petroleum hydrocarbons.[4] The still design was considered capable of removing components from equilibria even when minute vapour pressures are involved and as a result achieved the high molecular weight. This method proved successful for an extensive range of linear aliphatic polyesters.

Despite the decades of development of polycondensation, issues still remain. Polycondensation has not been the synthetic route of choice for industry or academia for polymers such as poly(lactic acid) (**P1**, Figure 1.4). **P1** at high molecular weights (MW) exhibits high mechanical strengths, necessary for medical implants and sutures.[5] However, the

MWs attained by the polycondensation of lactic acid do not display as high a mechanical strength.[6] The limited MWs achieved has been attributed to polyester, water and free acid equilibrium, and high melt viscosity inhibiting the release of water from the melt.[7] Other methods based on polycondensation such as solution polycondensation, melt-solid polycondensation, and solid state polycondensation have achieved higher MW, however, require multi-steps and or additional catalysts post-primary polycondensation.[8] The equilibrium dependent reaction is energy intensive as often temperatures in excess of 200 °C are required and in order to reach high MW **P1** a monomer that was more readily polymerised and did not require water to be eliminated during the polymerisation.

1.3 Ring-Opening Polymerisation

As a synthetic strategy, ring-opening polymerisation (ROP) differs greatly from polycondensation. The greatest difference derives from the contrast between step growth and chain growth polymerisations. Chain growth progresses *via* initiation, then propagation and finally termination. Initiation occurs generating a reactive species. It combines with a monomer to produce a molecule with a reactive chain end. This species takes part in propagation, reacting with monomers and elongating the reactive species. Termination occurs when the reactive moiety is extinguished.

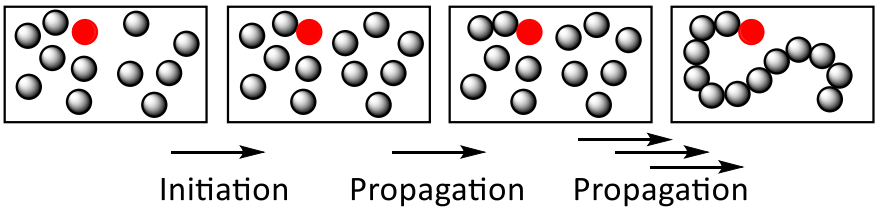

Figure 1.3. Initiation and propagation in chain growth polymerisation

Unlike in free radical polymerisation techniques where growing chains can terminate by coupling together, growing polyesters chains do not terminate and are considered to be living. During a living polymerisation, the polymer chain grows without termination until the introduction of an external quenching or termination source to the system. The molecular weight or the degree of polymerisation of the growing chain is aligned with the ratio of the monomer to the initiator. This living characteristic can be exploited to control the architectures of the synthesised polymers. Desirable architectures such a gradient and block can be realised through this route, and give polymers with unique properties for applications in thermoplastic elastomers and drug delivery systems.

Cyclic esters, such as glycolide (**M1**) and lactide (**M2**) have been frequently used as monomers in ROP (Figure 1.4).[9] The chain growth of cyclic esters is driven by the relief of ring strain.[10] The ring strain relieved upon the opening of **M2** is not usually associated with six membered rings, but it is derived from the two sp^2 hybridised ester moieties. These two planar conformations within the ring lead to its strained skew boat conformation.[10]

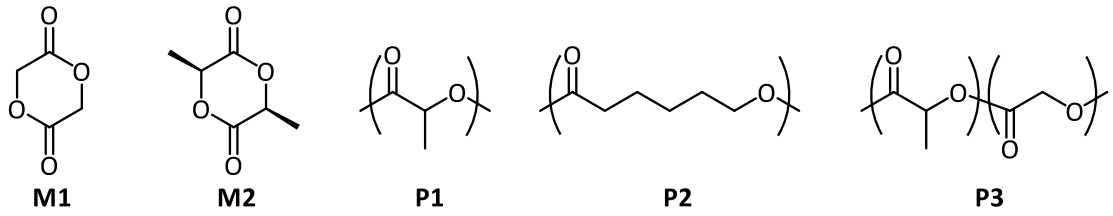

*Figure 1.4. Monomers **M1** and **M2** and polymers **P1**, **P2** and **P3***

The use of ROP has not been limited to academic research, as currently ROP is used to synthesise both polycaprolactone (**P2**) and poly(lactic-co-glycolic acid) (**P3**) in industry.[11] ROP goes by a pseudo-anionic mechanism in the presence of a catalyst. This provides control over the polymerisation and does not require the stringent conditions required for other mechanisms such as ionic. Metals have been central to the catalytic systems employed for the ROP of cyclic esters.[12] The most widely used catalyst in industry is tin(II) 2-ethylhexanoate or tin octanoate (**C1**). It remains the first-choice catalyst for polymerising cyclic esters due to multiple factors: its ease to handle, its aliphatic ligand framework exhibits good solubility in most common organic solvents or bulk monomer, and its high activity with typical reaction times ranging from minutes to hours rather than hours to days in polycondensation. It also achieves desired high molecular weights (10^5 g/mol). Although it is US food drug administration (FDA) approved for food additives, its toxicity is a drawback when the resultant polymer is desired for a biomedical application. **C1** promotes transesterification, a side reaction which leads to broad dispersities (*Đ*s).[13] The increase in *Đ* is caused by the active polymer chain end reacting with either another chain or undergoes backbiting. In order to circumvent these drawbacks a wide array of catalysts have been tested.

1.3.1 Ring-Opening Polymerisation Catalyst Development

In an effort to overcome the lack of activity shown by **C1**, the focus of research groups shifted towards testing a wide variety of metal alkoxides. The activity was greatly improved upon with the use of alkali metals magnesium,[13] transition metals titanium,[13] zirconium, [13] zinc,[13] rare earth metals yttrium,[14] and lanthanides.[15,16] Higher activities were achieved but broad dispersities and polymerisations not displaying a living nature were observed. This is

considered to be caused by aggregation of polymer chains and hence, led to the desire for discrete single site catalysts.

Aluminium complexes have received a lot of attention in the pursuit for more active catalysts. Spassky pioneered the first ligated aluminium complexes for ROP. In 1989, a simple (R)-3,3-dimethyl-1,2-butanediol was used in tandem with an equivalent of trialkyl aluminium for the polymerisation of β-butyrolactone (**M3**), though activity was found to be poor, reaching < 20% conversion after 18 days at 20 °C. It was thought that the simple ligand did not result in a well-defined system and likely formed stable clusters and a chelating ligand was thought to be needed to counteract this. Spassky found that using a (N,N′-bis(salicylidene)-1,2-ethanediamine) (salen) ligated aluminium alkoxide species (**C3**) helped to install control and the polymerisation displayed living characteristics until 70% conversion, however the activity was still considered to be low.[17] In other variations such as a cyclohexyl (**C4**) and binaphthyl (**C5**) diimine bridged salen complexes, side reactions such as transesterification were prevalent at conversions greater than 70%, causing broad molar mass distributions.[18,19]

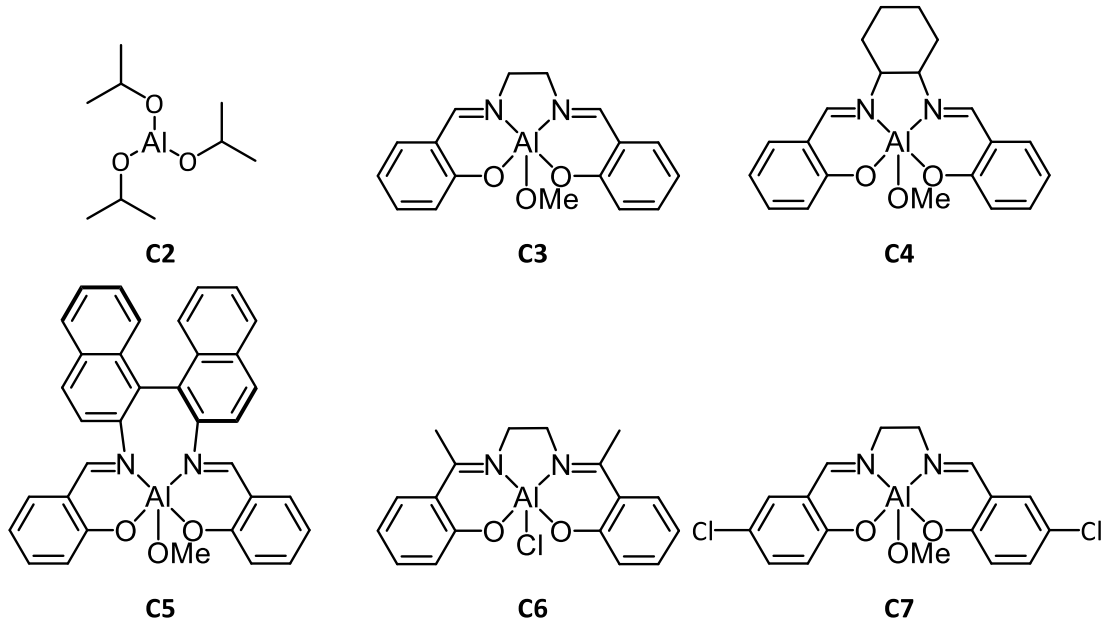

Figure 1.5. Early development of aluminium alkoxide catalysts.

A subsequent report investigated a similar species of salen ligand derived from 2-hydroxyacetophenone, resulting in methyl groups on each of the imine carbons (**C6**). This resulted in a significant increase in polymerisation rate, nearly three times faster than **C1** (k_{obs} = 374 h^{-1} vs. 138 h^{-1}).[20] Gibson found the polymerisation of both L- and *rac*-**M2** could be performed in solution at room temperature by installing electron withdrawing groups on a

salen ligated Al catalyst.[21] The lower temperature largely mitigated transesterification, indicated by dispersities as low as 1.06.

Gibson later went on to systematically synthesise MeAl(salen) complexes and screen them for the polymerisation of *rac*-M2. The experiments were conducted in order to gain an insight into the influence of the ligand's phenoxide substituents and diimine bridge over polymerisations. From these studies a number of factors about the polymerisation initiating species were better understood.[22] The alkyl aluminium species is a stable precursor for polymerisation which overcomes aluminium alkoxides' tendencies towards aggregation to form bridging and clustered species.[23] Monitoring the addition of exogenous alcohol to the complex by ^{1}H nuclear magnetic radiation (NMR) spectroscopy displayed a clean reaction and complete conversion to active aluminium alkoxide initiating species, visually observed by the formation of bubbles. The stability of aluminium halide species is detrimental when acting as an initiating species for the ROP of cyclic esters. Often alkali alkoxides are used to obtain the active initiating species, however, unlike the alkyl aluminium reaction with alcohol, this reaction typically leads to a mixture of products including aluminium halide alkoxides adducts.[24,25]

Across the ethylene diimine bridged MeAl(salen)s **C8**, **C9** and **C10** the variations between phenoxide substituents has a substantial impact upon the rates of polymerisation (Figure 1.6). For example, from **C8** to **C10** the rate is dramatically lowered by almost 60 times, this is due to the increase in steric bulk from proton to tertiary-butyl (^{t}Bu). Despite an increase in bulk at the ortho position of the phenoxide, the chloro substituents of **C9** enhance the rate three-fold due to the inductive electron withdrawing group compared to **C8**. Lengthening the backbone between the imines by one CH_2 unit also brought about a large increase in polymerisation rate. Again, the dichloro substituted **C12** has the highest rate of polymerisation. The C_2 to C_3 linker exchange had the most dramatic impact when R = H, comparing **C8** and **C11** presents a rate increase of 11 times. The change in rate from **C10** to **C13** follows the same trend and increases dramatically by 133 times. The steric hindrance provided by the chloro and ^{t}Bu substitutions display an important role by achieving a very narrow dispersities of 1.08 and 1.07. The rates of **C11-C13** can be further improved upon by the addition of a 2,2-dimethyl substituted propylene linker across all substituents on **C14**, **C15** and **C16**. The C_3 phenylene group **C17**, **C18** and **C19** display far greater polymerisation rates than their ethylene counter parts confirming the role of the linker length. Gibson attributes the increase in polymerisation rates to "the greater flexibility imparted to the metal coordination sphere and thus better accommodation of the geometric requirements of the transition state(s) for the ring-opening

process", despite the rates of **C17** and **C18** being greater than their less constrained **C11** and **C12** counterparts.

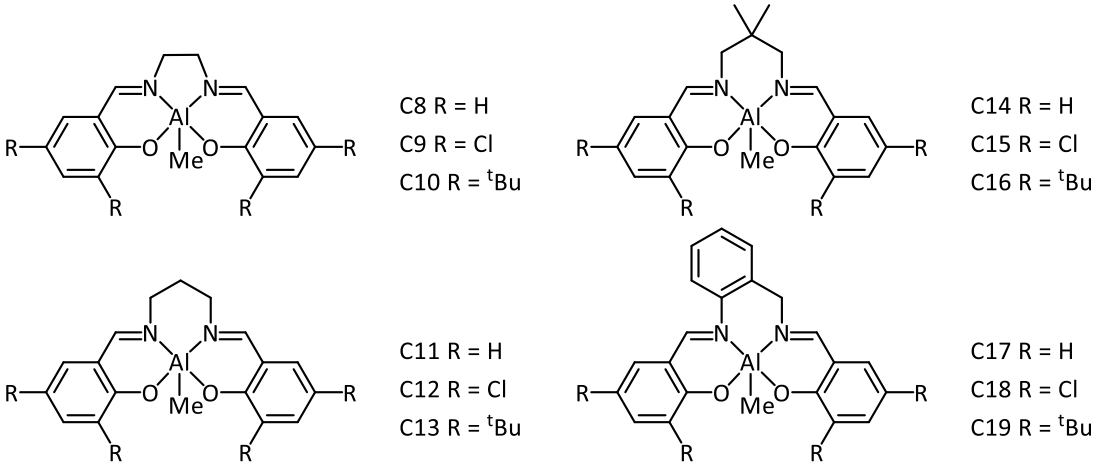

Figure 1.6. Select MeAl(salen)s synthesised by Gibson for comparison

*Table 1.1. rac-**M2** polymerisation data and rates of MeAl(salen)s*

	R	k_{obs} (s^{-1})	M_n	$Đ$		R	k_{obs} (s^{-1})	M_n	$Đ$
C8	H	59 x 10^{-6}	4390	1.76	**C14**	H	1073 x 10^{-6}	6190	1.35
C9	Cl	181 x 10^{-6}	4290	1.43	**C15**	Cl	6420 x 10^{-6}	7470	1.37
C10	^{t}Bu	1 x 10^{-6}	5900	1.58	**C16**	^{t}Bu	159 x 10^{-6}	7430	1.20
C11	H	661 x 10^{-6}	6560	1.40	**C17**	H	928 x 10^{-6}	7570	1.40
C12	Cl	1009 x 10^{-6}	9700	1.08	**C18**	Cl	4380 x 10^{-6}	9320	1.13
C13	^{t}Bu	133 x 10^{-6}	9590	1.07	**C19**	^{t}Bu	84 x 10^{-6}	7920	1.08

*The rac-**M2** was added to the initiator solution (MeAl(salen), BnOH in toluene) at 70°C. [M]:[I] = 50:1 [**M2**]$_0$ = 0.416 M; [Al]$_0$ = 8.33 mM; Polymerisation taken to high (90%) conversion. $M_{n,th}$ = 7200.*

1.3.2 Ring-Opening Polymerisation Mechanism

The mechanism for aluminium mediated ROP has been well studied with the first hypothesis of the coordination-insertion mechanism developed by Dittrich and Schulz.[26] The mechanism has been shown to follow a route consisting of initiation, propagation and termination (Figure 1.7):

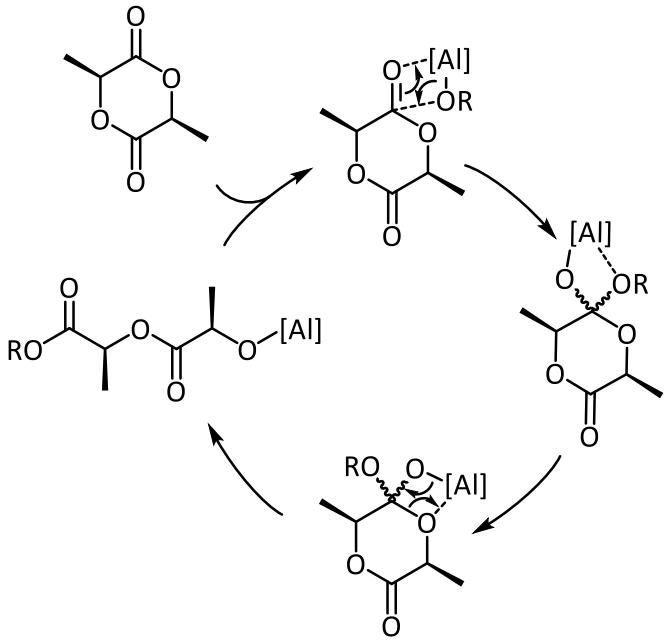

*Figure 1.7. Coordination insertion mechanism of **M2** ring-opening polymerisation with aluminium alkoxide catalyst.*

Initiation and propagation: aluminium coordinates to the oxygen of the carbonyl and promotes the alkoxide's insertion into the carbonyl. Whilst bound to the monomer, aluminium coordination to the acyl oxygen promotes reformation of the carbonyl and leads to acyl bond cleavage.

Termination: occurs upon the addition of exogenous alcohol, leading to alkoxide exchange between the polymer chain end and alcohol.

Initial support for the mechanism, experimentally, was provided by both Kricheldorf[13] and Teyssie by utilising ^{1}H NMR, ^{13}C NMR and IR spectroscopy to identify the product of a single isopropoxide insertion into an equivalent of **M2** and the end groups of **P1**.[27] Further support for the three-step process came both experimentally as Dubois illustrated the polymer chain was capped isopropoxide groups *via* NMR spectroscopy analysis, and theoretical calculations.[28,29] Hence, it is widely accepted that aluminium alkoxides catalyse *via* a coordination insertion mechanism.

1.4 The Synthesis of Poly(α-Hydroxy acid)s and Their Properties

Polymers **P1** and **P3** exhibit high mechanical strength,[30–32] while having the ability to be shaped and moulded is ideal for a variety of applications in the polymer industry.[33,34] Many applications of polymeric materials depend on the polymer's glass transition temperature (T_g).[30] This is often due to changes in the polymer's physical properties as they are heated through their glass transition temperature. These changes include but are not limited to increased permeability, loss of dimensional stability, and increased resilience.[35]

1.4.1 The Tacticities of Poly(lactic acid) and Their Properties

M2 exists as three diastereomers meso-, L and D. Without stereocontrol two tacticities of **P1** may synthesised: atactic from racemic **M2** (a 1:1 mixture of D-**M2** and L-**M2**) or meso-**M2**, and isotactic from either D-**M2** or L-**M2**. From a thermoplastic application perspective, the T_g of isotactic **P1** is low, at 50-60 °C. However, for applications such food packaging,[33] resorbable sutures and surgical fixtures semi-crystalline **P1** has near ideal properties.[36] In contrast, atactic **P1** is an amorphous polymer and has a decreased T_g near room temperature. This rubbery material degrades at a higher rate and is preferred for controlled drug delivery systems. Despite this lower T_g, atactic **P1** is not optimal for applications requiring lower T_g such as lubricants, due to its low decomposition temperature or injectable polymers, due to its stiffness and inability to form a gel. To expand from these easily accessible tacticities alternative catalysts were tested, modifications were made to polymerisation conditions and stereocomplexations were conducted.[37–39]

Four tacticities of **P1** may be obtained from racemic-**M2** or meso-**M2** (Figure 1.8). The desire for tacticites drove the research of stereoselective polymerisations *via* catalyst development. Previously discussed in the catalyst development section catalyst (*R*)-binapthylene (binap) imine bridged MeOAl(salen) (**C5)** was synthesised and used by Spassky as the first successful stereoselective catalyst for the polymerisation of *rac*-**M2**. The catalyst exhibited a 20:1 preference for the polymerisation of D-**M2** over L-**M2** forming a gradient stereoblock, though reaching full conversion required extended reaction times due to the sluggish rate of L-**M2** polymerisation.[18] Catalyst capable of forming stereoblock-**P1** with reduced reaction times were developed by both Coates and Feijen. Coates did so first by using a less costly *rac*-SalBinap ligand which produced stereoblock-**P1**. Through tetrad analysis they concluded this occurs by a chain exchange mechanism.[40] Following the same principles as

Spassky and Coates, Feijen was able to produce a stereoblock-**P1** by kinetic resolution using an o-*R,R*-cyclohexyl diimine bridged Al(salen) complex and by a chain exchange mechanism with the racemic equivalent.[39] Formation of stereoblock-**P1** achieved higher thermal properties than atactic-**P1** from a racemic feedstock and the melting temperature (T_m) was found to be 20 °C higher than **L-P1**. 2,6-Diisopropylaniline was used to synthesis a bulky β-diimine ligand that when complexed with zinc proved to be extremely efficient for the polymerisation of **M2**. Through a chain-end control mechanism it produced heterotactic **P1**. Despite its stereoregularity heterotactic **P1** was found to be an amorphous polymer with a T_g (59 °C) similar to that of L-**P1**.

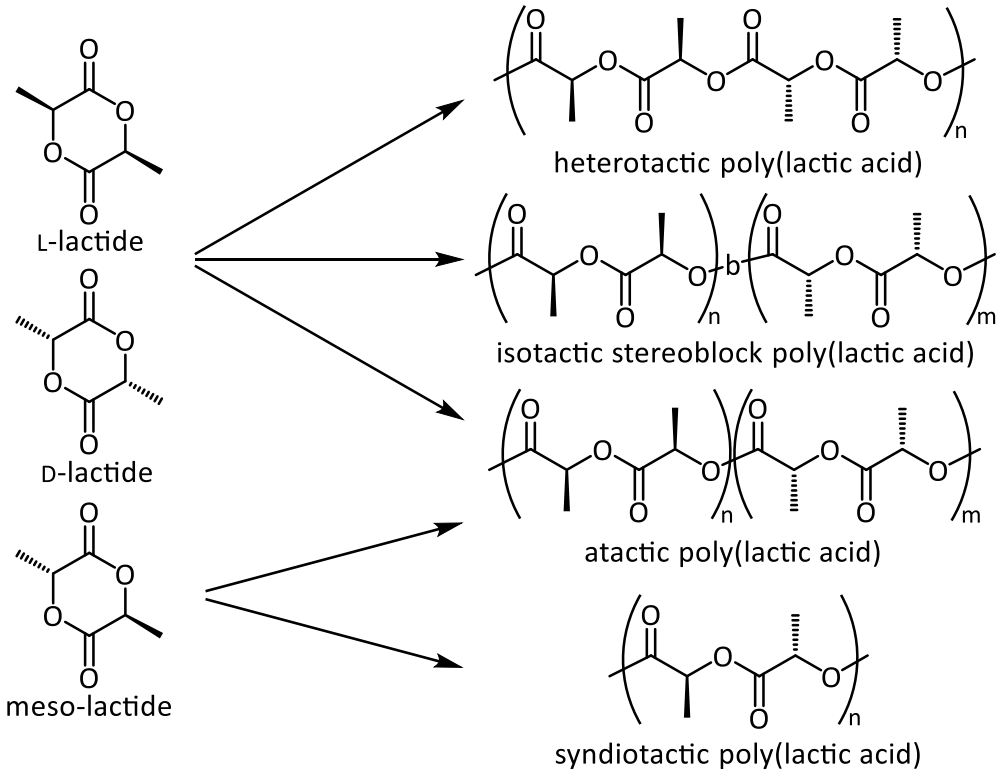

*Figure 1.8. **M2** diastereomers and tacticities of **P1***

Stereocomplexation can be achieved when L-**P1** and poly(D-lactic acid) (D-**P1**) are mixed. After cocrystallisation the T_m of the resulting stereocomplex is 230 °C.[41] This route suffers from the high cost of D-**P1** synthesis, as the *R,R*-diastereomer is far more expensive than the *S,S*-diastereomer.[42]

Stereoselective control over the ROP of *rac*-**M2** has been used to attain a variety of higher thermal properties than atactic **P1**, however, it also has an upper bound in T_g similar to L-**P1**. Stereocomplexation has been found to reach higher T_ms than any single stereoregular **P1**, but does not exceed the evident T_g upper bound.

Another approach to adapting a polymer's physical properties has been to blend the polymer with another. There has been a vast amount of research into polymer blends and selected examples relevant to this text are discussed. The most common method to blend polymers is for two or more polymers to be mixed in the molten state in extruders or batch mixers. Another biocompatible polymer, poly(ethylene glycol) (**P4**), has been blended with **P1**. Although initial changes in physical properties are observed they disappear with aging. Aging leads to the presence of two T_gs, evident of phase separation. While highly stereoregular **P1** led to two amorphous phases, **P1** with little to no stereoregularity led to semi-crystalline and amorphous phases.[43,44] Other methods include chain end modification and then subsequent use to form graft copolymers. However, this requires further difficult synthetic steps often giving poor yields,[45] formation of copolymers,[46–55] and higher architectures such as combs from macroinitiators.[56,57]

1.4.2 Synthesis of Poly(α-Hydroxy acid)s from Cyclic Diesters and Their Properties

P1 has been the base for many researchers to build upon and expand the physical properties of polyesters. As one of the simplest polyesters with an aliphatic backbone it was thought to have a high potential for tuning by replacing the methyl substituent of lactic acid to various other functional groups. These may be obtained through two significantly different general methods. The first is post-polymerisation functionalisation, this involves the addition of functional species to a pre-made polymer chain via reaction with (usually pendant) reactive groups such as alkenes or carboxylic acids. Such modification can provide access to a wide range of functionalised polymers starting with the same polymeric species and resulting in a range of functional species. An example of post-polymerisation modification was completed by Shaver *et al.* on modifying a poly(β-heptenolactone-co-lactic acid).[58] The polymer was used as the starting material to synthesise 15 different polymers by olefin cross metathesis. However, this method may have issues achieving complete functionalisation, as it relies on all of the reactive groups being readily accessible for reaction. This can prove to be problematic if there is significant coiling of the polymer chain.

An alternative method of functionalisation is achieved pre-polymerisation through the synthesis of functionalised monomers. Every repeat unit is already functionalised and complete incorporation of the desired functional species may be achieved. However, using this method, functional groups are limited to those which will not react or otherwise interfere with the polymerisation species or conditions. This means that particularly reactive species must be

protected in order to be used in ROP. Doing so reintroduces the problem of incomplete conversion of some protected species during deprotection.

1.4.3 The Synthesis of Alkyl and Aryl Substituted Cyclic Diesters

For a given polymer backbone increasing the rotational barriers along the polymer backbone is thought to lead to an increase in T_g. To increase the rotational barrier the methyl group of **P1** is replaced with more sterically encumbering groups such longer alkyl chains, increased branching of alkyl chains. In order to access more polyesters substituted with more sterically demanding groups Baker synthesised a variety of novel cyclic diesters monomers. The cyclic esters were synthesised in two methods (Scheme 1.1);

1. Oligomers were formed by refluxing α-hydroxy acid with an acid catalyst for several days. The cyclic ester was then formed by cracking (refluxing over a zinc oxide catalyst) the oligomers under vacuum. Monomer isolation was carried out by vacuum distillation.

2. The α-hydroxy acid was reacted with an equivalent of α-bromoacyl bromide in the presence of triethylamine. The monomer underwent a basic work up to complete the cyclisation.

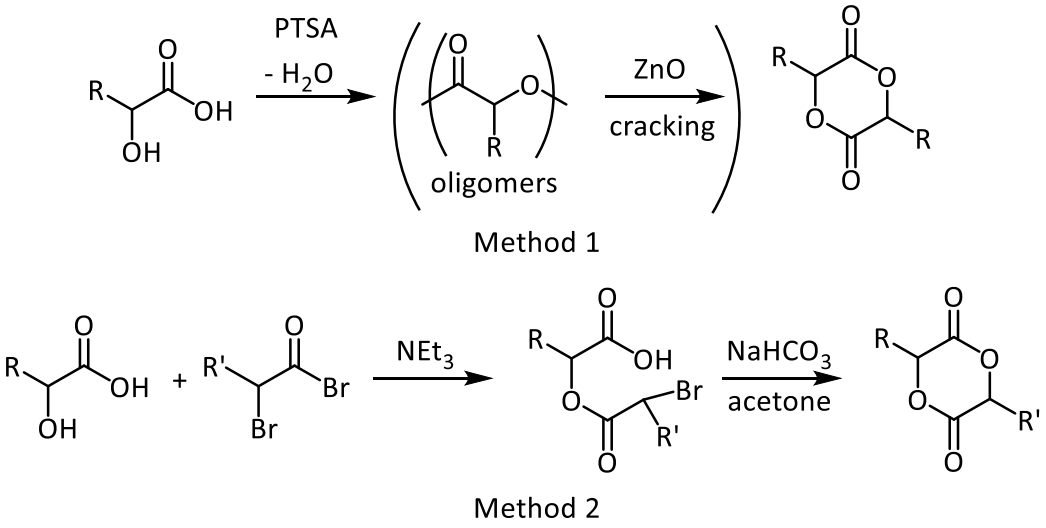

Scheme 1.1. Synthetic methods for cyclic diesters

Baker was able to access ethyl (monomer **M4**, 63% yield) using method 1 and later cyclohexyl (**M5**, 21%), ^{i}propyl (**M6**, 16%), phenyl (**M7**, 47%) and benzyl (**M8**, 90%) disubstitutions without the need for the cracking step (Figure 1.9).[59–62] Möller used the first method to synthesise ^{n}hexyl disubstituted glycolide (**M9**) again without the need for the cracking step.[63] The second method can be used to synthesise bifunctional and disubstituted monofunctional glycolides, the latter was synthesised with ^{i}butyl (**M10**, 71%) and ^{n}hexyl (**M9**,

65%) substituents.[60] Bifunctionalised monomers synthesised were methyl paired with ^{i}propyl(**M11**, 35%), ^{n}butyl (**M12**, 40%), ^{n}hexyl (**M13**, 45%), benzyl (**M14**, 35%) and cyclohexyl (**M15**, 59%).[59,63]

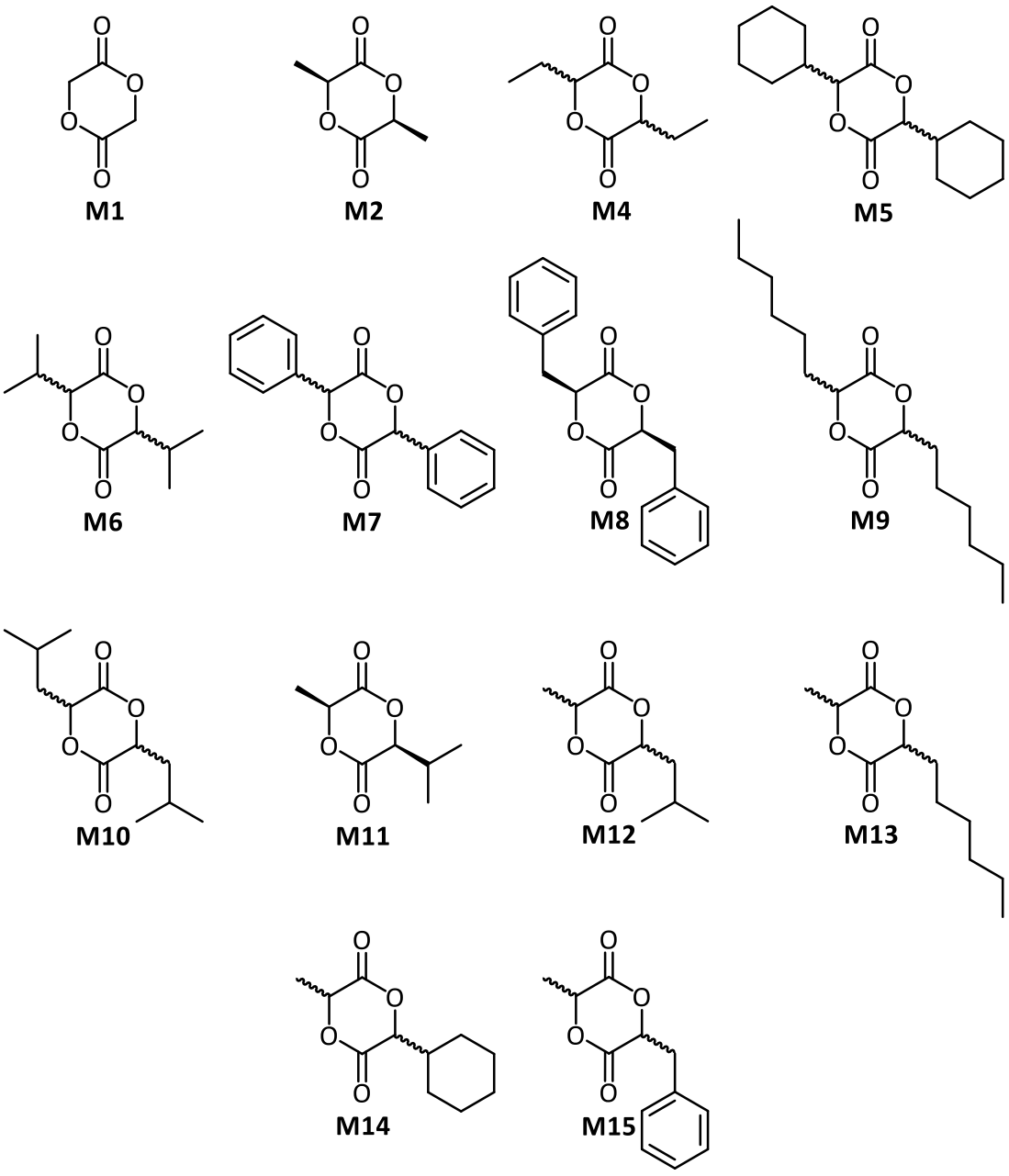

Figure 1.9. Cyclic diester monomers synthesised by Baker and Möller

The ROP of monomers **M3, M8, M9** proceeded in the presence of several tin-based catalysts, with or without alcohol initiator, at relatively high temperatures (130-180 °C), in the

absence of solvent. Polymerisations were high yielding, however, the elevated temperatures and extended reaction times (several days) led to polymers having broad dispersities (>1.7). In some cases, monomer insolubility is likely why they were completed without solvent and high melting temperatures was the probable cause for the use of such harsh polymerisation conditions. **M4**, **M5**, and **M10** were found to be living when polymerised in dilute solutions at 90 °C, but required several days to reach moderate conversions. When polymerised in bulk they achieved high molecular weights, while maintaining low to moderate dispersities (1.18-1.42). Monomer **M7** suffered from the same solubility issues, but conducting the polymerisation in a heterogeneous slurry at a moderate temperature (70 °C) afforded poly(mandelic acid) (**P5**) with narrower dispersities (<1.2). This displays a better control over the polymerisation. Möller found the polymerisation of monomers **M11**, **M12**, **M13** and **M15** to proceed more readily than **M6**, **M10**, **M9** and **M8** respectively using the same **C1** catalyst. The polymerisation of **M8** was completed in toluene due to its high melting point (>100 °C). The polymers obtained showed narrow dispersities ($Đ$ = 1.1-1.2) and moderate conversions of 65–85% were reached within one hour. It was noted, however, that as conversions exceeded 90%, molecular weight distributions began to broaden ($Đ$ = 1.4). These undesired side reactions were circumvented with the use of an organocatalyst 4-dimethylaminopyridine (DMAP). DMAP exhibited increased polymerisation rates as conversions reached ~ 90% in one hour, while maintaining narrow dispersities (<1.2). Synthesising the substituted poly(α-hydroxy acid)s (PAHAs) expanded upon **P1**s narrow range of physical properties, especially T_g. Longer alkyl chains decreased T_g, while branched chains displayed higher T_gs than straight chains. The proximity of branching to the polymer backbone also proved important, as a drop of 41 °C is seen between poly(valeric acid) (**P6**) and poly(ⁱbutyric acid) (**P7**). As one would expect from comparing the T_g of polystyrene and atactic polypropylene, directly attaching a phenyl ring at the α-position dramatically increased the T_g of the polyester. **P5** was found to be an amorphous glassy solid with a high T_g (100 °C) similar to polystyrene. Again, shifting the phenyl ring in the case of poly(phenyllactic acid) (**P8**), one carbon away from the polymer backbone proved detrimental as its T_g was 50 °C. This was to be expected as the T_g of poly(allylbenzene) is 30 °C lower than polystyrenes. The hydrogenated equivalent of **P5**, poly(hexahydromandelic acid) (**P9**), proved to be just as useful, achieving a comparable T_g = 98 °C.

1.4.4 Other Functionalised Cyclic Diesters

The alkyl and aryl substituted PAHAs' properties have been tested for use in biomedical applications, however, these substituents offer low solubilities and limited interactions with

biomedical ingredients and thus reduces their versatility.[64,65] PAHAs functionalised at the chain end have been shown to enhance their properties for use in biomedical applications, such as Kricheldorf and Stupp's use of vitamins, hormones and drugs to initiate **M2** polymerisation.[66,67] Although chain terminal functionalisation has made PAHAs useful for a number of applications, it is limited by its relatively minor impact to the polymer's properties and does not reach the demands for biomaterials.[68] Incorporating functionalities along the polymer chain, again, has been used to obtain the desired structures and property tuning capability. Various functionalities, other than the alkyl and aryl side chains discussed previously, have been researched with the aim of attaining the desired properties and as result their applications in biomedical areas have been demonstrated (Figure 10).

Method 1 proved vital in delivering symmetrical monomers containing two arms of the desired functional group (Table 1.2), among these **M16**,[69] **M17**,[70] **M18**,[71] **M19**,[72] **M20**, **M21**, **M22**, **M23**[73] and **M24**[74] were synthesised (Figure 10). Isolated yields were poor and no correlation with functional groups was evident. Method 2, with some minor variations in reagents, was used to synthesis **M25**[69] **M26**,[75] **M27**,[76] **M28**,[77] **M29**, **M30**,[78] **M31**,[79] **M32**,[80] **M33**,[81] **M34**,[82] **M35** and **M36** (Figure 10).[83]

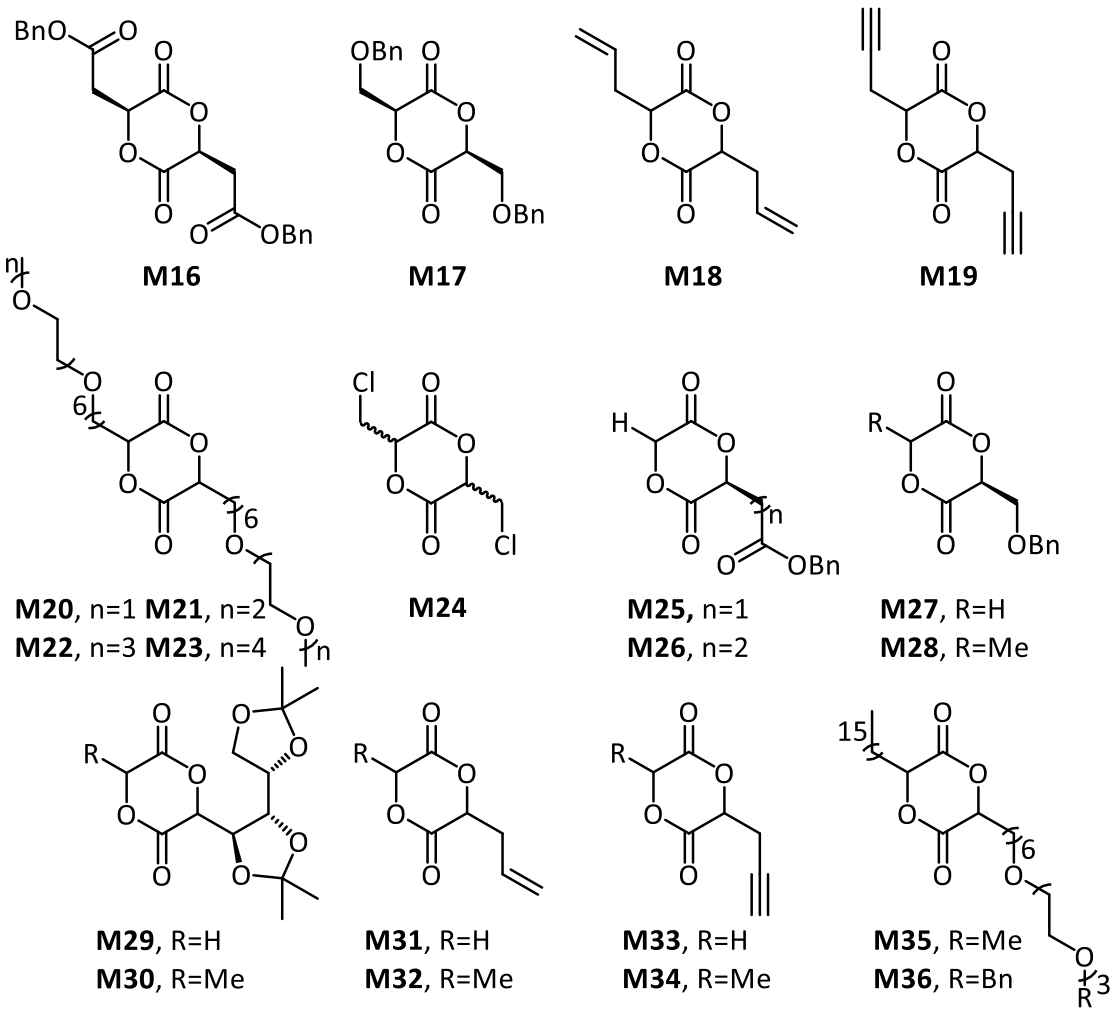

Figure 10. Functionalised cyclic diesters

Table 1.2. Synthetic method used for various functionalised diesters and yields

Monomer	Method	1st functional group	Protecting group	2nd functional group	Yield (%)
M16	1	Carboxyl	Benzyl	Carboxyl	30
M17	1	Hydroxyl	Benzyl	Hydroxyl	27
M18	1	Alkenyl	None	Alkenyl	40
M19	1	Alkynyl	None	Alkynyl	34
M20	1	Ethereal	None	Ethereal	41
M21	1	Ethereal	None	Ethereal	28
M22	1	Ethereal	None	Ethereal	21
M23	1	Ethereal	None	Ethereal	15
M24	1	Chloromethyl	None	Chloromethyl	21
M25	2	Carboxyl	Benzyl	Proton	30
M25	2*	Carboxyl	Benzyl	Proton	66
M26	2	Carboxyl	Benzyl	Proton	37
M27	2	Hydroxyl	Benzyl	Proton	40
M27	2*	Hydroxyl	Benzyl	Proton	40
M28	2	Hydroxyl	Benzyl	Methyl	42
M29	2	Hydroxyl	Isopropylidene	Proton	30
M30	2	Hydroxyl	None	Methyl	49
M31	2	Alkenyl	None	Proton	45
M32	2	Alkenyl	None	Methyl	34
M33	2	Alkynyl	None	Proton	45
M34	2	Alkynyl	None	Methyl	34
M35	2	Ethereal	None	Hexadecyl	12
M36	2	Ethereal	None	Hexadecyl	10

**Modified method involving halogen exchange prior to final cyclisation*

Bourissou and Dove polymerised the glutamic and malic acid bifunctional diesters **M26** and **M25** respectively utilizing a thiourea paired with (-)-sparteine or DMAP to excellent conversions (98 and 92%). The polymerisations took a matter of minutes and proceeded faster than the polymerisation of **M2** with the same catalyst system. Both poly(α-malic acid) homopolymer and **P1** copolymer were found to degrade hydrolytically as well as *in vitro*.[80] Poly(glycolic acid-co-α-malic acid) degrades to small molecules in water. The products of degradation are monomeric and dimeric units after 6 days and the degradation is described as autocatalytic.[69]

M17 was first polymerised to form a copolymer with **M2** (Scheme 1.2).[84] Following deprotection the hydroxyl group was reacted with succinic anhydride and was subsequently used as a tethering point for an RGD-peptide (GGRGDSPGGK). This functionalisation has the ability to be used in tissue engineering, displayed by the increased adhesion of epithelial Madin-Darby canine kidney cells to functionalised polymer films. Zhang was later able to homopolymerise **M17** and deprotect the resulting polymer to form a water soluble polyester.[70] The telechelic homopolymer was used to form a diblock copolymer with **P1**. The amphiphilic diblock copolymer was shown to self-assemble to form micelles in solution.

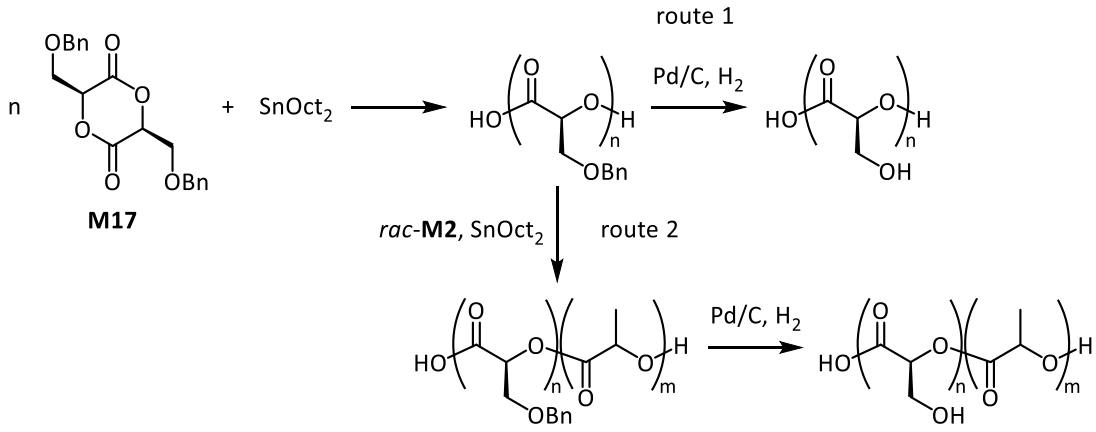

*Scheme 1.2. Ring-opening polymerisation of **M17** using C1. The polymer produced was then reacted in two pathways. Route 1: the benzyl group was deprotected in a hydrogenation catalysed by palladium on carbon. Route 2: The polymer was used a macroinitiator in the ring-opening polymerisation of rac-**M2** and the copolymer was subsequently deprotected by a hydrogenation*

Hennink pursued the use of **M27** and **M28** over **M17**. Over a 12 year span from the initial synthesis and polymerisation, including *in vitro* degradation studies, protein release modelling, and biocompatibility testing, hydroxyl functionalised polymer microparticles have shown great promise for sustained and local delivery of anti-cluster of differentiation-40 and anti-cytotoxic t-lymphocyte associated protein-4 in immunotherapy of cancer.[85–89] **M29** and **M30** meanwhile have enabled the use of greener and renewable starting materials. ROP of **M29** led

to a polyester with a high T_g (95 °C). However, the deprotection of the hydroxyl groups proved difficult to complete without degradation of the polymer backbone and a maximum of 50% deprotection was reached while the majority of backbone remained intact. **M29** and **M30** were later copolymerised with *rac*-**M2.** These polymers showed an increase in T_g, with incorporation of 31% **M29** and 11% **M30** determined to be 73 °C and 58 °C respectively.

The motivation for the synthesis and polymerisation of alkene functionalised monomers **M31** and **M32** was driven by the olefins ability to be modified post-polymerisation. Among the wide variety of reactions possible for the olefin, epoxidation and thiol-ene cross linking have received the main focus.[79,90] Epoxidised copolymers of **M2** and **M31** were synthesised with the intent to target dihydrolysed products, however, chain scission caused a very large drop in molecular weights and at high mol% (>75%) of **M31** no tractable polymer was obtained. **M32** was also copolymerised with **M2**, and olefin enabled them to crosslink polymer chains *via* a UV-induced thiol-ene reaction, to make biodegradable nanoparticles and nanocapsules.

Polymerisation of **M19**, like its alkenyl counterpart, produces a polymer with a functional group capable of undergoing further reaction to modify the polymer post-polymerisation. The copper catalysed Huisgen 1,3-dipolar cycloaddition is a reaction between two unsaturated reactants. An example of such a cycloaddition is the reaction between an azide and an alkyne to produce a triazole. This type reaction is otherwise known as click chemistry and is extremely versatile.[91] The versatility and reliability of click chemistry has been shown to be applicable to modifying PAHAs in a multitude of ways. Click chemistry enabled Baker and Smith to modify the homopolymer of **M19** as well as the random and block copolymers of **M19** and **M2**. They were modified to form a family of degradable and thermoresponsive materials. The thermoresponsive materials exhibited lower critical solution temperatures over a broad, physiologically relevant temperature range.[72] A variety of applications, including controlled cell adhesion to surface modified compartmentalised fibre scaffolds, siRNA delivery by polymeric nanoparticles, chemically controlled bending of microcylinders and antifouling biomaterials have been accessed through **M19**.[92–97] **M34** has been limited to one use to form an amphiphilic graft copolymer.[81] However, **M35** has been used to form novel graft polymer–drug conjugates with paclitaxel and doxorubicin for sustained release or pH triggered drug delivery.[82,98,99]

Baker and Smith wanted to add to their oligo(ethylene glycol) grafted polyester without the need for post-polymerisation modification, they completed this firstly through the diester approach. Monomers **M20-23** were successfully polymerised, however they found **M20** and

M21 produced polymers insoluble in water. ROP of monomers **M22** and **M23** resulted in two polymers with defined, unique lower critical solution temperature in water. The other oligo(ethylene glycol) grafted monomers **M35** and **M36** were not designed to meet the same criteria. The long alkyl chain and the hydrophilic oligo(ethylene glycol) chains led to polymers capable of side chain crystallisation. This amphiphilic behaviour was exploited to form micelles capable of encapsulating azobenzene and thus displaying their potential as drug delivery vehicles.[83]

M24 was copolymerised with **M2** to form a **P1**, incorporating 5% alkyl halide functionalisation.[74] Dehydrochlorination of the copolymer with Hunig's base brought about a novel α-vinyl PLA. It was illustrated that the olefin was capable of installing various substituted sulphides through radical addition. It was found that aryl containing sulphides impacted positively on the T_g, increasing by 10 °C. The addition potential was exemplified through the demonstration of thiol functionalised fluorescent dye conjugation to an α-vinyl PLA film.

Cyclic diesters have proven a useful route to access a wide variety of substituted PAHAs. However, as illustrated above the synthesis of the diester monomers is often challenging and low yielding. The high temperatures used during synthesis often results in a mixture of diastereomers, which in turn inhibits the access to isotactic PAHAs. The diesters display poor reactivity which leads to elongated polymerisation times and the need for elevated temperatures.

1.4.5 The Use of O-Carboxyanhydrides as a Monomer in Ring-Opening Polymerisation

O-Carboxyanhydrides (OCAs) have recently emerged as a monomer feedstock and has drawn the attention of many research groups. The shift of focus from cyclic esters to OCAs, as a monomer source, has been due to several factors including the prevalence of literature on OCA synthesis and the synthesis often being high yielding. However, the biggest difference is OCAs ability to circumvent the low reactivity of cyclic diesters.

OCAs are typically prepared via carbonylation of α-hydroxy acids. Phosgene, diphosgene and triphosgene are typically used as carbonylating agents. Despite diphosgene and triphosgene requiring activated charcoal and stoichiometric tertiary-amines, they are often preferred over phosgene due to their lower volatility making them easier to handle.

Carbonylating lactic acid following this preparation produces lacOCA (**M37**) (Figure 1.11), the prototype used for investigating the ROP of OCAs.[100]

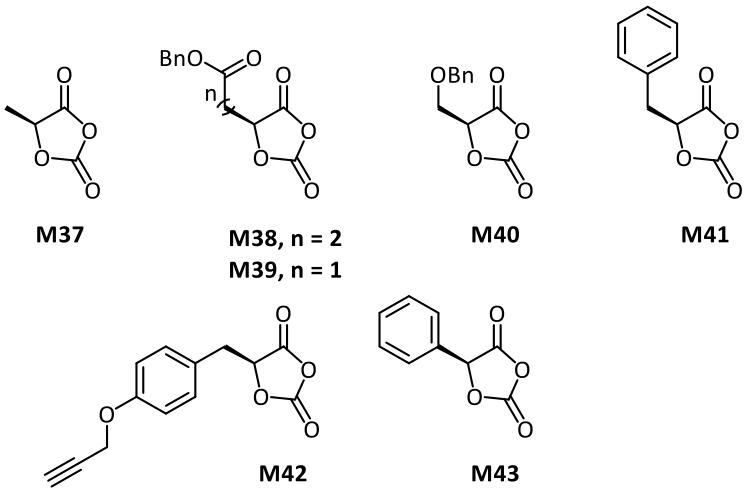

Figure 1.11. O-Carboxyanhydride monomers

In the presence of a primary or secondary alcohol DMAP acts as an organocatalyst towards **M37**. **M37** is polymerised at a far higher rate than **M2**. 20 equivalents of **M37** were found to ring open in five minutes at room temperature, in comparison to 10 equivalents of **M2** opened in 4 days in refluxing dichloromethane (DCM). Only 19 minutes were required to polymerise 600 equivalents of **M37**, epitomizing the activity of the monomer and potential of this route. The polymerisation was also shown to display a living nature, as observed MWs aligned well with the expected MWs and the polymerisation was found to proceed upon addition of a second monomer feedstock. It was suggested that the mechanism of the ROP of OCAs proceeds *via* a nucleophilic addition of the catalyst to the ester carbon followed by displacement by the alcohol. However, it was illustrated that ROP of **M37** using DMAP and an alcohol initiator follows an initiator activation pathway (Scheme 1.3).[101]

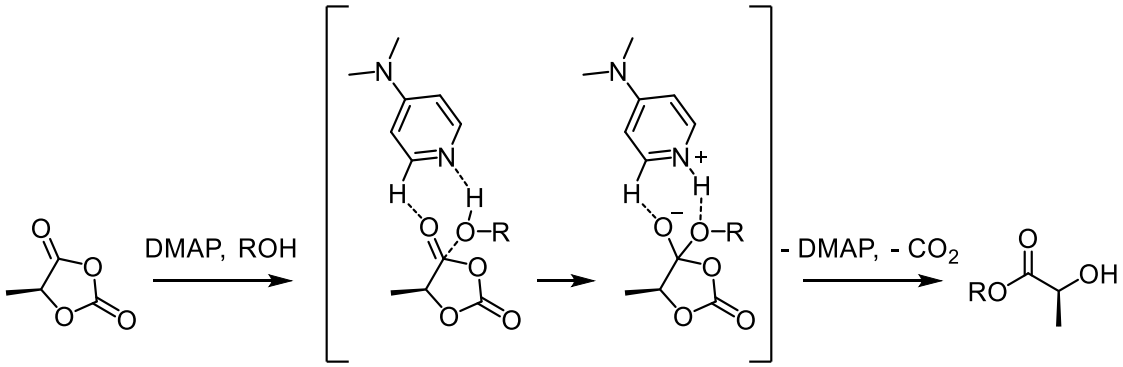

*Scheme 1.3. The alcohol addition to and ring-opening of **M37** promoted by DMAP. The mode of action presented is the basic activation of alcohol initiation proposed by Bourissou and Martin Vaca.*[101]

1.4.6 The Synthesis and Use of O-Carboxyanhydrides to Form Functionalised Poly(α-hydroxy acids) and Their Properties

The rapid and efficient polymerisation of **M37** pathed the way for others to follow with more complex OCA monomers. High demands in biomedicine led the focus away from simple alkyl and aryl groups. Bourissou and Dove used **M38** and **M39** respectively to overcome **M16**, **M25** and **M26**'s poor polymerisation conversions.[102,103] High conversions were reached in mild conditions in minutes, contrasting with the days the cyclic esters took to reach lower conversions. The polymerisations displayed living characteristics while dispersities remained relatively low ($Đ$ < 1.28). Block copolymers were formed by both Bourissou and Dove through divergent routes (Scheme 1.4). The polymer produced from **M38** was shown to be a telechelic polymer and was used to initiate the ROP of **M37** forming a block copolymer. The reverse approach was taken by Dove as **P1** and **P4** were used as a macroinitiators to ring-open **M39**. The catalytic hydrogenation of the benzyl esters was performed under an atmosphere of hydrogen gas in the presence of a catalytic amount of palladium on carbon (Pd/C). The deprotected carboxylic acid side chains led to the resulting polymer being water soluble. The acidic functional group was thought to auto-catalyse the hydrolytic degradation of the polymer to monomeric units or small oligomers in a short degradation time of 10 days.

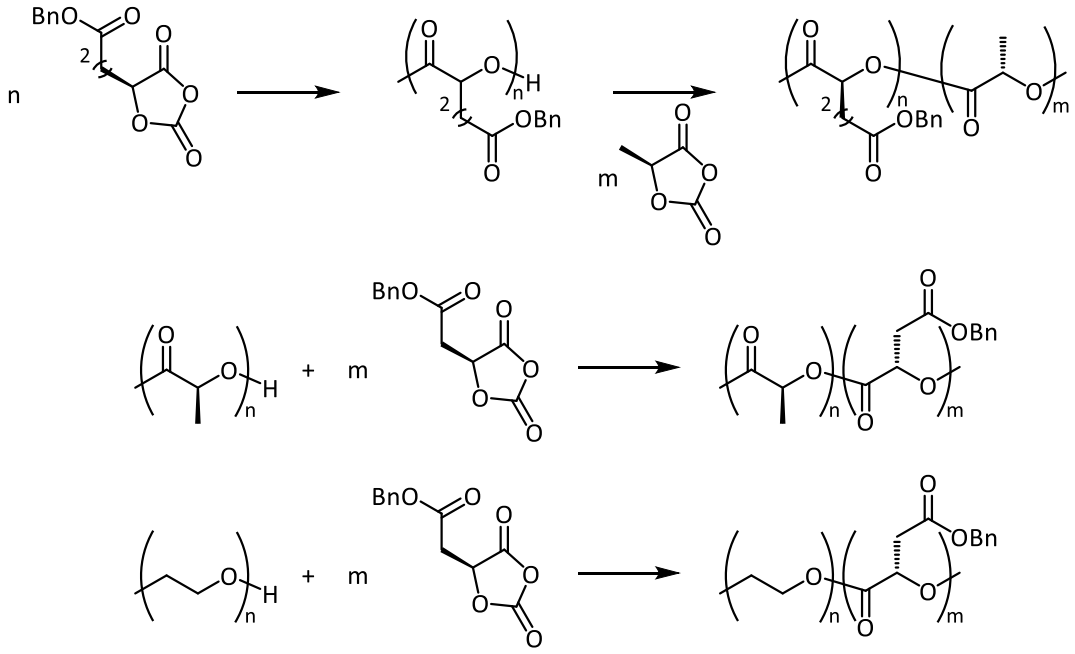

*Scheme 1.4. The polymerisations of monomers **M38** and **M39**. The homopolymer formed from the polymerisation of **M38** is used as a macroinitiator for the ROP of **M37**. **P1** and **P4** were used as macroinitiators to form block copolymers with **M39**.*

Diazotisation of *S*-2-amino-3-benzyloxypropionic acid followed by ring closure with diphosgene gave **M40** in 50% yield, improving upon the yield of **M17**.[104] The polymerisation reached comparable conversions without the need for high concentrations or elevated temperatures. It was illustrated that **M40** has the ability to be copolymerised with **M37** and benzyl substituted OCA **M41** to form block copolymers. The presence of free hydroxy groups of deprotected poly(α-glyceric acid) improved the adhesion of Henrietta Lacks (HeLa) cells to polymer films.

Similar to the diester, the alkyne functionalised OCA received a lot of attention. A different synthetic approach was taken to reach **M42**, using a renewable amino acid, tyrosine as the starting material rather than ethyl glyoxalate used for the synthesis of **M19**. The overall yield of **M42 (**29%) nearly doubled that of **M19** (15%).[105] Post-polymerisation modification in the form of thiol radical addition has been used several times to reach a range of applications in the biomedical field. Polyesters with pendant ammonium hydrochlorides were efficient in cell penetration and gene delivery with low toxicity, while disulphide bridged diazides formed redox active crosslinks were among the modifications made.[104] The reduction of crosslinks triggered macrostructure disassembly and drug release. A spiropyran chromophore was attached by azide-alkyne click chemistry.[106] The resulting polymer was light responsive. Under ultra-violet (UV) light the polymer was triggered to disassemble its micelle structure and released a hydrophobic drug model (coumarin 102).

Further utility of the OCA route was shown by Carbery through synthesis of an enantiopure OCA derivative from mandelic acid **M43** with a 75% yield.[107] Control over tacticity was observed to be readily reproduced by performing the polymerisation using preformed catalyst initiator systems from pyridine and mandelic acid. The lack of epimerization resulted in the isolation of isotactic **P5**, which exhibited an increase of T_g (105 °C) over atactic **P5**.

OCAs have provided an extremely useful synthetic route to PAHAs. While boosting the monomer's activity in polymerisations, the monomers were also frequently obtained in higher yields than their diester counterparts. Higher activity has led to the use of ambient temperatures which has likely played a large factor in the increased control over polymerisations. The simplicity of OCA synthesis and its high yields have been beneficial for synthesising polymers unique to those synthesised from cyclic diesters. However, there are several drawbacks to using OCAs as a monomer source. Firstly, the cost of monomer synthesis is increased dramatically. This is due to the price of phosgene being far greater than the α-hydroxy acid, for example 500 g of triphosgene is 20 times higher than 1 L of lactic acid (80%) (prices from

Sigma Aldrich January 2018). The health and safety of the chemist and those in the wider area are put at a far greater risk when synthesising OCA monomers. Phosgene gases are extremely toxic by acute inhalation exposure and toxic levels that put a person's life and well-being in jeopardy can be as low as 2 parts per million (ppm).[108] Phosgene's high toxicity led to the compound being used in chemical warfare and was the primary agent that led to 100,000 casualties during World War I.[109–111] These two factors make have made it a pressing issue to devise a synthetic route in a cost effectively, without the use of highly toxic materials, whilst also tackling the issues such as poor yields present in the cyclic diester route to polyesters.

1.5 A New Synthetic Approach to Making Polyesters

Hillmyer *et al.* has provided key inspiration for this project with the discovery of a new divergent synthetic route to synthesise a polyester and a polyesteracetal. A six-membered ring was synthesised *via* a Baeyer-Villiger oxidation of a widely available starting material, 2-methyltetrahydrofuran-3-one, using an easy to handle oxidant meta-chloroperbenzoic acid. The resultant monomer 2-methyl-1,3-dioxan-4-one (**M44**) was made anhydrous and isolated with a good yield (75%). $ZnEt_2$ (**C20**), known to ring open a wide variety of lactones, was chosen as the catalyst. The catalyst concentration was found to play a pivotal role in the polymerisation. It was found that two distinct repeat units could be obtained from the same monomer (**M44**).[112] The monomeric unit could be selected by having either high or low catalyst loadings. At high catalyst loadings (30-100 mM) monomer conversion reached >99% after eight hours at 25 °C. It was found that the isolated white solid had no acetal units present in either ^{1}H or ^{13}C NMR spectra. In agreement with the NMR spectra electron spray ionisation mass spectroscopy (ESI-MS) confirmed the mass difference between polymer chains has a mass to charge ratio (m/z) = 72.02 and the polymer to be poly(3-hydroxypropionic acid). The divergence occurs at low catalyst loadings (0.4-14 mM). Though conversions are limited to 60%, acetal linkages in the polymer backbone are retained and lead to an observed repeat unit m/z = 116.05 in the ESI-MS spectrum. As discussed earlier the metal alkoxide species tend to aggregate and Hillmyer speculates that it is the aggregation of propagating zinc species that facilitates acetal elimination. To establish the order of polymerisation in $[\mathbf{C20}]_0$ double logarithmic plots of k_{obs} vs. $[\mathbf{C20}]_0$ were created. The system that eliminates the acetal was found to have a second order rate dependence suggesting that two zinc centres are taking part in the rate determining step.

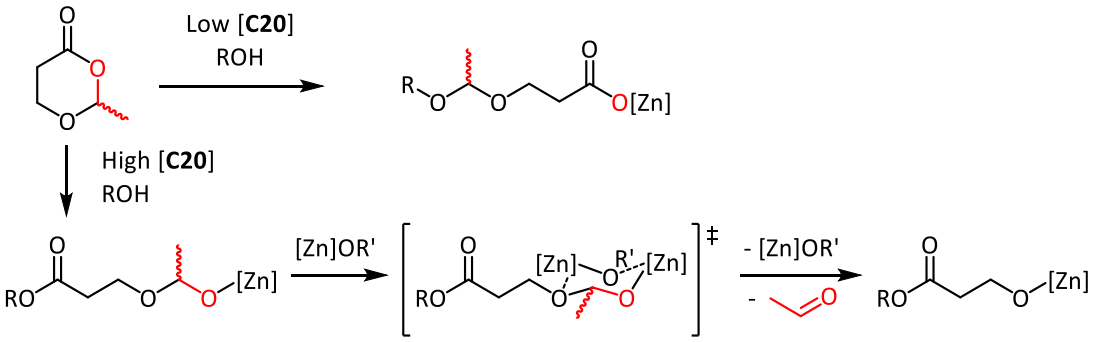

Scheme 1.5. Divergent mechanistic pathways for the polymerisation of 2-methyl-1,3-dioxan-4-one.[112]

1.6 Project Aims

The two current synthetic routes used to synthesise PAHAs have each been shown to have major flaws, such as poor yields for many monomers including the vast majority of the cyclic esters, elaborate synthetic procedures primarily involving the need for extra protection and deprotection steps before the carbonylation of OCA monomers **M38**-**M40**, low polymerisation activity, toxic synthesis and cost issues. To tackle these major issues, it has become vital to synthesise PAHAs from a different monomer pool from cyclic diesters or OCAs. A family of 1,3-dioxolan-4-ones was targeted as a potential monomer source to address these issues. This monomer feedstock was sought after with the intention of achieving high yields due to stability of the five-member ring. It was hypothesised that the stability of the 5-membered cyclic ester could be overcome with the expulsion of a stable small molecule in order to achieve high conversions during the polymerisation process. In Chapter 2 the focus surrounds the most basic unsubstituted monomer synthesised from glycolic acid. The monomer underwent the initial polymerisation testing. The compatibility of 1,3-dioxolan-4-ones ROP with other standard common ROP monomers was tested. The compatibility testing opened this synthetic route to a wider array of copolymerisations possibilities. Chapter 3 explored the homopolymerisation of methyl and phenyl substituted 1,3-dioxolan-4-ones. The polymerisation was conducted with a variety of catalysts and reactions set ups with the intention of achieving high rates of polymerisation whilst instilling control over the polymerisation. Finally, Chapter 4 looked to diversify the range of 1,3-dioxolan-4-ones available for ROP by varying the functional group substituted at the α-carbon. Not only has the wide variety of functional groups been shown to expand the range of thermal properties available from the ROP of 1,3-dioxolan-4-ones, but they have also been tested for use in biomedical applications.

1.7 References

(1) Carothers, W. H.; Arvin, J. A. *J. Am. Chem. Soc.* **1929**, *51* (8), 2560–2570.

(2) Carothers, W. H.; Natta, F. J. Van. *J. Am. Chem. Soc.* **1930**, *52* (1), 314–326.

(3) Carothers, W. H.; Hill, J. W. *J. Am. Chem. Soc.* **1932**, *54* (4), 1557–1559.

(4) Carothers, W. H.; Hill, J. W. *J. Am. Chem. Soc.* **1932**, *54* (4), 1559–1566.

(5) Kulkarni, R. K.; Pani, K. C.; Neuman, C.; Leonard, F. *Arch. Surg.* **1966**, *93* (5), 839–843.

(6) Ajioka, M.; Enomoto, K.; Suzuki, K.; Yamaguchi, A. *J. Environ. Polym. Degrad.* **1995**, *3* (4), 225–234.

(7) Idumah, C.; Nwachukwa, A.; Akubue, B. *J. Text. Sci. Eng.* **2013**, *3* (3), 40–45.

(8) Maharana, T.; Mohanty, B.; Negi, Y. S. *Progress in Polymer Science (Oxford)*. 2009, pp 99–124.

(9) Nuyken, O.; Pask, S. D. *Polymers (Basel).* **2013**, *5* (2), 361–403.

(10) Duda, A.; Penczek, S. *Macromolecules* **1990**, *23* (6), 1636–1639.

(11) Lunt, J. *Polym. Degrad. Stab.* **1998**, *59*, 145–152.

(12) Löfgren, A.; Albertsson, A.-C.; Dubois, P.; Jérôme, R. *J. Macromol. Sci. Part C Polym. Rev.* **1995**, *35* (3), 379–418.

(13) Kricheldorf, H. R.; Berl, M.; Scharnagl, N. *Macromolecules* **1988**, *21* (2), 286–293.

(14) Stevels, W. M.; Ankoné, M. J. K.; Dijkstra, P. J.; Feijen, J. *Macromolecules* **1996**, *29* (19), 6132–6138.

(15) Mclain, S. J.; Ford, T. M.; Drysdale, N. E. *Abstr. Pap. Am. Chem. Soc.* **1992**, *204* (1), 188–192.

(16) Stevels, W. M.; Ankoné, M. J. K.; Dijkstra, P. J.; Feijen, J. *Macromolecules* **1996**, *29* (9), 3332–3333.

(17) Le Borgne, Alain; Wisniewski, Muriel; Spassky, N. *Polym. Prepr. (American Chem. Soc. Div. Polym. Chem.* **1995**, *36* (2), 217–218.

(18) Wisniewski, M.; Le Borgne, A.; Spassky, N. *Macromol. Chem. Phys.* **1997**, *198* (4), 1227–1238.

(19) Vincens, V.; Le Borgne, A.; Spassky, N. *Makromol. Chemie. Macromol. Symp.* **1991**,

47 (1), 285–291.

(20) Bhaw-Luximon, a.; Jhurry, D.; Spassky, N. *Polym. Bull.* **2000**, *44* (1), 31–38.

(21) Cameron, P. a; Jhurry, D.; Gibson, V. C.; White, A. J. P.; Williams, D. J.; Williams, S. *Macromol. Rapid Commun.* **1999**, *20* (12), 616–618.

(22) Hormnirun, P.; Marshall, E. L.; Gibson, V. C.; Pugh, R. I.; White, A. J. P. *Proc. Natl. Acad. Sci. U. S. A.* **2006**, *103* (42), 15343–15348.

(23) Wengrovius, J. H.; Garbauskas, M. F.; Williams, E. A.; Going, R. C.; Donahue, P. E.; Smith, J. F. *J. Am. Chem. Soc.* **1986**, *108* (5), 982–989.

(24) Aoshima, S.; Higashimura, T. *Macromolecules* **1989**, *22* (3), 1009–1013.

(25) Gianopoulos, C. G.; Kumar, N.; Zhao, Y.; Jia, L.; Kirschbaum, K.; Mason, M. R. *Dalt. Trans.* **2016**, *45* (35), 13787–13797.

(26) Dittrich, V. W.; Schulz, R. C. *Die Angew. Makromol. Chemie* **1971**, *15* (1), 109–126.

(27) Dubois, P.; Jacobs, C.; Jérôme, R.; Teyssté, P. *Macromolecules* **1991**, *24* (9), 2266–2270.

(28) Parenté, V.; Brédas, J. L.; Dubois, P.; Ropson, N.; Jérôme, R. *Macromol. Theory Simulations* **1996**, *5* (3), 525–546.

(29) Von Schenck, H.; Ryner, M.; Albertsson, A. C.; Svensson, M. *Macromolecules* **2002**, *35* (5), 1556–1562.

(30) Albertsson, A. C.; Varma, I. K. *Biomacromolecules* **2003**, *4* (6), 1466–1486.

(31) Dechy-Cabaret, O.; Martin-Vaca, B.; Bourissou, D. *Chem. Rev.* **2004**, *104* (12), 6147–6176.

(32) Mecking, S. *Angew. Chem. Int. Ed. Engl.* **2004**, *43* (9), 1078–1085.

(33) Auras, R.; Harte, B.; Selke, S. *Macromol. Biosci.* **2004**, *4* (9), 835–864.

(34) Chiellini, E.; Solaro, R. *Adv. Mater.* **1996**, *8* (4), 305–313.

(35) Sperling, L. H. *Introduction to Physical Polymer Science*; Wiley, 2001; Vol. 207.

(36) Ulery, B. D.; Nair, L. S.; Laurencin, C. T. *J. Polym. Sci. Part B Polym. Phys.* **2011**, *49* (12), 832–864.

(37) Ovitt, T. M.; Coates, G. W. *J. Am. Chem. Soc.* **2002**, *124* (7), 1316–1326.

(38) Cheng, M.; Attygalle, A. B.; Lobkovsky, E. B.; Coates, G. W. *J. Am. Chem. Soc.* **1999**,

121 (49), 11583–11584.

(39) Zhong, Z.; Dijkstra, P. J.; Feijen, J. *J. Am. Chem. Soc.* **2003**, *125* (37), 11291–11298.

(40) Ovitt, T. M.; Coates, G. W. *J. Polym. Sci. Part A Polym. Chem.* **2000**, *38* (S1), 4686–4692.

(41) Ikada, Y.; Jamshidi, K.; Tsuii, H.; Hyon, S. H. *Macromolecules* **1987**, *20* (4), 904–906.

(42) Vink, E. T. H.; Rábago, K. R.; Glassner, D. A.; Gruber, P. R. *Polym. Degrad. Stab.* **2003**, *80* (3), 403–419.

(43) Hu, Y.; Rogunova, M.; Topolkaraev, V.; Hiltner, A.; Baer, E. *Polymer (Guildf).* **2003**, *44* (19), 5701–5710.

(44) Hu, Y.; Hu, Y. S.; Topolkaraev, V.; Hiltner, A.; Baer, E. *Polymer (Guildf).* **2003**, *44* (19), 5711–5720.

(45) Ouchi, T.; Miniari, T.; Ohya, Y. *J. Polym. Sci. Part A Polym. Chem.* **2004**, *42* (21), 5482–5487.

(46) Zhu, K. J.; Xiangzhou, L.; Shilin, Y. *J. Appl. Polym. Sci.* **1990**, *39* (1), 1–9.

(47) Zhu, K. J.; Lei, Y. **1997**, *43*, 210–216.

(48) Jie, C.; Zhu, K. J. *Polym. Int.* **1997**, *42* (4), 373–379.

(49) Shirahama, H.; Mizuma, K.; Umemoto, K.; Yasuda, H. *J. Polym. Sci. Part A Polym. Chem.* **2001**, *39* (9), 1374–1381.

(50) Schmidt, P.; Keul, H.; Höcker, H. *Macromolecules* **1996**, *43* (95), 3674–3680.

(51) Grijpma, D. W.; Pennings, A. J. *Macromol. Chem. Phys.* **1994**, *195* (5), 1633–1647.

(52) Feng, Y.; Klee, D.; Hocker, H. *Macromol. Biosci.* **2004**, *4* (6), 587–590.

(53) Chen, X.; McCarthy, S. P.; Gross, R. A. *Macromolecules* **1998**, *31* (3), 662–668.

(54) Cai, Q.; Bei, J.; Wang, S. *Polym. Adv. Technol.* **2002**, *13* (2), 105–111.

(55) Buchholz, B. *J. Mater. Sci. Mater. Med.* **1993**, *4* (4), 381–388.

(56) Gadzinowski, M.; Sosnowski, S. *J. Polym. Sci. Part A Polym. Chem.* **2003**, *41* (23), 3750–3760.

(57) Tasaka, F.; Ohya, Y.; Ouchi, T. *Macromolecules* **2001**, *34* (16), 5494–5500.

(58) Sinclair, F.; Chen, L.; Greenland, B. W.; Shaver, M. P. *Macromolecules* **2016**, *49* (18), 6826–6834.

(59) Jing, F.; Smith, M. R.; Baker, G. L. *Macromolecules* **2007**, *40* (26), 9304–9312.

(60) Yin, M.; Baker, G. L. *Am. Chem. Soc. Polym. Prepr. Div. Polym. Chem.* **1998**, *39* (2), 158–159.

(61) Liu, T.; Simmons, T. L.; Bohnsack, D. A.; Mackay, M. E.; Smith, M. R.; Baker, G. L. *Macromolecules* **2007**, *40* (17), 6040–6047.

(62) Simmons, T. L.; Baker, G. L. *Biomacromolecules* **2001**, *2*, 658–663.

(63) Trimaille, T.; Möller, M.; Gurny, R. *J. Polym. Sci. Part A Polym. Chem.* **2004**, *42* (17), 4379–4391.

(64) Khadka, P.; Ro, J.; Kim, H.; Kim, I.; Kim, J. T.; Kim, H.; Cho, J. M.; Yun, G.; Lee, J. *Asian Journal of Pharmaceutical Sciences*. 2014, pp 304–316.

(65) Köping-Höggård, M.; Sánchez, A.; Alonso, M. J. *Expert Rev. Vaccines* **2005**, *4* (2), 185–196.

(66) Kricheldorf, H. R.; Kreiser-Saunders, I. *Polymer (Guildf).* **1994**, *35* (19), 4175–4180.

(67) Klok, H. A.; Hwang, J. J.; Iyer, S. N.; Stupp, S. I. *Macromolecules* **2002**, *35* (3), 746–759.

(68) Barakat, I.; Dubois, P.; Jérôme, R.; Teyssié, P. *J. Polym. Sci. Part A Polym. Chem.* **1993**, *31* (2), 505–514.

(69) Pounder, R. J.; Dove, A. P. *Biomacromolecules* **2010**, *11* (8), 1930–1939.

(70) Zhang, X.; Dai, Y. *Macromol. Rapid Commun.* **2017**, *38* (2), 1600593.

(71) Radano, C. P.; Baker, G. L.; Smith III, M. R. *Polym. Prepr. (American Chem. Soc. Div. Polym. Chem.* **2002**, *43* (2), 727–728.

(72) Jiang, X.; Vogel, E. B.; Smith, M. R.; Baker, G. L. *Macromolecules* **2008**, *41* (6), 1937–1944.

(73) Jiang, X.; Smith, M. R.; Baker, G. L. *Macromolecules* **2008**, *41* (2), 318–324.

(74) Kalelkar, P. P.; Alas, G. R.; Collard, D. M. *Macromolecules* **2016**, *49* (7), 2609–2617.

(75) Du Boullay, O. T.; Saffon, N.; Diehl, J. P.; Martin-Vaca, B.; Bourissou, D. *Biomacromolecules* **2010**, *11* (8), 1921–1929.

(76) Samadi, N.; Van Nostrum, C. F.; Vermonden, T.; Amidi, M.; Hennink, W. E. *Biomacromolecules* **2013**, *14* (4), 1044–1053.

(77) Gerhardt, W. W.; Noga, D. E.; Hardcastle, K. I.; García, A. J.; Collard, D. M.; Weck,

M. *Biomacromolecules* **2006**, *7* (6), 1735–1742.

(78) Marcincinova-Benabdillah, K.; Boustta, M.; Coudane, J.; Vert, M. *Biomacromolecules* **2001**, *2* (4), 1279–1284.

(79) Leemhuis, M.; Akeroyd, N.; Kruijtzer, J. A. W.; van Nostrum, C. F.; Hennink, W. E. *Eur. Polym. J.* **2008**, *44* (2), 308–317.

(80) Vogeley, N. J.; Baker, G. L.; Smith III, M. R. *Polym. Prepr. (American Chem. Soc. Div. Polym. Chem.* **2005**, *46* (1), 336.

(81) Coumes, F.; Darcos, V.; Domurado, D.; Li, S.; Coudane, J.; Law, W. C.; Cheng, C.; Frechet, J. M. J.; Sharpless, K. B.; Fokin, V. V.; Gellert, P. R.; Washington, C. *Polym. Chem.* **2013**, *4* (13), 3705–3713.

(82) Yu, Y.; Zou, J.; Yu, L.; Ji, W.; Li, Y.; Law, W. C.; Cheng, C. *Macromolecules* **2011**, *44* (12), 4793–4800.

(83) Jiang, X.; Vogel, E. B.; Smith, M. R.; Baker, G. L. *J. Polym. Sci. Part A Polym. Chem.* **2007**, *45* (22), 5227–5236.

(84) Noga, D. E.; Petrie, T. A.; Kumar, A.; Weck, M.; García, A. J.; Collard, D. M. *Biomacromolecules* **2008**, *9* (7), 2056–2062.

(85) Leemhuis, M.; van Steenis, J. H.; van Uxem, M. J.; van Nostrum, C. F.; Hennink, W. E. *European J. Org. Chem.* **2003**, *2003* (17), 3344–3349.

(86) Leemhuis, M.; Kruijtzer, J. A. W.; van Nostrum, C. F.; Hennick, W. E. *Biomacromolecules* **2007**, *8* (9), 2943–2949.

(87) Ghassemi, A. H.; Van Steenbergen, M. J.; Talsma, H.; Van Nostrum, C. F.; Crommelin, D. J. A.; Hennink, W. E. *Pharm. Res.* **2010**, *27* (9), 2008–2017.

(88) Kazazi-Hyseni, F.; Zandstra, J.; Popa, E. R.; Goldschmeding, R.; Lathuile, A. A. R.; Veldhuis, G. J.; Van Nostrum, C. F.; Hennink, W. E.; Kok, R. J. *Int. J. Pharm.* **2015**, *482* (1–2), 99–109.

(89) Rahimian, S.; Fransen, M. F.; Kleinovink, J. W.; Amidi, M.; Ossendorp, F.; Hennink, W. E. *Biomaterials* **2015**, *61*, 33–40.

(90) Zou, J.; Hew, C. C.; Themistou, E.; Li, Y.; Chen, C. K.; Alexandridis, P.; Cheng, C. *Adv. Mater.* **2011**, *23* (37), 4274–4277.

(91) Kolb, H. C.; Finn, M. G.; Sharpless, K. B. *Angew. Chemie - Int. Ed.* **2001**, *40* (11), 2004–2021.

(92) Tu, Q.; Wang, J. C.; Liu, R.; Chen, Y.; Zhang, Y.; Wang, D. E.; Yuan, M. Sen; Xu, J.; Wang, J. *Colloids Surfaces B Biointerfaces* **2013**, *108*, 34–43.

(93) Saha, S.; Copic, D.; Bhaskar, S.; Clay, N.; Donini, A.; Hart, A. J.; Lahann, J. *Angew. Chemie - Int. Ed.* **2012**, *51* (3), 660–665.

(94) Portis, A. M.; Carballo, G.; Baker, G. L.; Chan, C.; Walton, S. P. *Microsc. Res. Tech.* **2010**, *73* (9), 878–885.

(95) Bhaskar, S.; Nandivada, H.; Deng, X.; Lahann, J. *Polym. Prepr.* **2010**, *51* (1), 482–483.

(96) Mandal, S.; Bhaskar, S.; Lahann, J. *Macromol. Rapid Commun.* **2009**, *30* (19), 1638–1644.

(97) Bhaskar, S.; Roh, K. H.; Jiang, X.; Baker, G. L.; Lahann, J. *Macromol. Rapid Commun.* **2008**, *29* (20), 1655–1660.

(98) Yu, Y.; Chen, C. K.; Law, W. C.; Weinheimer, E.; Sengupta, S.; Prasad, P. N.; Cheng, C. *Biomacromolecules* **2014**, *15* (2), 524–532.

(99) Yu, Y.; Chen, C. K.; Law, W. C.; Mok, J.; Zou, J.; Prasad, P. N.; Cheng, C. *Mol. Pharm.* **2013**, *10* (3), 867–874.

(100) Thillaye Du Boullay, O.; Marchal, E.; Martin-Vaca, B.; Cossío, F. P.; Bourissou, D. *J. Am. Chem. Soc.* **2006**, *128* (51), 16442–16443.

(101) Martin Vaca, B.; Bourissou, D. *ACS Macro Lett.* **2015**, *4* (7), 792–798.

(102) Du Boullay, O. T.; Bonduelle, C.; Martin-Vaca, B.; Bourissou, D. *Chem. Commun.* **2008**, *12* (15), 1786–1788.

(103) Pounder, R. J.; Fox, D. J.; Barker, I. A.; Bennison, M. J.; Dove, A. P.; Jerome, R.; Jerome, C.; Dubois, P. *Polym. Chem.* **2011**, *2* (10), 2204–2212.

(104) Lu, Y.; Yin, L.; Zhang, Y.; Zhang, Z.; Xu, Y.; Tong, R.; Cheng, J. *ACS Macro Lett.* **2012**, *1* (4), 441–444.

(105) Zhang, Z.; Yin, L.; Xu, Y.; Tong, R.; Lu, Y.; Ren, J.; Cheng, J. *Biomacromolecules* **2012**, *13* (11), 3456–3462.

(106) Niu, Y.; Li, Y.; Lu, Y.; Xu, W.; Xia, X. N.; Lu, Y. B.; Ji, J.; Cheng, J. J.; Ren, J.; Cheng, J. J. *RSC Adv.* **2014**, *4* (102), 58432–58439.

(107) Buchard, A.; Carbery, D. R.; Davidson, M. G.; Ivanova, P. K.; Jeffery, B. J.; Kociok-

Köhn, G. I.; Lowe, J. P. *Angew. Chemie - Int. Ed.* **2014**, *53* (50), 13858–13861.

(108) Olson, K. R. In *McGraw-Hill's AccessMedicine*; 2012; p xvi, 815 .

(109) Hoenig, S. L. In *Compendium of Chemical Warfare Agents*; Springer New York, 2007; Vol. 25, p 222.

(110) Haber, L. F. *The Poisonous Cloud: Chemical Warfare in the First World War*; Oxford University Press, 1986.

(111) Eckert, W. G. *Am. J. Forensic Med. Pathol.* **1991**, *12* (2), 119–125.

(112) Neitzel, A. E.; Petersen, M. A.; Kokkoli, E.; Hillmyer, M. A. *ACS Macro Lett.* **2014**, *3* (11), 1156–1160.

Chapter 2. Poly(glycolic acid) Copolymers from 1,3-Dioxolan-4-one

2.1 Introduction

The use of 1,3-dioxolan-4-ones as monomers to form polymers was first patented 22 years ago.[1] Hermes stated that "useful polymeric material" was obtained from the homopolymerisation of 1,3-dioxolan-4-one (**M45**). The composition of the ring-opened monomer was not reported in the text and some examples of polymerisations suggest that when **M45** is polymerised with **M1** a copolymer is formed. This differs from our hypothesis that the copolymerisation of **M45** and **M1** would generate a poly(glycolic acid) (**P10**) homopolymer (Scheme 2.1).

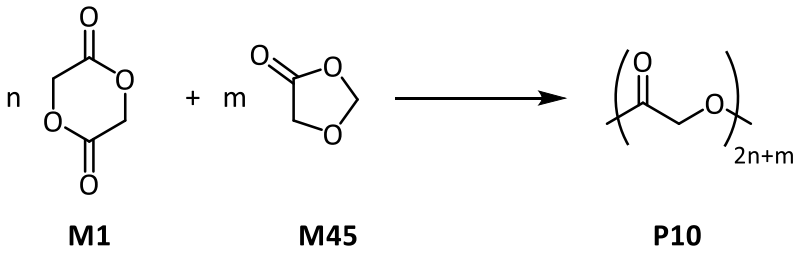

*Scheme 2.1. The polymerisation of **M1** and **M45** to form **P10** following the discussed hypothesis.*

In 2010, Miller patented a less ambiguous invention of the polymerisation of 1,3-dioxolan-4-ones as a monomer feedstock.[2] The patent specifies the polymerisation of 1,3-dioxolan-4-ones produces a polymer and its repeat unit retains the acetal present in the monomer. The copolymerisation of **M45** was later reported by Miller in 2014.[3] The goal of the work was to synthesise a polyesteracetal and tackle the inability of **P1** to hydrolytically degrade. **M45** was copolymerised with **M2** using the standard ROP catalyst **C1** and BnOH as an initiator (Scheme 2.3). The copolymerisation was conducted in solution at 100 °C for 24 h. The ring-opening of the **M45** was determined computationally to be energetically unfavourable, and similar to that of γ-butyrolactone.[3] It was suggested that the unfavourable polymerisation enthalpy of **M45** is overcome by the favourable polymerisation enthalpy of **M2**, due to the release of ring strain present in this monomer. Miller and co-workers modified the composition of the copolymer by varying the monomer feedstock ratio, and thus produced polymers with different hydrolytic degradation rates. It was claimed that the acetal unit, known to be cleaved by water and

accelerated by acidic conditions, led to the observed hydrolytic degradation. However, upon further analysis of the characterisation data supplied in the supplementary information we suggest that the composition of the polymers was incorrectly assigned. The ^{13}C NMR spectrum of the product from the copolymerisation of monomers **M2** and **M45** is displayed in Figure 2.. Despite an initial monomer feedstock ratio of 7:3, **M2**:**M45**, no acetal carbons are detected and a very weak signal is present for the protons alpha to the carbonyl of the ring-opened **M45.**[3]

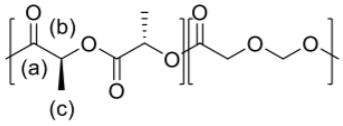

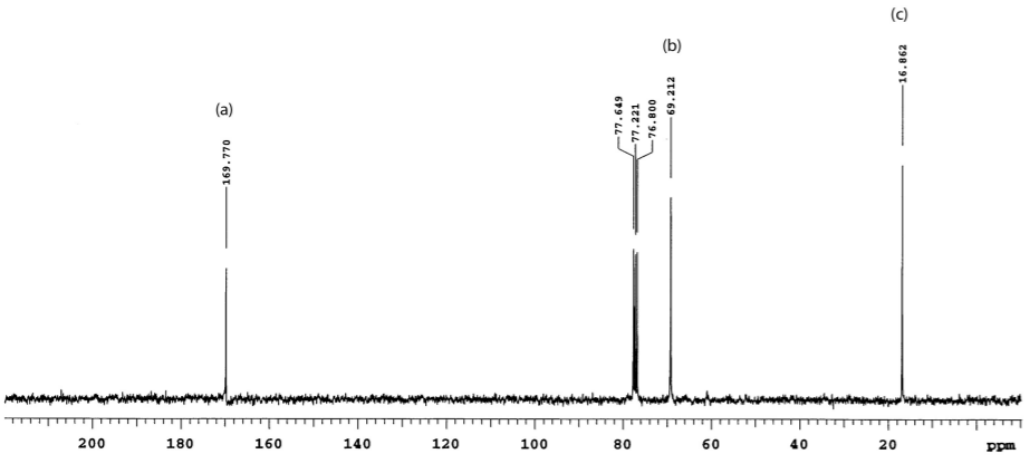

*Figure 2.1. ^{13}C NMR spectrum of copolymer synthesised by Miller et al, from a monomer feedstock of **M2**:**M45** = 70:30 ($CDCl_3$, frequency not presented).*[3] *Carbon signals for the acetal are not present.*

The ^{13}C NMR spectra are inconsistent with the claim that the acetal functionality is retained in the resultant copolymer and are consistent with the loss of the acetal during the polymerisation. The spectra show the incorporation of a second α-hydroxy acid, glycolic acid, in both ^{1}H and ^{13}C NMR spectra. The formation of **P3** is not only consistent with the NMR data presented in Miller's supplementary information, but also the hydrolytic and pH dependent degradation as first shown by Gilding in 1981.[4] This chapter explores the copolymerisations of monomer **M45**.

2.2 Copolymerisation of **M45** and **M2**

Monomer **M45** was synthesised following Miller's procedures by refluxing glycolic acid with an excess of paraformaldehyde (1.2 equivalents) in the presence of *p*-toluenesulfonic acid (PTSA), a weak acid catalyst (Scheme 2.2).[3] A Dean-Stark apparatus was used to actively remove water, a reaction product. Miller *et al.* modified the original protocol used by Salomaa and Loili by reducing the reaction time from 20 to 12 hours and reducing the molar ratio of glycolic acid to paraformaldehyde from 1:6.7 to 1:1.2.[5] The change to the reaction set up eliminated the formation of what Salomaa and Loili describe as a "thick tarlike polymeric mass" and sublimation of excess paraformaldehyde was minimised. Modifying Miller's procedures, it was found that reducing the reaction time further to six hours had no impact upon the product yield of 26%.

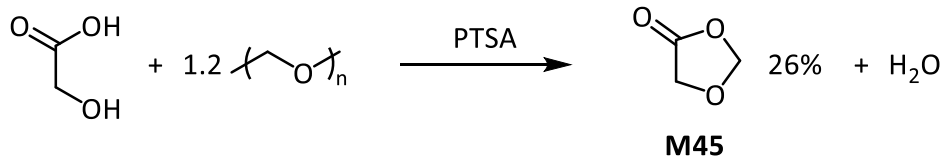

*Scheme 2.2. Synthesis of monomer **M45** from glycolic acid and paraformaldehyde in the presence of PTSA.*

As a preliminary experiment, the polymerisation of **M45** was conducted following the protocol Miller *et al.* described. **M45** and **M2** were copolymerised as described earlier and in Scheme 2.3, where m + n = 500. After 24 h at 100 °C, the reaction was quenched and ^{1}H NMR spectroscopy was conducted on a crude sample to reveal a similar monomer conversion of **M45** and **M2** to what Miller *et al.* had achieved.

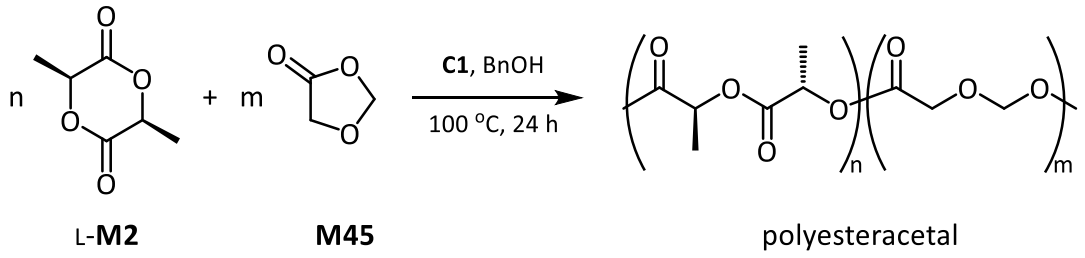

*Scheme 2.3. The copolymerisation of L-**M2** and **M45** conducted by Miller et al. using **C1** and BnOH to form a polyesteracetal.*[3]

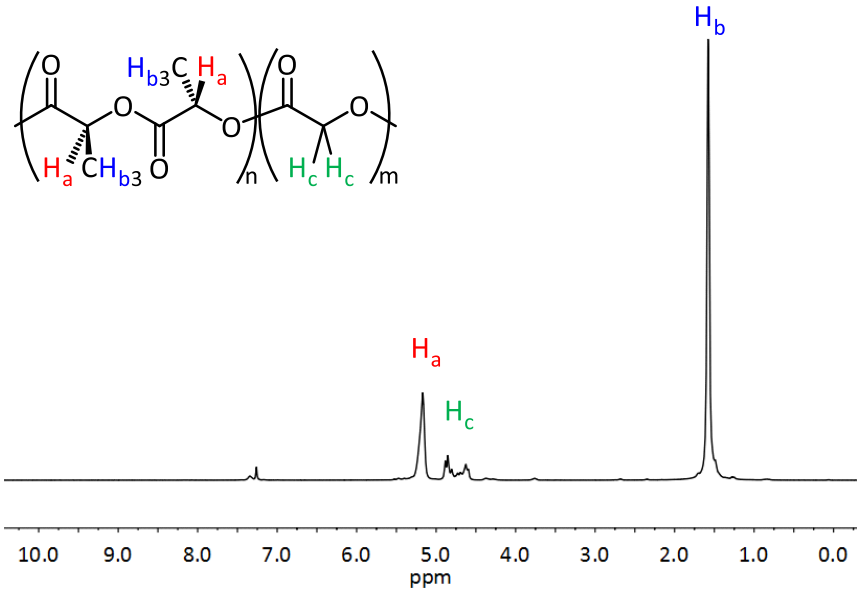

*Figure 2.2. ^{1}H NMR spectrum of **P3** following the literature polymerisation protocol of **M45** and **M2** ($CDCl_3$, 300 K, 500 MHz).*

The ^{1}H NMR spectrum (Figure 2.2) matched those reported by Miller, including the methylene region previously assigned to both the α-protons and acetal protons. However, the ^{13}C NMR spectrum (Figure 2.3) displays no peaks other than those associated with **P3** and it has been concluded that the polymer produced is a polyester and not a polyesteracetal.

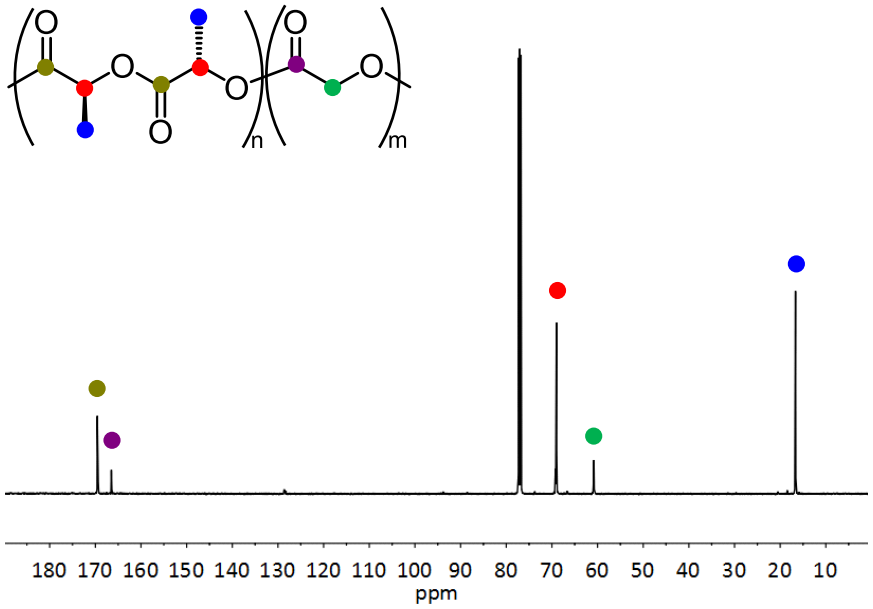

*Figure 2.3. ^{13}C NMR spectrum of **P3** following the literature polymerisation protocol of **M45** and **M2** ($CDCl_3$, 300 K, 100 MHz).*

Residual insoluble white solid was noted to have formed on the walls of the reaction vessel suggesting the formation of either insoluble **P3** or another polymerisation by-product. The unknown white solid was confirmed to be paraformaldehyde following the comparison of the infrared (IR) spectra of the unknown to paraformaldehyde. The spectra were found to overlap and matched across the entire frequency range recorded (4000-600 cm^{-1}). Oligomerisation of the expelled formaldehyde occurs, and sublimation occurs to deposit the solid onto the reaction vessel walls. To improve upon the reaction performance (increasing the polymerisation activity, obtaining expected MWs and narrow dispersities) the catalyst and reaction conditions were varied. The ring-opening polymerisation of monomers **M45** and **M2** was investigated using four additional catalysts which are proposed to operate *via* different mechanisms (Scheme 2.4).[6–8] The catalysts were tested with one equivalent of BnOH as a chain initiator.

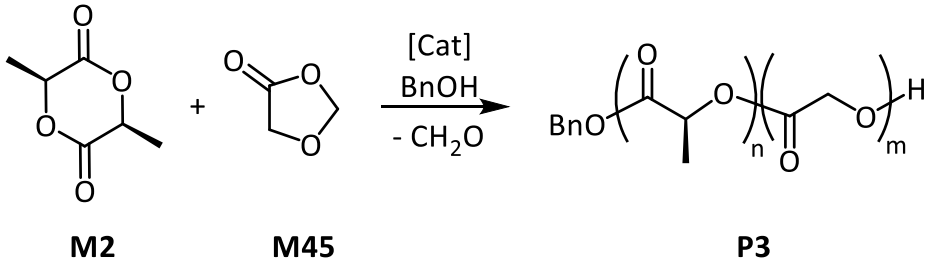

M2 **M45** **P3**

[Cat] = **C13**, DBU, TBD, **C20**

*Scheme 2.4. The copolymerisation of **M2** and **M45**, using various catalysts and BnOH.*

All copolymerisations of **M2** and **M45** were conducted with a total initial monomer concentration of 1 M in anhydrous, degassed solvents. The reaction vessel was an ampoule, sealed under a dry, nitrogen atmosphere. The reaction progress was monitored by removing crude samples from the polymerisation, quenching with excess methanol before performing analysis by ^{1}H NMR spectroscopy. The relative concentrations of monomer and polymer were determined from the relative integration values of each polymer methine peaks at 5.10-5.30 and 4.50-4.90 ppm and the monomer methine peaks at 5.10 and 4.27 ppm. The relative concentrations were used to calculate the monomer conversion. The copolymerisations were conducted with an initial monomer to initiator ratio ([M]/[I]) of 100:1. MWs were obtained by analysing the purified and dried polymer sample by gel permeation chromatography (GPC) equipped with a triple detection system (Table 2.3).

*Table 2.3. **M2** and **M45** copolymerisation with various catalysts.*

Entry	Catalyst	Time (h)	M2 conv. (%)[a]	**M45** conv. (%)[a]	$M_{n,th}$[c]	M_n [c]	$Đ$[c]
1	**C13**	7	96	90	10000	11100	2.23
2	DBU	1	91	10	7000	6700	1.12
3	DBU	24	99	71	9800	9100	1.57
4	TBD	7	12	4	1300	/	/
5	**C20**	7	99	83	9700	4000	1.83

M2*:*M45*:Catalyst*:BnOH = 50:50:1:1. Monomer concentration = 1 M in toluene. The reaction was conducted at 40 °C. Conv. = Monomer conversion. [a] Monomer conversion determined from crude ^1H NMR spectrum. [b] $M_{n,th}$ (g/mol) = ([*M2*]/[BnOH]) × MW(*M2*) × (% conv.) + ([*M45*]/[BnOH]) × MW(glycolyl unit) + MW(end group). [c] Đ and M_n (g/mol) determined by gel permeation chromatography.*

1,5,7-Triazabicyclo[4.4.0]dec-5-ene (TBD), a highly active organocatalyst for the ROP of **M2**, surprisingly, showed no activity in the copolymerisation (Entry 4, Table 2.3). The other organocatalyst tested, 1,8-diazabicyclo(5.4.0)undec-7-ene (DBU), was active toward the copolymerisation. After one hour the polymerisation of **M2** had nearly reached completion, however the conversion of **M45** was far lower at 10% (Entry 2, Table 2.3). After a further 23 hours **M2** had reached greater than 99% conversion and **M45** had reached 71% (Entry 3, Table 2.3). Despite controlling the initial polymerisation of **M2** well and giving a narrow dispersity ($Đ$ = 1.11), after 24 hours the dispersity broadens ($Đ$ = 1.57). DBU showed greater activity toward the polymerisation **M2** over **M45** and likely installs a strong gradient architecture in the polymer but this was not studied further and broadening of the dispersity suggests transesterification has likely interrupted the architectural control. The coordination-insertion catalysts **C13** and **C20** reached the highest conversions of monomers **M2** and **M45** in 7 hours (Entries 1 and 5, Table 2.3). The control over the dispersity was poor, however **C13** produced **P3** with an observed MW (M_n) more in line with the expected MW ($M_{n,th}$) than **C20**.

To confirm the formation of a copolymer and to test for the presence of any homopolymer a diffusion-ordered spectroscopy (DOSY) (^1H) NMR experiment was conducted on the copolymer following purification by precipitation. The presence of only a single diffusion coefficient confirms that a copolymer is the sole polymer product (Figure 2.4).

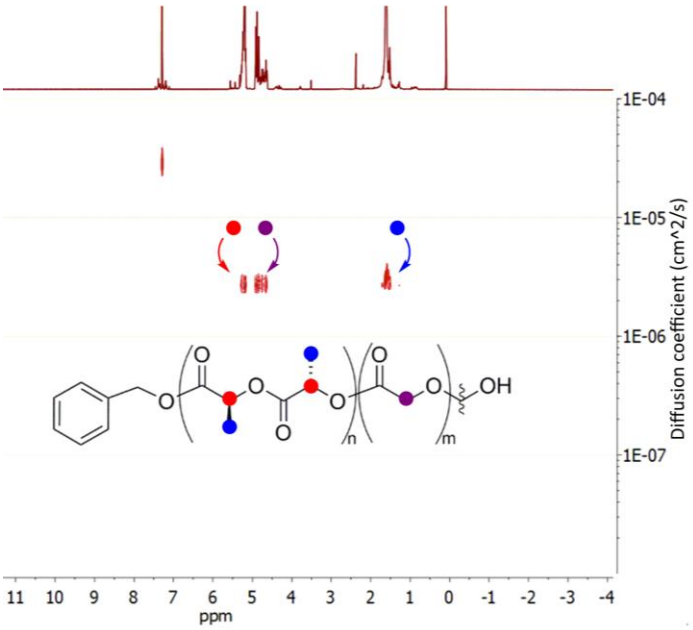

*Figure 2.4. DOSY NMR spectrum of **P3** copolymer from **M2** and **M45***

The copolymerisation was optimised with a monomer feedstock ratio of 90:10 (**M2**:**M45**) using **C13**. Temperature, solvent and time were all varied, with the goal of achieving control over dispersity with high conversion. The polymerisations conducted at higher temperatures were the least well-controlled, noted by their high dispersities (Entries 1, 2 and 3, Table 2.4). A high conversion (98%) and low the dispersity ($Đ$ = 1.08) was achieved at 40 °C in toluene. Although, the observed MW (M_n) did not align well with the expected value ($M_{n,th}$), it is thought that the lower reaction temperature promotes a side reaction. The difference between the polarity of DCM and toluene did not have a significant effect on the dispersity ($Đ$ = 1.10 versus 1.08) (Entries 4 and 5, Table 2.4), though using DCM resulted in a decreased observed MW. Dispersity was significantly higher, indicating loss of control when using THF as the polymerisation solvent, which is possibly due to THF having the ability to coordinate to the polymerisation mediator. Thus, **C13** was used in toluene at 40 °C to copolymerise **M2** and **M45**.

*Table 2.4. Optimisation of **M2** and **M45** copolymerisation catalysed by **C13***

Entry	Solvent	Temp. (°C)	Time (h)	**M2** conv. (%)[a]	**M45** conv. (%)[a]	$M_{n,th}$[b]	M_n [c]	$Đ$[c]
1	Toluene	110	3	99	100	14500	11900	1.46
2	Toluene	70	7	95	95	11020	12000	1.82
3	THF	70	7	98	100	11456	12700	1.23
4	DCM	40	7	96	100	11312	3700	1.10
5	Toluene	40	7	98	100	13980	7300	1.08
6	THF	40	7	100	100	13930	1600	3.20

__M2__:__M45__:__C13__:BnOH = 90:10:1:1. Monomer concentration = 1 M in toluene. Conv. = Monomer conversion. [a] Monomer conversion determined from crude ^{1}H NMR spectrum. [b] $M_{n,th}$ (g/mol) = ([__M2__]/[BnOH]) × MW(__M2__) × (% conv.) ([__M45__]/[BnOH]) × MW(GA) × (% conv.) + MW(end group). [c] Đ and M_n (g/mol) determined by gel permeation chromatography.

Various monomer feedstocks were used to test the capabilities of the system to control the chemical composition of the polymer. The ratio of lactic acid (LA) to glycolic acid (GA) in **P3** was varied, with monomer feedstocks varying from 90:10 to 50:50 (Table 2.5). It was noted that small amounts of insoluble polymer were produced at **M2**:**M45** < 50:50. As the number of equivalents of **M2** was increased dispersity was reduced. This is thought to be due to the more sterically encumbering methyl group inhibiting transesterification.

*Table 2.5. **M2** and **M45** copolymerisation with various monomer ratios*

M2:**M45**	**M2** conv.[a] (%)	**M45** conv.[a] (%)	$M_{n,th}$[b]	M_n[c]	$Đ$[c]
60:40	98	96	10800	14100	1.60
70:30	67	100	8600	6100	1.38
80:20	82	100	10700	8300	1.15
90:10	98	100	11700	7300	1.08

(__M2__+__M45__):__C13__:BnOH = 100:1:1. Monomer concentration = 1 M in toluene. The reaction was conducted at 40 °C for 7 h. Conv. = Monomer conversion. [a] Monomer conversion determined from crude ^{1}H NMR spectrum. [b] $M_{n,th}$ (g/mol) = ([__M2__]/[BnOH]) × MW(__M2__) × (% conv.) + ([__M45__]/[BnOH]) × MW(glycolyl unit) × (% conv.) + MW(end group). [c] Đ and M_n (g/mol) determined by gel permeation chromatography.

In comparison to the copolymerisation of monomers **M1** and **M2**, the reaction times necessary to achieve higher conversion of **M2** and **M45** are prolonged.[9] However, using the standard method, the ratio of LA:GA in the resulting polymer has been difficult to control and significant fractions of the polymer are often insoluble due to having elongated GA sections. These problems were concluded to occur due the reactivity of **M1** being ten times greater than **M2** when an aluminium monoalkoxide catalyst/initiator system is used.[10] Using monomers

M2 and **M45** negates the reactivity issue seen in the ROP of monomers **M1** and **M2**, with no need for extra equipment such as a syringe pump.

The system was capable of achieving higher M_ns (> 37000 g/mol) by increasing the monomer to initiator ratio from 100:1 to 1000:1

(

Table 2.6). Despite prolonged reaction times and the presence of GA linkages, the dipersities remained lower than those observed in Table 2.3 and Table 2.5. New peaks were present in the crude ^{1}H NMR spectra taken from reactions which had large initial monomer feedstocks.

*Table 2.6. **M2** and **M45** copolymerisations with increased monomer feedstock*

M2:**M45**	Temp. (°C)	Time (h)	**M2** conv. [a] (%)	**M45** conv.[a] (%)	M_n[b]	$Đ$[b]
1000:0	70	23	64	/	50600	1.11
700:300	40	32	64	83	43600	1.67
500:500	40	48	60	86	36800	1.45

***(M2*+*M45)*:*C13*:*BnOH = 1000:1:1. Monomer concentration = 2 M in toluene. The reaction was conducted at 70 °C. Conv. = Monomer conversion. [a] Monomer conversion determined from crude ^{1}H NMR spectrum. [b] Đ and M_n (g/mol) determined by gel permeation chromatography.*

The reaction was conducted in a Young's tap NMR tube and ^{1}H NMR spectra were conducted at various time points to monitor the development of the new peaks during the reaction. Two unknown peaks were observed to increase in relative integration values at the same relative rate and were assigned to the methyl substituted monomer 5-methyl-1,3-dioxolan-4-one (**M46**). Shown in Figure 2.15, **M2** is nearly completely consumed in the first 2 hours of the polymerisation and the subsequent formation of **P1** is observed. As the reaction proceeds the concentration of **P1** decreases despite **M2** also slowly decreasing. **M45** is steadily consumed throughout the reaction producing **P1**. The formation of the by-product, formaldehyde, is observed through the sublimation of paraformaldehyde.

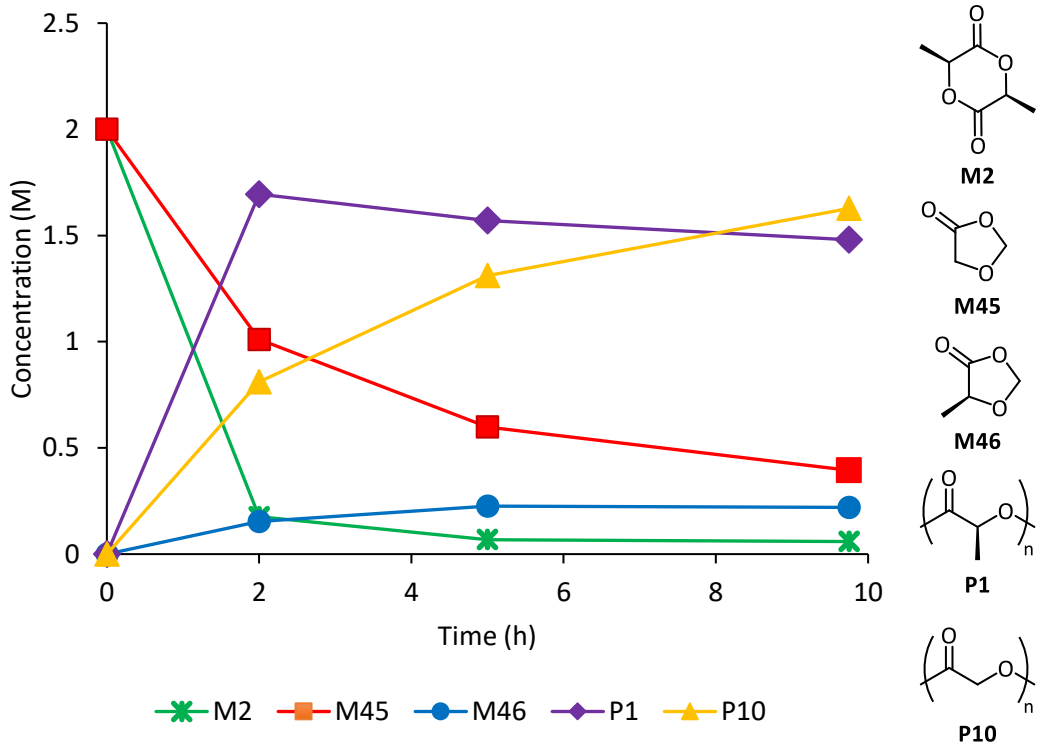

*Figure 2.5. Monitoring **M2** and **M45** copolymerisation by ^{1}H NMR spectroscopy. M:**C13**:BnOH = 500:1:1. **M2**:**M45** = 1:1. Copolymerisation was conducted at 70 °C in C_6D_6 at a concentration of 2 M.*

However, it is plausible that the formation of formaldehyde is not irreversible. A new polymer-monomer equilibrium could be introduced when **P1** is produced in the presence of paraformaldehyde, as a reaction between formaldehyde and **P1** may lead to the formation of **M46**. On the other hand, the new equilibrium could be present without re-dissolving paraformaldehyde and **M46** formed directly from the reaction of ring-opened **M45** and **P1**.

2.3 Copolymerisations of **M45** and **M47**

Polymer **P3** is a popular choice for synthesising nanoparticle drug carriers, but has proven to lack the appropriate mechanical properties for other applications. Thus, **M1** has been copolymerised with other monomers to install complimentary mechanical properties available for biodegradable polymers. One such monomer has been ε-caprolactone (**M47**). Monomer **M47** has been copolymerised with **M1** in the presence of **C1** to form poly(glycolic acid-*co*-caprolactone) (**P11**). Mechanical testing showed drastic differences between polymers **P3** and **P11**. Kim *et al.* found that copolymer **P11** is an elastomer with extensions of up 250% without

cracking and 96% recovery after 230% extension. They found that this contrasted heavily with **P3**'s 10-15% and failure (cracking) after an applied strain of 20%.[11] The polymer **P11** fabricated into sutures for biomedical applications was proven to be the suture that possesses the highest straight tensile strength and best handling properties of all the available monofilament absorbable sutures.[12] In previous publications, the synthesis of **P11** has been energy intensive and reaction times of 17 hours were required. It was hypothesised that the newly developed polymerisation system, the polymerisation of 1,3-dioxolan-4-one monomers to form PAHAs, could be used to synthesise the applicable, biodegradable polymer **P11** (Scheme 2.5). The polymerisation system was tested at lower temperatures in order to increase the control over the polymerisation. The ability to vary the composition of the **P11** was tested in a similar manner to the synthesis of **P3**. The copolymerisations of monomers **M47** and **M45** were conducted with the assistance of Ms Amelie Schultheiss.

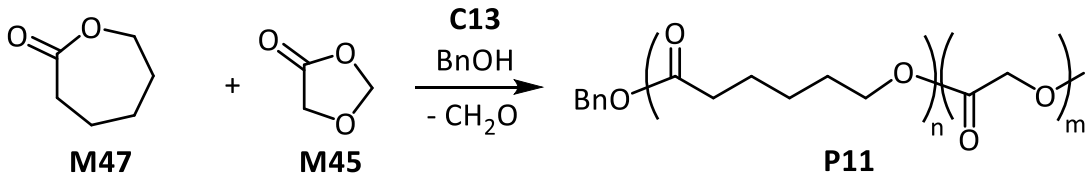

*Scheme 2.5. The copolymerisation of monomers **M47** and **M45**, using catalyst **C13** and BnOH as initiator.*

As expected, the reaction required a lower energy input, as the copolymerisation was active when conducted at room temperature (Table 2.7). The relative integration values of glycolyl and caproyl units obtained from ^{1}H NMR spectra of the purified polymers showed good agreement with the initial monomer feedstocks. All polymers were produced with a moderate control over dispersities, with $Đ$ varying from 1.25-1.78. Unlike copolymerisations of monomers **M2** and **M45**, no overall trend was observed between monomer ratio and dispersity. It was observed that as the fraction of **M45** was increased the observed MW decreased in relation to the expected MW. This can be explained by the two contrasting refractive index increment values of **P2** and **P10**. In Table 2.7, GPC calculations were performed using a calculation method that assumes the chemical composition is constant at all elution times. The refractive index increment (dn/dc) value of **P2** (0.05 mL/g) was used in these calculations, hence the observed trend.

*Table 2.7. **M47** and **M45** copolymerisations with various monomer ratios.*

M47:**M45**	**M47** conv.[a] (%)	**M45** conv.[a] (%)	$M_{n,th}$[b]	M_n[c]	$M_{n,NMR}$[d]	$Đ$[c]
90:10[e]	90	100	9900	7000	/	1.36
80:20	100	100	11100	6800	9800	1.47
70:30	73	100	8400	5400	5400	1.25
60:40	79	97	9000	2900	7100	1.29
50:50	78	97	8900	2700	5700	1.27
40:60	46	88	5300	1700	2400	1.45
40:60[f]	83	94	9300	2800	5700	1.45
30:70[f]	58	92	6800	1300	5400	1.78

***(M47**+**M45)**:**C13**:BnOH = 100:1:1. Monomer concentration = 1 M in toluene. The reaction was conducted at 25 °C over 7 h. Conv. = Monomer conversion. [a] Monomer conversion determined from crude ^{1}H NMR spectrum. [b] $M_{n,th}$ (g/mol) = ([**M47**]/[BnOH]) × MW(**M47**) × (% conv.) + ([**M45**]/[BnOH]) × MW(GA) × (% conv.) + MW(end group). [c] Đ and M_n (g/mol) determined by gel permeation chromatography. [d] Calculated from ^{1}H NMR spectrum integrations. [e] Time = 3 h. [f] Time = 17 h.*

The trend is not observed when the MW ($M_{n,NMR}$) is calculated using the relative integration values of the methylene peak of benzyl ester and a methylene peak of caprolactyl from ^{1}H NMR spectra. However, the $M_{n,NMR}$ are consistently lower than the expected value. The weight fraction of GA in **P11** can be increased further than was possible in **P3**. Increased reaction times were required for **M47**:**M45** < 1:1. The ability to vary the **P2**:**P10** ratios in **P11** has proven extremely beneficial for the polymers application. One such application for these elastic copolymers has been in a wound bed, where the ratio has been shown to provide differences in adsorption and degradation profiles, illustrating the importance of the ability to control the chemical composition of the copolymer.[13] A single diffusion coefficient was again observed in the DOSY (^{1}H) NMR spectrum of the copolymer **P11** indicating no homopolymer contaminants (Figure 2.6).

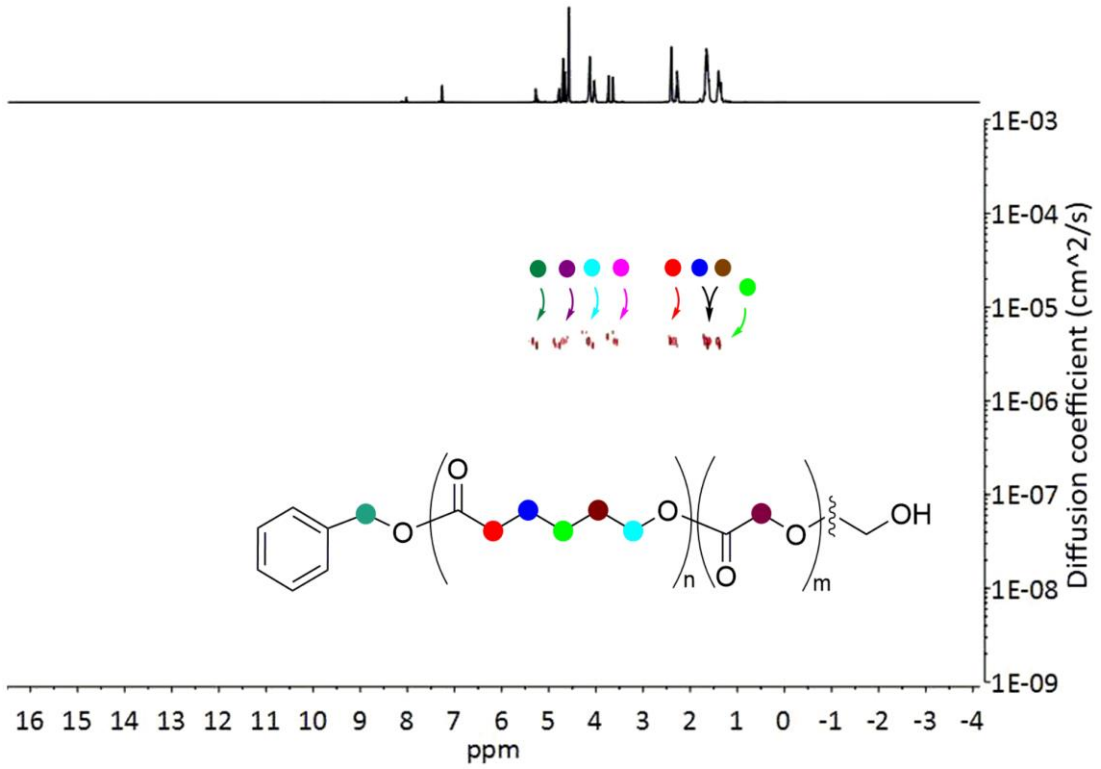

*Figure 2.6 . DOSY NMR spectrum of **P11** copolymer from **M47** and **M45.***

Unlike the copolymer **P3**, the copolymer **P11** composition and chain microstructure can be determined from the ^{1}H NMR spectra, as derived by Kasperczyk *et al.*[14] and simplified by Dobrzynski *et al.*[15] As observed from Figure 2.6 several of the caprolactone repeat unit protons resonate at two chemical shifts in the ^{1}H NMR spectrum of copolymer **P11**. The two chemical shifts corresponding to the same proton are known as diads and are a result of the caprolyl protons' chemical shift being influenced by the neighbouring monomeric unit. Each can be identified as a caprolyl unit next to glycolyl unit GC or a caprolyl unit next to a caprolyl unit CC. The diads that appears at 4.20 ppm (GC) and 4.10 ppm (CC) are well defined, this allows for integration and thus the calculation of the concentration of each diad [GC] and [CC], various concentrations of the diads are presented in Figure 2.7. Firstly, the molar ratio k is defined in Eq. 1, where [C] and [G] represent the concentration of each monomeric unit present in the copolymer **P11**. The experimental number average length of the caprolyl blocks L_C and glycolyl blocks L_G are calculated from equations Eq.2. and Eq.3. This differs from the L_C presented by Dobrzynski *et al.* and aligns with the equations for AB copolymers as presented by Herbert as **M1** incorporates two glycolyl units for every one ring-opened monomer.[16]

$$k = {}^{[C]}\!/_{[G]} \qquad \text{Eq.1}$$

$$L_C = {(2[CC] + [GC])}/{[GC]} \quad \text{Eq.2}$$

$$L_G = {L_C}/{k} \quad \text{Eq.3}$$

Based on a Bernoullian statistics model, the theoretical random lengths of caprolyl blocks (L_C^R) and glycolyl blocks (L_G^R) are calculated from equations Eq.4 and Eq.5. as also presented by Dobrzynski *et al.* and Herbert.[15,16] The degree of randomness (R) of the copolymer can be calculated using equation 6 (Eq.6) from both the experimental average length and the theoretical random average length. As the coefficient R approaches one the composition of the copolymer becomes closer to being completely random. Below one, the experimental average length is greater than the theoretical random chain length and as it decreases the copolymer becomes more block like. An R value of zero is calculated if the copolymer is diblock. Values of R greater than one indicate a preference for an alternating sequence.

$$L_C^R = k + 1 \quad \text{Eq.4}$$

$$L_G^R = {(k+1)}/{k} \quad \text{Eq.5}$$

$$R = {L_C^R}/{L_C} = {L_G^R}/{L_G} \quad \text{Eq.6}$$

*Table 2.8. Summary of chemical composition of **P11** copolymers*

Entry	[GC]	[CC]	k	L_C	L_G	L_C^R	L_G^R	R
1	9.58	90.42	9.00	19.88	2.21	10.00	1.11	0.50
2	25.79	74.21	4.88	6.75	1.38	5.88	1.20	0.87
3	61.38	38.62	1.78	2.26	1.27	2.78	1.56	1.23
4	79.08	20.92	1.63	1.53	0.94	2.63	1.61	1.72
5	85.09	14.91	1.38	1.35	0.98	2.38	1.72	1.76
6	86.92	13.08	0.69	1.30	1.87	1.69	2.44	1.30

As expected, the length of caprolyl chains decrease with a decrease in **M47** feedstock. At lower feedstock ratios of **M45** (Entries 1 and 2, Table 2.8) the R values of the copolymer are below one. At moderate and high ratios of **M45**:**M47** the degree of randomness is increased, illustrating the polymerisation is not truly random and has a preference toward alternating caprolactyl and glycolyl units. The trend suggests that once **M47** opens it has a preference to react with another equivalent of **M47**.

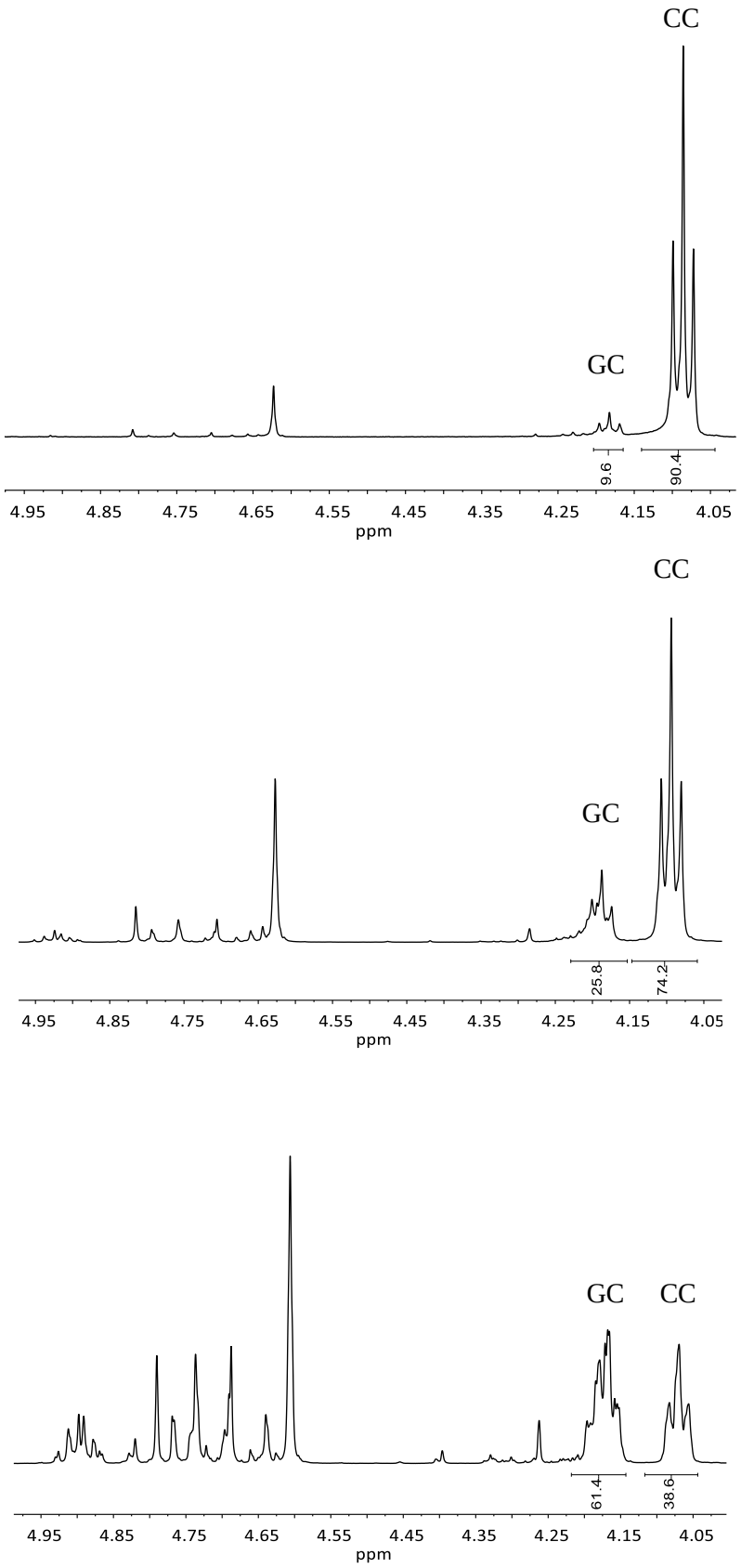

*Figure 2.7. ^{1}H NMR spectra showing the methine regions of **P11** with various **P2** and **P10** ratios, illustrating the concentrations of GC and CC diads*

The opposite is true for **M45**, as once opened it also has a preference to react with an equivalent of **M47**. The final entry in the table shows reduced selectivity (R = 1.30), however this observation may be a result of the increased reaction time required for a molar ratio of **M45**:**M47** greater than one. If the dispersity is an indicator for the level of transesterification and it occurs randomly between monomeric units, the increased level of this side reaction will lead toward randomness and thus R being closer to one.

The monomer feedstock was increased from 100 to 1000 and the system was shown to have the ability to reach higher MWs. When the initial ratio **M47**:**M45** was 1:1 the only product observed was an insoluble white solid. Analysis of the soluble portion of the reaction mixture by ^{1}H NMR spectroscopy revealed a decrease in **M45** concentration in the reaction mixture. This coupled with the presence of the insoluble solid suggests **M45** has formed **P11** containing chains of glycolic acid of insoluble lengths.

*Table 2.9. Copolymerisation of monomers **M47** and **M45** with increased monomer feedstock*

M47:**M45**	**M47** conv. (%)[a]	**M45** conv. (%)[a]	$M_{n,th}$[b]	M_n[c]	$M_{n,NMR}$[d]	$Đ$[c]
900:100	78	100	87700	34900	40200	1.48
800:200	91	100	101000	14600	40400	1.38

***(M47**+**M45)**:**C13**:BnOH = 1000:1:1. Monomer concentration = 2 M in toluene. The reaction was conducted at 25 °C over 48 h. Conv. = Monomer conversion. [a] Monomer conversion determined from crude ^{1}H NMR spectrum. [b] $M_{n,th}$ (g/mol) = ([**M47**]/[BnOH]) × MW(**M47**) × (% conv.) + ([**M45**]/[BnOH]) × MW(GA) × (% conv.) + MW(end group). [c] Đ and M_n (g/mol) determined by gel permeation chromatography. [d] Calculated from integrals values of caprolactyl and glycolyl units relative to the methylene peak of benzyl ester following ^{1}H NMR spectroscopy*

2.4 Copolymerisations of **M45** and **M4**

The monomer β-butyrolactone (**M4**) is used to form a biodegradable polymer, poly(3-hydroxybutyrate) (**P12**). Polymer **P12**, along with other poly(3-hydroxyalkanoates), are naturally occurring polymers in a wide variety of microorganisms and the cyclic ester monomer may be also produced by this route.[17] **M4** offers greater control over the polymerisation, whether it is the MW or stereoregularity which has a significant impact upon physical properties such as crystallinity and melt temperature.[18] Akin to the polymerisation of **M2**, a large portion of research surrounding **M4** has been the use of discrete metal alkoxide complexes capable of stereoselective polymerisation of racemic **M4**.[8,19–21] It was found that the stereochemistry also had an impact upon polymer **P12**s thermal stability and susceptibility to enzymatic degradation.[18,22] However, it did not have an impact on its hydrolytic degradation. The rate of hydrolytic degradation of **P12** is lower than that of **P1** *in vitro* (immersed in an

agitated phosphate buffer solution) at 37 °C as well as at an elevated temperature (70 °C).[23] Despite its low rate of hydrolytic degradation the potential of **P12** as a degradable plastic is great due to the final degradation product, 3-hydroxy butyric acid, being a nontoxic, naturally occurring chemical. Using our new synthetic route, we believed that it would be possible to synthesise the novel copolymer from monomers **M4** and **M45** with the aim of incorporating glycolic acid units throughout the **P10** polymer to produce poly(3-hydroxybutyrate-co-glycolic acid) (**P12**) (Scheme 2.6). Polymerisations were conducted at room temperature in three solvents: toluene, THF, and DCM (Table 2.10). The copolymerisations of monomers **M4** and **M45** were conducted with the assistance of Ms Amelie Schultheiss.

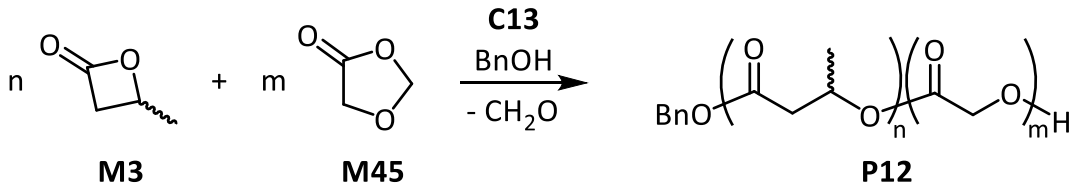

*Scheme 2.6. The copolymerisation of monomers **M4** and **M45**, using catalyst **C13** and BnOH the catalyst initiation system.*

*Table 2.10 . Optimisaton of **M45** and **M3** copolymerisation catalysed by **C13***

Solvent	Temp. (°C)	Time (h)	**M3** conv. (%)[a]	**M45** conv. (%)[a]	$M_{n,th}$[b]	M_n[c]	$Đ$[c]
Toluene	25	48	22	100	2690	1300	1.44
THF	25	48	15	100	2150	2500	2.13
DCM	25	48	18	100	2380	700	1.32
Toluene	40	24	28	100	3160	1700	1.20
Toluene	40	96	70	100	6106	5100	1.383
THF	40	24	31	100	3390	700	1.92
DCM	40	24	20	100	2540	ND[d]	ND[d]
Toluene	70	17	52	100	5010	6000	1.18
THF	70	17	50	100	4860	6900	1.13
Toluene	85	5	30	100	3310	2900	1.46
Toluene	85	24	55	100	4950	4500	1.50
Toluene	110	7	29	100	3230	2300	1.89

***M3*:*M45*:*C13*:BnOH = 90:10:1:1. Monomer concentration = 1 M in toluene. Conv. = Monomer conversion. [a] Monomer conversion determined from crude ^{1}H NMR spectrum. [b] $M_{n,th}$ (g/mol) = ([*M3*]/[BnOH]) × MW(*M3*) × (% conv.) + ([*M45*]/[BnOH]) × MW(GA) × (% conv.) + MW(end group). [c] $Đ$ and M_n (g/mol) determined by gel permeation chromatography. [d] ND = not determined due to no observed precipitation.**

The polymerisations conducted at 25 °C proceeded slowly. After two days conversions were less than 22%, regardless of the solvent used. Increasing the temperature to 40 °C led to greater activity. Upon conducting the reaction in DCM under reflux and addition of the reaction mixture to cold methanol no precipitation was observed, likely due to the formation of low MW products. At 25 and 40 °C, the reaction in THF promotes transesterification evident by the broadened dispersities. Conducting the polymerisation in toluene produces accurate MW **P12** with a narrower dispersity than polymerisations conducted in either THF or DCM. Increasing the temperature of the reaction in toluene leads to increased activity without loss of control. Interestingly, the same temperature increase has a more dramatic effect on the polymerisation in THF, as M_n approached the expected MW and a decrease in dispersity was observed. Increasing the reaction temperature further to 85 and 110 °C in toluene led to a broadening of dispersities without a significant increase in activity. It was concluded that 70 °C in either toluene or THF were the optimal reaction conditions for the copolymerisation of **M45** and **M3**. The monomer ratio **M45**:**M3** was increased from 1:9 until an insoluble polymer was produced in both toluene and THF.

*Table 2.11. **M3** and **M45** copolymerisations with various monomer ratios*

Solvent	**M3**:**M45**	**M3** conv.[a] (%)	**M45** conv.[a] (%)	$M_{n,th}$[b]	M_n[c]	$M_{n,NMR}$[d]	$Đ$[c]
Toluene	80:20	92	99	7600	4600	7008	1.25
Toluene	70:30	90	98	7200	3400	6698	1.19
Toluene	60:40	86	93	6700	1500	5835	1.60
Toluene[e]	50:50	100	97	7200	ND	ND	ND
THF	80:20	100	100	8100	4600	5300	1.20
THF	70:30	100	100	7900	3900	5300	1.18
THF	60:40	100	88	7300	3000	5400	1.15
THF[e]	50:50	100	70	6700	ND	ND	ND

***(M3+M45)*:*C13*:BnOH = 100:1:1. Monomer concentration = 1 M in toluene. Conducted over 24 h at 70 °C. Conv. = Monomer conversion. [a] Monomer conversion determined from crude ^{1}H NMR spectrum. [b] $M_{n,th}$ (g/mol) = ([*M3*]/[BnOH]) × MW(*M3*) × (% conv.) + ([*M45*]/[BnOH]) × MW(GA) × (% conv.) + MW(end group). [c] $Đ$ and M_n (g/mol) determined by gel permeation chromatography. [d] Calculated from integrals values of the monomeric units relative to the methylene peak of benzyl ester following ^{1}H NMR spectroscopy. [e] ND = not determined due to resultant polymer being partially insoluble.**

High conversions were attained by all polymerisations, other than **M3**:**M45** 50:50 in THF where only 70% conversion of **M45** was recorded. Overall, polymerisations conducted in THF produced polymers with narrower dispersities for all four feedstock ratios (90:10 – 60:40) that

were analysed. Following analysis of the MWs by NMR spectroscopy, the observed MWs compared well with the expected values, agreeing well with the preliminary polymerisations at 90:10. The $M_{n,NMR}$ of polymers produced in toluene aligned closer to their $M_{n,th}$, than in THF. The absence of any major differentiation between polymer structures produced in THF or toluene suggests the polymerisation of monomers **M3** and **M45** is robust.

2.5 Conclusions

The monomer **M45** and other substituted 1,3-dioxolan-4-ones were hypothesised to undergo ROP with the elimination of the -OCH_2- portion of the monomer. However, **M45** was previously shown by Miller *et al.* to ring-open in a copolymerisation with **M2**. The resultant polymer was presented as a polyesteracetal. Using the same polymerisation protocols, the previously identified polyesteracetal was not present by ^{1}H or ^{13}C NMR spectroscopy. As we had previously hypothesised, the ROP of **M45** and **M2** produced **P3**. Several catalysts were screened for the copolymerisation and catalysts known to follow a coordination-insertion type mechanism were found to be the most active. The optimal conditions for the copolymerisation were found using the catalyst **C13**. Polymer **P3** was synthesised with various chemical compositions by varying the monomer feedstock. The copolymerisation of monomers **M2** and **M45** also maintained good conversions at monomer feedstocks as high as 1000:1. In the literature, polymer **P11** was identified as a biodegradable polyester with increased elastomeric properties to **P3**. In comparison to literature procedures, **P11** was synthesised at reduced temperatures and times by copolymerising **M45** and **M47**. The ratio of glycolic acid and caprolactone units were varied in a greater range than possible for **P3**. The ^{1}H NMR spectra of **P11** copolymers were used to calculate the degree of randomness in the polymer and gain an insight to its microstructure. Finally, in a similar fashion to polymers **P3** and **P11**, **P12** was synthesised from monomers **M45** and **M4** with good control over the dispersity and chemical composition. Though **M45** was used to synthesise a range of copolymers, the capability of 1,3-dioxolan-4-one monomers to form homopolymer was inconclusive from **M45**. In order to synthesise homopolymer from 1,3-dioxolan-4-ones further substitution on the ring was necessary. The polymerisation of diversely substituted 1,3-dioxolan-4-one monomers is presented in Chapters 3 and 4.

2.6 References

(1) Hermes, M. E. Polymers of 1,3 dioxolan-4-ones. US5424136 A, 1995.

(2) Miller, S. A.; Martin, R. T. Polyesteracetals. US8653226, 2014.

(3) Martin, R. T.; Camargo, L. P.; Miller, S. A. *Green Chem.* **2014**, *16* (4), 1768–1773.

(4) Reed, A. M.; Gilding, D. K. *Polymer (Guildf).* **1981**, *22* (4), 494–498.

(5) Salomaa, P.; Laiho, S.; Cyvin, S. J.; Kvande, P. C.; Meisingseth, E. *Acta Chem. Scand.* **1963**, *17*, 103–110.

(6) Lohmeijer, B. G. G.; Pratt, R. C.; Leibfarth, F.; Logan, J. W.; Long, D. A.; Dove, A. P.; Nederberg, F.; Choi, J.; Wade, C.; Waymouth, R. M.; Hedrick, J. L. *Macromolecules* **2006**, *39* (25), 8574–8583.

(7) Dubois, P.; Jacobs, C.; Jérôme, R.; Teyssté, P. *Macromolecules* **1991**, *24* (9), 2266–2270.

(8) Rieth, L. R.; Moore, D. R.; Lobkovsky, E. B.; Coates, G. W. *J. Am. Chem. Soc.* **2002**, *124* (51), 15239–15248.

(9) Dechy-Cabaret, O.; Martin-Vaca, B.; Bourissou, D. *Chem. Rev.* **2004**, *104* (12), 6147–6176.

(10) Gilding, D. K.; Reed, A. M. *Polymer (Guildf).* **1979**, *20* (12), 1459–1464.

(11) Lee, S. H.; Kim, B. S.; Kim, S. H.; Choi, S. W.; Jeong, S. I.; Kwon, I. K.; Kang, S. W.; Nikolovski, J.; Mooney, D. J.; Han, Y. K.; Kim, Y. H. *J. Biomed. Mater. Res. - Part A* **2003**, *66* (1), 29–37.

(12) Bezwada, R. S.; Jamiolkowski, D. D.; Lee, I. Y.; Agarwal, V.; Persivale, J.; Trenka-Benthin, S.; Erneta, M.; Suryadevara, J.; Yang, A.; Liu, S. *Biomaterials* **1995**, *16* (15), 1141–1148.

(13) Cooper, K.; Nathan, A.; Vyakarnam, M. In *Biodegradable Polymers in Clinical Use and Clinical Development*; John Wiley & Sons, Inc.: Hoboken, NJ, USA, 2011; pp 401–415.

(14) Kasperczyk, J. *Macromol. Chem. Phys.* **1999**, *200* (4), 903–910.

(15) Dobrzynski, P.; Li, S.; Kasperczyk, J.; Bero, M.; Gasc, F.; Vert, M. *Biomacromolecules* **2005**, *6* (1), 483–488.

(16) Herbert, I. R. In *NMR Spectroscopy of Polymers*; Springer Netherlands: Dordrecht,

1993; pp 50–79.

(17) Steinbüchel, A.; Schlegel, H. G. *Mol. Microbiol.* **1991**, *5* (3), 535–542.

(18) Abe, H.; Matsubara, I.; Doi, Y.; Hori, Y.; Yamaguchi, A. *Macromolecules* **1994**, *27* (21), 6018–6025.

(19) Xu, C.; Yu, I.; Mehrkhodavandi, P. *Chem. Commun.* **2012**, *48* (54), 6806.

(20) Rieth, L. R.; Moore, D. R.; Lobkovsky, E. B.; Coates, G. W. *J. Am. Chem. Soc.* **2002**, *124* (51), 15239–15248.

(21) Liu, Y. C.; Lin, C. H.; Ko, B. T.; Ho, R. M. *J. Polym. Sci. Part A Polym. Chem.* **2010**, *48* (23), 5339–5347.

(22) Kurcok, P.; Kowalczuk, M.; Adamus, G.; Jedliński, Z.; Lenz, R. W. *J. Macromol. Sci. Part A* **1995**, *32* (4), 875–880.

(23) Bonartsev, A. P.; Boskhomodgiev, A. P.; Iordanskii, A. L.; Bonartseva, G. A.; Rebrov, A. V.; Makhina, T. K.; Myshkina, V. L.; Yakovlev, S. A.; Filatova, E. A.; Ivanov, E. A.; Bagrov, D. V.; Zaikov, G. E. *Mol. Cryst. Liq. Cryst.* **2012**, *556* (1), 288–300.

Chapter 3. Poly(lactic acid) and Poly(mandelic acid) from 1,3-Dioxolan-4-ones

3.1 Introduction

Monomer **M45** was used in tandem with common ring-opening polymerisation monomers to successfully synthesise three different copolymers and each copolymer was made with an array of chemical compositions. To overcome the negative factors of other routes, it was of interest to utilise this new pathway to obtain homopolymers solely from 1,3-dioxolan-4-ones. The homopolymerisation of the unsubstituted 1,3-dioxolan-4-one monomer **M45** was attempted, and it produced an intractable white solid. The insoluble white solid was indicative of the formation of poly(glycolic acid), though without full characterisation by NMR spectroscopy or mass-spectrometry it was still unclear of the exact species present. It was necessary to target a more soluble homopolymer that could be fully characterised in order to test the potential of this synthetic protocol to make homopolymers.

3.1.1 Synthesis of Poly(lactic acid)

As discussed in Chapter 1 and Chapter 2, polymer **P1** has become an increasingly important polyester for its uses in food packaging and the biomedical field.[1,2] **P1** is synthesised from **M2**, which is viewed as green alternative for petroleum based monomers due to the renewable nature of its starting material; the renewability is rooted in nature. Plants such as corn, sugar beets or rice are utilised as they produce starch from the photosynthesis of carbon dioxide and water. Following separation, the starch is broken down to dextrose *via* enzymatic hydrolysis.[3]

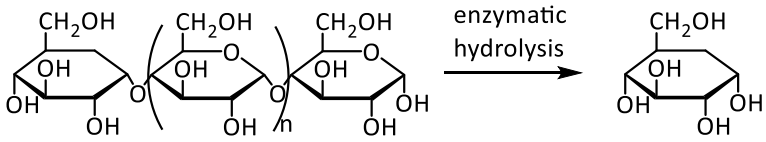

Scheme 3.1. Enzymatic hydrolysis of starch to dextrose.[3]

Companies, such as Cargill Dow, then ferment dextrose into lactic acid. The industrial two-step process widely used to synthesise **M2** is the polymerisation-depolymerisation

strategy. Firstly, lactic acid is polymerised to form low MW **P1** as a prepolymer at low pressure and high temperature (180 °C). The same low pressure and high temperature conditions are required in the second step to ensure a rapid reaction and to distil the **M2** from the reaction mixture once formed. Yields are typically low at *ca.* 50%.[4–7]

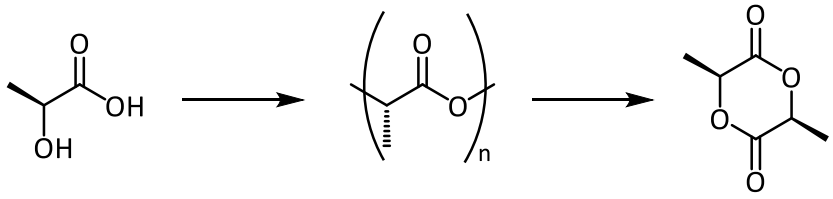

*Scheme 3.2. The two-step process to synthesis **M2**: prepolymerisation of lactic acid to form low molecular weight **P1**, followed by depolymerisation to synthesise **M2**.*[8]

3.1.2 Synthesis of Poly(mandelic acid)

The backbone of **P1** is relatively flexible and leads to a relatively low T_g of 55 °C. In comparison, poly(mandelic acid) (**P5**) has a far bulkier substituent group. The structure of **P5** is analogous to polystyrene (PS) as **P1** is analogous to polypropylene (PP), and the difference in T_gs between **P5** and **P1** conform with the difference observed between PS and PP.

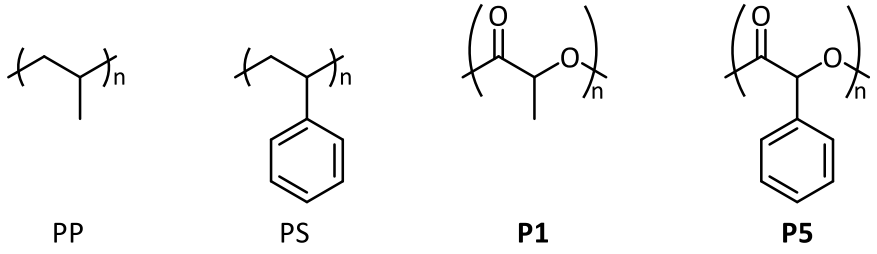

*Figure 3.1. The structural analogy between PP, PS, and **P1** and **P5**.*

P5's bulkier pendant group on the polyester chain is thought to increase the polymer's internal rotational barrier and hence cause the increase in T_g. Mandelic acid undergoes polycondensation in both the melt and in acidified solutions to synthesis **P5**.[9] Conducting the polymerisation of mandelic acid, *via* polycondensation, a higher average length **P5** with a degree of polymerisation (DP) 20 was reached by Whitesell and Pojman.[10] They achieved this by comparing various methods and higher DPs were attained by employing Nafion superacid catalyst beads. Another polycondensation route was explored for **P5**, taking inspiration from the synthesis of **P1** from a haloacetic acid in the presence of a tertiary amine.[11] Though more costly, α-bromophenyl-acetic acid proved a good starting material as the reaction reached 77% yield after two hours at room temperature. However, analysis of the **P5** by GPC did not reveal increased MW. It was suggested that the less harsh reaction conditions also led to retention of

configuration around each monomeric unit, despite no crystallinity being observed by the X-ray powder diffraction. The monomer **M6** was turned to in order to obtain polymer with a higher MW.[12] As discussed in Chapter 1, **M6**'s poor solubility seemed useful as low dispersities (<1.2) were achieved when the polymerisation was conducted in a heterogeneous reaction mixture. However, high MW **P5** was obtained at temperatures >150 °C in the absence of solvent. Despite rigorous attempts to eliminate impurities the highest MW samples (68,000 g/mol, DP > 250) were produced with adventitious initiator, as a monomer:catalyst:initiator (M:C:I) ratio of 500:1:0 was used. The high MW samples resulted in completely amorphous polymer regardless of the initial stereochemistry of monomer. This was thought to be due to the facile racemisation of the methine proton in **M6**. The activated equivalent of **M6**, **M42** was thought to have the potential to eliminate the need for the harsh polymerisation conditions that cause epimerisation. **M42** proved a success for obtaining isotactic **P5**.[13] When pyridine is complexed with an equivalent of mandelic acid, it forms a pyridine mandelic acid adduct capable of acting as an efficient initiator/mediator for the polymerisation of **M42**.

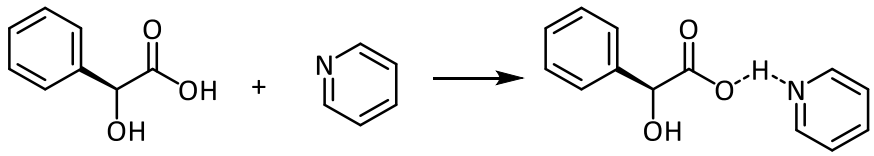

Scheme 3.3. Formation of pyridine malic acid adduct catalyst initiator system.[13]

The complexed pyridine mandelic acid system was utilised to produce **P5** over a range of predictable MWs, as they varied M:C:I from 50:1:1 to 500:1:1. Only at very high loadings of 500:1:1 did the obtained MW deviate from the calculated weight from monomer conversion.[13] The control over $Đ$ was not lost at any point, as all polymers exhibited very low dispersities <1.10, other than when M:C:I = 500:1:1 the dispersity broadened slightly to 1.17. Most importantly the system was capable of producing isotactic **P5**. The stereoretention was illustrated by a large optical rotation and a sharpening of the polymer's methine region in the ^{1}H NMR spectrum. The stereoregularity of the **P5** led to an increase in the polymer's T_g to 105.5 °C. The monomer **M42** has proven very beneficial as the monomer is easier to synthesise, higher yielding, displays an increased polymerisation rate and was capable of producing isotactic **P5**. However, the drawbacks associated with the polymerisation of monomer **M42** are shared with all OCA monomers due to the carbonylating agent used in their syntheses. In Chapter 1, phosgene as well as its derivatives diphosgene and triphosgene's high toxicity and use in chemical warfare was discussed. Coupled with the high cost of carbonylating agent there has yet to be a simple, low risk and economic synthetic route to obtain this synthetically demanding polymer.

3.2 Polymerisation of 5-Methyl-1,3-dioxolan-4-one

Previous studies of monomer **M46** being utilised as a monomer have not been published in scientific documents other than the patents discussed in Chapter 2. It has been studied as a diastereoselective lactaldehyde enolate surrogate, a substrate for chlorine initiated oxidation, and studying the ^{13}C NMR spectra of various alkyl substituted 1,3-dioxolan-4-ones. Hence, it was selected as the first monomer to attain soluble homopolymer **P1**.

3.2.1 Initial Formation of Poly(lactic acid) from 5-Methyl-1,3-dioxolan-4-one

Previously reaction optimisation in the Shaver group revealed 85 °C to be the optimal temperature for polymerising **M2** to form **P1**.[14] This was found to be the ideal temperature, as high rates of polymerisation are achieved without broadening of the *Đ*s. It was hypothesised that transesterification was minimised at this temperature, while still having increased rates of polymerisation, hence it was chosen as the temperature for the initial test to form **P1** from **M46**. Like **M2** and **M45**, **M46** was polymerised at 1 M in toluene with **C13** and an equivalent of alcohol as the initiation and mediation system.

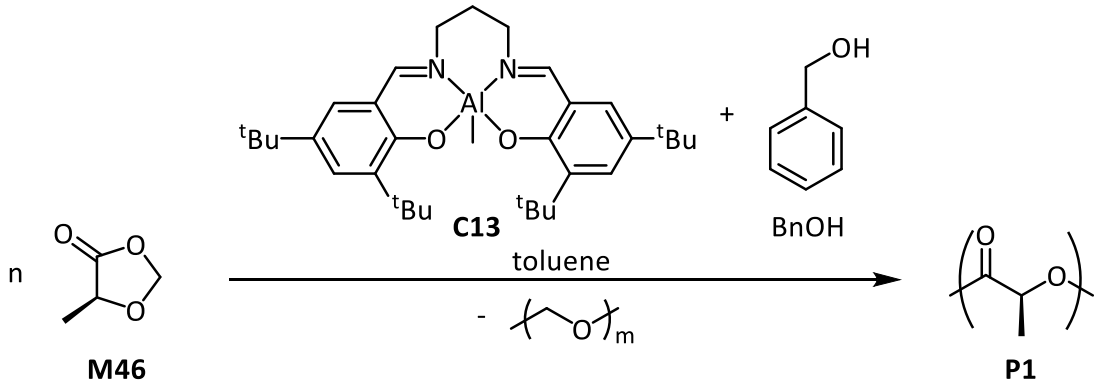

*Scheme 3.4. The polymerisation of **M46** utilising **C13** and BnOH as the initiation and mediation system to form **P1** and release formaldehyde, observed as paraformaldehyde.*

Expulsion of formaldehyde was observed directly by the sublimation of paraformaldehyde on the walls of the reaction vessel. After 24 hours, a significant quantity had sublimed. An aliquot was removed from the ampoule and analysed by ^{1}H NMR spectroscopy and the conversion was determined to be 59%. The conversion was calculated from relative integrations of the methine peak attributed to the polymer **P1** at 5.30-5.10 ppm and the methine peak attributed to **M46** a quartet at 4.30 ppm. Two further reactions were conducted for 48 and 72 hours and gave conversions of 78% and 86% respectively. The reactions were quenched with excess alcohol and the quenched reaction mixture was added dropwise to methanol.

Precipitation of a white solid was observed from the polymerisation mixture that was reacted for 72 hours. Analyse of the resulting white solid by ^{1}H NMR spectroscopy showed the desired polymer **P1** peaks, however, unidentifiable peaks with significant integrations relative to the polymer **P1** were also present. The small amount of white solid isolated was analysed by GPC and was found to be oligomers of DP less than 5 (290 g/mol).

3.2.2 Initial Optimisation with Common Ring-Opening Polymerisation Catalysts

The poor purity of the product and low MW called for screening of more common ROP catalysts and variations in reaction conditions. Utilising catalyst **C13** and decreasing the reaction temperatures led to a need for elongated reaction times and an increase in the number of impurities present in resulting ^{1}H NMR spectra. This was found to be independent of solvent. Solvents tested included toluene, THF and DCM. Pleasingly, an increase in reaction temperature to 110 °C resulted in an increased conversion of **M46**, of 81% after 24h (Table 3.12, Entry 1). The crude ^{1}H NMR spectrum did not display the impurities present in polymerisations conducted at lower temperatures. The product was polymeric and displayed a far higher MW than previously reached, with a narrow dispersity ($Đ$ = 1.16).

*Table 3.12. Initial optimisation of **M46** polymerisation utilising **C13**, **C1**, and **C20***

Entry	Catalyst	Solvent	Temp. (°C)	Time (h)	Conv. (%)[a]	$M_{n,th}$ [b]	M_n[c]	$Đ$[c]
1	**C13**	Toluene	110	24	81	5900	8300	1.16
2	**C1**	Toluene	110	24	28	2100	ND	ND
3	**C1**	Toluene	110	72	52	3900	ND	ND
4	**C1**[d]	NA	120	1.5	59	4400	2300	1.73
5	**C20**	DCM	40	48	2	250	ND	ND
6	**C20**	THF	50	48	0	NA	ND	ND
7	**C20**	THF	75	48	88	6400	4300	1.45

***M46**:Catalyst:BnOH = 100:1:1. Monomer concentration = 1 M in toluene. Conv. = Monomer conversion. [a] Monomer conversion determined from crude ^{1}H NMR spectrum. [b] $M_{n,th}$ (g/mol) = ([M]/[BnOH]) ×MW(monomer) ×(% conv.) + MW(end group). [c] $Đ$ and M_n (g/mol) determined by gel permeation chromatography. [d]* Conducted *in the absence of solvent. NA = Not applicable. ND = not determined due to polymer not being isolated.*

C1 catalysed the reaction with a lower activity than **C13** when performing the reaction in solution at 110 °C. No precipitate was observed following a reaction time of 72 hours and addition to methanol. Polymer did precipitate from the reaction mixture's addition to methanol when the polymerisation was conducted in the absence of solvent, however the resultant **P1** had much broader dispersity ($Đ$ = 1.73) despite a reduced reaction time. Chapter 1 discussed

how **C20** was used by Hillmyer *et al.* to promote the elimination of acetaldehyde during the polymerisation of **M44**, hence it was postulated that **C20** could be utilised for the polymerisation of **M46**. Little to no conversion was observed at temperatures below 50 °C in either THF or DCM (Table 3.12, Entries 5 and 6). When conducted at 75 °C a dramatic increase in activity was observed, as 88% conversion is reached in 48 hours. The *Đ* of **P1** produced with **C20** was broader than that produced by **C13** (1.45 vs 1.16). Matrix assisted laser desorption/ionisation-time of flight mass spectrometry (MALDI-ToF MS) was used to characterise the mass of the repeat unit. The mass difference between signals in the mass spectrum is assigned as the mass of the repeat unit. The observation of only a single main series in the spectrum is indicative of a lack of side reactions and variations in the polymer composition including repeat unit.

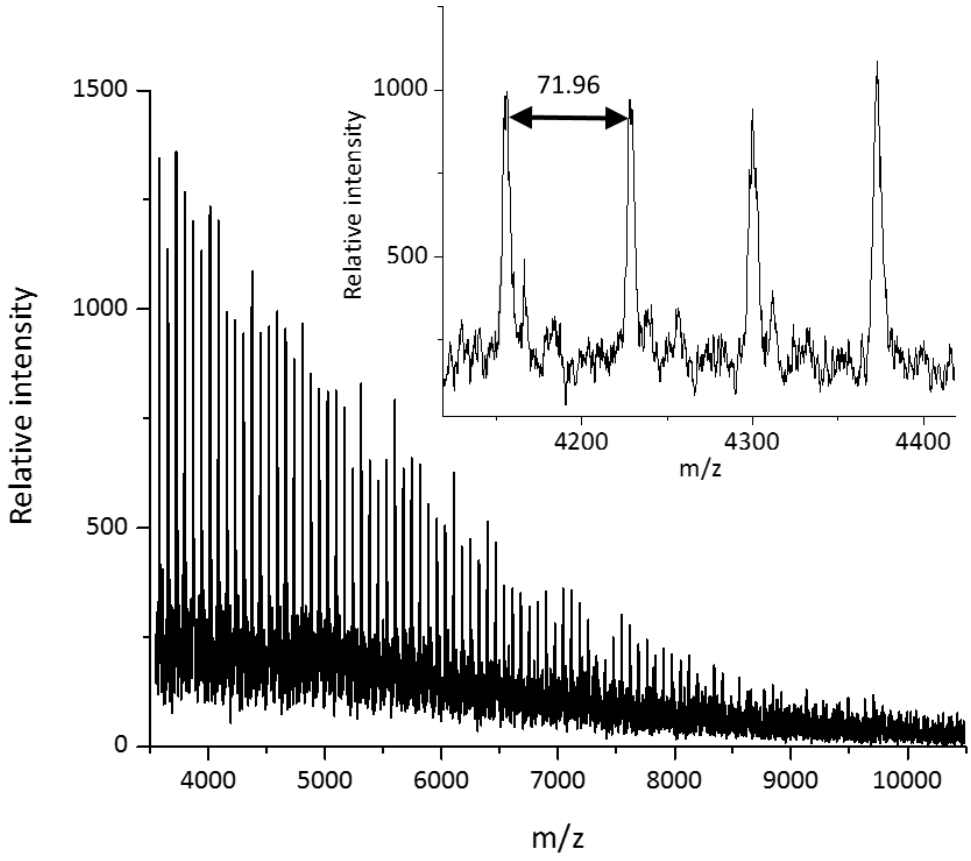

*Figure 3.2. MALDI-ToF spectrum of **P1** produced from the polymerisation of **M46** utilising **C20***

Further characterisation by ^{1}H and ^{13}C NMR spectroscopy was conducted and agreed well with the structure of **P1**. Defined multiplets of **P1**'s methine and methyl protons were observed in the ^{1}H NMR spectrum, this suggested that the stereochemistry of the monomer was retained in the polymer producing isotactic **P1**. Performing differential scanning calorimetry (DSC) on

the polymer sample proved the polymer sample was isotactic **P1**, as the thermal properties such as T_g (58.9 °C), T_m (153.4 °C) and enthalpy of melting (ΔH_m) (56.34 J/g) were in good agreement with literature values.[15] In comparison to other polymer **P1** literature values, a lower onset degradation temperature ($T_{5\%}$) was observed. This may be due to its low MW.

3.2.3 Role of Initial Monomer Concentration

The ROP of monomer **M2** to form **P1** exists in equilibrium. Assuming the rate of initiation is far greater than the rate of polymerisation the general reversible rate form can be described by Figure 3.3. The monomer, **M2**, is polymerised to form lactic dimers incorporated at the end of the initiated/active polymer chain. Due to this equilibrium, the conversion of a monomer is often limited by its monomer equilibrium concentration.

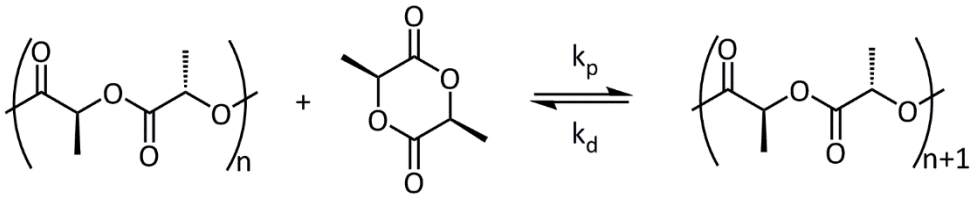

*Figure 3.3. The equilibrium of **M2** and **P1**, when the rate of polymerisation (k_p) and depolymerisation (k_d) are equal.*

Analysis of the crude ^{1}H NMR spectra taken from the polymerisations of **M46** revealed the presence of an additional methine peak indicative of potential side products. The methine was confirmed to be the cyclic diester **M2**. This suggested that the polymerisation of **M46** does not have the same straight forward monomer equilibrium between **P1** and **M46** as is between **M2** and **P1**. Knowing the influence of initial monomer concentration, **M46** was polymerised to form **P1** at three concentrations consecutively one lower than the next. The graphs presented below in Figure 3.4 are constructed from ^{1}H NMR data gathered from polymerisations conducted in Young's tap NMR tubes sealed under an inert atmosphere. The total height of the bar represents the total concentration of methine protons in the NMR tube and is presumed to be constant throughout the polymerisation. Each section of the bars represents the portion of methine concentration in the three forms present during the polymerisation: **M2**, **M46** and **P1**. After six hours, the polymerisation with an initial monomer concentration of 0.5 M (Figure 3.4, left) had moderate monomer conversion and a significant portion of the lactyl units had been converted to **M2**. After 24 hours monomer **M46** conversion had not notably increased and allowing the reaction to proceed for a further two days conversion of **M46** approached completion despite the low concentration. Despite achieving a high conversion of **M46**, a significant amount of **M2** was produced due to the decreased

initial monomer concentration. Decreasing the initial monomer concentration from 0.5 to 0.25 M (Figure 3.4, middle) aligned with the findings at 0.5 M, as it led to an increase in the **M2** portion at all-time points and at 72 hours the methine ratio of **P1**:**M2** was roughly equal.

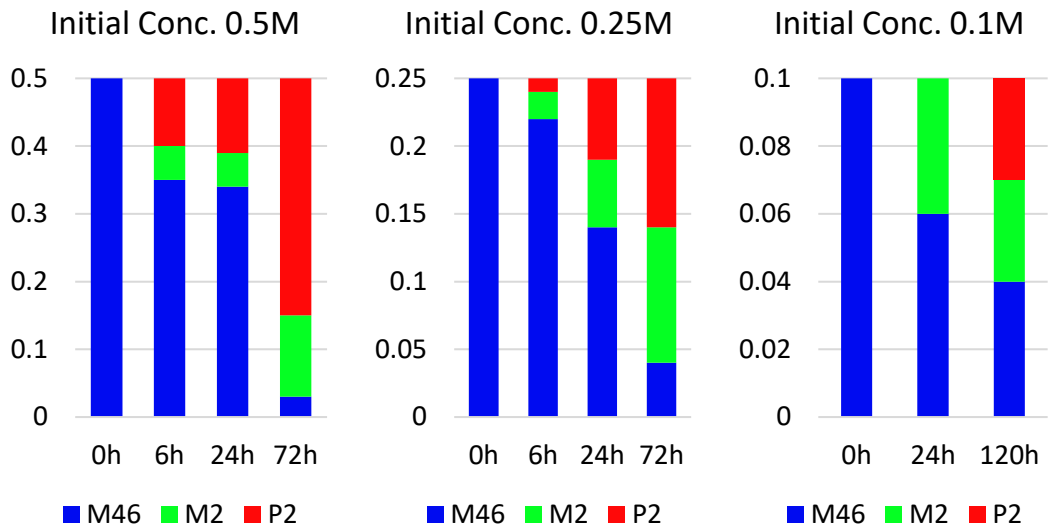

*Figure 3.4. Polymerisation of **M46** at three initial monomer concentrations. Polymerisations were conducted at 120 °C in toluene with an initial loading of **M46**:**C1**:BnOH = 500:1:1.*

At an initial monomer concentration of a tenth the standard concentration (0.1 M) a dramatic impact on the products was observed. After 24 hours, no **P1** was present despite the expulsion and sublimation of paraformaldehyde being observed inside the NMR tube. The sole reaction product was found to be **M2**. Whether **M2** is produced directly from **M46** or all **P2** is depolymerised is not known. After an additional 4 days, **M46** was converted into an equal amount of the **P1** and **M2.** This displays an intriguing dynamic surrounding the ROP of **M46** and the impact of initial monomer concentration on it. These findings have outlined the importance of conducting the polymerisations at higher concentrations. The versatility of utilising the expulsion of a small molecule like paraformaldehyde to assist in overcoming a monomer polymer equilibrium is observed, however lower concentrations do lead to the introduction of the diester polyester monomer polymer equilibrium.

3.2.4 Reaction Set Up

As discussed in Chapter 1, during the formation of polyester *via* polycondensation the choice of reaction vessel had a major impact upon conversions, as MWs were significantly affected. Consequently, it was thought that with more efficient elimination of the formaldehyde (or paraformaldehyde) had the potential to decrease the rate of depolymerisation.

A comparison was made between the areas of heat contact. Two identical polymerisations were conducted in the same reaction vessel, however, each reaction was heated in a different fashion (Figure 3.5). In the first setup (Figure 3.5, 1) The ampoule was submerged in the oil bath until the level of the contents were submerged below the level of the oil bath. While in the second setup ((Figure 3.5, 2), the ampoule was submerged until the oil was in contact with all of the outer glass areas of the reaction vessel. In the second setup, it was observed that the volume of the solution dramatically decreased over 24 hours. The crude ^{1}H NMR spectra of the polymerisations showed heating the entire vessel causes an increased conversion, however, upon dissolution into DCM and addition to hexane minimal precipitation was observed. It was concluded that no tractable polymer was obtained from setup 2. In comparison, setup 1 behaved in line with previous results and resulted in polymer with an accurate MW. It was hypothesised that sublimation could be used as a method to remove the generated formaldehyde. A third setup (Figure 3.5, 3) was possible utilising a carousel type reactor, as an aluminium reflux head cooled the walls 4 cm above the reaction mixture. No improvement to conversion was observed using setup 3.

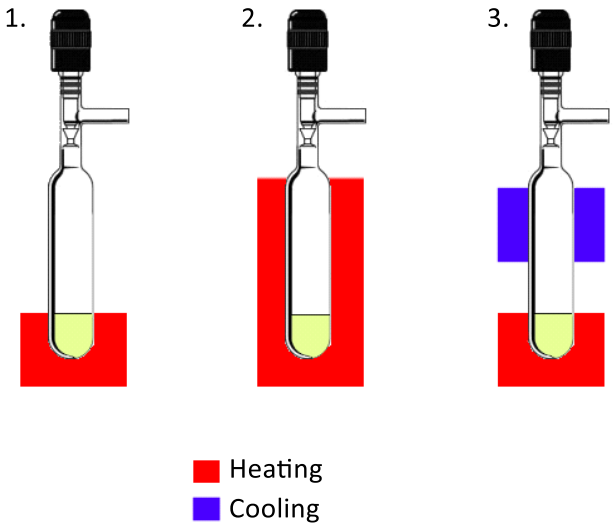

Figure 3.5. Three reaction setups tested with various areas of heating and or cooling

*Table 3.13. Variations in **M46** polymerisation reaction heating/cooling setup*

Setup	Conv.[a] (%)	$M_{n,\,th}$[b]	M_n[c]	$Đ$[c]
1. Heating the glass contacting reaction mixture	93	3456	3000	1.35
2. Heating the entirety of the vessel	99	3672	/	/
3. Heating the glass contacting reaction mixture & cooling above	93	3456	4600	1.52

M46*:*C13*:*BnOH = 50:1:1. Conducted *at 120 °C in toluene 2M for 24h. Conv. = Monomer conversion. [a] monomer conversion% determined from crude ^{1}H NMR spectrum. [b] $M_{n,th}$ (g/mol) = ([M]/[BnOH]) × MW(monomer) ×(% conv.) + MW(end group). [c] Đ and M_n (g/mol) determined by gel permeation chromatography. Đ=dispersity=M_w/M_n.*

3.2.5 Attempts to Actively Remove Formaldehyde with Molecular Sieves

Following the unsuccessful attempts to remove the eliminated molecule using heating or cooling, molecular sieves (MS) were turned to. MS are aluminasilicates that build networked material in three dimensions which creates porous material. These materials are commonly used to separate and purify liquids and gases, as well as catalyse reactions.[16–19] Polymerisations were conducted following the optimised conditions as established through this work. MS were added to the reaction vessel with the aim of removing the eliminated formaldehyde from the reaction mixture. MS of various pore sizes were chosen. Loading the reaction mixture with MS at 10 W/V% and conducting the reaction for seven hours saw no increase in conversion to **P1** at any pore size. An increased conversion of monomer was observed utilising 5 Å MS, however, surprisingly a significant fraction was converted to **M2**. Increasing the reaction time to 15 hours or conducting the polymerisation at higher loadings of MS displayed no increase in monomer conversion and the result at 10%W/V could potentially be an anomaly. Overall it was found that even at higher loadings of MS and extended reaction times, MS of all pore sizes tested resulted in an inhibition of **P1** formation. Alumina silicates are known for their ability to catalyse reactions often due to the Lewis acidic sites and surface aluminium present in alumina silicates.[20] It was hypothesised that increased Lewis acidity would lead to an increase in polymerisation activity, however, this was not observed. Alumina silicates are not restricted to Lewis acidity alone, as replacing Si with Al in a silicate structure generates a pair of ions and in the case of the cation being a proton a Bronsted site is produced.[21–23] The presence of the Bronsted acid is the likely cause of the polymerisation inhibition, as it may cause interference between polymer-catalyst and monomer-catalyst interactions.

*Table 3.14. Addition of MS to the polymerisation of **M46***

Pore size	MS (W/V%)	Time (h)	**P1** (%)	**M2** (%)
None	/	7	84	12
3 Å	10	7	65	20
5 Å	10	7	67	26
10 Å	10	7	55	13
None	/	15	89	9
3 Å	10	15	75	11
5 Å	10	15	51	8
10 Å	10	15	79	13
None	/	13	88	7
3 Å	20	13	75	15
5 Å	20	13	71	15
10 Å	20	13	61	8

***M46*:*C13*:*BnOH* = *100:1:1*.** Conducted *at 120 °C in toluene.*

3.2.6 Alterations to MeAl(salen) Ligand Framework and Its Impact Upon the Polymerisation of 5-Methyl-1,3-dioxolan-4-one

As discussed in Chapter 1, Gibson *et al.* synthesised and tested a wide variety of methyl aluminium salen type (MeAl(salen)) catalysts for the polymerisation of *rac*-**M2**. From screening, it was obvious that variations across the diimine backbone and the phenoxide substitution played a significant role in activity, *Đ* and the stereoselectivity. Hence, at series of salen ligands were synthesised following modified literature procedures: one equivalent of diamine was reacted with two equivalents of substituted salicylaldehyde in an imine condensation. Following recrystallisation and drying under vacuum the proligands were complexed with trimethylaluminium following modified literature procedures. Complexes were purified on a Schlenk line simply by filtering, washing with hexane repeatedly and dried under vacuum. Yields achieved were comparable to literature values and spectroscopic data matched those previously reported.[24] To acquire rates of polymerisation, kinetic investigations were conducted in Young's tap NMR tubes. The polymerisation mixtures were charged to NMR tubes and sealed under an inert nitrogen atmosphere. Polymerisations were conducted by heating the NMR tubes in oil baths. Time points were taken in the following fashion: The NMR tube was removed from the oil bath and rapidly cooled with liquid nitrogen, before being

allowed to reach room temperature and loaded onto the NMR spectrometer. The time elapsed while the reaction was out of the oil bath was noted and the reaction replaced until the next time point. Identical polymerisations were conducted in ampoules parallel with those in NMR tubes (these polymerisations were constantly in the oil bath) and gave comparable final results to ensure the changes in temperatures to the NMR tube reaction did not have an adverse effect on the polymerisation.

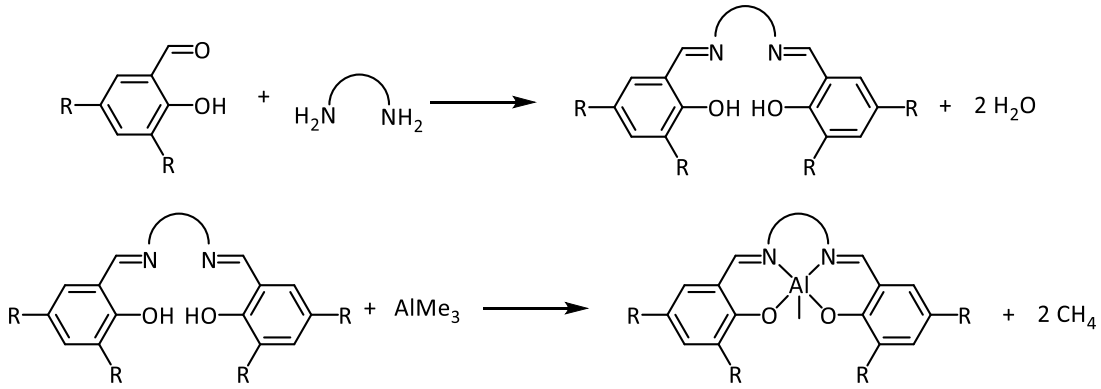

Scheme 3.5. Top: The imine condensation of two equivalents of salicylaldehyde with a diamine. and Bottom: The complexation of a pro salen ligand with trimethylauminium.

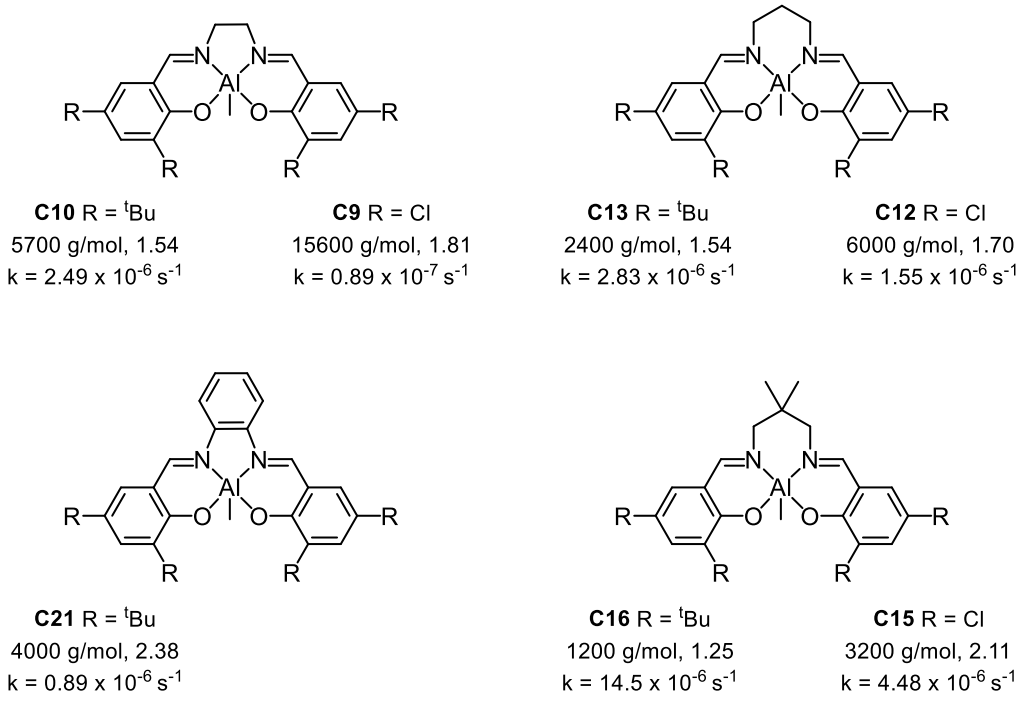

*Figure 3.6. Various MeAl(salen) complexes displayed with their resultant polymer data (M_n, Đ) and their polymerisation rate constant. Polymerisations conducted in Youngs tap NMR tubes, in C_6D_6 at 80 °C, with an initial **M46**:catalyst:BnOH = 200:1:1.*

From previous literature ligand systems substituted with electron withdrawing groups such as halides have been used to achieve higher polymerisation rates, as the ligated metal has

increased Lewis acidity.[24] The increased Lewis acidity is hypothesised to have a better ability to promote the nucleophilic addition of the ester carbonyl. Comparing between the three diimine bridges tested with both substituents, changing the tert-butyl groups for chloro groups induced a decrease in the observed polymerisation rate. The most dramatic decrease was observed when **C13** and **C12** were compared (Figure 3.6), as **C13** polymerises **M46** at an observed rate greater than 25 times that of **C13**. A major difference was also observed in the reaction mixture, polymerisations conducted with chloro substituted MeAl(salen)s gave a red colour, followed by precipitation of a white solid. It was also confirmed by NMR spectroscopy that catalyst concentration decreased over time, and an appreciable decline in the rate was observed. The decreased rate of polymerisation could potentially be caused by catalyst participating in competing side reactions, which would lead to a colour change in the solution and precipitation. The prominence of a side reaction has the potential to be caused by either the electronic change or reduced steric hindrance.

1,2-Diaminoethane, 1,3-diaminopropane, 2,2-dimethyl-1,3-diaminopropane and ortho-phenylenediamine were used to synthesis the various diimine bridges. The two catalysts ligated by salen with C3 linkers (propyl, dimethylpropyl) displayed higher observed rates of polymerisation than the two containing C2 linkers (ethyl, *o*-phenyl). The catalyst with a dimethylpropyl ligand backbone achieved the highest observed rate, five times higher than that of the catalyst containing a propyl backbone. The most prolific increase observed for the rate of polymerisation of **M2** is ethyl *vs* propyl. This suggested that though the linker length has an impact on the ROP of **M46**, it is not as great as that observed for the ROP of **M2**. The C2 linker ortho-phenylene backbone has the most dramatic decrease in polymerisation, so much so that after 9 days only 50% conversion was obtained. This catalyst **C21**, though well known for its ability to copolymerise carbon dioxide and cyclohexene oxide to form polycarbonates,[25] was shown to be an ineffective catalyst for the ROP of **M2** in 2017.[26] The catalyst showed poor activity for the polymerisation of **M2**, taking 24 hours to reach 85% conversion at reduced monomer catalyst loadings of 50:1. These findings fit well with the trend observed for the polymerisation of **M46.** The crystal structure of the catalyst displays distorted square pyramidal geometry about the metal centre. If indicative of the geometry that complex exists in solution, this could be the cause of the reduced rates. Square pyramidal complexes have been reported to have slower observed rates than those with a trigonal bipyramidal geometry. It was observed that across both chloro and ^{t}butyl substituents the MWs of the polymer produced followed the trend ethyl>propyl>dimethylpropyl, the opposite trend of rates. No trend between rates and MWs can be deciphered from the catalysts' polymerisations of **M2** by Gibson *et al.* It was thought that acetal linkages were being retained

in the polymer chain and their cleavage during the polymerisation is what leads to the reduction in the experimental MW in comparison to the theoretical MW.

If the polymerisation of **M46** is pseudo first order with respect to monomer concentration the plot should follow a straight line. However, plotting the results obtained from the kinetic investigation a straight line was not observed (Figure 3.7). The polymerisation was quenched below 50% conversion, far lower than the conversion where deviations from first order kinetics are observed in the polymerisation of **M2** using similar aluminium alkoxide catalysts. This suggests the presence of an undesired side reaction that has the potential to reduce the rate of polymerisation.

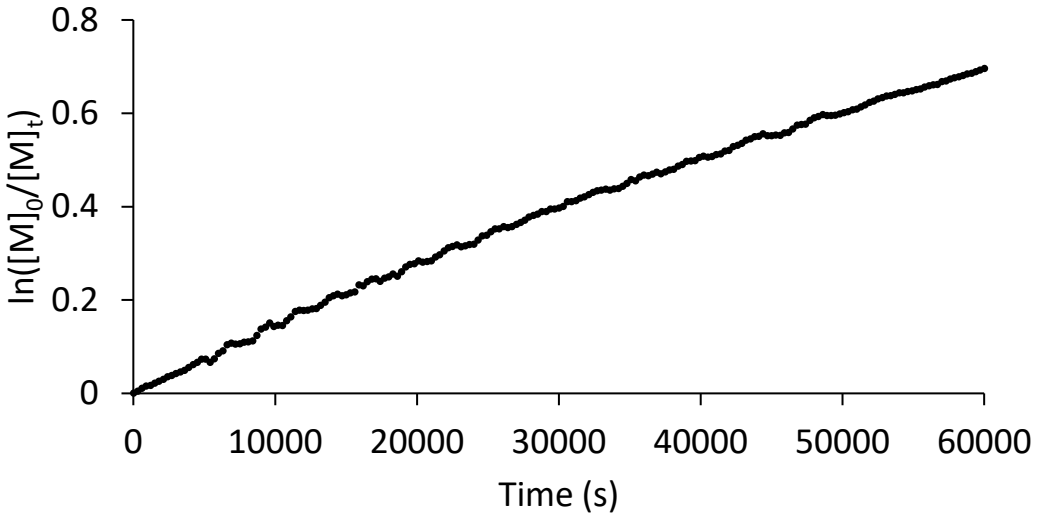

*Figure 3.7. Kinetic plot of **M46** polymerisation using **C16.***

To investigate at what point during the polymerisation the realised MW deviates from the theoretical MW further polymerisations were conducted. Multiple polymerisations that were being conducted in parallel with one another were stopped and worked up at various time points (Table 3.15). After 45 minutes, the polymerisation had reached 12% conversion and theoretically the polymer should have been 1834 g/mol, despite this no polymer was recovered from the precipitation of the crude mixture. After two hours, precipitation was indeed observed after reaching a conversion of 32%. The MW by GPC was notably lower than the expected MW at the beginning of the polymerisation, this suggests a side reaction is present in the reaction during the early stages of the polymerisation and results in the MWs to be lower than expected from the initial stages of the polymerisation. Continuing the polymerisation and taking a sample after 5 hours the MWs were observed to remain at 23% of the expected weight. Longer reactions times were found to produce polymers with decreasing $M_n/M_{n,th}$s, indicating that the side reaction continues to produce chain transfer agent during the polymerisation but

a lesser rate than at the initial stages. Ultimately, at 99% conversion the polymer's MW is only 8% of the expected MW. The narrow dispersity of the polymers agrees with the rapid production of chain transfer agent and initiation at the early stages of the polymerisation. Narrow dispersities also disagree with the theory that acetals were retained during the polymerisation, if an acetal unit is retained they would be distributed through the polymer chain with a random number of lactyl units between each. A range of lactyl units between acetal units would lead to a broad dispersity after the acetal linkages were cleaved and that would be contradictory to the narrow dispersities of the resultant polymer samples.

*Table 3.15. Polymerisation of **M46** with **C16**, stopped at various time points*

Entry	Time (h)	Conv. (%)[a]	$M_{n,th}$[b]	M_n[c]	M_w[c]	$Đ$[c]	$M_n/M_{n,th}$
1	0.75	12	1834	/	/	/	/
2	2	32	4715	1100	1300	1.17	0.23
3	5	63	9181	2100	2500	1.16	0.23
4	7	68	9901	1900	2500	1.37	0.19
5	16	84	12205	1900	2600	1.39	0.16
6	97	99	14366	1200	1600	1.25	0.08

M46*:*C16*:BnOH = 100:1:1. Monomer concentration = 2 M in toluene. The reaction was conducted at 100 °C. Conv. = Monomer conversion. [a] Monomer conversion determined from crude ^{1}H NMR spectrum. [b] $M_{n,th}$ (g/mol) = ([M]/[BnOH]) ×MW(monomer) ×(% conv.) + MW(end group). [c] Đ and M_n (g/mol) determined by gel permeation chromatography.*

3.2.7 Identification of the Chain Transfer Agent

Upon further inspection of the ^{1}H NMR spectrum of **P1**, from the polymerisation of **M46** using **C16** and BnOH, the appearance of new previously unidentified peaks at 8.07 and 3.74 ppm was noted (Figure3.8). Upon repeated purification by precipitation the peaks were still present. Their presence was also noted in previous spectra, but their integrations, relative to the peaks assigned to the repeat unit, were previously insignificant. Both peaks are singlets not coupling to any other polymer peak. They diffuse at the same diffusion coefficient as the lactyl unit peaks confirming they are a part of the polymer chain. From distortionless enhancement by polarisation transfer 135° (DEPT135) edited ^{13}C and heteronuclear single quantum correlation (HSQC) NMR spectroscopic experiments (Figure3.8), both peaks were assigned as CH or CH_3 groups and it was noted that the proton at 8.07 ppm was coupled to a carbon at 159.91 ppm, a chemical shift typically associated with carbonyl carbons or on the periphery of the aromatic chemical shift range. No other aromatic protons were found having similar integrations, nor was the peak at 8.07 ppm coupled to any other aromatic carbon in a heteronuclear multiple-bond correlation (HMBC) NMR spectroscopy experiment. Hence, the

peak at 8.07 ppm could be ruled out as an aromatic proton. Further studies were required to determine the structure of the chain transfer agent.

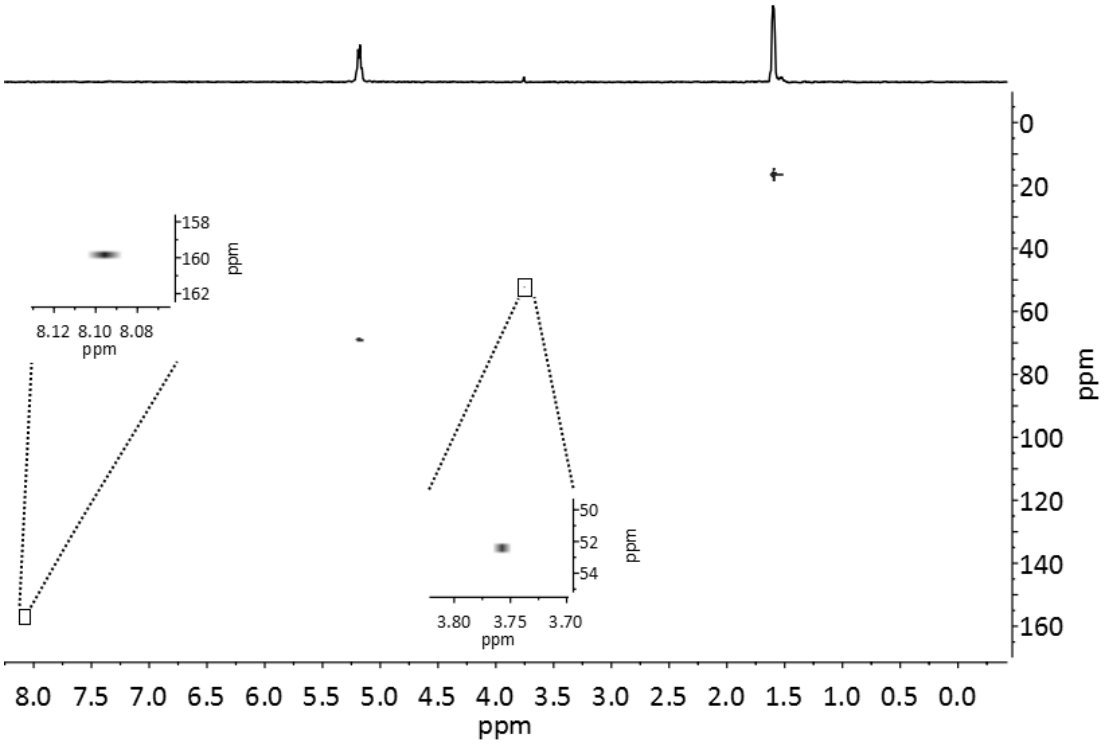

*Figure3.8. HSQC 2D NMR spectrum of **P1** synthesised from **M46** using **C16**. NMR spectroscopy conducted in the following conditions: $CDCl_3$, 300 K, 600 MHz.*

P1 samples with these unidentified NMR peaks produced MALDI-ToF spectra with more than one series present, an example is Figure 3.9. Each series displays a repeat unit mass consistent with **P1**. Upon an initial inspection, it was thought the spectrum consisted of two series, one more prevalent than the other.

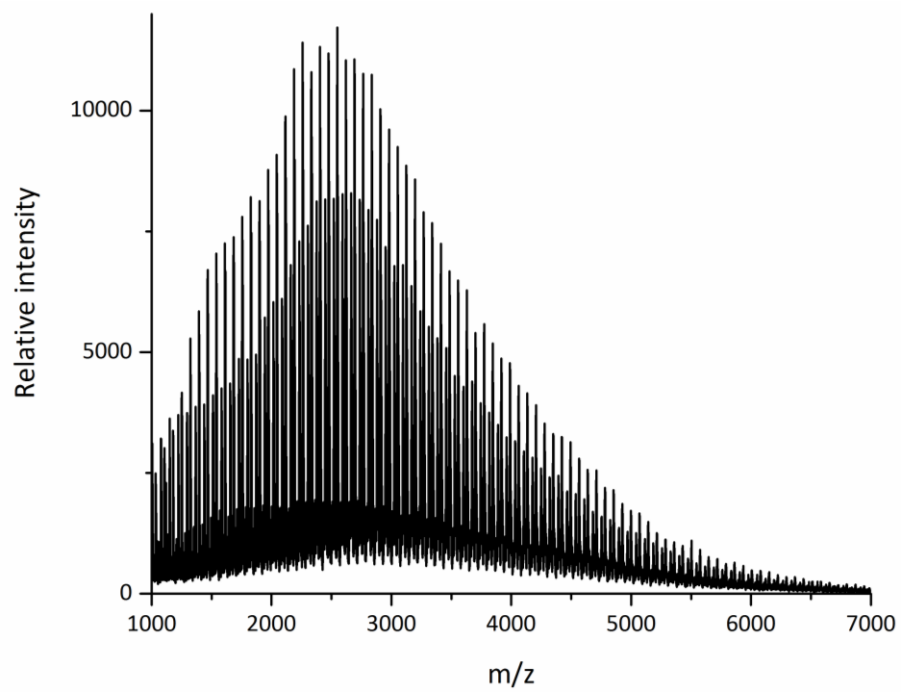

*Figure 3.9. MALDI-ToF Spectrum of **P1** containing unidentified NMR peaks*

Two series would have been in line with the generation of an additional initiator to benzyl alcohol. The ^{1}H NMR peak at a chemical shift of 3.74 ppm is indicative of a methyl ester and supports the assumption that methanol is an initiator. The peak-list of the most intense series was compared to the calculated mass-lists of both benzyl alcohol and methanol initiators; however, it was found neither sets were consistent with the expected values. Taking a closer look at each series, the peaks' shapes followed the expected isotope pattern (Figure 3.10), however were spread over too wide a mass range (5 g/mol). The shoulder of each peak was therefore assumed to be an independent series. Two additional very minor series were also identified at the foot of the peak. Peak lists were generated from the 6-repeating series each labelled in Figure 3.10. The series 3 and 4 were identified as hydroxy terminated **P1** with methyl ester and benzyl ester end groups.

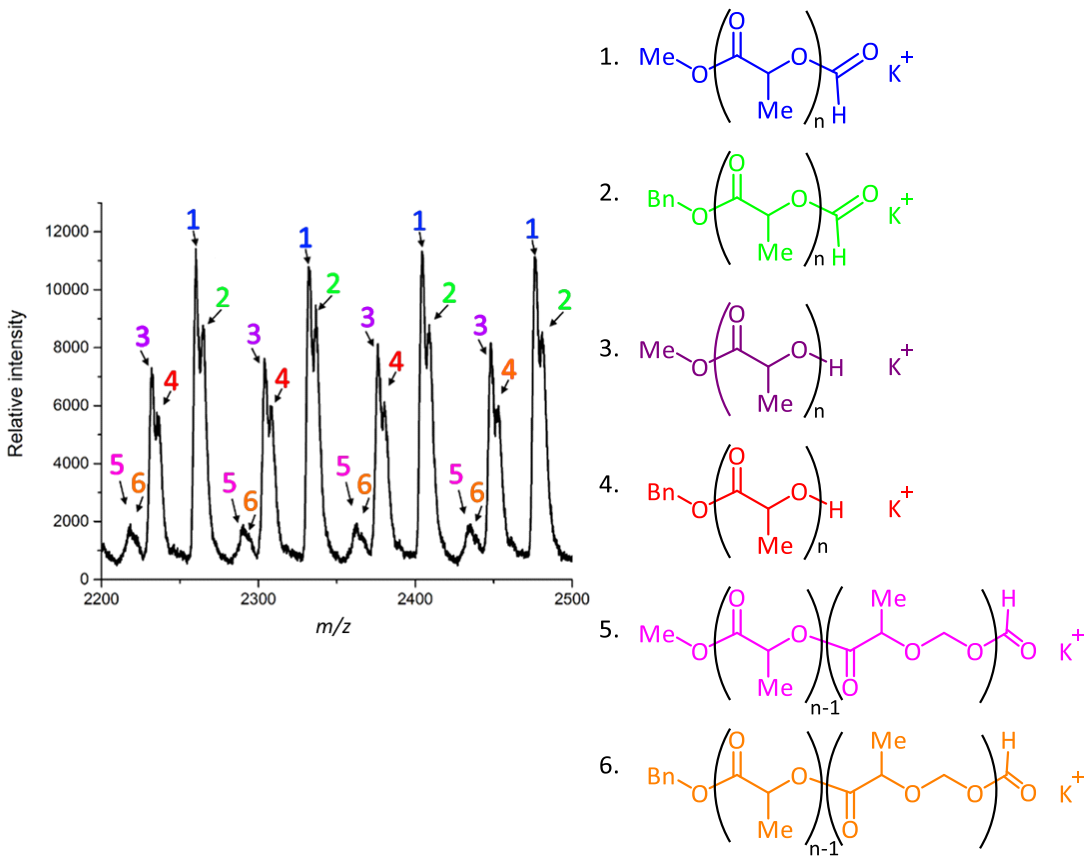

*Figure 3.10. MALDI-ToF of **P1** synthesised from the polymerisation of **M46** catalysed by C13 and initiated by BnOH. The mass spectrum is plotted from 2200-2500 g/mol to illustrate defined peak shapes. Each repeating series is labelled to the identified series on the right.*

Taking in consideration the generation of the newly identified methoxy initiator, a new theoretical MW can be calculated and has been added to Table 3.16 below. This calculated MW, though not the expected MW, aligns very well with the observed MW by GPC and confirms the theory that chain transfer agent is being generated during the polymerisation.

*Table 3.16. Polymerisation of **M46** with **C16** stopped at various time points and incorporating data from additional methoxy initiators*

Time	Conv (%)[a]	$M_{n,th}$[b]	M_n[c]	$Đ$[c]	$M_n/M_{n,th}$	# MeO[d]	$M_{n,th}$
0.75	12	1800	/	/	/	2.72	500
2	32	4700	1100	1.17	0.23	3.37	1100
5	63	9200	2100	1.16	0.23	4.31	1700
7	68	9900	1900	1.37	0.19	4.40	1800
17	84	12200	1900	1.39	0.16	6.20	1700
97	99	14400	1200	1.25	0.08	9.51	1400

M46*:*C13*:BnOH = 200:1:1. Monomer concentration = 2 M in toluene. The reaction was conducted at 100 °C. Conv. = Monomer conversion. [a] monomer conversion determined from crude 1H NMR spectrum. [b] Mn,th (g/mol) = (M:BnOH) × MW(monomer) × (conv (%)) + MW(end group). [c] Đ and M_n (g/mol) determined by gel permeation chromatography. [d]determined by comparing the relative integrations of the methoxy CH_3 and the ***P1 CH.**

At this point, the source of the methanol was still unknown, as was the end groups of the most intense repeating series 1 and 2. The relative intensities of series 1. and 2. appear to be the same as the relative intensities of series 3. MeO-$(C_3O_2H_4)_n$-OH and 4. BnO-$(C_3O_2H_4)_n$-OH. This indicates that they were likely methyl ester and benzyl ester end groups. A list of potential mass differences from 3 to 1 and 4 to 2 were generated using the mass differences to the nearest set of peaks on either side and a combination of n ± 1,2,3 etc. Studying the polymer with multiple characterisation tools in great depth has allowed for partial structural determination and led to the assumption that methanol is generated and acts as a polymerisation initiator.

3.2.8 Determining the Source of Methanol Initiator

With the knowledge that methanol is a product of the side reaction combined with the data obtained from MALDI-ToF MS, a literature search led to the identification of a relevant reaction, the Tishchenko reaction. The reaction is the disproportionation of two equivalents of aldehydes to form a single equivalent of alcohol and ester (Figure 3.11). The reaction's relevance comes with the catalyst, as the most common and active catalysts used for the Tishchenko reaction are Lewis acids, such as Al^{3+}, ligated with alkoxides. The hypothesis that the Tishchenko reaction is a side reaction present during the polymerisation, is strengthened when the products of the disproportionation of formaldehyde are realised as methyl formate. Methyl formate may be trans-esterified with a propagating chain end to form a methoxy aluminium and a formate capped polymer chain. Methanol was found to be the initiator of two repeating series in the MALDI-ToF mass spectrum. From the lists of mass differences between 1 and 3, and 2 and 4 a mass difference of 30 g/mol agrees well with the polymer having a formate end group.

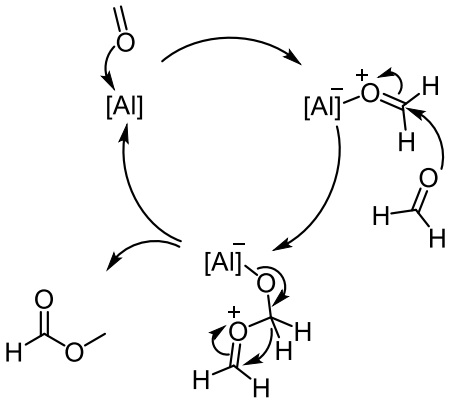

Figure 3.11. Example of the Tishchenko reaction, and the suggested mechanism of the disproportionation of formaldehyde with non-participating alkoxide ligands

The repeating series 1 and 2 are in agreement with the calculated mass list of MeO-$(C_3O_2H_4)_n$-OCHO and BnO-$(C_3O_2H_4)_n$-OCHO. A formate terminated chain *vs* a carboxylic terminated chain would produce a polymer with the same repeating mass formula. A propagating carboxylate aluminium species could not be ruled out, as work conducted by Hillmyer *et al.* concluded that low zinc concentration system mediated the polymerisation in this fashion.[27] It was not until comparing the plausible chain ends with the final unidentified ^{1}H resonance in the NMR spectrum, the sharp singlet at $\delta = 8.07$ ppm coupled to the ^{13}C peak at 159.91 ppm, was the carboxylic acid discounted. The hypothesised side reaction, the Tishchenko reaction, agrees well with the presence of methanol initiators and formate terminating groups.

The minor repeating series was difficult to identify due to its poor resolution. Firstly, it was the hypothesised a minute amount water was present in the monomer after the drying procedure of stirring and distilling over calcium hydride. The expected mass of a water initiating species did not align with the mass of the minor series. The g/mol range of the minor series was indicative toward there being two series present, akin to the other pairs 1,2 and 3,4. Scanning through the spectrum, the minor peak was resolved into two series: 5 and 6, in the range displayed in *Figure 3.10*. The two series were a match for CH_3O-$(C_3O_2H_4)_{n-1}$-$C_4O_3H_6$-OCHO and $C_6H_5CH_2$-O-$(C_3O_2H_4)_{n-1}$-$C_4O_3H_6$-OCHO. These masses represent each the methoxy and benzyloxy initiated polymerisation and terminated with a formate group and differ by a single repeat unit retaining the acetal linkage. This hypothesis was not confirmed by any other characterisation technique due to its lack of abundance.

3.2.9 Proposed Mechanism

As discussed in Chapter 1, aluminium alkoxide catalysts proceed *via* a coordination-insertion mechanism. It is proposed that the mechanism of this new synthetic route would follow the same mechanism as a standard coordination-insertion mechanism (Figure 3.12). Specifically, this mechanism is hypothesised to follow the following steps: aluminium coordinates to the oxygen of the carbonyl and promotes nucleophilic attack by the alkoxide at the carbonyl carbon. This breaks the carbonyl's π-bond leading to the former carbonyl carbon having sp^3 hybridisation and the former carbonyl oxygen being bound to the aluminium in the intermediate. Coordination of aluminium to the acyl oxygen promotes the reformation of the carbonyl and leads to the cleavage of the acyl bond. During the coordination-insertion polymerisation, the catalyst is found to be bound to the propagating alkoxide as discussed above. This was observed by DOSY NMR as all the peaks in an unquenched, conducted

polymerisation (**M46**:**C16**:BnOH 20:1:1) were associated with the same diffusion coefficient, including peaks assigned to ^{t}Bu groups of **C16**.

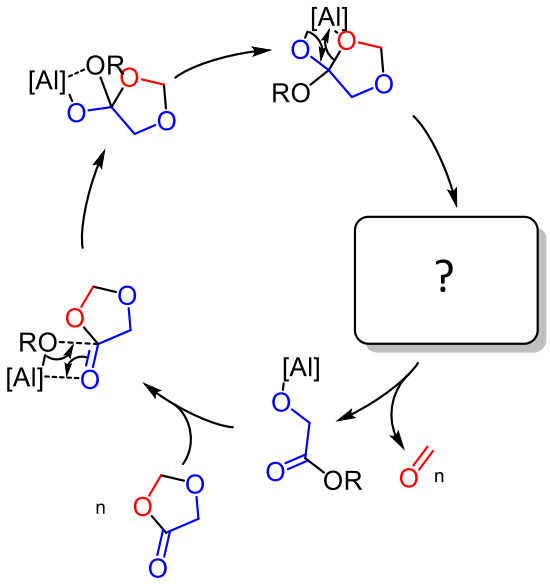

Figure 3.12. Coordination-insertion mechanism of the polymerisation of 1,3-dioxolan-4-ones

The step which leads to the elimination of formaldehyde has not yet been identified. One suggested route is that a backbiting type event occurs. The backbiting process outlined in Figure 3.13 would occur after the acyl bond cleavage step and involve the aluminium coordinating to the acetal oxygen and pass through a four membered metallo-cycle transition state to eliminate an equivalent of formaldehyde. An alternate elimination route involves two propagating aluminium alkoxide species. A six-membered ring is suggested as a plausible route for the two aluminium alkoxide mechanism to pass through. In Figure 3.13 the six-membered ring arrangement is illustrated. In the proposed arrangement one aluminium, Al^{A}, is coordinated to the oxygen alpha to the carbonyl of the other propagating species. The other aluminium, Al^{B}, is coordinated to the alkoxide of Al^{A}. The alkoxide is exchanged from Al^{A} to Al^{B}, Al^{A} exchanges its alkoxide for the beta oxygen of Al^{B} and thus promoting the formation of formaldehyde.

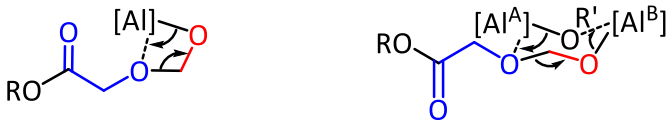

Figure 3.13. Plausible mechanisms for the elimination of formaldehyde from the polymerisation of 1,3-dioxolan-4-ones

The standard coordination-insertion mechanism and the plausible elimination mechanisms of formaldehyde have been combined with the hypothesised Tishchenko reactions in Figure

3.14. Both current theories of the Tishchenko are displayed. Shown in Figure 3.11 and Figure 3.14 is the disproportionation of two equivalents of formaldehyde to form methylformate. Shown in the bottom right of the Figure 3.14, methylformate is incorporated in the polymerisation following reaction with a propagating polymer-aluminium species. Alternatively, the Tishchenko reaction could occur prior to the elimination of acetal from the propagating polymer. In Figure 3.14 centre top an equivalent of formaldehyde adds to aluminium and is followed by a 1,5-hydride shift to cap the propagating chain with formaldehyde and produce a methoxyaluminium species. The hypothesised mechanism should allow for better planning of experiments to probe this new synthetic route to polyesters in the future. One such example is to widen the catalytic screening to coordination-insertion type ROP catalysts which act a weak Lewis acid towards either the monomer, acetal or formaldehyde.

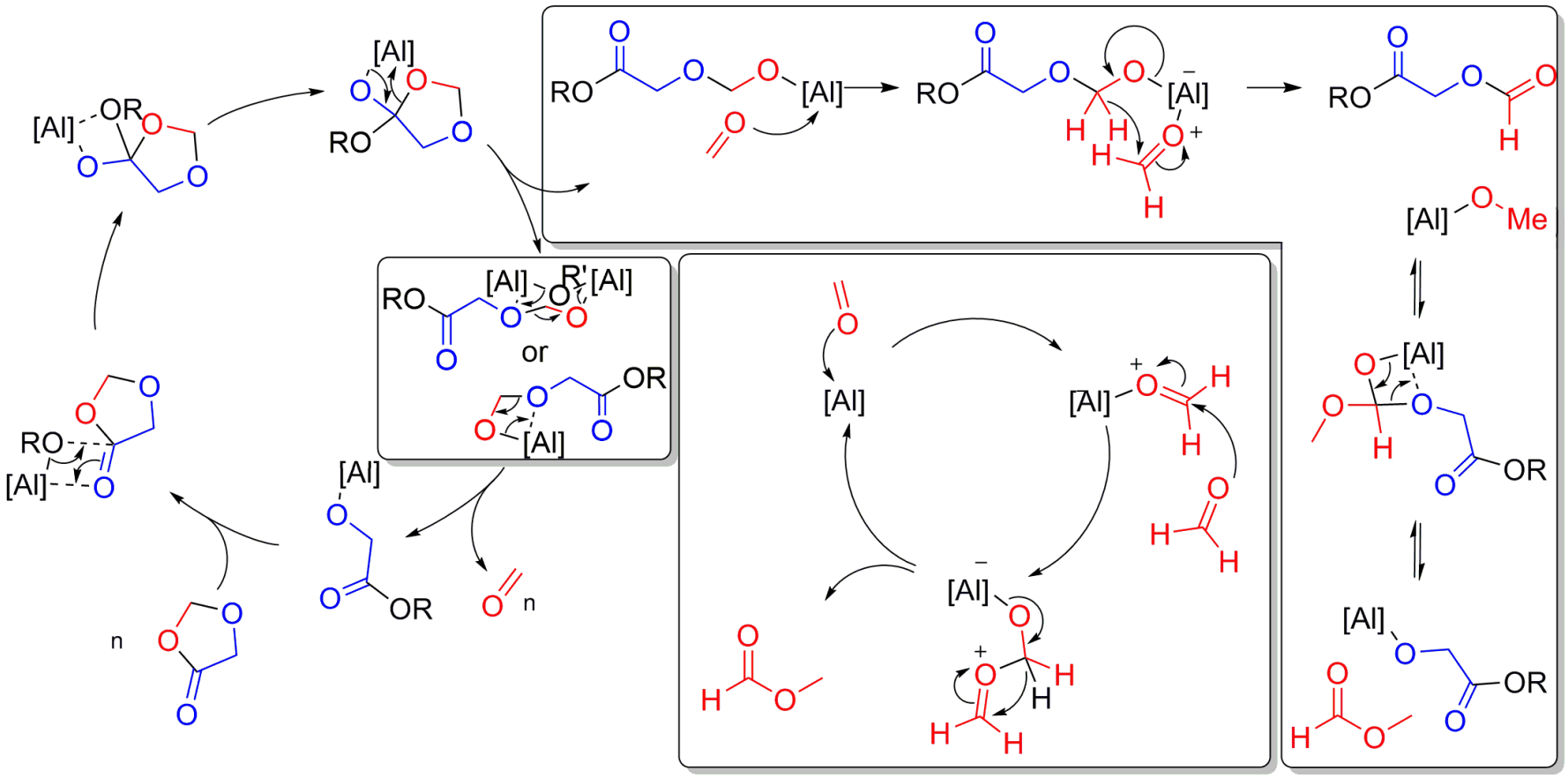

Figure 3.14. Hypothetical ring-opening polymerisation of 1,3-dioxolan-4-one mechanism

3.2.10 Attempted Retention of Acetal

It has been shown that monomer **M46** is capable of homopolymerisation to form PAHA. However, there has been a pressing need to synthesise a **P1** type polymer with increased hydrolytic degradation capabilities. In Chapter 2, the copolymerisation of a 1,3-dioxolan-4-one was studied in order to attain the hydrolytically degradable copolymer **P3** in a more efficient and controlled manner than **M2**. However, it was noted that the yield of the monomer to attain the copolymer was poor. It was hypothesised that retention of acetal units during the homopolymerisation of **M46** could lead to a hydrolytically degradable homopolymer. Hillmyer *et al*. observed an increased hydrolytic degradation rate of the polyesteracetal over the polyester synthesised from the ring-opening polymerisation of **M44** (Scheme 3.6).[27] The importance of polyesteracetals has been illustrated by patents describing the potential utility of the polymers.[28] Increased hydrolytic degradation rates have been described as desirable for applications such drug delivery and to replace slow degrading commercial plastics.[28] Taking inspiration from the divergent mechanism pathways shown for **M44**, it was hypothesised that by reducing the catalyst loading and or reduce the catalyst concentration another mechanistic pathway could be evoked to synthesise a polyesteracetal from **M46**. However, neither reducing the catalyst concentration or loading led to the formation of polymer differing from **P1**, this merely led to a reduced rate of polymerisation.

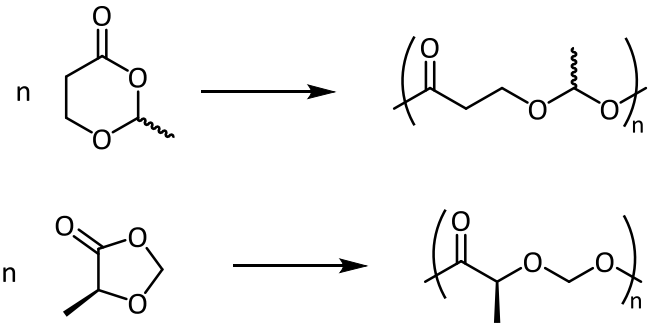

*Scheme 3.6. Polymerisation of **M44** and **M46** to form polyesteracetals*

The ring strain of **M45**, as previously discussed in Chapter 2, was found to be similar to that of γ-butyrolactone **M48**. The polymerisation of **M48** has been attempted with limited success and has been referred to as 'non-polymerisable' in textbooks.[29–31] It was not until Chen *et al.* used a lanthanum complex or a tert-butyl P_4 phosphazene super-base (*Figure 3.15*) as a catalyst under a very low temperature was poly(γ-butyrolactone) formed at high conversions (>90%).[32,33] The combination of a very active catalyst and low temperature had the capability of overcoming the entropic penalty associated with polymerisation. It was thought that the

same approach could be taken in order to polymerise **M44** to retain the acetal units and synthesise a polyesteracetal.

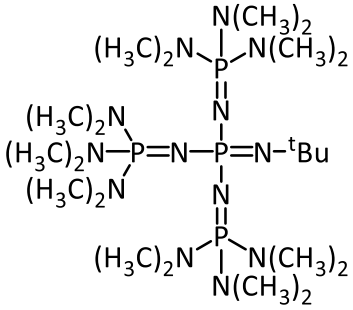

Figure 3.15. Phosphazene base P4-t-Bu

Polymerisations were set up using standard Schlenk techniques in order to complete the addition of the tert-butyl P_4 phosphazene and benzyl alcohol solution to the monomer solution at the desired temperature. No conversion of monomer was observed after 5 hours at -78 °C. Increasing the temperature to -40 °C, near complete consumption of the monomer was observed in the same time period. The crude ^{1}H NMR spectrum was found to be undecipherable. Formation of a precipitate was observed upon the addition of the reaction mixture to cold hexane. Following filtration and drying, analysis by ^{1}H NMR spectroscopy of the precipitated sample (5% yield) showed peaks typically associated with **P1**, an additional methylene peak at 4.88 ppm was identified as retained acetal units. The integration the acetal peak relative to the methine peak at 5.17 ppm indicated that lower than 25% of the acetal units were retained. The integration of the methyl ester peak associated with methoxy initiated polymer chains was very large relative to the polymer peak. As observed with the coordination-insertion type polymers at lower temperatures undesirable side reactions were occurring and this was avoided by increasing the polymerisation temperature. The monomer was found to be consumed after 5 hours at 0 °C, however, no precipitation was observed upon addition of the reaction mixture to cold methanol or cold hexane and no peaks associated with **P1** were present in the crude ^{1}H NMR spectrum indicating none of the expected polymer was present. No further attempts to form the polyesteracetal were made with this system due to the prevalence of side reactions consuming the monomer or polymer at 0 °C and -40 °C or no reaction at -78 °C.

3.2.11 Functional Group Tolerance Screening

In Chapter 1 the importance of the pendant functional group was discussed. The variety of pendant groups outlined the impact of the functional group on its properties and thus the applications the resultant polymer could be used for. Thus, it was desirable to test the

capabilities of this new polymerisation route in the presence of various functional groups, in order to gain an insight into the most desirable groups to install on 1,3-dioxolan-4-ones.

The polymerisations were set up according to standard procedure modified to screen functional group tolerance: **M46** was dissolved in toluene with **C13**, benzyl alcohol and a compound containing the functional group being tested. The compound of interest was added equimolar to **M46**. From *Table 3.17*, it can be observed that a number of functional groups have very little effect on the polymerisation including: ester, ether, sulphide, and tertiary amine. Interestingly some functional group's impact on the polymerisation varied greatly depending on the substitution. Firstly, comparing the amides tested, the presence of methylacetamide inhibited the polymerisation, such that no conversion was observed. However, when substituting the amide with another methyl, dimethylacetamide showed little effect over the polymerisation. The functional group guanidine showed similarities to the amide. The guanidines containing nitrogens bearing protons inhibited the formation of any polymer. Again, no polymer was observed when imidazole was tested, as the group contains a nitrogen bearing a proton. The role of the nitrogen baring is poorly understood due to the variety of nitrogen proton bonds illustrated in these examples. Examples such as methylacetamide and TBD have the ability to disrupt the polymerisation through reaction with the catalyst. However, the other less substituted nitrogens have the ability to react, nucleophilically, with the monomer causing the observed monomer conversion without the subsequent formation of polymer.

*Table 3.17. Polymerisation of **M46** in the presence of various functional groups.*

Functional Group	Compound	Conv. (%)	Polymer	$M_{n,th}$	M_n	$Đ$
none		99	Y	7200	2700	1.40
indole	indole	10	N	800		
amide	methylacetamide	0	N			
ester	ethyl acetate	99	Y	7200	2500	1.50
ether	diethyl ether	99	Y	7200	2600	1.40
sulphide	thioanisole	94	Y	6900	2300	1.31
imidazole	imidazole	99	N	7300	200	1.60
3° amine	TEA	99	Y	7200	2300	1.50
2° amide	DMA	94	Y	6900	2300	1.25
guanidine	TBD	0	N			
imidazole	2-amino-1-ethylbenzimidazole	99	N	7200	140	1.43

***M46*:*C13*:*BnOH = 100:1:1. Monomer concentration = 2 M in toluene. The reaction was conducted at 120 °C over 15h. Conv. = Monomer conversion. [a] monomer conversion% was determined by crude sample ^{1}H NMR spectroscopy. [b] $M_{n,th}$ (g/mol) = ([M]/[BnOH]) ×MW(monomer) ×(% conv.) + MW(end group).[c] Đ and M_n (g/mol) determined by gel permeation chromatography.**

3.2.12 Recycling of Paraformaldehyde

The desire to synthesise new materials, especially polyesters, is fundamentally driven by the need for greener and more sustainable chemistry. Polyesters align with these goals as the product is designed for degradation, however, to align with other green principles such as reducing waste during synthesis, using less hazardous syntheses, and using renewable feedstocks the synthetic route must be scrutinised. Atom efficiency was of particular interest, due to OCA's poor efficiency during polymerisation and synthesis, while 1,3-dioxolan-4-one's efficiency is still poor during polymerisation. In contrast, the ROP of diesters is extremely efficient. Comparing the atom economy of each route firstly by their monomer syntheses, the synthesis of **M46** is 54% economic and however the synthesis of **M36** is far lower at 14%. Secondly, the polymerisation of **M36** has an atom economy of 62%, whereas the polymerisation of **M46** is 71%. Both polymerisation techniques are a large fraction lower than 100% due to the need to expel a small molecule during each turnover. Collection of the expelled formaldehyde is done with great ease, as solid paraformaldehyde is sublimed on the walls of the reaction vessel, whereas once the polymerisation an OCA is complete and the reaction vessel is opened, the carbon dioxide is released to the atmosphere. This provided an easy opportunity to tackle and improve the "greenness" of the polymerisation of 1,3-dioxolan-4-ones and to prevent waste. Upon completion of a **M46** polymerisation the expelled paraformaldehyde was recovered from the walls of the reaction vessel by simply scraping with a spatula. This provided an opportunity to close the cycle for paraformaldehyde by entering it back into the polymer synthesis, as it was subsequently used to synthesise 5-phenyl-1,3-dioxolan-4-one (**M49**). Comparing with standard paraformaldehyde purchased from Sigma Aldrich, the recovered paraformaldehyde achieved the same conversion to monomer **M49** upon analysing the crude samples by ^{1}H NMR spectroscopy. This allowed us to close the loop and make for a far more efficient polymerisation route. In contrast, this is not possible for the OCA polymerisation synthetic pathway, as a side product, carbon dioxide, cannot be reintroduced directly to further synthesise OCA monomers.

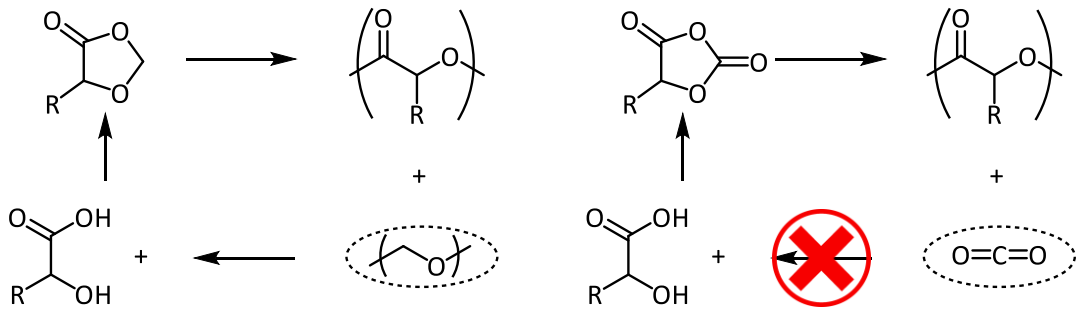

Figure 3.16. Recycling paraformaldehyde vs carbon dioxide

3.3 Ring-Opening Polymerisation of 5-Phenyl-1,3-dioxolan-4-one

Few reports of **M49** are presented in the literature. Some examples include using **M49** as a precursor in the stereospecific synthesis of (3S,4S)-3-hydroxy-4-phenylbutyrolactone,[34] and the synthesis of O-trimethylsilyl-DL-mandelic N,N-dimethylamide, a monochelating ligand for germanium chlorides.[35] This may be due to it having few uses in synthesis or any wider applications. The only document recording the aim to polymerise **M49** to form **P5** was produced as a result of this work.[36] Thus, it was of interest to investigate **M49** as a monomer for ring-opening polymerisation, with the intention to form **P5**.

3.3.1 Formation of Poly(Mandelic acid) from 5-Phenyl-1,3-dioxolan-4-one

Following the successful polymerisation of **M46** using catalysts known to follow a coordination-insertion type mechanism, the polymerisation of **M49** was attempted using the same type of catalysts. Initial polymerisation attempts were made with **C20** as the catalyst and exogenous benzyl alcohol for the initial insertion (Scheme 3.7).

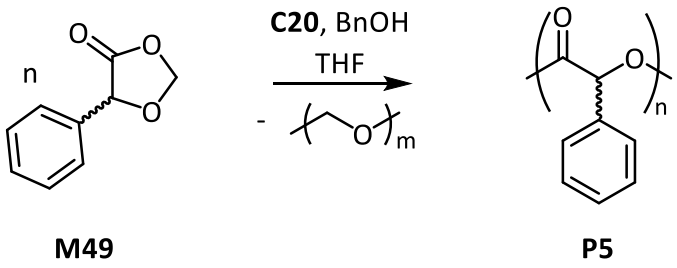

*Scheme 3.7. Initial attempt to polymerise **M49** with **C20** and BnOH in THF heated at reflux.*

The initial polymerisation was conducted in a THF solution heated at reflux (Table 3.18, Entry 1). Very little sublimation of paraformaldehyde was observed,[37] and the reaction was allowed to proceed over 8 days. Analysing the crude polymerisation mixture by ^{1}H NMR spectroscopy, formation of peaks assigned to **P5** in previous work were observed,[34] and the monomer conversion was calculated by comparing the relative methine integrations of the polymer (6.25-5.90 ppm) and monomer (5.30 ppm). The amount of sublimed paraformaldehyde was indicative of the slow rate of polymerisation as only 15% conversion was reached over the long reaction time. The polymerisation was conducted in the absence of solvent and at an elevated temperature of 180 °C and this led to a higher monomer conversion. MALDI-ToF was used to confirm the MW of the repeating unit as a mandelyl unit (Figure 3.17). It is apparent from Figure 3.17 that three main series are present in the MALDI-ToF spectrum, the most intense series, at this molecular weight region, was identified as **P5**

containing 2 acetal groups retained in the polymer, and this series was flanked with **P5** containing 1 and 3. The intensity of each series varies through the mass distribution and is indicative of loss of control over the formaldehyde expulsion step.

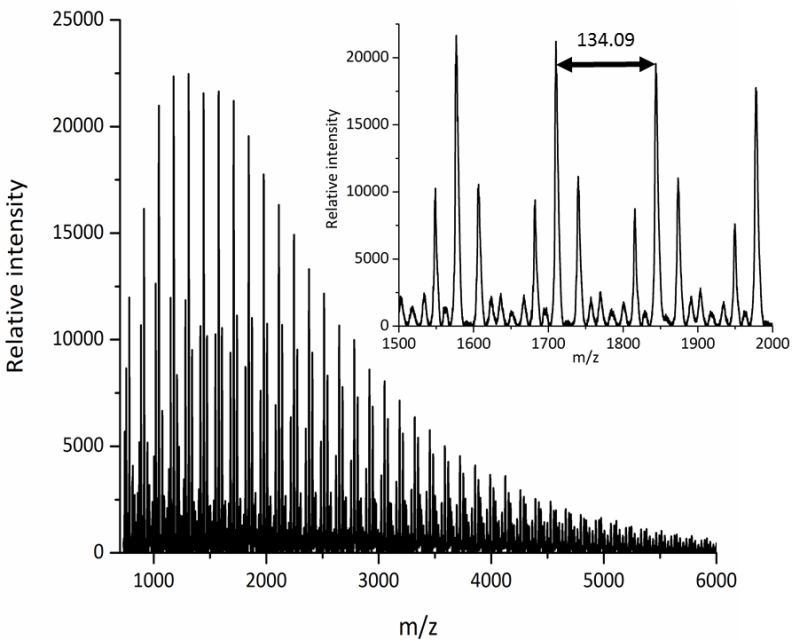

*Figure 3.17. MALDI-ToF spectrum of **P5** including zoomed in region*

A conversion of 42% was reached after four hours and extending this reaction time to 24 hours a monomer conversion of 97% was reached (Table 3.18, Entries 2 and 3). Despite the harsh polymerisation conditions, the dispersity after 24 hours was low at 1.07. Using the most common ring-opening polymerisation catalyst, **C1**, the solution polymerisation achieved higher conversions, but this was likely due to the to the higher reaction temperature (Table 3.18, Entry 4). Despite a conversion of 20%, no precipitation was observed upon adding the crude mixture to cold methanol. Precipitation was observed when the polymerisation was conducted in the bulk (Table 3.18, Entry 5), however, 19 hours was required to reach approximately the same conversion reached in 4 hours in solution. In order to reduce the time taken to complete catalyst screening the equivalents of monomer to catalyst was reduced from 100 to 50. Polymerisations were conducted using the single enantiomer *S*-**M49** in order to synthesise the desirable isotactic **P5**, which as discussed in Chapter 1 showed an increase in T_g of 10 °C from the atactic equivalent. Polymerising with Sn and Zn outlined the same difficulties that were observed when attempting the polymerisation of either **M7** and **M43**, as epimerisation resulted in the **P5** being atactic. The catalyst **C13** proved to be very efficient for the polymerisation of **M49** as it achieved a higher conversion, lower dispersity and the chirality was retained (Table 3.18, Entry 7). *S*-**M49** (ee = 89.3%) and *R*-**M49** (ee = 90.2%)

were used to synthesise **P5** in Entries 13 and 14, Table 3.18 and retention of chirality resulted in **P5** with specific rotations of +110 and -122 respectively. When the tert-butyl substituents were replaced for chloro groups the conversion was decreased (Table 3.18, Entry 8), the decrease in rate aligned well with the observations made conducting polymerisations of **M46**. The polymer's dispersity was very narrow (1.05). The ^{1}H NMR spectrum illustrated that the catalyst caused a distinctive broadening of the methine proton region of the polymer indicative of an atactic polymer, comparative methine regions of isotactic and atactic **P5** samples are shown below in Figure 3.18. This was also confirmed by optical rotation as the polymer had a specific rotation of -6.9.

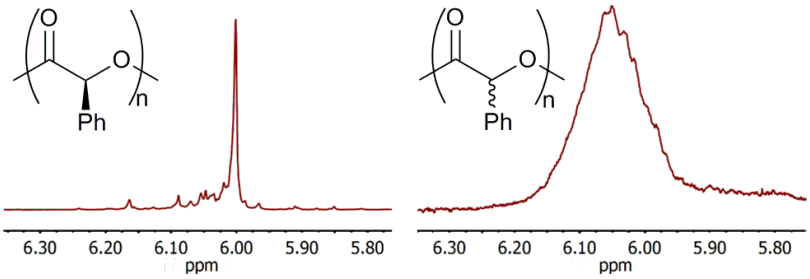

*Figure 3.18. Comparative ^{1}H NMR methine regions of isotactic **P5**, product of Entry 13, Table 3.18 (left) and atactic **P5**, product of Entry 8, Table 3.18 (right)*

Another adjustment can be made to the ligand framework by replacing the imine functional groups with amine. This ligand framework, named salan,[38] bearing chloro substituted phenoxide rings and benzyl substituted amines complexed with trimethyl aluminium was used to polymerise **M49** (Table 3.18, Entry 9). A further decrease in monomer conversion was observed using this catalyst and the resultant polymer exhibited a very broad dispersity (3.71). Akin to the polymerisations of **M46** resulting in low MW **P1**, **P5** samples all exhibited lower MWs than the expected MWs.

In order to outline the importance of this work, higher MWs were targeted. To do so the M:C:I ratio was increased from 50:1:1 to 100:1:1 and then to 200:1:1 and finally to 500:1:1 (Table 3.18, Entries 11-15). Drastically longer reaction times were needed to achieve higher conversions. The resultant polymers, though lower than the expected MWs, still retained the input stereochemistry and had low dispersities (<1.20). Poor conversions were observed when the ratio 500:1:1 was polymerised in solution, even with prolonged reaction times. To overcome this the polymerisation was conducted in the absence of solvent and the polymerisation temperature was increased to 180 °C. The polymer produced had a higher DP than **P5** formed by polycondensation and had a narrow *Đ*. These reaction conditions though enabling a higher DP, led to an atactic product.

The monomer **M49** was polymerised to form the polymer **P5**. Polymer **P5** has previously been synthesised from monomers **M6** and **M42** with drawbacks in areas such as monomer synthesis, and long reaction times. **M49** was synthesised in a greater yield than either **M6** or **M42,** and the synthesis of **M49** required less toxic reagents than those utilised to synthesise **M42**. Extended reaction times were required to achieve control over the molecular weight distribution of **P5** and reach high conversions. Utilising **C13** the monomer's stereochemistry was retained in the polymer and isotactic polymers were synthesised. However, at higher monomer loadings conversion was limited and forcing reaction conditions were required. It was hypothesised that this limitation was correlated with the build-up of large quantities of paraformaldehyde in the reaction vessel and hence further attempts to actively remove the polymerisation by-product were required.

*Table 3.18. Polymerisations of **M49***

Entry	M	M:C:I	Catalyst	Temp. (°C)	Time (h)	Conv. (%)[a]	$M_{n,th}$[b]	M_n[c]	$Đ$[c]	Tacticity[d]
1	*rac*-**M49**	100:1:1	**C20**	75	192	15	2100	/	/	atactic
2	*rac*-**M49**[e]	100:1:1	**C20**	180	4	42	5700	1600	1.47	atactic
3	*rac*-**M49**[e]	100:1:1	**C20**	180	24	97	13100	4000	1.07	atactic
4	*rac*-**M49**	100:1:1	**C1**	120	4	22	3100	/	/	atactic
5	*rac*-**M49**[e]	100:1:1	**C1**	120	19	20	2800	1700	1.38	atactic
6	*S*-**M49**	50:1:1	**C1**	120	4	65	4500	3400	2.15	atactic
7	*S*-**M49**	50:1:1	**C13**	120	4	89	6100	3700	1.30	isotactic
8	*S*-**M49**	50:1:1	**C12**	120	4	59	4100	3900	1.05	atactic
9	*S*-**M49**	50:1:1	MeAl(salan)	120	4	43	3000	1000	3.71	isotactic
10	r*ac*-**M49**	100:1:1	**C13**	120	72	92	12500	4000	1.17	atactic
11	*R*-**M49**	100:1:1	**C13**	120	72	98	13300	4800	1.30	isotactic
12	*S*-**M49**	100:1:1	**C13**	120	72	96	12990	4900	1.22	isotactic
13	*S*-**M49**	200:1:1	**C13**	120	120	83	22370	8400	1.14	isotactic
14	*R*-**M49**	200:1:1	**C13**	120	120	96	25860	7700	1.47	isotactic
15	*S*-**M49**[e]	500:1:1	**C13**	180	72	55	37000	19700	1.18	atactic

Monomer concentration = 2 M in toluene. Conv. = Monomer conversion. [a] monomer conversion% was determined by crude sample ^{1}H NMR spectroscopy. [b] $M_{n,th}$ (g/mol) = ([M]/[BnOH]) ×MW(monomer) ×(% conv.) + MW(end group).[c] Đ and M_n (g/mol) determined by gel permeation chromatography.[d] Determined from the ^{1}H NMR spectrum's methine region. [e] Conducted in the absence of solvent

3.3.2 Attempts to Actively Remove Formaldehyde

Elongating the reaction time used in Table 3.18, Entry 15, it was found that the monomer conversion was not increased. The presence of large amounts of paraformaldehyde were hypothesised to be hindering the polymerisation. Hence, in order to achieve greater monomer conversion of **M49** at high the monomer loading of 500:1:1 a number of different reaction set ups were tested. A sealed ampoule as the standard below was compared with a sublimator with a cold finger cooled with liquid nitrogen, an ampoule with constant nitrogen flow over the top of the reaction, and finally a reaction in an ampoule under vacuum (<0.5 bar) and attached to liquid nitrogen trap.

The premise of conducting the reaction in a sublimator was to increase the rate that paraformaldehyde was sublimed away from the reaction mixture and with hope that the cold surface would keep the paraformaldehyde from re-entering the reaction mixture. Conducting the reaction in a sublimator achieved an identical conversion (25%) to the reaction set up in a sealed ampoule, though the polymer had an increased MW. It was observed that the cold finger did not encourage sublimation of the paraformaldehyde, but condensed the monomer instead, despite the reaction being conducted below its boiling point.

The goal of having nitrogen flow above the reaction mixture was to eliminate formaldehyde or paraformaldehyde from the reaction mixture by expelling their vapours with the flowing nitrogen gas. An increase of *ca*. 10% monomer conversion was achieved, surprisingly this did not lead to an increase in MW. It was thought that the increase in monomer conversion could be due to loss of monomer vapours with the nitrogen flow.

Lastly the polymerisation was conducted under vacuum. The idea of conducting the polymerisation under vacuum was conceived when a batch of **M49** was being purified by vacuum distillation. A significantly lower yield was achieved and the majority of the crude product had polymerised in the round bottom flask during the distillation. The paraformaldehyde was found to have condensed in the liquid nitrogen trap. The same conditions were tested for the polymerisation using a controlled monomer feedstock (same as above). The reaction was conducted under vacuum at 90 °C (the monomer's boiling point). After 2 days, no polymer was formed. No reaction set ups were found to increase the level of polymer formation.

*Table 3.19. Polymerisations of **M49** using **C13** with various reaction set ups*

Monomer	Condition	Temp. (°C)	Time	Conv. (%)[a]	M_n[b]	$Đ$[b]
rac-**M49**	Sealed amp	180	3 d	25	6100	1.16
rac-**M49**	Sublimator	180	3 d	25	7500	1.21
rac-**M49**	Amp N_2 flow out	180	3 d	36	6500	1.30
rac-**M49**	Under vacuum	90	2 d	0	ND	ND

M49*:*C16:*BnOH = 500:1:1. Conducted in the absence of solvent. Conv. = Monomer conversion. [a] Monomer conversion determined from crude ^{1}H NMR spectrum. [b] Đ and M_n (g/mol) determined by gel permeation chromatography. ND = not determined due to polymer not being isolated.*

3.3.3 Attempted formation of a stereocomplex

In Chapter 1, formation of a **P1** stereocomplex was briefly discussed as a method to alter the thermal properties of the polyester. The two isotactic **P5**s were obtained from *R*-**M49** and *S*-**M49** monomers with the retention of stereochemistry by utilising **C13**. The goal of achieving a similar increase in thermal properties of **P5** was targeted by attempting to form the stereocomplex of **P5**.

The most prevalent procedure for stereocomplexation in the literature is solution casting into films.[39,40] This was conducted by making a solution of equal quantities of each isotactic **P5** and the film was formed by allowing the solvent to evaporate. Multiple solvents were tested including DCM, chloroform and THF. The solvent evaporation rates were modified by either conducting the casting in an open PTFE crystallisation dish in a fumehood or covering with a glass plate and placing it into an un-ventilated cupboard. Another common method for stereocomplex formation that was tested was by simply dissolving the two polymers together in DCM or THF and then precipitating from methanol.[41] Despite best efforts no changes were observed in the resulting DSC thermograms. The formation of a stereocomplex occurs between D-and L-**P1** due to the polymers configuring into a highly organised crystalline structure.[42] However, the theory behind stereocomplex formation and its higher stability were relatively unknown.[40,41] Keller *et al.* went about studying the crystalline structure of D-and L-**P1** stereocomplexes in order to better understand the key principles as to why it forms and use these principles to be able to predict future stereocomplex formation. The formation of D-and L-**P1** have been shown to grow in the presence of one another and their structure has been elucidated *via* x-ray diffraction, neutron diffraction, and computational modelling.[43,44] Presented in Figure 3.19 in the crystal structure. Firstly, upon visual inspection it is clear the disruption exchanging the methyl group of **P1** for the phenyl group of **P5** would be to this structure. Secondly, on predicting the potential of a pair of enantiomeric polymers forming a

stereocomplex Keller *et al.* state that the force field locking the structure together is sensitive to steric effects. Hence it is clear that the steric bulk of the phenyl that induces an increase in the glass transition temperature of **P5** has a role in hindering the growth of a stereocomplex from D-and L-**P5**.

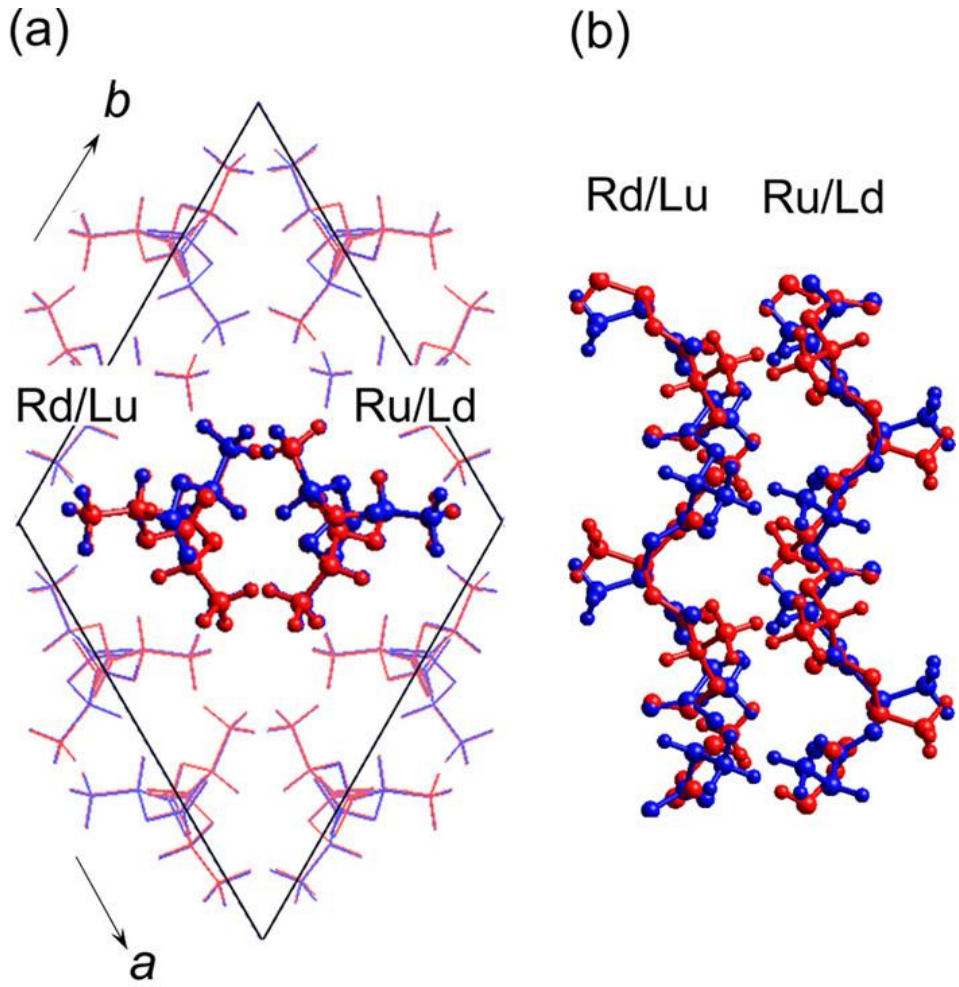

Figure 3.19. Crystal structure of PLLA/PDLA stereocomplex. One lattice site is statistically occupied by a pair of right hand down(Rd) and left hand up(Lu) chains and the neighbouring site by a pair of right hand up (Ru) and left hand down (Ld) chains: (a) along the c-axis and (b) along the 110 plane.

3.3.4 Enzymatic degradation

Polymer **P5** is a polyester that shows great promise toward the future of polyesters and their potential to be used in applications requiring shape retention at higher temperatures. It is common for aliphatic polyesters to be biodegradable, but the aromatic side chain of **P5** was identified as a potential threat to this. The ability for **P5** to degrade enzymatically was tested

following similar protocols used for the biodegradation of **P1**. The enzyme proteinase K was used rather than an esterase enzyme due to its cost and ease of access. The biodegradation was conducted on a 0.1 mm thick square film of **P5** (10 x 10 mm) and was incubated for 24 hours at 37 ˚C in a 1 mL buffer solution (H_2O, 30 mM TrisHCl (pH 8), 10 mM $CaCl_2$) containing proteinase K from tritirachium album (10 mg). The **P5** film was found to have lost 12% of its mass confirming its ability to degrade enzymatically.

3.4 5,2,2-Trimethyl-1,3-dioxolan-4-one and 2,2-Dimethyl-5-phenyl-1,3-dioxolan-4-one

The Tishchenko reaction has proven to a key issue for several factors of the polymerisation of both **M46** and **M49**. Primarily, it is hypothesised to be the cause of the misalignment between attained molecular weights and those expected and the inhibition of polymerisation rates due to the competition for catalyst between the reactions. Multiple attempts were made to remove the formaldehyde and or paraformaldehyde from the reaction to stop this occurring. Attempts were made by adjusting the reaction set up by different heating/cooling methods, by introducing a vacuum, a cold finger, and adding molecular sieves. However, all attempts failed to increase molecular weights, or monomer conversions. Another method to eliminate the Tishchenko reaction was to remove paraformaldehyde or any aldehydes from the equation completely. It was hypothesised that the polymerisation of a 1,3-dioxolan-4-one with two substituents at the two position would produce a PAHA with observed MWs in a greater alignment with the expected values. To do so it was necessary to ring close the α-hydroxy acids with a ketone.

3.4.1 The Synthesis of 2,2,5-Trimethyl-1,3-dioxolan-4-one and 2,2-Dimethyl-5-phenyl-1,3-dioxolan-4-one

To minimise the steric bulk increase at the 2 position of the monomers that is associated with increased substitution methyl groups were selected as the target substituents. Firstly, 2,2,5-trimethyl-1,3-dioxolan-4-one (**M50**) was synthesised by refluxing lactic acid in a solution of 50:50 acetone and benzene in the presence of PTSA. The reaction mixture was refluxed for 6 hours in a Deans-Stark apparatus to produce the desired product in a 60% yield (Scheme 3.8). Secondly, 2,2-dimethyl-5-phenyl-1,3-dioxolan-4-one (**M51**) was synthesised using the same method and a high yield of 95% was attained.

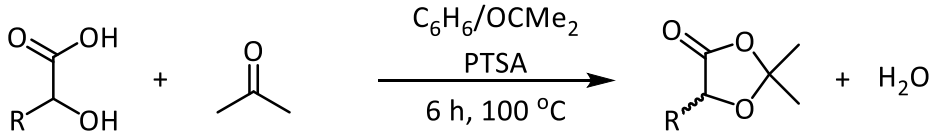

*Scheme 3.8. The synthesis of monomers **M50** and **M51** from lactic acid and mandelic acid respectively.*

Both of these monomers had been previously synthesised with acetone in the presence of a variety of catalysts. In the synthesis of monomer **M50** does not differ greatly from the previously reported one, however the use of benzene as the solvent in place of petroleum ether led to a 70 % increase in yield and a decrease in the reaction time from 40 h to 6 h.[45] The synthesis of monomer **M51** is aligned with the highest yields achieved for ring closing mandelic acid with acetone, as a 95% yield was also attained when conducting the synthesis using boron trifluoride diethyl etherate as the catalyst.[46] Purification of the monomer **M50** was similar to those performed for monomers **M45**, **M46** and **M49**, as it was conducted firstly by stirring the monomer over calcium hydride for 16 h, followed by vacuum distillation. The purification method of monomer **M51** was recrystallisation from anhydrous toluene. After purification the monomers were used for ROP.

3.4.2 Ring-opening polymerisation of 2,2,5-Trimethyl-1,3-dioxolan-4-one and 2,2-Dimethyl-5-phenyl-1,3-dioxolan-4-one

Attempted polymerisation of monomers **M50** and **M51** was firstly conducted under the similar conditions as those used for **M46** and **M49** (Scheme 3.9). A decreased monomer feedstock of M:C:I of 50:1:1 was used. An extended reaction period was required to achieve high conversion of monomer **M50**.

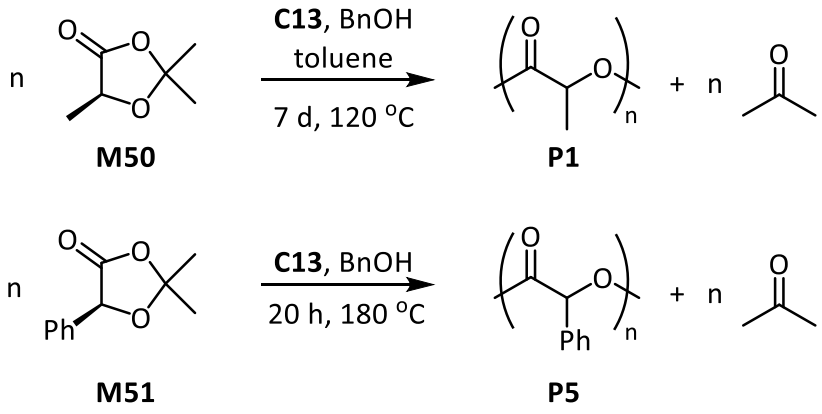

*Scheme 3.9. Polymerisations of monomers **M50** and **M51** using **C13** and BnOH to form polymers **P1** and **P5**.*

Due to the extended reaction time at 120 °C, the polymerisation of **M50** produced **P1** with a broader dispersity than from monomer **M46** (Entry 1, Table 3.20). Indicating that despite the reduced monomer feedstock the polymerisation of **M50** is difficult due to its stable nature along with the increased steric bulk proximal to the acyl oxygen. The same factors were the probable cause of the low conversion observed in Entry 2, Table 3.20, as no polymer was recovered from the polymerisation of **M51**, despite conducting the polymerisation at 120 °C for 7 days. A further increase in temperature was required for the polymerisation of **M51** (Entry 3, Table 3.20). The polymerisation was conducted in the absence of solvent at 180 °C and after 20 h an excellent conversion was reached. The polymerisation was thought to have been well controlled as the polymer **P5** produced had a narrow dispersity ($Đ$ = 1.23). Above all, the observed MW (M_n = 12800) of polymer **P5** aligned with the expected MW, as result that had not been previously realised through the polymerisation of **M49**. However, upon inspection of the ^{1}H NMR spectrum of the polymer produced from Entry 3, Table 3.20 it was observed that the polymer was atactic as a result of epimerisation. The harsh reaction conditions though leading to a well-controlled polymerisation of **M51** was also the cause of loss of isotacticity.

*Table 3.20. The polymerisation of monomers **M50** and **M51***

Entry	Monomer	Conc.	Temp.	Time	Conv.	$M_{n,\,th}$	M_n	$Đ$
1	**M50**	1M	120	7 d	95%	6948	4600	1.49
2	**M51**	1M	120	7 d	6%	/	/	/
3	**M51**	bulk	180	20 h	91%	13000	12800	1.23

*Monomer:**C13**:BnOH = 50:1:1. Conducted in the absence of solvent. Conv. = Monomer conversion. [a] Monomer conversion determined from crude ^{1}H NMR spectrum. [b] Đ and M_n (g/mol) determined by gel permeation chromatography.*

3.5 Conclusion

The monomers **M46** and **M49** were utilised to synthesise homopolymers **P1** and **P5**. The ring-opening polymerisation of both monomers were found to be well controlled and active when catalysed by catalyst **C13**. The polymerisation of **M49** was screened with a variety of MeAl(salen) catalysts. The rate of polymerisation was observed to be impacted by both the diimine bridge and phenoxide substituents. The dimethylpropyl bridged catalyst (**C16**) gave the highest rate of polymerisation, however, the M_n *vs* the expected MW of the resultant

polymer was the lowest produced by the range of MeAl(salen) screened. This was found to be caused by the prevalence of a side reaction. The products of the side reaction were observed to be **P1** with MeO- end groups and **P1** chains terminated with formate groups. The end groups were assumed to be the source of the decrease in MW. In order to circumvent the side reaction attempts to remove the polymerisation product, formaldehyde or its oligomer, were made, however various methods attempted failed. An alternate route to remove the Tishchenko reaction was to polymerise **M50** and **M51**, as replacement for **M46** and **M49**. The polymerisation though had poor rates and this led to undesired results such as an increased dispersity to **P1** and epimerisation of **P5**.

3.6 References

(1) Auras, R.; Harte, B.; Selke, S. *Macromol. Biosci.* **2004**, *4* (9), 835–864.

(2) Ikada, Y.; Tsuji, H. *Macromol. Rapid Commun.* **2000**, *21* (3), 117–132.

(3) Sawyer, D. J. *Macromol. Symp.* **2003**, *201* (1), 271–282.

(4) Drysdale, N. E.; Lin, K.; Stambaugh, T. W. Rare earth metal catalyzed oligomerization of alpha-hydroxycarboxylic acids and conversion to dimeric cyclic esters. WO1993018021A1, 1993.

(5) O'Brien, W. G.; Cariello, L. A.; Wells, F. Integrated process for the manufacture of lactide. WO1996006092A1, 1996.

(6) Riedel, J. D.; de Haën, E. Verfahren zur Darstellung von ß-Aminoäthylharnstoff. DE267826C, 1929.

(7) Gruber, P. R.; Hall, E. S.; Kolstad, J. J.; Iwan, M. L.; Benson, R. D.; Borchardt, R. L. Continuous process for manufacture of lactide polymers with controlled optical purity. US5247058, 1993.

(8) Vink, E. T. H.; Rábago, K. R.; Glassner, D. A.; Gruber, P. R. *Polym. Degrad. Stab.* **2003**, *80* (3), 403–419.

(9) Kobayashi, S.; Yokoyama, T.; Kawabe, K.; Saegusa, T. *Polym. Bull.* **1980**, *3* (11), 585–591.

(10) Whitesell, J. K.; Pojman, J. A. *Chem. Mater.* **1990**, *2* (3), 248–254.

(11) Pinkus, A. G.; Subramanyam, R. *J. Polym. Sci. Polym. Chem. Ed.* **1984**, *22* (5), 1131–1140.

(12) Liu, T.; Simmons, T. L.; Bohnsack, D. A.; Mackay, M. E.; Smith, M. R.; Baker, G. L. *Macromolecules* **2007**, *40* (17), 6040–6047.

(13) Buchard, A.; Carbery, D. R.; Davidson, M. G.; Ivanova, P. K.; Jeffery, B. J.; Kociok-Köhn, G. I.; Lowe, J. P. *Angew. Chemie - Int. Ed.* **2014**, *53* (50), 13858–13861.

(14) Macdonald, J. P.; Shaver, M. P. In *ACS Symposium Series*; 2015; Vol. 1192, pp 147–167.

(15) Numata, K.; Srivastava, R. K.; Finne-Wistrand, A.; Albertsson, A. C.; Doi, Y.; Abe, H. *Biomacromolecules* **2007**, *8* (10), 3115–3125.

(16) Kisler, J. M.; Dähler, A.; Stevens, G. W.; O'Connor, A. J. *Microporous Mesoporous*

Mater. **2001**, *44* (Supplement C), 769–774.

(17) Min Wang, Q.; Shen, D.; Bülow, M.; Ling Lau, M.; Deng, S.; Fitch, F. R.; Lemcoff, N. O.; Semanscin, J. *Microporous Mesoporous Mater.* **2002**, *55* (2), 217–230.

(18) Westheimer, F. H.; Taguchi, K. *J. Org. Chem.* **1971**, *36* (11), 1570–1572.

(19) Williams, D. B. G.; Lawton, M. *J. Org. Chem.* **2010**, *75* (24), 8351–8354.

(20) Coster, D.; Blumenfeld, A. L.; Fripiat, J. J. *J. Phys. Chem.* **1994**, *98* (24), 6201–6211.

(21) Jansen, J. C.; Creyghton, E. J.; Njo, S. L.; van Koningsveld, H.; van Bekkum, H. *Catal. Today* **1997**, *38* (2), 205–212.

(22) Woolery, G. L.; Kuehl, G. H.; Timken, H. C.; Chester, A. W.; Vartuli, J. C. *Zeolites* **1997**, *19* (4), 288–296.

(23) Corma, A.; Planelles, J.; Sánchez-Marín, J.; Tomás, F. *J. Catal.* **1985**, *93* (1), 30–37.

(24) Hormnirun, P.; Marshall, E. L.; Gibson, V. C.; Pugh, R. I.; White, A. J. P. *Proc. Natl. Acad. Sci. U. S. A.* **2006**, *103* (42), 15343–15348.

(25) Sugimoto, H.; Ohtsuka, H.; Inoue, S. *J. Polym. Sci. Part A Polym. Chem.* **2005**, *43* (18), 4172–4186.

(26) Luo, W.; Shi, T.; Liu, S.; Zuo, W.; Li, Z. *Organometallics* **2017**, *36* (9), 1736–1742.

(27) Neitzel, A. E.; Petersen, M. A.; Kokkoli, E.; Hillmyer, M. A. *ACS Macro Lett.* **2014**, *3* (11), 1156–1160.

(28) Miller, S. A.; Martin, R. T. Polyesteracetals. US8653226, 2014.

(29) Stockmayer, W. H. *J. Polym. Sci. Polym. Lett. Ed.* **1979**, *17* (4), 246–247.

(30) Pearce, E. M. *J. Polym. Sci. Part A Polym. Chem.* **1992**, *30* (7), 1508–1508.

(31) Allcock, H. R.; Lampe, F. W.; Mark, J. E. *Contemporary polymer chemistry (3rd edition).*; John Wiley & Sons, Ltd., 2003; Vol. 53.

(32) Hong, M.; Chen, E. Y.-X. *Nat. Chem.* **2015**, *8* (1), 42–49.

(33) Hong, M.; Chen, E. Y.-X. *Angew. Chemie Int. Ed.* **2016**, *55* (13), 4188–4193.

(34) Vidyasagar Reddy, G.; Sreevani, V.; Iyengar, D. S. *Tetrahedron Lett.* **2001**, *42* (3), 531–532.

(35) Bylikin, S. Y.; Shipov, A. G.; Kramarova, E. P.; Negrebetsky, V. V.; Korlyukov, A. A.; Baukov, Y. I.; Hursthouse, M. B.; Male, L.; Bassindale, A. R.; Taylor, P. G. *J.*

Organomet. Chem. **2009**, *694* (2), 244–248.

(36) Cairns, S. A.; Schultheiss, A.; Shaver, M. P. *Polym. Chem.* **2017**, *8* (19), 2990–2996.

(37) Połoński, T. *Tetrahedron* **1983**, *39* (19), 3139–3143.

(38) Hormnirun, P.; Marshall, E. L.; Gibson, V. C.; White, A. J. P.; Williams, D. J. *J. Am. Chem. Soc.* **2004**, *126* (9), 2688–2689.

(39) *Polymer (Guildf).* **1999**, *40* (24), 6699–6708.

(40) Fumitaka, H. T.; Hyon, H. S.; Ikada, Y. **1990**, 2719–2724.

(41) Tsuji, H.; Hyon, S.-H.; Ikada, Y. *Macromolecules* **1991**, *24*, 5657–5662.

(42) Ikada, Y.; Jamshidi, K.; Tsuii, H.; Hyon, S. H. *Macromolecules* **1987**, *20* (4), 904–906.

(43) Wasanasuk, K.; Tashiro, K.; Hanesaka, M.; Ohhara, T.; Kurihara, K.; Kuroki, R.; Tamada, T.; Ozeki, T.; Kanamoto, T. *Macromolecules* **2011**, *44* (16), 6441–6452.

(44) Brizzolara, D.; Cantow, H.-J.; Diederichs, K.; Keller, E.; Domb, A. J. *Macromolecules* **1996**, *29* (1), 191–197.

(45) Watanabe, K.; Andou, Y.; Shirai, Y.; Nishida, H. *Chem. Lett.* **2013**, *42* (2), 159–161.

(46) Cavelier, F.; Gomez, S.; Jacquier, R.; Verducci, J. *Tetrahedron: Asymmetry* **1993**, *4* (12), 2501–2505.

Chapter 4. Functionalised Poly(α-hydroxy acid)s from Substituted 1,3-Dioxolan-4-ones

4.1 Introduction

In Chapters 2 and 3, a new and competitive strategy to synthesise PAHAs from 1,3-dioxolan-4-ones has been realised (Scheme 4.1). Monomer **M45** was copolymerised with three monomers, that are commonly used in ROP, to synthesise copolymers **P3**, **P11** and **P12**. The monomer **M45** granted better control of the copolymer's chemical composition directly from the initial monomer feedstock ratio than previously achieved from copolymerising monomers **M1** and **M2**. The methyl substituted equivalent, **M46**, was first observed as an equilibrium side product from ring-closing a single unit of lactic acid unit from **P3** with expelled formaldehyde from the polymerisation of **M44**. The homopolymerisation of **M46** was an efficient strategy to synthesise **P1**, more specifically L-**P1**, as the synthetic route left the chirality of lactyl units unchanged. Investigating the effects of ligand alterations to MeAl(salen)'s ability to polymerise **M46** provided critical information to understand the side reactions that limit MWs. The phenyl substituted PAHA was then targeted to benchmark the synthetic strategy against other synthetic routes due to the inherent difficulty to obtain isotactic **P5**. Following catalyst screening, *S*-**M49** and *R*-**M49** were polymerised to form L-**P5** and D-**P5** respectively. Higher MW **P5** was obtained by simply increasing the initial monomer to initiator ratio and reaction temperature.

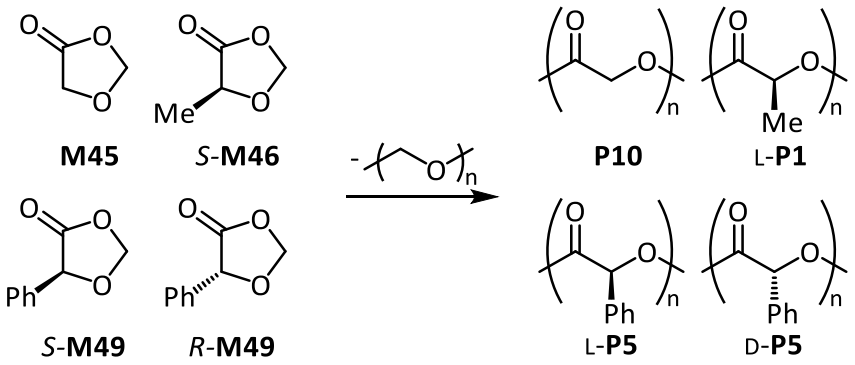

Scheme 4.1. Summary of 1,3-dioxolan-4-one polymerisations thus far.

As discussed in Chapter 1, a variety of substituted diesters were synthesised and polymerised by tin catalysts to form PAHAs with pendant functional groups including alkyl, aryl, alkyl chloride, alkenyl, alkynyl, hydroxyl and carboxyl groups. The pendant groups were found to have significant influence over the polymers' properties. Hence a wide variety of functionalised PAHAs have been synthesised and have been tested for an even wider variety of applications.

4.2 Alkyl Substituted Poly(α-hydroxy acid)s

A variety of substituent groups were selected as they were previously found to have a significant impact on the thermal properties of the resultant polymer.[1–4] A variety of simple carbon chains were substituted to the PAHA backbone in order to alter the rotational barrier around the polymer chain and thus alter the polymer's T_g. The ROP of diesters illustrated that PAHAs were capable of having a wide array of T_gs, however, as outlined in Chapter 1 the synthesis of the diester monomers was both challenging and low yielding. Hence, a variety of alkyl substituted 1,3-dioxolan-4-ones were used as monomers in order to install carbon chains of different lengths and branching. The impact of the selected substituents on polymerisation activity was a focus of the research presented in this chapter.

4.2.1 Synthesis of Alkyl Substituted 1,3-Dioxolan-4-one Monomers

A variety of alkyl substituted 1,3-dioxolan-4-ones were selected with the objective of obtaining the monomers in greater yields than the poor yields outlined previously for their diester counterparts. The appropriate α-hydroxy acids were needed in order to subsequently synthesise the 1,3-dioxolan-4-ones. The α-hydroxy acids available without the need for any prior reaction were hexahydromandelic acid and α-hydroxy^{n}caproic acid. The number of naturally occurring α-hydroxy acids are rather limited and hence it was necessary to turn to other precursors for the route to remain sustainable. Cohen-Arazi *et al.* used amino acids to reach a number of PAHAs in 2008, but only attempted the polycondensation.[5] They used a diazotisation to convert the amino functionality to a hydroxy inexpensively and reliably.[6] The amino acids valine, ^{i}leucine and ^{t}leucine were reacted with sodium nitrite in acidified water to form valic acid, α-hydroxy^{i}caproic acid and α-hydroxy^{t}caproic acid, respectively, in good to excellent yields (Scheme 4.2).

Scheme 4.2. Diazotisation of amino acids to form α-hydroxy acids.

All five α-hydroxy acids were subsequently used to synthesise substituted 1,3-dioxolan-4-ones by refluxing the appropriate acid with an excess of paraformaldehyde in the presence of a weak acid (Scheme 4.3). The reaction mixture was refluxed with a Deans-Stark apparatus in order to remove the reaction by-product. The reaction was also conducted in very dilute conditions in order to avoid the formation of oligomeric or polymeric side products.

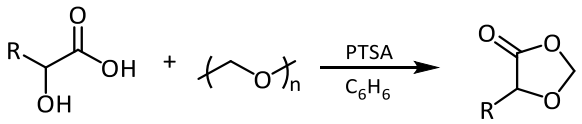

Scheme 4.3. Formation of substituted 1,3-dioxolan-4-ones from α-hydroxy acids.

Table 4.1. Alkyl substituted diesters, 1,3-dioxolan-4-ones, and their yields.

Entry	Functional group	Diester monomer	Diester monomer yield (%)	1,3-dioxolan-4-one monomer	1,3-dioxolan-4-one yield (%)
1	^{i}propyl	**M6**	16[1]	**M52**	90
2	cyclohexyl	**M5**	21[1]	**M53**	92
3	^{n}butyl	**M57**	10[a][7]	**M54**	60
4	^{i}butyl	**M10**	71[2]	**M55**	94
5	^{t}butyl	/	/	**M56**	60

[a] Previously not discussed as the polymerisation of the monomer has not yet been reported and the yield is presented from a patent.[8]

The 1,3-dioxolan-4-one monomers were all improved upon the yields of their diester counterparts, as observed by comparing the yields between the synthetic routes in Table 4.1. The yields of ^{i}propyl, ^{n}butyl and cyclohexyl substituted monomers were increased by greater than five, four and six times, respectively (Entries 1, 2 and 3, Table 4.1), while the increase for monomer **M55** baring a ^{i}butyl substituent was not as great at 23% (Entry 4, Table 4.1). No comparisons could be made for the ^{t}butyl substituents as the synthesis of the diesters has not yet been reported.

4.2.2 Polymerisation of Alkyl Substituted 1,3-Dioxolan-4-ones

Monomers **M52**-**M56** were polymerised following the optimal conditions found for **M46** and **M49**. Monomers were polymerised with a **C13** and benzyl alcohol initiating/mediating system at a monomer loading of 100:1:1. Polymerisations were undertaken in toluene (1 M)

at 120 °C. Polymerisations were halted by cooling and adding several drops of methanol to quench the reaction. A crude sample was removed and dissolved in $CDCl_3$. The monomer conversion was calculated *via* ^{1}H NMR spectroscopy by comparing the relative integrations of monomer and polymer peaks. The appropriate peaks used for each monomer were as follows in the form Monomer (monomer, polymer): **M52** (4.04, 5.08-4.83), **M53** (4.03, 5.05-4.87), **M54** (4.16, 5.21-5.03), **M55** (4.20, 5.14-5.04) and **M56** (3.82, not determined). **M50** was polymerised to low conversion in 20 hours and the polymer's dispersity was broad (Entry 1, Table 4.2). However, the M_n of the polymer aligned well with the expected value. From Entries 2 and 3 the observed MW (M_n) was lower than the expected MW ($M_{n,th}$), while Entry 4's observed MW was also decreased in comparison to the expected MW. This suggests that side reactions were most prolific for **M53** and **M54**. Whether this was due to NMR inactive impurities, competing transesterification reactions or the Tishchenko reaction was not investigated. No reaction was observed following the attempted polymerisation of **M56** over 3 days.

*Table 4.2. Polymerisation data for **M52 - M56**.*

Entry	Monomer	Time (h)	Conv.[a]	$M_{n,th}$[b]	M_n[c]	$Đ$[c]
1	**M52**	20	33	3400	3800	1.48
2	**M53**	72	65	9200	1500	1.26
3	**M54**	72	97	11160	1800	1.42
4	**M55**	72	99	11390	7500	1.06
5	**M56**	72	0	/	/	/

*Monomer:**C13**:BnOH = 100:1:1. Monomer concentration = 1 M in toluene. The reactions were conducted at 120 °C. Conv. = Monomer conversion. [a] monomer conversion (%) determined from crude 1H NMR spectrum. [b] $M_{n,th}$ (g/mol) = (Monomer:BnOH) × (MW(monomer) – 30) × (conv (%)) + MW(end group). [c] Đ, M_n (g/mol), and M_w (g/mol) determined by gel permeation chromatography using a fixed dn/dc = 0.05g/mL.*

Kinetic experiments were conducted in Youngs tap NMR tubes. Each monomer was dissolved in a toluene-d_8 solution of **C13** and BnOH. The reaction mixture was charged to an NMR tube, sealed, removed from the glovebox and loaded into an NMR spectrometer preheated to 100 °C. NMR spectra were recorded periodically over 8 hours (Figure 4.1).

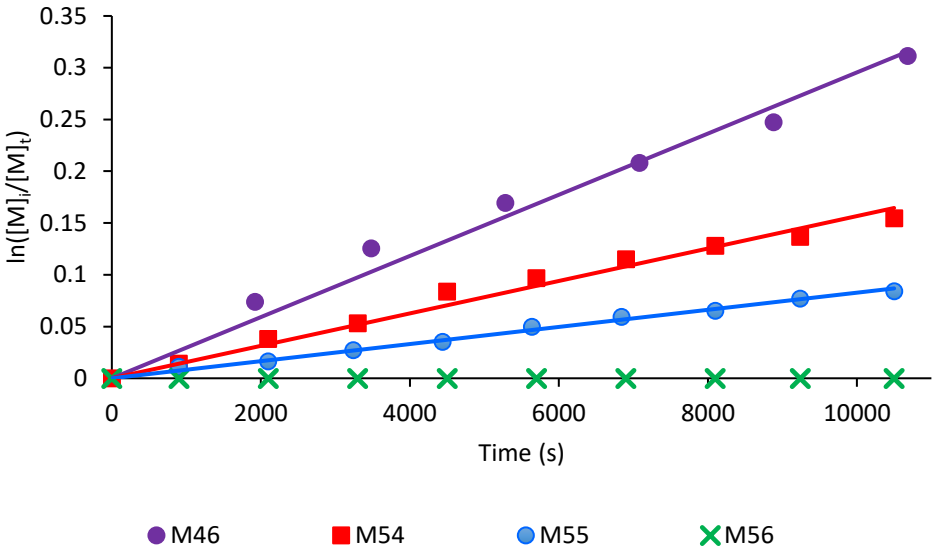

*Figure 4.1. Pseudo first order kinetics of **M46**, **M54**, **M55** and **M56**.*

The kinetic profile of these polymerisations confirm that they are well controlled, however, low conversions were observed under these conditions. The observed first order rate constants were found to follow the trend: **M46** >**M54** >**M55** (k_{obs} = 3.0 × 10^{-5} s^{-1}, 1.6 × 10^{-5} s^{-1}, 8.3 × 10^{-6} s^{-1}). The trend illustrates that the larger butyl substituents have a significant impact on the rate. The rates between butyl isomers were also significantly different. It was found that bulk proximity to the body of the monomer and or the degree of branching decreased the rate dramatically (Figure 4.2). In the case for monomer **M56**, substituted with the most sterically encumbering group, no polymer formed.

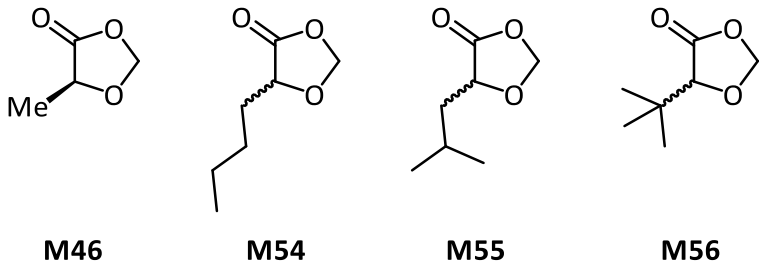

*Figure 4.2. Monomers **M46**, **M54**, **M55**, and **M56***

These studies were found to be in support of our mechanistic hypothesis that steric bulk dictates the observed rate, by impacting monomer coordination to the bulky catalyst **C13**. Though the impurities suspected to be present in **M54**, due to its decreased M_ns, does mean that no definitive conclusions can be made. The thermal properties accessible through this new synthetic route have been diversified by polymerising this range of alkyl substituted monomers. The T_g values for PAHAs synthesised thus far vary from 22 – 115 °C (Table 4.3).

Table 4.3. Glass transition temperatures of PAHAs synthesised from 1,3-dioxolan-4-ones.

Entry	Monomer	R	T_g (°C)	
1	**M46**	*R*-Me	59	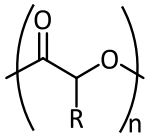
2	*rac*-**M49**	*rac*-Ph	100	
3	*S*-**M49**	*R*-Ph	115	
4	**M50**	^{i}Pr	41	
5	**M53**	Cy	98	
6	**M55**	^{i}Bu	22	

Glass transition temperatures as originally reported.[1,2,9,10]

Though the thermal properties of a polymer have a significant impact on the applications it can be used for, the other properties of PAHAs, such as polarity, are still limited when substituted with an alkyl or aryl group. A variety of pendant functional groups were added to 1,3-dioxolan-4-ones to broaden the available functionalities of the PAHAs synthesised from this new synthetic strategy.

4.3 Alkyne Substituted Poly(α-hydroxy acid)

One of the most dynamic functional groups installed onto a PAHA has been an alkyne group. As discussed in Chapter 1, the versatility of the alkyne functionality was illustrated in its ability to be modified in post-polymerisation reactions, such as using azide-alkyne click chemistry to attach paclitaxel-poly(ethylene glycol) to a polyester backbone, thus synthesising a drug conjugate graft copolymer. Monomers **M19**, **M33**, **M34** and **M42** have been polymerised to form both homopolymers or copolymers with **M2**. The resultant polymers were modified post-polymerisation to achieve the appropriate properties for implementation across a range of applications in biomedical fields by grafting various side chains *via* click chemistry or by radical thiol addition (Scheme 4.4).[11–15] However, the synthesis of **M19**, **M33** and **M34** are poor yielding and the synthesis of **M42** requires the use of toxic and expensive reagents. Thus, the importance of implementing alkyne substituted 1,3-dioxolan-4-ones to synthesise functionalised PAHAs has been established, as substituted monomers **M46** and **M49** displayed increased yields in comparison to their diester equivalents and avoided the use of extremely toxic reagents.

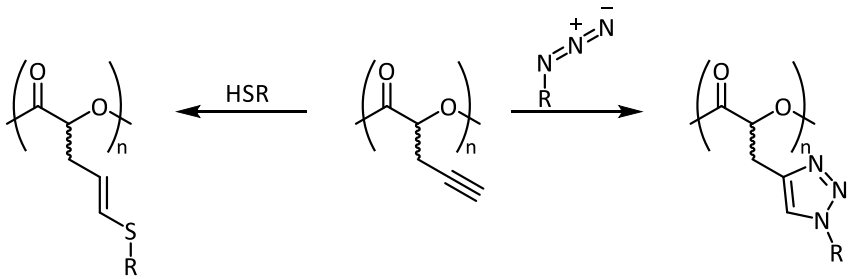

Scheme 4.4. Examples of post-polymerisation modifications to aryl functionalised PAHA.[15,16]

Alkyne functionality has been selected for use in imaging drug delivery *via* Raman spectroscopy, an emerging tool in the biomedical field. Due to their Raman shift/vibrational stretching frequency being *ca.* 2100 cm^{-1}, alkyne groups have been used as a bioorthoganal chemical reporter. Sodeoka *et al.* found that natural cellular molecules are Raman inactive between 1800 and 2800 cm^{-1} (cell silent region).[17] Hong *et al.* used stimulated Raman spectroscopy to acquire a spectrum of a single HeLa cell and also noted that a cellular silent region between 1800 and 2800 cm^{-1} was present in live cells (Figure 4.3).[18]

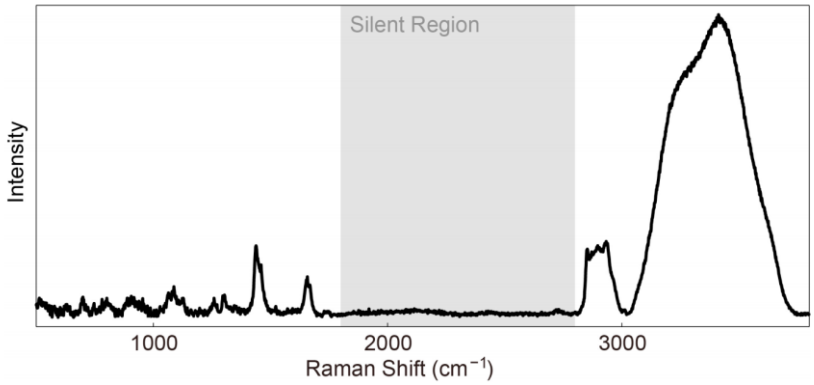

Figure 4.3. Spontaneous Raman spectrum acquired from a single live HeLa cell.[18]

The Raman shift of an alkyne functionality provided an excellent opportunity to image biomolecules in live cells. An alkyne tagged thymidine, 5-ethynyl-2'-deoxyuridine (EdU), was shown *via* Raman spectroscopy to be taken up into cellular DNA and was found to accumulate in the nucleus of the cell (Figure 4.4).

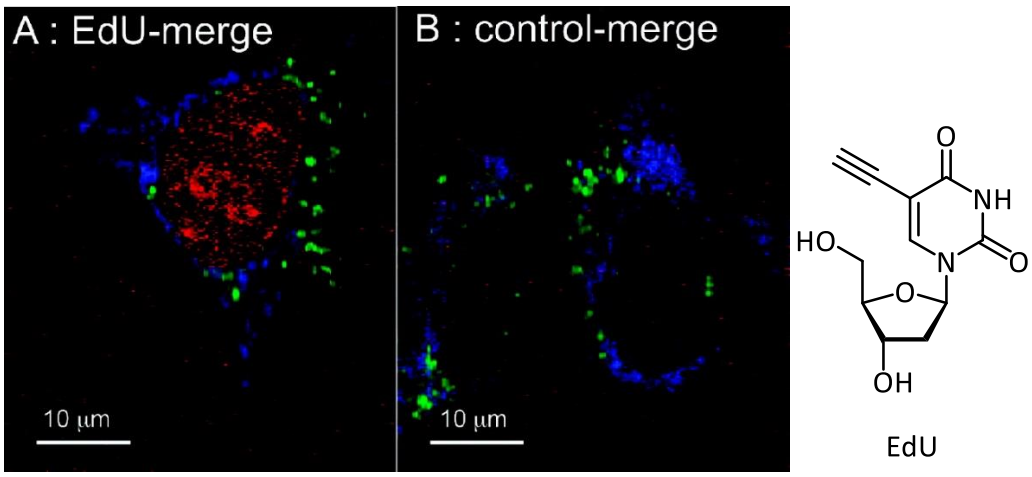

Figure 4.4. Merged Raman imaging of HeLa cell (749 cytochrome, 2123 EdU, and 2849 lipid cm^{-1}). A. Raman image obtained from HeLa cells treated with EdU. B. Raman image from control HeLa cells.[17]

Our goal of incorporating alkyne functionality to a PAHA has the potential use for imaging nanoparticles of **P3**. Nanoparticles of **P3** have been approved by the FDA for use in the body as a drug delivery system and imaging the delivery *via* Raman spectroscopy would provide a further handle to monitor nanoparticles. Nanoparticles are used as they encapsulate therapeutic drugs and deliver them *in vivo,* in their active form with elongated lifetimes. Nanoparticles release the bioactives over a sustained period which allows for the active ingredient to reach therapeutic window concentrations.[19] A novel alkyne functionalised 1,3-dioxolan-4-one was designed and synthesised. The monomer was polymerised to firstly synthesise homopolymer and secondly to synthesise a copolymer. The copolymer synthesised primarily consisted of **P3**, and was doped with alkyne functionalised α-hydroxy acid units.

4.3.1 Synthesis of 5-Propargyl-1,3-dioxolan-4-one

Unlike the alkyl substituted α-hydroxy acids, the amino acid counterpart to the propargyl substituted α-hydroxy acid is not commercially available and thus a new route was needed. The parent α-hydroxy acid had been synthesised previously by several groups and a similar procedure was used for this work.[20,21] Glyoxalate based compounds offer the opportunity to provide α-hydroxy acids after a nucleophilic addition to the aldehyde and hydrolysis of the ester. To obtain the propargyl substituent, propargyl bromide was reacted with ethyl glyoxalate catalysed by Zn in a Barbier reaction (Scheme 4.5). The ethyl ester was then modified to form the carboxylic acid by acid hydrolysis.

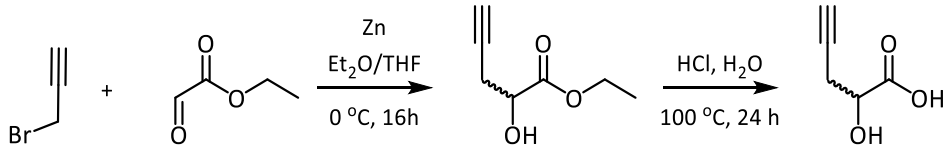

Scheme 4.5. Synthesis of 2-hydroxy-4-pentynoic acid from ethyl glyoxalate and propargyl bromide.

Using the same conditions used to synthesise the other substituted 1,3-dioxolan-4-ones, propargyl substituted 1,3-dioxolan-4-one was cyclised with paraformaldehyde in 66% yield. The yield of 5-propargyl-1,3-dioxolan-4-one (**M58**) was moderate and was greater than the yields of the diester equivalents **M19**, **M33**, **M34** and the OCA based on alkyne functionalised tyrosine **M42** by at least 20%.

4.3.2 Homopolymerisation of 5-Propargyl-1,3-dioxolan-4-one

The polymerisation of **M58** was conducted following the optimised conditions found for **M46**, and **M49**, as **C13** and BnOH were used as the initiation system (Scheme 4.6). Polymerisations were conducted with an initial monomer concentration of 1 M in toluene at 120 °C. Monomer conversion was obtained by conducting ^{1}H NMR spectroscopy on a crude sample and was calculated from the relative integrals of the monomer (**M58**) and polymer (**P15**) methine peaks, 4.42-4.35 and 5.31-5.46, respectively.

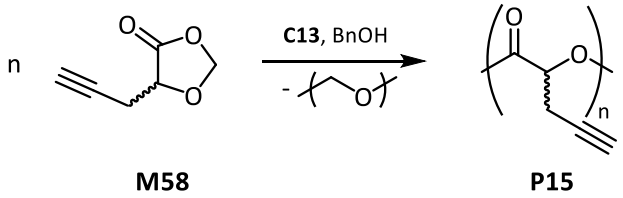

*Scheme 4.6. Homopolymerisation of **M58** to form **P15**, using **C13** and BnOH as the catalyst and initiator respectively.*

A kinetic experiment was undertaken to investigate if the polymerisation was living. The experiment was conducted by periodically removing aliquots from an ongoing polymerisation, quenching the sample and conducting ^{1}H NMR spectroscopy on the crude sample (Figure 4.5). From Figure 4.5, the polymerisation is found to follow first order reaction kinetics. The first two points of the kinetic plot lie significantly beneath the line drawn to represent the pseudo first order kinetic profile. This is a sign of an induction period and is likely caused by slow insertion of the benzyloxide due to its steric bulk clashing with the propargyl substituent of **M58**. The reaction does not proceed any slower than expected for the substituent's steric bulk and suggests that the alkyne functionality does not interfere with the activity of the polymerisation.

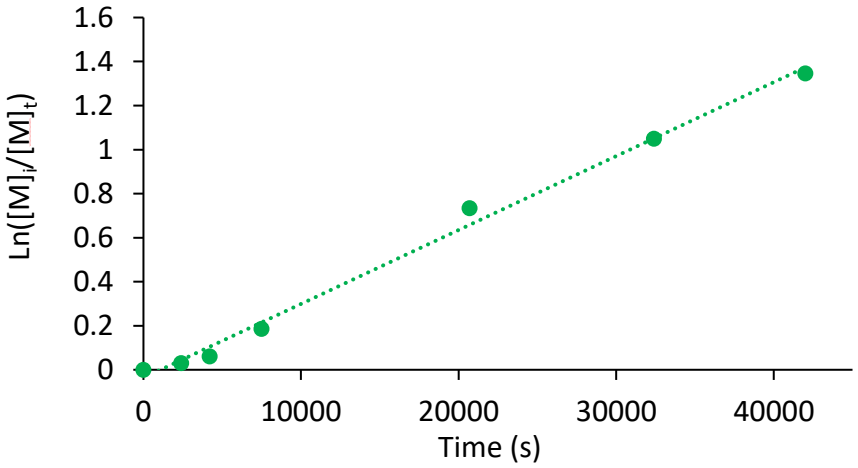

*Figure 4.5. First order kinetics plot of the homopolymerisation of **M58**.*

The MW of the growing polymer chains was investigated during the reaction (Figure 4.6). Homopolymerisations of **M58** were conducted to various time-points. Each polymer was worked up and GPC analysis was conducted on the samples. Due to overlapping of the peak of interest with permeation peaks in the GPC chromatograms an accurate representative of M_n could not be obtained. However, the MW at the peak of the chromatogram (M_p) was used as a more accurate representation of the MW of the sample and for comparative purposes all data points were obtained in this manner.

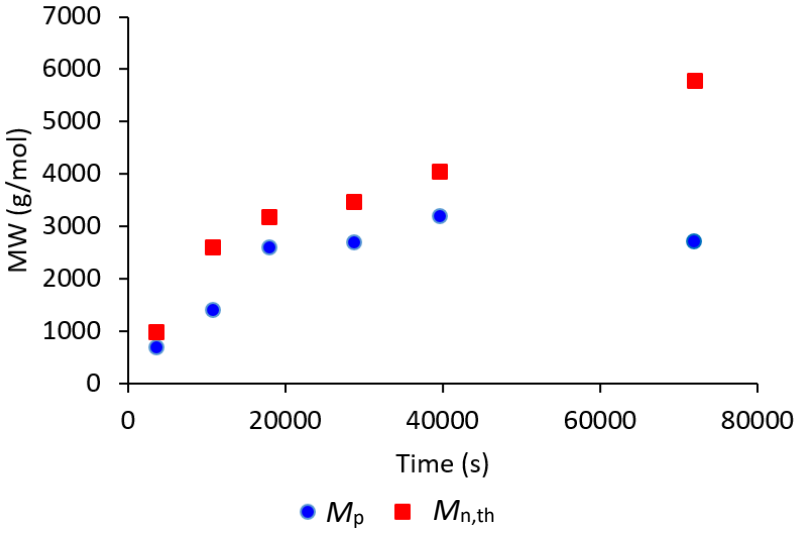

*Figure 4.6. The observed and theoretical MWs of the homopolymerisation of **M58** at various times.*

The observed MW of **P15** aligned with the expected MW during the early period of the polymerisation. As expected all M_p points were lower than their related $M_{n,th}$ values. From the penultimate point to the final a larger time period was used, between these time-points an 18%

increase in monomer conversion was observed. However, over this period the M_p was found to decrease, a similar phenomenon was presented in Chapter 3. As an elongated time period was required to reach the final point in the polymerisation of **M46**, the observed MW (M_p) decreased. Deviations from the expected values are likely to be caused by an increase in paraformaldehyde available to participate in Tishchenko reactions at high conversions. It was hypothesised that this problem would not have an impact as significant when forming the final copolymer target, as the relative levels of eliminated formaldehyde to polymer would be reduced.

4.3.3 Copolymerisation of 5-Propargyl-1,3-dioxolan-4-one with Lactide and Glycolide

The homopolymerisation of 1,3-dioxolan-4-ones have been most well controlled using **C13** and was used in the initials attempts to copolymerise monomers **M1**, **M2** and **M58** to form copolymer **P16**. Copolymerisations were set up as previously described, the entire monomer feedstock was placed into the reaction vessel followed by the catalyst/initiator solution. Copolymerisations were conducted in the toluene at 120 °C (Table 4.4). ^{1}H NMR spectroscopy showed the incorporation of 2-hydroxypropynoic acid units in the worked-up polymer (Figure 4.7). It was necessary to increase polymerisation times, to two, five and five hours for one, five and ten percent of **M58**, respectively, in order to reach high conversions and insure complete incorporation (Entries 2, 3 and 4, Table 4.4.) and. As loadings of **M58** and reaction times were increased a trend was seen as the dispersity of the resultant copolymers increased.

*Table 4.4. Copolymerisations of **M1**, **M2** and **M58***

Entry	n	m	l	Time (h)	**M1**[a] conv.	**M2**[a] conv.	**M58**[a] conv.	$M_{n,th}$[b]	M_n[c]	$Đ$[c]
1	49.95	49.95	0.1	1	100	100	/	13100	25300	1.08
2	49.5	49.5	1	2	100	100	/	13000	21700	1.26
3	47.5	47.5	5	5	100	100	100	13000	23000	1.43
4	45	45	10	5	100	100	92	12800	6000	1.57

*(**M1**+**M2**+**M58**):**C13**:BnOH = 100:1:1. Monomer concentration = 1 M in toluene. The reactions were conducted at 120 °C. Conv. = Monomer conversion. [a] monomer conversion (%) determined from crude ^{1}H NMR spectrum. [b] $M_{n,th}$ (g/mol) = (**M1**:BnOH) × MW(**M1**) × (conv (%)) + (**M2**:BnOH) × MW(**M2**) × (conv (%)) + (**M58**:BnOH) × (MW(**M58**) – 30) × (conv (%)) + MW(end group). [c] Đ and M_n (g/mol) determined by gel permeation chromatography*

The polymerisations from Entries 1, 2 and 3, Table 4.4, formed a large portion of insoluble solid when dissolution of the reaction mixture was attempted. As presented in Chapter 2, polymers with large fractions of **P10** or have elongated **P10** chains become insoluble. This is

likely to have caused the increase in the observed MW, as insoluble polymer chains are removed during the reaction the ratio of monomer to propagating chains is increased. Entry 4 was the only polymerisation to form polymer samples with no insoluble portion, however, it produced polymer with half the expected MW. The obtained polymers permitted preliminary Raman spectroscopy to be conducted. All Raman spectroscopy in Section 4.3.3 was conducted with the assistance of Ms Sally Vanden-Hehir. A peak was present at a Raman shift of 2128 cm^{-1}. However, it was not present in the polymer produced from Entries 1 and 2 in Table 4.4. From the preliminary Raman spectra, it was concluded that 10% alkyne functionalised repeat units were required to give an intense Raman signal in the cell silent region and provided the best opportunity to image the polymer in cells.

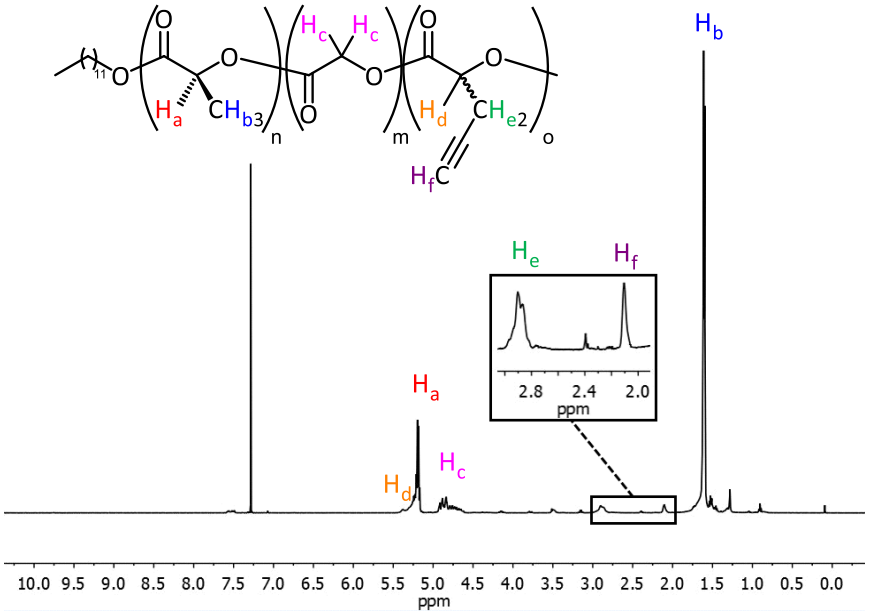

*Figure 4.7. ^{1}H NMR spectroscopy of resultant polymer **P16** from the copolymerisation of **M1**, **M2** and **M58**, Entry 3, Table 4.4 ($CDCl_3$, 300 K, 500 MHz).*

Another route was needed to be devised to increase the accuracy of the alkyne loadings, in order to obtain the loadings required for an intense alkyne Raman signal. The route was primarily designed to mitigate the deviation of the observed MW from the expected MW caused by the polymerisation of monomer **M58**. It was also necessary to insure all the resultant polymer was soluble. The aluminium based catalyst used has not received FDA approval and hence catalyst **C1** was used in the polymerisations henceforth. Polymer **P3** was firstly formed from the copolymerisation of monomers **M1** and **M2** with a ratio of 3:7, this ratio was used in order to decrease the amount of insoluble polymer obtained. The polymerisation was initially loaded with all of **M2** and monomer **M1** was fed into the polymerisation as small portions

over the course of the reaction (Scheme 4.7). Conversions of > 90% were achieved and the polymer produced had a M_n of 5700 g/mol and $Đ$ = 1.11.

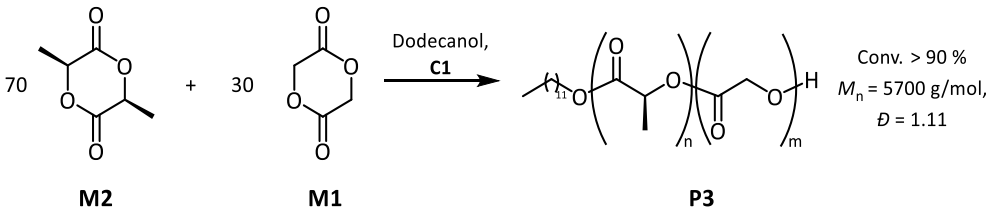

*Scheme 4.7. Copolymerisation of **M1** and **M2**, initiated with dodecanol and catalysed by **C1**.*

The telechelic property of **P3** was subsequently used to add the alkyne functionality. The polymerisation of **M58** was conducted using **P3** as a macroinitiator and was catalysed by **C1** (Scheme 4.8). The ability of catalyst **C1** to participate in transesterification reactions is often regarded as a detriment to its ability to control MW distributions. However, in this experiment, an elongated reaction time permitted 2-hydroxy-pentynoic acid units to be statistically distributed through the polymer. The polymerisation resulted in an increase in both in the observed MW (M_n = 5900 g/mol, calculated using the dn/dc value of **P3** = 0.05 mL/g[22]) and dispersity ($Đ$ = 1.88). Incorporation of the alkyne was illustrated by ^{1}H NMR spectroscopy and confirmed by the presence of only a single diffusion coefficient present following DOSY NMR spectroscopy.

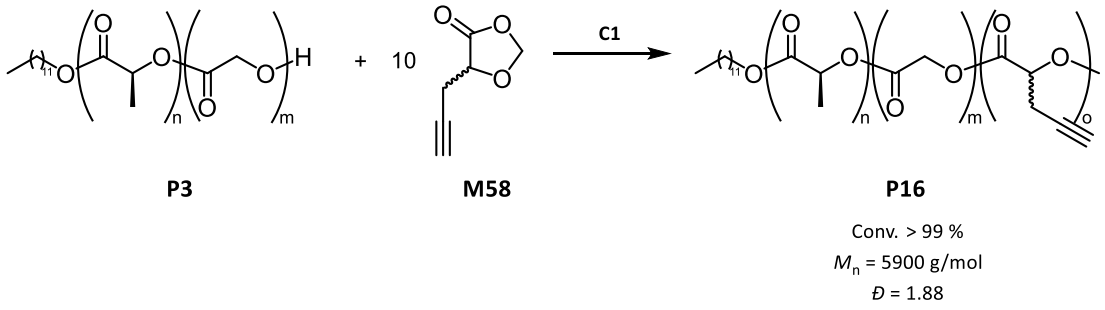

*Scheme 4.8. Polymerisation of **M58** using a **P3** macroinitiator and catalysed by **C1**.*

Raman spectroscopy was conducted on both pre- and post-alkyne functionalisation of the **P3**. The spectra are stacked below to illustrate the presence of the alkyne shift in polymer only after reaction with **M58** (Figure 4.8). This confirms that upon functionalisation with pendant alkyne groups may a peak appear in the cell silent region.

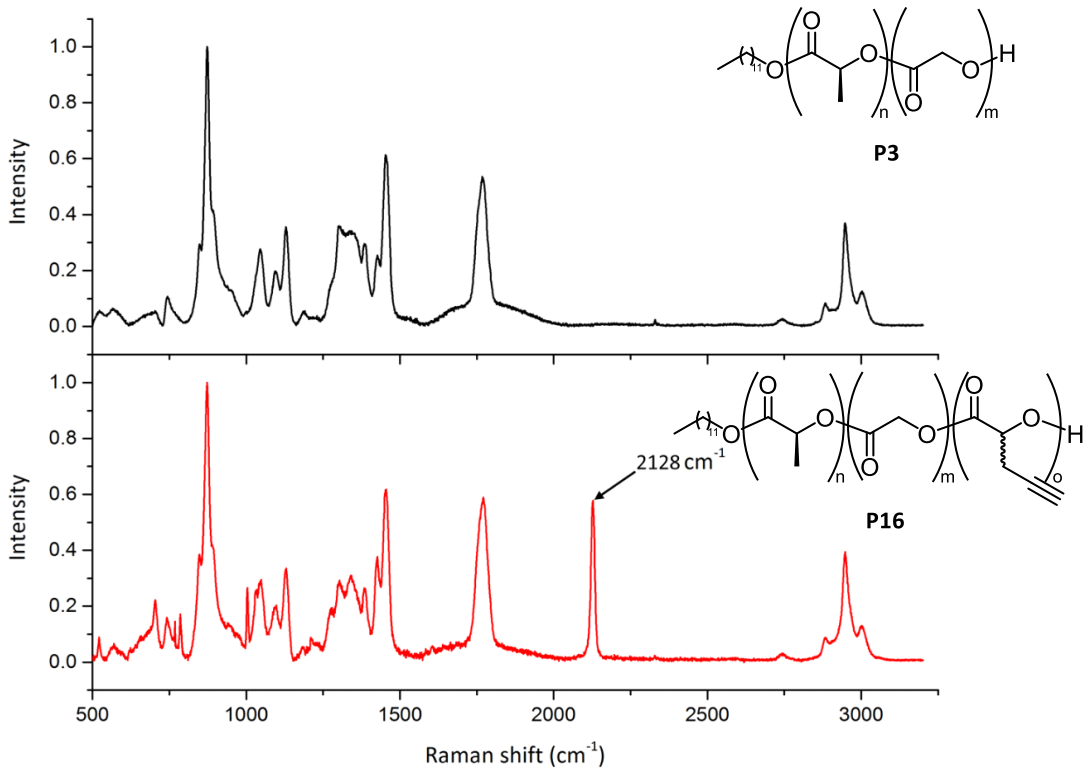

*Figure 4.8. Spontaneous Raman spectra recorded solid polymer samples **P3**(top) and **P16** (bottom). Raman spectra were normalised to the intensity of the peak at 873 cm^{-1}. The alkyne peak has been annotated at 2128 cm^{-1}. Raman spectra were acquired at λ_{ex} = 785 nm for 10 s using a 20× objective.*

The polymerisation of monomer **M58** with **P3** has demonstrated that this synthetic strategy can be used to obtain polymers with a controlled loading of alkyne functionalised monomeric units. The experiments have led to the continuation of this collaborative project. Nanoparticles of **P16** are currently being made target to the treatment of cells, first microglia and then oligodendrocyte precursor cells, to investigate if the cells uptake the nanoparticles and if this can be visualised using Raman spectroscopy. The propargyl functionalised PAHA will be used to image the uptake of P3 nanoparticles in cells, more specifically the goal will be to visualise them and their role in delivering drugs to oligodendrocyte precursor cells to promote remyelination in collaboration with Ms Sally Vanden-Hehir and Professor Alison Hulme.

4.4 Alkene Substituted Poly(α-hydroxy acid)

Olefin substituted PAHAs have been found to be as useful as their alkyne counterparts.[23–25] Though they do not have the ability to participate in the Huisgen 1,3-dipolar cycloaddition click chemistry, however, they do have the ability to react *via* other avenues

such as epoxidation and thiol-ene type radical additions.[26,27] Although thiol-ene chemistry is akin to the thiol-yne chemistry, it was not used in the same fashion to add a consecutive functional group. Instead, it was used to crosslink polymer chains through a di thiol (Scheme 4.9).

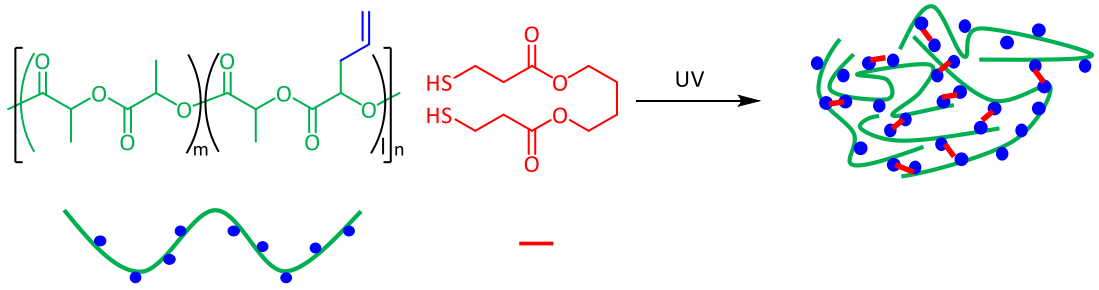

Scheme 4.9. UV induced thiol-ene crosslinking.

As discussed in Chapter 1, Collard *et al.* synthesised a copolymer with **M2** and **M24**.[28] Following post-polymerisation modification, an olefin alpha to the carbonyl was produced. The copolymer underwent further modification. Sulphide groups were reacted in thiol-ene additions to incorporate various groups, such as phenol, 4-methoxybenzyl and *N*-acetylcysteine. This particular polymer was attention drawing due to its α-vinyl ester functionality. This type of functionality is present in some common monomers that undergo radical polymerisation, such as acrylic acid, and is known otherwise as an acrylate monomer. If the acrylate functionality of the copolymer was to participate in polymerisation, a network of polyesters bound together by polyacrylates would arise. Polyacrylates are not typically biodegradable, however, the polyester portion is known to be both biodegradable and compostable.[29] This type of network is of interest to obtain novel polyacrylate-polyester networks and potentially be able to biodegrade. Hence, a chloromethyl substituted 1,3-dioxolan-4-one was synthesised in order to produce a copolymer with **P1** containing acrylate type functional groups enchained within the polymer backbone.

4.4.1 Synthesis of 5-Chloromethyl-1,3-dioxolan-4-one

A β-chloro substituted PAHA provides a key opportunity to synthesise an α-vinyl functionality. The α-vinyl ester functionality was noted to be akin to an acrylate type functionality. Acrylate monomers are used in free radical polymerisations to synthesise a wide variety of polymers. It was hypothesised that an acrylate functionalised polyester could be used to synthesise a crosslinked polyester-polyacrylate network. The α-hydroxy acid for the synthesis of 5-chloro-1,3-dioxolan-4-one (**M59**) was not readily available and it was necessary

to synthesise 3-chloro-2-hydroxypropanoic acid. 3-Chloro-1,2-propanediol is an undesired by-product formed in some food processing and refining e.g. oils and soy sauce.[30] Oxidation of this food by-product provided Collard *et al.* the opportunity to synthesise monomer **M24**.[28] We used similar reaction conditions to also reach to same α-hydroxy acid starting material. 3-Chloro-1,2-propanediol was oxidised by nitric acid, and the excess nitric acid was neutralised, before the α-hydroxy acid was extracted and crystallised from chloroform.[31] The same conditions were used to form monomer **M59** as the other 1,3-dioxolan-4-ones in a good yield (80%). This improved upon the crude yield, containing all three possible diastereomers of **M24**, Collard *et al.* obtained by 47%. With this chloro substituted monomer in hand, copolymers of various loadings of **M59** were then targeted in order to synthesise a variety of networked copolymers.

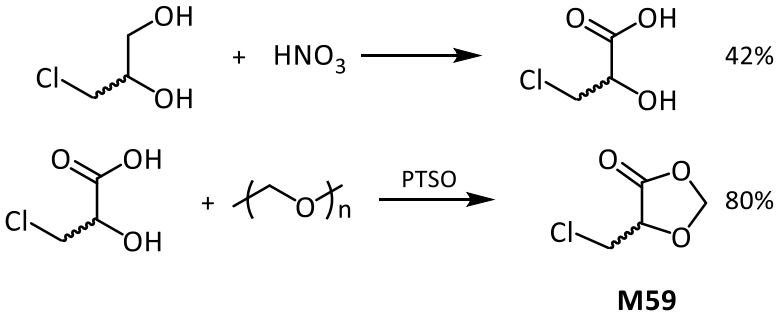

*Scheme 4.10. Top: Synthesis of 3-chloro-2-hydroxypropanoic acid. Bottom: Synthesis of 5-chloromethyl-1,3-dioxolan-4-one (**M59**).*

4.4.2 Copolymerisation of 5-Chloromethyl-1,3-dioxolan-4-one with Lactide

Monomers **M2** and **M59** underwent ROP in the presence of BnOH initiator and catalyst **C13**. After four hours at 120 °C, both monomers had reached quantitative conversion. ^{1}H NMR spectroscopy was conducted on the resultant polymer and the spectrum below (Figure 4.9) illustrated that the copolymer poly(lactic acid-co-3-chloro-2-hydroxypropanoic acid) (**P17**) had formed. In line with observations from other 1,3-dioxolan-4-one polymerisations, the observed MW (M_n = 9000 g/mol, uncorrected from **P1**) was again lower than the expected MW ($M_{n,th}$ = 13800 g/mol). The high reaction temperature did not disrupt the catalyst's ability to produce **P17** with a low dispersity ($Đ$ = 1.08).

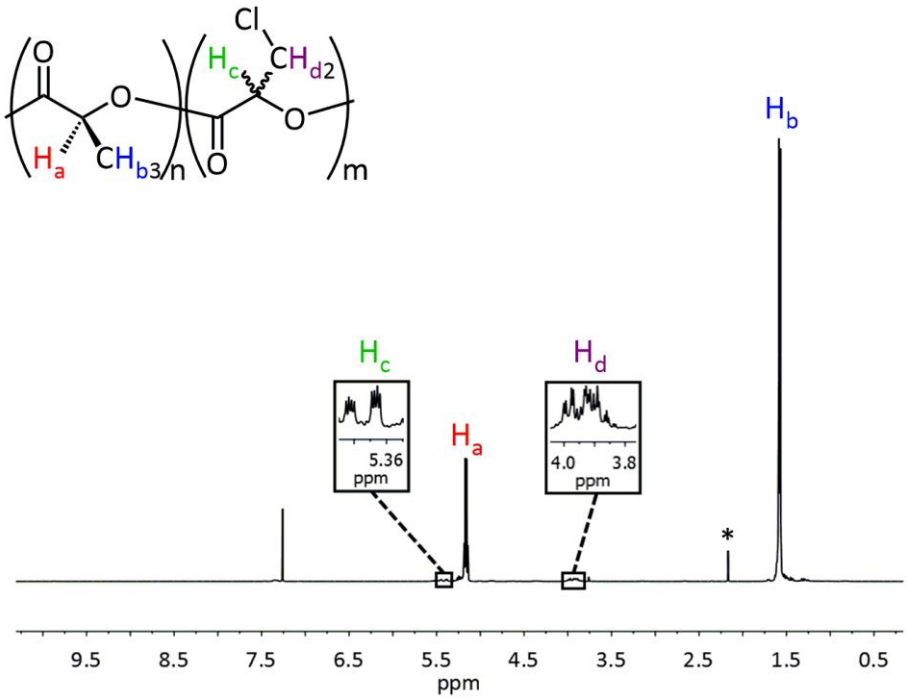

*Figure 4.9. [1]H NMR spectrum of polymer **P17** synthesised from the copolymerisation of **M2** and **M59**, initiated with BnOH and catalysed by **C13**. * indicates residual acetone from cleaning the NMR tube. ($CDCl_3$, 300 K, 600 MHz).*

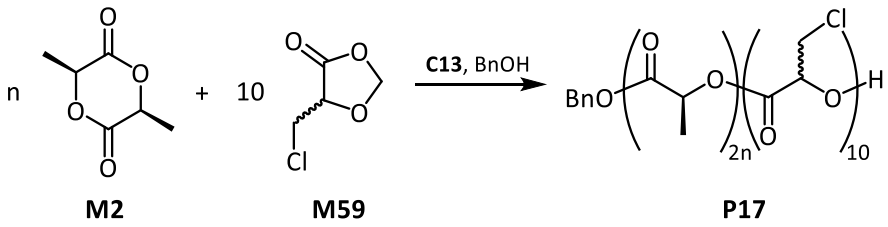

*Scheme 4.11. Copolymerisation of **M2** and **M59**, initiated with BnOH and catalysed by **C13**.*

The monomer feedstock provided the opportunity to control the average length of **P1** chain between pendant chloromethyl groups and thus the density in which the polyacrylates would be crosslinked through the polyester chain. Polymerisations were varied by altering the loading of **M2**, while keeping the initial loadings of **M59**, **C13** and BnOH constant (Table 4.5). Entries 1-3 were polymerised on a small scale (1 mmol of total monomer). The observed MWs of the polymers produced at the small scale aligned well with the expected values. Conducting the polymerisations on an increased scale (*ca.* 11 mmol) (Entries 4-6, Table 4.5) led to a decrease in the observed MW across all monomer feeds, this occurred despite an increase in monomer conversion in Entries 5 and 6. The dispersities remained low throughout. Collard *et al.* produced similar copolymers with two ratios of **M2**:**M24**.[28] Slight deviations are seen when comparing the poly(3-chloro-2-hydroxypropanoic acid) methine region of ^{1}H NMR

spectroscopic data of **P17** (94:6 mol%) synthesised from **M59** and **P17** (95:5 mol%) synthesised from **M24** (Figure 4.7). The different multiplets are likely a result of various polyads from sequences of repeat units and/or stereochemistry. In terms of repeat unit sequences, **M24** produces two consecutive 3-chloro-2-hydroxypropanoic acid units, whereas **M59** only produces a single repeat unit with each ring-opened monomer. From a stereochemistry perspective, the different synthetic methods, monomers and catalyst could potentially be selective for different monomer sequences.[32]

*Table 4.5. Copolymerisations of **M2** and **M59**, with varying **M59** loadings. Polymerisations were initiated with BnOH, and catalysed with **C13**.*

Entry	n	Time (h)	**M2**[a] conv.	**M59**[a] conv.	$M_{n,th}$[b]	M_n[c]	M_w[c]	$Đ$[c]
1	100	3	83	83	12900	11400	12600	1.11
2	50	2	78	81	6600	7600	8100	1.07
3	20	1.5	84	80	3400	3900	4600	1.17
4	100	3	94	97	14500	10200	11100	1.09
5	50	2	82	82	6700	5100	5700	1.11
6	20	1.5	73	86	3100	2100	2700	1.28

*Entries 1-3 were conducted at a 1 mmol scale, while entries 4-6 were condcted at an 11 mmol scale. **M2**:**M59**:**C13**:BnOH = n:10:1:1. Conducted in toluene at 1 M at 120 °C. Conv. = monomer conversion (%) [a] Monomer conversion (%) determined by performing ^{1}H NMR spectroscopy on a crude sample. [b] $M_{n,th}$ (g/mol) = (**M2**:BnOH) × MW(**M2**) × **M2** conv. + (**M59**:BnOH) × (MW(**M59**) – 30) × **M59** conv. + MW(end group). [c] Đ, M_n (g/mol) and M_w (g/mol) determined by GPC.*

The polymerisation of monomer **M59** was used to obtain copolymer **P17** and the chemical composition of the copolymer was varied by altering the feedstock. By using this synthetic procedure, a greater control over the polymer's expected MW, as the M:I was controlled and did not rely on adventitious protic impurities. Using this synthetic strategy allowed for a reduced reaction temperature, from 135 °C to 110 °C and reduced reaction times from 16 h to 1-5 h). The synthetic route also permitted greater control over the molecular weight distribution of **P17**, observed by the decrease in dispersities from $Đ$ = 1.81 to $Đ$ = 1.07-1.28.

4.4.3 Post-polymerisation Modification of Poly(lactic acid)-co-Poly(3-chloro-2-hydroxypropanoic acid)

Dehydrohalogenation is a common method for the synthesis of alkenes from haloalkanes by treatment of base.[33] Use of dehydrohalogenation for post-polymerisation modification of **P17** was conducted by Collard *et al*. in order to add thiol groups to the PAHA.[28] Optimised conditions were obtained by modifying conditions used Collard *et al*. Initial testing was conducted with **P17** (M_n = 10200 g/mol, $Đ$ = 1.09)(94:6 mol%). It was found that when using triethylamine as the base, the reaction proceeded and all the peaks associated with the chloro-

hydroxypropanoic acid units were consumed in 24 h. ^{1}H NMR spectroscopy showed the presence of peaks associated with a triethylamine like structure were still present and a DOSY NMR spectroscopy experiment showed these peaks had the same diffusion coefficient as other polymer peaks. It was thus determined that a less nucleophilic base was required to produce the dehydrochlorination product selectively. Hunig's base was selected as a bulkier, non-nucleophilic base and under the same reaction conditions this produced the desired alkene functionalised copolymer (**P18**) without the presence of any peaks associated with the amine (Scheme 4.12).

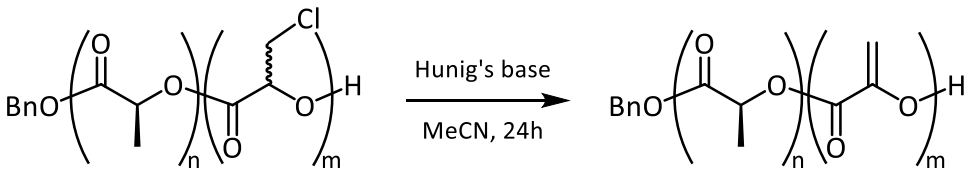

P17 **P18**

*Scheme 4.12. Dehydrochlorination of **P17**, with Hunig's base, to form poly(lactic acid-co-2-hydroxypropenoic acid) (**P18**).*

^{1}H NMR spectroscopy experiments proved the polymer produced *via* this synthetic method differs from the polymer produced previously (Figure 4.11). From the diester pathway four doublets are produced whereas the 1,3-dioxolan-4-one pathway produces two multiplets and several smaller peaks present in the base also associated with 2-hydroxypropenoic acid units and are likely different polyads. The random nature of the polymer is also evident by the large number of overlapping peaks in the carbonyl region of the polymer's ^{13}C NMR spectrum.[34,35] Following the post-polymerisation of **P17** (M_n = 10200 g/mol, $Đ$ = 1.09)(94:6 mol%) the observed MW and dispersity of the new copolymer, poly(lactic acid-co-2-hydroxypropenoic acid) (**P18**), were both increased (M_n = 12100 g/mol, $Đ$ = 1.26) (96:4 mol%). The change in the copolymer's composition was likely the result of the observed increase in the M_n, as the GPC calculation parameters were not adjusted and no attempts were made to determine the dn/dc value of this polymer. The modification of the lower MW **P17** (5100 g/mol, $Đ$ = 1.11)(92:8 mol%) under the same conditions led to copolymer **P18** having a significant increase in M_w (35900 g/mol) and thus $Đ$ (M_n = 8800 g/mol, $Đ$ = 4.08) (97:3 mol%). This observation was consistent with the ^{1}H NMR spectrum, as the mol% of alkene present in the copolymer was found to have decreased. The reduced alkene content and increased M_w are likely caused by crosslinking between **P18** chains as shown in Figure 4.10. The polymer produced in Entry 6 was reacted in the same fashion as the two higher MW copolymers. Following treatment of base, the product obtained was found to have degraded, as only

oligomers were present in the GPC chromatogram. The synthetic route was used to produce of polymer capable of undergoing elimination with a non-nucleophilic base in the same procedure as previously shown by Collard *et al.*, however the ^{1}H NMR spectrum of the polymer underlined the differences between the synthetic routes as monomer **M59** was used to enchain single α-hydroxy units.

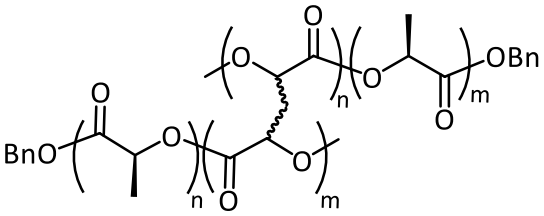

Figure 4.10. Potential self-cross linking of poly(lactic-co-2-hydroxypropenoic acid) via spontaneous radical formation.

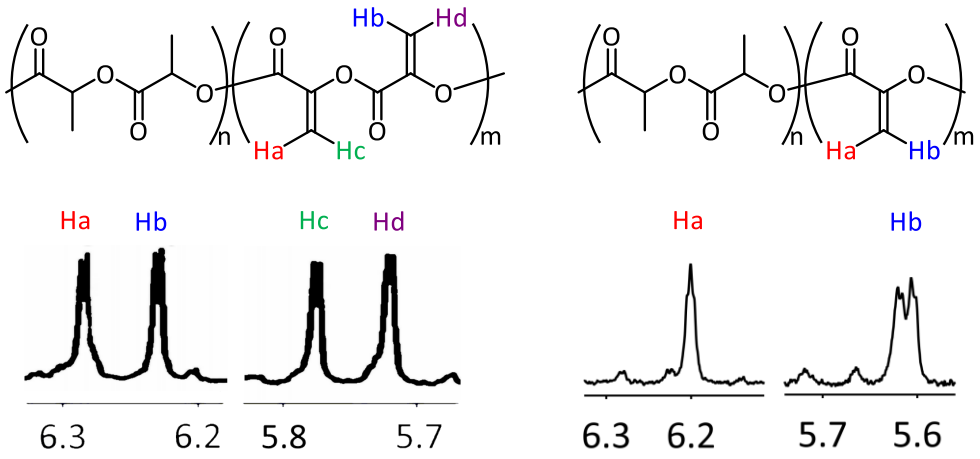

*Figure 4.11. ^{1}H NMR spectrum of poly(lactic-co-2-hydroxypropenoic acid) from ROP of **M2** and **M16** taken from the supporting information of the publication by Collard et al. (left, faded edges removed from spectrum to reduce blurs and sharpen the image for better comparison, $CDCl_3$, 500 MHz)[28] and ROP of **M2** and **M50** (right) ($CDCl_3$, 300 K, 500 MHz).*

4.4.4 Crosslinking of Poly(lactic acid)-co-poly(2-hydroxypropenoic acid)

Methyl methacrylate (**M60**) is used to make poly(methyl methacrylate) (**P19**) which has a wide range of uses, from clear plastic sheets sold under trade names such as Plexiglas, and Perspex, to medicine and dentistry.[36] Biodegradable cross-linked polymers are of interest for biomedical applications, as they are employed as surgical implants,[37] glues,[38] drug delivery devices,[39] and scaffolds for tissue engineering.[40] **P17** provides a unique opportunity crosslink poly(acrylate)s throughout the polymer chain as a opposed to chain-end crosslinking that **P1**

has previously been limited to.[41,42] The formation and potential degradation of the crosslinked network is illustrated in the Figure 4.12.

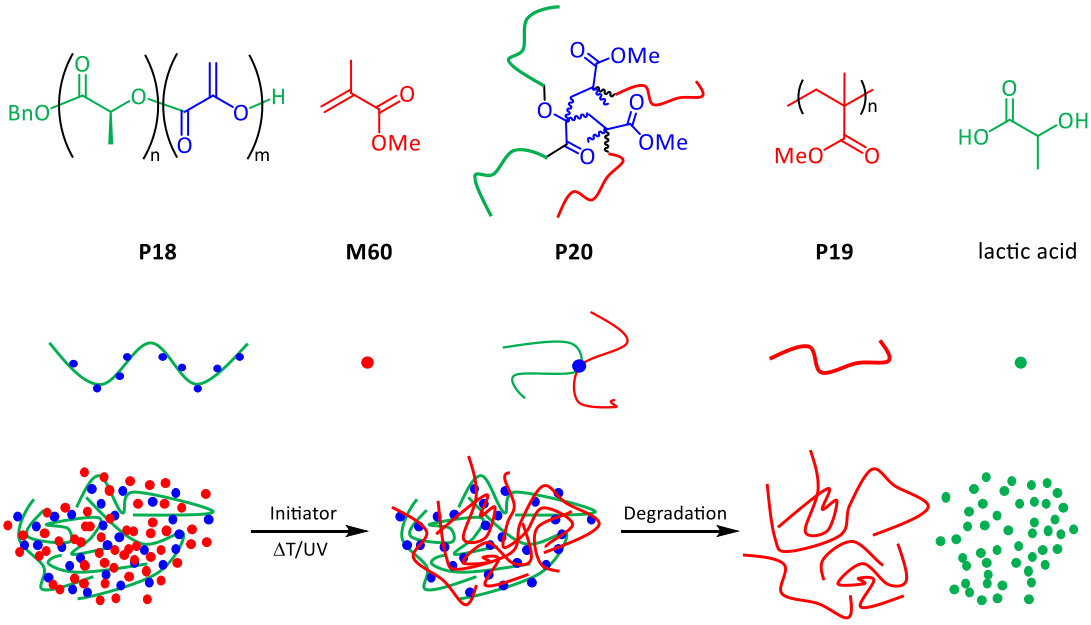

*Figure 4.12. Polymerisation of **M60** in the presence of **P18** via thermal or UV-initiated free radical polymerisation. Crosslinking occurs as radicals propagate through the vinyl functionality of **P18** to form a networked copolymer **P20**. Followed by degradation of crosslinked **P20** to lactic acid and **P19**.*

Firstly, the formation of a copolymer network was tested using a thermal azo-initiator azobisisobutyronitrile (AIBN). As a comparison to crosslinking experiments a standard free radical polymerisation was conducted: 100 equivalents of **M60** was polymerised with 0.6 equivalents of AIBN in toluene at 120 °C for one hour (Entry 1, Table 4.6).

*Table 4.6. Thermal iniated free radical polymerisation of **M60** crosslinked with **P18***

Entry	**M60**	**P18**	AIBN	Olefin conversion[a]	M_n[b]	M_w[b]	$Đ$[b]	α[c]
1	100	0	0.6	n/a	5500	11400	2.07	0.59
2	100	0.1	0.6	/	/	/	/	
3	100	.05	0.6	74	32600	433900	13.3	0.31
4	100	0.01	0.6	60	6900	23800	3.47	0.57
5	100	0.1	3	63	16500	157600	9.56	0.39
6	100	0.1	6	81	3700	26100	6.99	0.41

*Polymerisations were conducted in toluene 50% w/w at 120 °C for one hour. [a] Olefin conversion (%) of the olefin functionalised **P18** determined by performing ^1H NMR spectroscopy on a crude sample. [b] $Đ$, M_n(g/mol), M_w(g/mol) determined by GPC. α is the Mark Houwink α parameter and was determined GPC.*

The polymerisation was conducted in the presence of 0.1% olefin functionalised PAHA (Entry 2, Table 4.6). After 20 minutes the reaction mixture became so viscous that the magnetic stir bar no longer moved. The reaction formed a gel encapsulating the reaction

solvent evident of the formation of a polymeric network.[43] High MW linear **P19** also entraps solvent approaching high conversions when the polymerisation is conducted in 50% w(monomer)/w(monomer + toluene). However, it differs from the gel produced with 0.1% crosslinking, because the networked copolymer **P20** was not able to be dissolved. Reducing the input of crosslinker to 0.05% gelation did occur, however > 99% of the networked copolymer was soluble and was recovered (Entry 3, Table 4.6). Conversion of the polyester's olefin was calculated by comparing the relative integrations of the methylene peak at 5.61 ppm and the methine peak at 5.16 ppm in both the starting material and the crosslinked polymer. GPC can be performed on the polymer and the differences between the polymerisation with 0% and 0.05% crosslinker are noted. The M_n is increased by nearly six times and the dispersity is increased by greater than 6 times. Conversion of the olefin functionalised are relatively high at 74%. Conducting DOSY NMR spectroscopy on the polymer shows only a single diffusion coefficient present in the spectrum and both the peaks associated with **P1** and **P19** are present along this single coefficient (3.5×10^{-7} cm^2/s) (Figure 4.13).

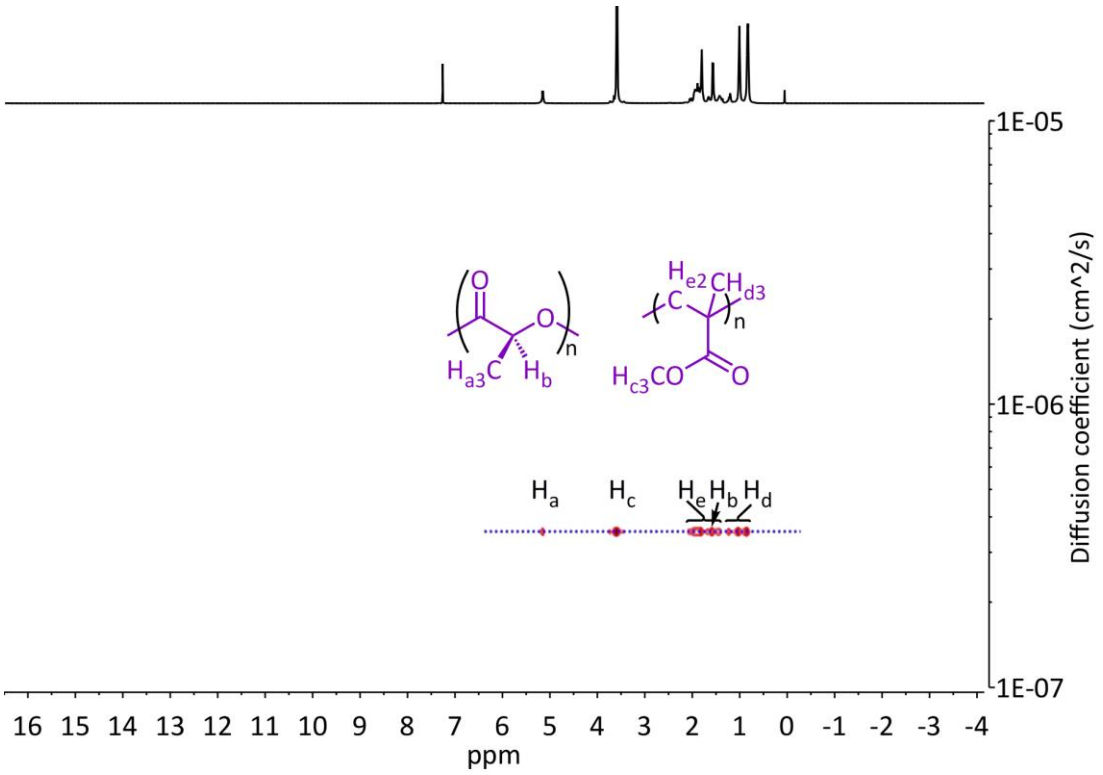

*Figure 4.13. DOSY NMR spectroscopy of **P19** (0.05% **P1** crosslink) Entry 3, Table 4.6. Peaks associated with both **P1** and **P19** present on the same diffusion coefficient ($CDCl_3$, 300 K, 600 MHz).*

Reducing the amount of crosslinker to 0.01% (Entry 3, Table 4.6) the M_n is similar to Entry 1 and exhibited an increase in dispersity though lower than that of Entry 2. The conversion of crosslinker olefin was lower than Entry 2. During propagation a large fraction of the **P19** must not have reacted with crosslinker illustrated by the M_n being lower than that of the crosslinker. All **P1** peaks were present on a single diffusion coefficient (1.1×10^{-6} cm^2/s) exhibited in the spectrum produced by DOSY NMR spectroscopy.

To reduce the MW of the networked polymer and make a soluble, but highly crosslinked polymer, the same ratio of **M60** to **P18** as Entry 1 was used and polymerised with an increased ratio of initiator. During the polymerisation of Entry 5 no gelation was observed and the polymer was quantitatively recovered. The dispersity is broad and Entry 5 has a larger M_n than the **P19** synthesised with no crosslinker, suggesting a large degree of crosslinking has occurred. Increasing the equivalence of AIBN even further to 10 times that of Entries 1 and 2 again no gel is formed during the polymerisation, however similarly to Entry 4, the average polymer chain does not contain a single crosslinker molecule. The polymer exhibits two diffusion coefficients in the DOSY NMR spectrum (Figure 4.14). **P1** and **P19** peaks are each on defined coefficients, despite high olefin conversions of **P18**.

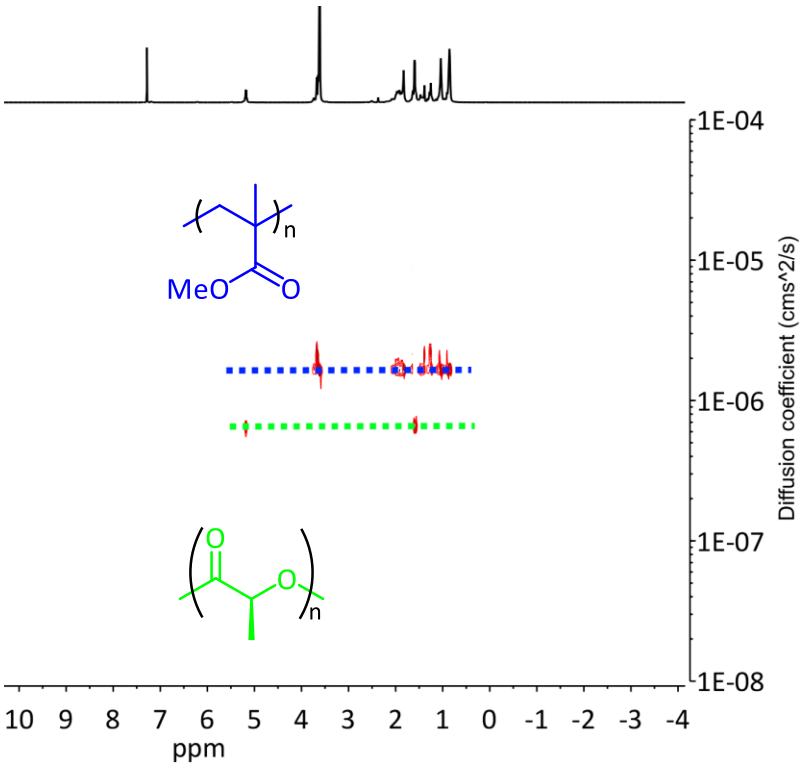

*Figure 4.14. DOSY NMR spectroscopy of **P19** (0.1% **P1** crosslink) Entry 6, Table 4.6. Peaks associated with both **P1** and **P19** present on the different diffusion coefficients ($CDCl_3$, 300 K, 600 MHz).*

Comparing the Mark-Houwink parameters exhibited by the crosslinked polymers the amount of networking or crosslinking can be seen. The free radical polymerisation of **M60**, with no added **P18**, has a Mark-Houwink α parameter of 0.59, and similar to the previosuly reported values for linear **P19** of 0.69.[44] Entry 3 has an α parameter furthest from linear of 0.31. The 0.01% of crosslinker has the most similar parameter to Entry 1 and thus this percentage of **P18** has had little effect on the resulting polymer's overall macrostructure. Despite the presence of two diffusion coefficients presented by both Entries 5 and 6 the Mark-Houwink α parameters 0.39, and 0.41 respectively indicate that the polymers are highly crosslinked. The acrylate functionalised PAHA and **M60** system has been shown to have to ability to polymerise and crosslink **P19** in a single step without the presence of a catlayst. Relatively low mol percentages of PAHA (0.1%w/w) were required to produce highly crosslinked materials that were insoluble. Decreased mole percentages of PAHA were used to produce soluble polymers. The increased solubility allowed for vital characterisation of the polymer's architecture, noted by the change in Mark-Houwink α parameter (0.59 to 0.31). High degress of crosslinking were also produced by increasing the equivalents of radical initiator to monomer and crosslinker, as theoretically shorter polyacrylates were produced with increased radical equivalents. Thermal initiation has been useful for conducting the crosslinking polymerisation of **M60** in solvent. However when conducted in bulk monomer **M60** at 120 °C, to ensure fast initiation, monomer **M60** vigorously refluxed and the reaction mixture solidfied to form a solid foam with uncontrolled large pores (~1-3 mms) and large qunatities of **M60** are left unreacted condensed along the reaction vessel walls. If the reaction were to take place at lower temperatures the initiation would require an extended period of time. In an open system this would often lead to loss of monomer to the atmosphere. UV initiators provide systems that are easy to control without the need for cold storage or heat for initiation. Using a UV radical source, 1-hydroxycyclohexyl phenyl ketone, the polymerisation and crosslinking was conducted in a reaction vessel open to the atmosphere to illustrate the robustness of this network synthetic route. The network formation was conducted by firstly dissolving the α-vinyl funtionalised copolymer **P18** (Entry 5, Table 4.5) and 1-hydroxycyclohexyl phenyl ketone in bulk monomer **M60**, in a ratio of **M60**:**P18**:1-hydroxycyclohexyl phenyl ketone of 100:0.1:1. The reaction mixture was charged to a vial, the reaction mixture was noted to have a depth of 2-3 mm. Upon irradiation by UV light for 15 minutes, the reaction mixture was observed to solidify into a clear solid glass-like disk. No portion of the disk was found to be soluble, suggestive of homogenous network formation. Conducting a comparative **M60** homopolymerisation under the same conditions 60 minutes of UV irradiation was required to reach > 90% conversion. The MW of **P19** and dispersity were

relatively low (M_n = 5700 and $Đ$ = 1.47) and the macrostructure was linear. The presence of copolymer **P18** during the polymerisation of **M60** not only allows for the formation of highly networked **P19** formation a solid occurs in a quarter of the irradiation time, compounding the robustness of this method to form networks in short time.

Crosslinked polyacrylate and polyester **P20** was synthesised using small fractions (0.01 to 0.1%w/w) of **P18** in the presence of thermally and photolytically initiated free radical polymerisation of **M60**. At loadings of 0.1%w/w **P18**, increasing the the loadings initiator reduced the MW and reduced the crosslinking, so much so that at [**M60**]:[AIBN] = 100:6 two distinct diffusion coefficients were observed in the DOSY ^{1}H NMR spectrum. The Mark-Houwink α parameter was used as an indication of the level of networking present in **P20**. UV light initiated free radical polymerisation was used to eliminate the need for solvent or elevated temperatures. The reaction was performed with great ease as it did not require an inert atmosphere or any additional equipment other than the UV light source and a reaction vessel.

To further explore networking between polyester and vinyl polymers, our focus shifted towards a pendant ethylene group. A pendant ethylene group would likely impact upon the potential networking due to both decreased steric hindrance and conjugation.

4.4.5 Attempted Synthesis of 5-Ethylene-1,3-dioxolan-4-one

With the intention of synthesising a pendant ethylene group to a PAHA, the synthesis of 5-ethylene-1,3-dioxolan-4-one. The work carried in Section 4.4.5 was conducted with the assistance of Ms. Francesca Ballard. In order to synthesise the monomer, the synthesis of the α-hydroxy acid was necessary. A route similar to that of the synthesis of 2-hydroxy-4-pentynoic acid was attempted to form 2-hydroxy-3-butenoic acid. Following the attempted Barbier reaction between vinyl bromide and ethyl glyoxalate, the formation of the desired product was not observed. In another attempt, the reaction was conducted under an inert atmosphere using dry solvent, reactants and reagents, however, again no product was observed under these conditions.

To increase the reactivity of the addition, a Grignard reagent was selected to form the desired product. The reaction between ethyl glyoxalate and vinyl-magnesium bromide was investigated. The reaction was carried out at two different temperatures, -40 °C and -78 °C, and using dry or wet ethyl glyoxalate in toluene. The course of the reaction was monitored using ^{1}H NMR spectroscopy, and thus the reactions were left to proceed for varying lengths of times, with cooling and then at room temperature. Analysing the spectra produced by conducting ^{1}H NMR spectroscopy on the crude mixture was difficult due to the presence of a

vast number of peaks, however, three major compounds were identified in the product mixture; ethyl glyoxalate, the desired ethyl 2-hydroxy-3-butenoate product and other major side-products based on the production of ethanol (formation and structure discussed below). The quantities of each product in the crude mixture were quantified by comparing relative integral values in the ^{1}H NMR spectra.

Table 4.7. Reaction between ethyl glyoxalate and vinyl-magnesium bromide and the identified products

Entry	Temp. (°C)	Fractional quantity of three major identifiable compounds / ± 5%		
		Desired-product	Ethyl glyoxalate	Ethanol
1[a]	-40	26	71	3
2[a]	-78	75	24	1
3[b]	-40	50	33	17
4[b]	-78	75	25	0

[a] Dry ethyl glyoxalate, 1 hours at -40 or -78 °C as stated and subsequent 22 hours at room temperature. [b] Wet ethyl glyoxalate, 1.5 hours at -40 or -78 °C as stated and subsequent 16 hours at room temperature.

At -78 °C (Entries 2 and 4) more of the target product was formed than at -40 °C (Entries 1 and 3). The hypothesised mechanism was based on the reactivity of the aldehyde being greater than the ester (Figure 4.15). This is attributed to the reduced electrophilicity of the ester carbonyl in comparison to the aldehyde as well as the kinetic availability of the aldehyde, leading to steric and electronic selectivity. The hypothesis of selectivity towards the kinetic product was bolstered by increased formation of the desired product at lower and decreased at higher temperatures.

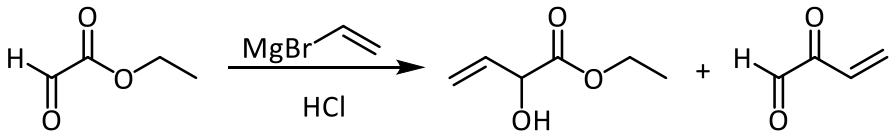

Figure 4.15 Reaction between vinyl-magnesium bromide and ethyl glyoxalate and the formation of desired product (ethyl 2-hydroxy-3-butenoate) and a major side product (2-oxo-3-butenal).

The ethanol was expected to form in higher quantities when the reaction was run at higher temperatures. The generation of an α,β-unsaturated ketone following the loss of ethanol may have led to another side reaction between vinyl-magnesium bromide and the ketone or aldehyde functionalities, or even a 1,4-addition. There was only an increased formation of the ethanol at higher temperatures when wet ethyl glyoxalate was used wet (Entry 4 versus Entry

3). Around 17% of the ethanol was observed after the reaction was run at -40 °C, but there was no evidence of the side-product after the reaction was run at -78 °C. The differences in the formation of the side-product when ethyl glyoxalate was used wet or dry indicated that the presence of water contributed to an increase in the rate of formation of the side-product. This could be explained by the aldehyde undergoing addition with water, to generate a hydrated product. If this did occur, it could be followed by the Grignard reagent reacting with the ester functionality, to generate a vinyl-functionalised compound with similar chemical shifts to that of the other major product. Another possible side reaction when using wet ethyl glyoxalate was a hydrolysis reaction of the ester, leading to formation of a carboxylic acid.

The large number of products in the reaction mixture were evidenced by convoluted ^{1}H NMR spectra, and several mixtures of products were also evident when separated by thin layer and flash column chromatography. A smaller mixture of products, believed to include the target compound, was isolated by flash column chromatography. This crude sample was used in a base hydrolysis reaction, with the aim to hydrolyse the ethyl ester, in order to generate the α-hydroxy acid and isolate this. However, performing ^{1}H NMR spectroscopy on the crude product mixture did not show the expected signals for the α-hydroxy acid within the vast number of peaks of the spectrum. Unfortunately, due to the large mixture of products obtained, and being unable to isolate the target α-hydroxy acid, it was concluded that the synthetic route followed was not viable. Work was not continued to synthesise the pendant vinyl-functionalised DOX compound.

4.5 Benzyloxymethyl Substituted Poly(α-hydroxy acid)

Hydroxyl functionality has been identified as an alternative route to increase the PAHA's hydrophilicity. Polymerising **M17** and following the hydrogenation of **P13** a water-soluble polymer (**P14**) was produced and no auto-catalysis of the hydrolytic degradation was observed (Scheme 4.13). The hydrophilic nature of **P14** was used in conjunction with the hydrophobicity of **P1** to form an amphiphilic block copolymer, which was used to form polymeric micelles.

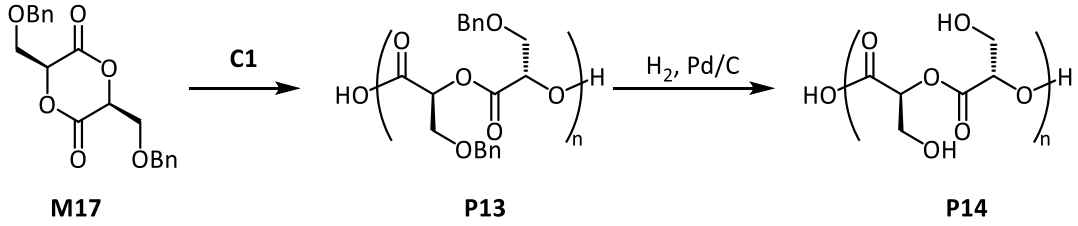

*Scheme 4.13. ROP of **M17** using **C1**. The benzyl group was then deprotected in a hydrogenation catalysed by palladium on carbon to form **P14**.*

M27 and **M28** were polymerised and copolymerised with **M1** and or **M2** and once deprotected, they were also formed water soluble polymers.[45,46] Their degradation was studied *in vitro* and the rate of degradation was found to vary with composition, which was suggested to be beneficial for potential biomedical and pharmaceutical applications. The OCA **M40** achieved the greatest yield out of the benzyloxymethyl monomers at 50%, in comparison to **M17**, **M27** and **M28** at 27, 40, and 42% yields respectively.[47] **M40** was polymerised to high conversions at room temperature and at a faster rate than the other diester monomers. Cheng *et al.* found **P14** to have good cell viability, a necessity for an application such as hydrogel scaffolds for tissue engineering.

4.5.1 Synthesis of 5-Benzyloxymethyl-1,3-dioxolan-4-one

Benzyl-serine was chosen as a renewable starting material to synthesise 5-benzyloxymethyl-1,3-dioxolan-4-one (**M61**), as amino acids were found to yield their equivalent α-hydroxy acid in Section 4.2.1 with ease and were then used to reach a variety of substituted PAHAs. The work carried in this Sections 4.5.1 and 4.5.2 was conducted with the assistance of Ms. Francesca Ballard. The diazotisation of benzyl-serine was conducted with sulphuric acid and sodium nitrite, following a procedure Matthes *et al.* had previously reported and achieved a 99% yield (Scheme 4.14).[48] The α-hydroxy acid was subsequently refluxed with paraformaldehyde in the presence of PTSA (10%), and upon the expulsion of water **M61** was isolated (Scheme 4.14). The ^{1}H NMR spectrum of **M61** is illustrated in Figure 4.16. **M61** was dried over calcium hydride and distilled under vacuum as conducted for all other liquid monomers polymerised in this thesis. **M61** was obtained with a poor isolated yield of 55%, however was greater than the yields obtained for monomers **M17**, **M27**, **M28** and **M40**.

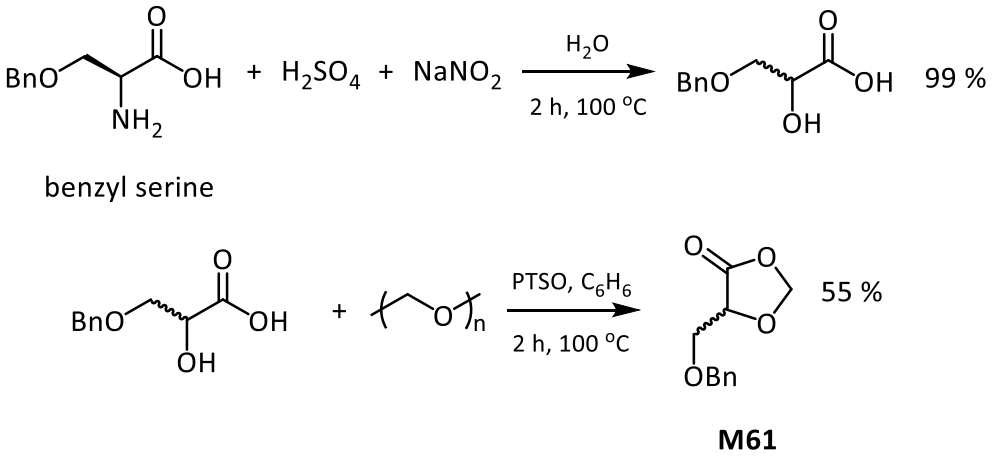

Scheme 4.14. Synthesis of 3-benzyloxy-2-hydroxypropanoic acid via *the diazotisation of benzyl-serine and the subsequent ring closing with paraformaldehyde catalysed by PTSA to form* ***M61***.

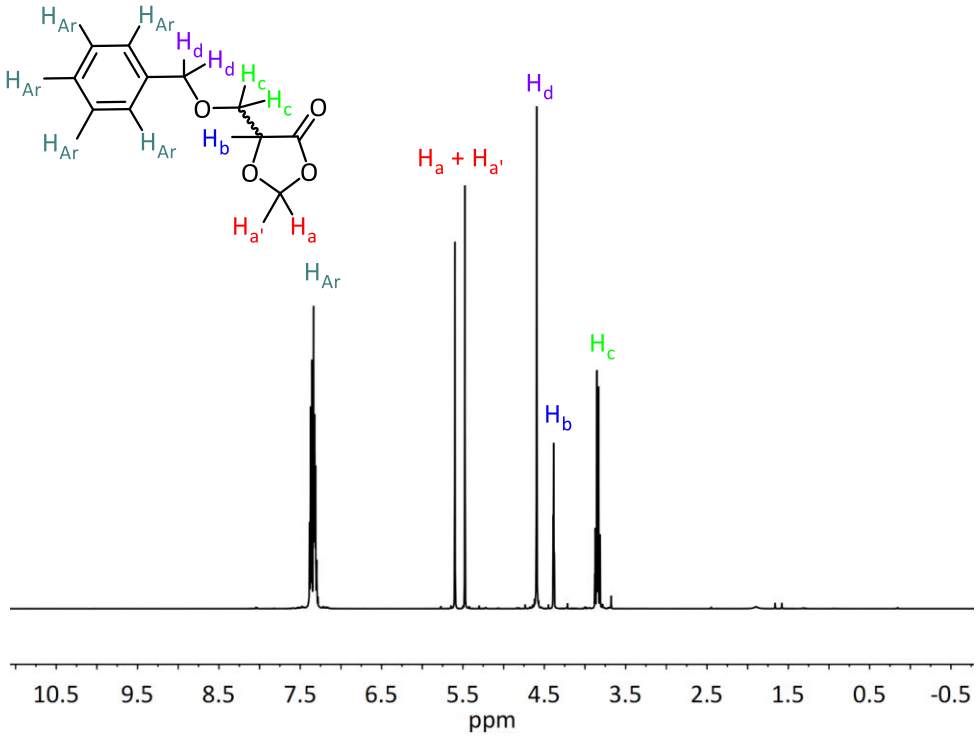

Figure 4.16. The ^{1}H NMR spectrum of ***M61*** *($CDCl_3$, 300 K, 500 MHz)*

After obtaining dry **M61**, the next steps were to conduct the polymerisation of the monomer in the same fashion as was used for the other 1,3-dioxolan-4-ones. MeAl(salen) catalysts were selected once again due to their performance with other monomers.

4.5.2 Polymerisation of 5-Benzyloxymethyl-1,3-dioxolan-4-one

Attempted polymerisations were conducted with catalysts **C13** and **C9** in toluene at 85 or 120 °C and are summarised in Table 4.8. Monomer conversions were calculated from the relative integrations of monomer and polymer methine regions: 4.52 ppm and 5.37-5.54 ppm, respectively. Firstly, as shown in Entry 1, Table 4.8, conducting the polymerisation at 85 °C with catalyst **C13** resulted in no formation of polymer over 24 hours. Increasing the reaction temperature to 120 °C and elongating the reaction time to a week, 50% of monomer **M61** was converted to polymer. However, no solid was formed upon addition to cold methanol. After the methanol and toluene were removed under vacuum, the polymer was separated using size-exclusion chromatography. The polymer was analysed using GPC (MWs vs PS standards *via* calibration curve) and this revealed the MW to be <15% of the expected MW while achieving a narrow dispersity. Using the chloro substituted catalyst **C9**, under the same reaction conditions, only 35% conversion was observed after 120 hours, however, the isolation of the polymer from the reaction mixture failed and GPC data was not collected. The low conversion using **C9** was akin to the slower polymerisations of **M46** using chloro substituted MeAl(salen) catalysts. Attempted purification of the polymer from the reaction mixture was unsuccessful. The prolonged reaction times caused by the increased steric bulk of this substituent allows for an increased time for the disproportionation of formaldehyde to occur.

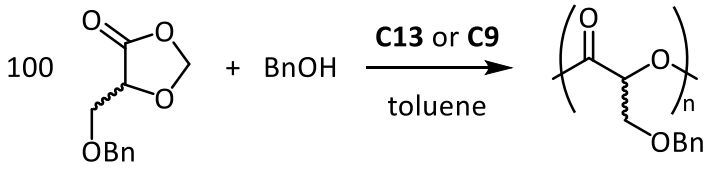

M61 **P13**

*Scheme 4.15. The polymerisation of **M61** controlled by a **C13** or **C9**, and BnOH mediation/initiation system.*

*Table 4.8. Attempted polymerisations of **M61**, using **C13** or **C9**, and BnOH.*

Entry	Cat	T (°C)	Time (h)	Conv.[a]	$M_{n,th}$[b]	M_n[c]	$Đ$[c]
1	**C13**	85	24	0	/	/	/
2	**C13**	120	168	50	10500	1500	1.14
3	**C9**	120	120	35	7400	/	/

***M61**:Cat:BnOH = 100:1:1. Conducted in toluene at 1 M. Conv. = monomer conversion (%) [a] Monomer conversion (%) determined by performing ^{1}H NMR spectroscopy on a crude sample. [b] $M_{n,th}$ (g/mol) = (**M61**:BnOH) × (MW(**M61**) - 30) × **M50** conv. + MW(end group). [c] Đ, M_n(g/mol) and M_w(g/mol) determined by GPC.*

Despite the successful increase in monomer yield, the polymerisation of monomer **M61** was slow. The ROP of **M61** produces polymer of very low MWs and are not aligned with the

expected MWs. The low MW of the polymer increased the difficulty of polymer isolation. Hence it was concluded that this synthetic route was not viable to produce hydroxyl functionalised PAHA.

4.6 Benzyloxyester Substituted Poly(α-Hydroxy acid)

Carboxyl functionalised PAHAs have been accessed efficiently in literature, from diester and OCA monomers **M16**,[45] **M25**,[45] **M26**,[46] **M38**,[49] and **M39**.[50] These monomers were polymerised with organocatalyts to achieve high conversions (92 – 99%) and obtain polymers of low dispersity (1.04 – 1.27). The final goal of obtaining a PAHA functionalised with pendant free carboxylic acids was achieved through each monomer successfully. Dove *et al.* polymerised **M25** with a (-)-sparteine and alcohol initiation/mediation system, the resultant polymer was deprotected *via* hydrogenation of the benzyl ester group (Scheme 4.16).[45]

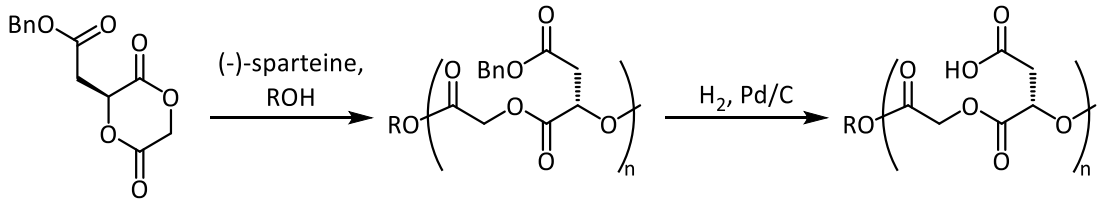

*Scheme 4.16. Polymerisation of **M25** and subsequent hydrogenation to form a carboxylic acid functionalised PAHA.*

An increased hydrolytic degradation rate was observed and was attributed to the functional group's ability to increase the polymer's solubility in water. Making the degradation a homogeneous process and decreasing the pH of the solvent promotes hydrolysis of ester linkages. The synthesis of diesters **M16**, **M25** and **M26** is, however, poor yielding at the final cyclisation step. As discussed previously, the OCA synthetic procedure is not ideal due to the toxicity and cost of the carbonylating agent, furthermore the synthesis of **M38** and **M39** is laborious. On top of the benzyl protection and carbonylation step, it involves two additional steps: protection and deprotection. To eliminate issues of cost, poor yields and reduce the number of synthetic steps a benzyl ester substituted 1,3-dioxolan-4-one has been synthesised in order to attain a hydrophilic and hydrolytically degradable carboxylic acid functionalised PAHA.

The likely failure of the polymerisation of **M61** and the inability to achieve accurate MWs was the production/presence of chain transfer agent. Previously in this thesis the disproportionation of formaldehyde was realised as the source for excess initiator. The use of acetone as a ring closing agent rather than paraformaldehyde produced monomers capable of producing **P1** and **P5** of MWs in accordance with their expected MWs. In the introduction it

was noted that a protection and deprotection steps were required prior to the formation of **M16**, **M25**, **M26**, **M38** and **M39**. 5-Benzyloxyester-2,2-dimethyl-1,3-dioxolan-4-one (**M61**) was an intermediate during the synthesis of both the diester and OCA. This protected species was identified as a potential monomer to form the benzyloxyester substituted PAHA *via* the expulsion of acetone.

4.6.1 Synthesis of 5-Benzyloxyester-2,2-dimethyl-1,3-dioxolan-4-one

The ring-closure of L-malic acid was attempted using acetone as the ring-closing reagent and PSTO as the weak acid catalyst in various conditions, however, the desired product was not observed in any mixture of solvents attempted (1:1 acetone:chloroform, 1:1 acetone:toluene, 1:1 acetone:benzene, chloroform, toluene or benzene). The ring-closed product was obtained following procedures previously reported in literature: L-Malic acid was dissolved in excess 2,2-dimethoxypropane and the product was formed after 3.5 hours of stirring at room temperature (Scheme 4.17).[50] The benzyl protection was again conducted following a literature procedure *via* a reaction with benzylbromide and triethylamine. The product was recrystallized from diethyl ether to yield monomer **M62**.

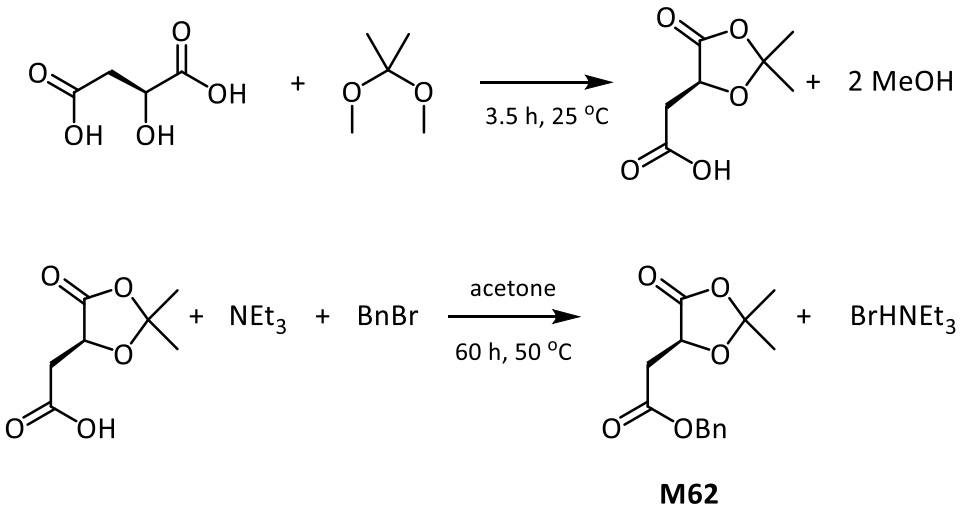

*Scheme 4.17. Top: Ring closure of L-malic acid with dimethoxypropane. Bottom: Benzyl protection to form monomer **M62**.*

4.6.2 Attempted Polymerisations of 5-Benzyloxyester-2,2-dimethyl-1,3-dioxolan-4-one

Using **C13** and BnOH, polymerisations of **M62** were attempted firstly at 85 and 120 °C in toluene solutions. After long reaction times (>5 days), no reaction had been observed by ^{1}H NMR spectroscopy. Polymerisations were conducted at 120 °C in the absence of solvent and

again, no polymerisation was observed. Increasing the reaction temperature to 180 °C, after two hours 10% monomer conversion was observed. A large portion of the reaction mixture was found to be insoluble in DCM when the reaction time was extended to 24 hours. The DCM soluble portion of the crude sample was analysed by ^{1}H NMR spectroscopy. The signals associated with **P21** were observed in the NMR spectrum. However, the concentration of **P21** was very low, as integration values of other unidentified peaks were substantially higher. The other fraction of the sample was found to be soluble in THF. **P21** was also present in this portion, as shown by ^{1}H NMR spectroscopy analysis. Again, however, its concentration was very low. It was concluded that the formation of benzylester functionalised PAHA was not viable *via* this synthetic pathway due to the lack of reactivity of **M60** in the system tested.

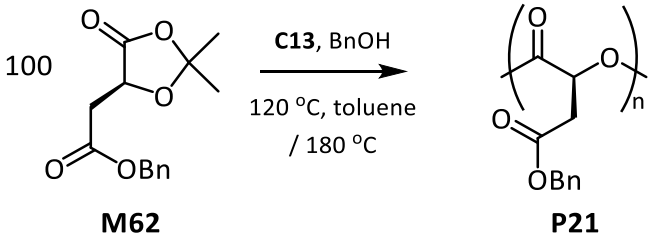

M62 **P21**

*Scheme 4.18. Attempted polymerisation of monomer **M62** using an equivalent of BnOH and catalyst **C13** to form polymer **P21**.*

4.7 Conclusions

The synthetic pathway that is the ROP of 1,3-dioxolan-4-ones has proven to be a success synthetic tool to form a variety of substituted PAHAs. The polymerisations of monomers **M50**, **M53**, **M54**, **M55** and **M56** were tested and all the monomers other than **M56** were shown to be capable of undergoing ROP with the elimination of formaldehyde. The monomers were all higher yielding than their diester equivalents. The differences in rates between various substituted monomers gave an insight into the potential coordination-insertion mechanism at play during the polymerisation. The variety of substituted PAHAs synthesised boasts the ability of the synthetic pathway to produce polymers with a wide array of T_g values. Alkynyl substituted 1,3-dioxolan-4-one, **M58**, was successfully synthesised in a greater yield than any diester or OCA monomers previously polymerised to access alkynyl functionalised PAHAs. **M58** was homopolymerised to produce a PAHA with pendant propargyl groups, polymer **P15**. It was found that observed MWs deviate from the expected MWs. A similar observation was seen in Chapter 3 and was attributed an increase in methanol concentration due to formaldehyde undergoing disproportionation. These deviations were largely mitigated when copolymerised with **M1** and **M2** at lower feedstocks of **M58**. **P3** was also successfully used as a macroinitiator and elongated reaction times were used to distribute alkynyl functionality

through the copolymer. The copolymer was shown to have a distinct and intense Raman shift located in the cell silent region. Monomer **M59** was synthesised in a greater yield than the diester equivalent. **M2** and **M59** were copolymerised, in a controlled fashion, with a variety chemical compositions. Treatment of **P17** with Hunig's base produced PAHA containing acrylate type olefin functional groups, however, isolation of the lowest MW olefin functionalised copolymer failed. The acrylate functionalised PAHA was copolymerised with **M60** in thermal and UV initiated free radical polymerisations to form a networked copolymer **P20** with a variety of compositions. Attempted synthesis of a pendant olefin functionalised 1,3-dioxolan-4-one failed. **M61** was synthesised with a greater yield than either of the diester or OCA equivalents. Homopolymerisation of **M61** was achieved, however, the highest conversion reached was 50% and only low MW polymer was obtained in a very low yield. **M62** was synthesised by modified literature procedures, however, attempts to obtain polymer **P21** failed.

4.8 Future Work

Various alkyl substituted monomers produced polymers of low MWs in comparison to similar substituents, to investigate this, steps to identify and source the chain transfer agent causing the decrease in MW by combining further NMR spectroscopy and mass spectrometry studies would be carried out. As noted previously, the ultimate goal of propargyl functionalised PAHA will be for this project to investigate the fate of the drug delivery system *in vivo* and gain an insight into how to better design future drug delivery systems in collaboration with Ms Sally Vanden-Hehir and Professor Alison Hulme. Further investigations surrounding **P20** such as tensile testing, rheology, and degradation is currently being carried out to investigate the impact of the networking on the physical properties and the degradation products in order to identify the polymer's potential applications.

4.9 References

(1) Jing, F.; Smith, M. R.; Baker, G. L. *Macromolecules* **2007**, *40* (26), 9304–9312.

(2) Yin, M.; Baker, G. L. *Am. Chem. Soc. Polym. Prepr. Div. Polym. Chem.* **1998**, *39* (2), 158–159.

(3) Baker, G.; Vogel, E.; Smith, M. *Polym. Rev.* **2008**, *48* (1), 64–84.

(4) Trimaille, T.; Möller, M.; Gurny, R. *J. Polym. Sci. Part A Polym. Chem.* **2004**, *42* (17), 4379–4391.

(5) Cohen-Arazi, N.; Katzhendler, J.; Kolitz, M.; Domb, A. J. *Macromolecules* **2008**, *41*

(20), 7259–7263.

(6) Deechongkit, S.; You, S. L.; Kelly, J. W. *Org. Lett.* **2004**, *6* (4), 497–500.

(7) Sels, B.; Dusselier, M. PROCESS FOR PREPARING CYCLIC ESTERS AND CYCLIC AMIDES. WO2014122294, 2014.

(8) Sels, B.; Dusselier, M. Process for preparing cyclic esters and cyclic amides. WO 2014122294, 2014.

(9) Liu, T.; Simmons, T. L.; Bohnsack, D. A.; Mackay, M. E.; Smith, M. R.; Baker, G. L. *Macromolecules* **2007**, *40* (17), 6040–6047.

(10) Buchard, A.; Carbery, D. R.; Davidson, M. G.; Ivanova, P. K.; Jeffery, B. J.; Kociok-Köhn, G. I.; Lowe, J. P. *Angew. Chemie - Int. Ed.* **2014**, *53* (50), 13858–13861.

(11) Jiang, X.; Vogel, E. B.; Smith, M. R.; Baker, G. L. *Macromolecules* **2008**, *41* (6), 1937–1944.

(12) Coumes, F.; Darcos, V.; Domurado, D.; Li, S.; Coudane, J.; Law, W. C.; Cheng, C.; Frechet, J. M. J.; Sharpless, K. B.; Fokin, V. V.; Gellert, P. R.; Washington, C. *Polym. Chem.* **2013**, *4* (13), 3705–3713.

(13) Yu, Y.; Zou, J.; Yu, L.; Ji, W.; Li, Y.; Law, W. C.; Cheng, C. *Macromolecules* **2011**, *44* (12), 4793–4800.

(14) Wang, H.; Tang, L.; Tu, C.; Song, Z.; Yin, Q.; Yin, L.; Zhang, Z.; Cheng, J. *Biomacromolecules* **2013**, *14* (10), 3706–3712.

(15) Yu, Y.; Chen, C. K.; Law, W. C.; Weinheimer, E.; Sengupta, S.; Prasad, P. N.; Cheng, C. *Biomacromolecules* **2014**, *15* (2), 524–532.

(16) Zhang, Z.; Yin, L.; Xu, Y.; Tong, R.; Lu, Y.; Ren, J.; Cheng, J. *Biomacromolecules* **2012**, *13* (11), 3456–3462.

(17) Yamakoshi, H.; Dodo, K.; Okada, M.; Ando, J.; Palonpon, A.; Fujita, K.; Kawata, S.; Sodeoka, M. *J. Am. Chem. Soc.* **2011**, *133* (16), 6102–6105.

(18) Hong, S.; Chen, T.; Zhu, Y.; Li, A.; Huang, Y.; Chen, X. *Angew. Chemie - Int. Ed.* **2014**, *53* (23), 5827–5831.

(19) Allen, T. M.; Cullis, P. R. *Science* **2004**, *303* (5665), 1818–1822.

(20) Dyker, G.; Hildebrandt, D. *J. Org. Chem.* **2005**, *70* (15), 6093–6096.

(21) Hawkins, E. G. E.; Maddams, W. F. *J. Chem. Soc.* **1963**, No. 0, 3466–3468.

(22) Belibel, R.; Avramoglou, T.; Garcia, A.; Barbaud, C.; Mora, L. *Mater. Sci. Eng. C* **2016**, *59*, 998–1006.

(23) Jing, F.; Hillmyer, M. A. *J. Am. Chem. Soc.* **2008**, *130* (42), 13826–13827.

(24) Fuoco, T.; Finne-Wistrand, A.; Pappalardo, D. *Biomacromolecules* **2016**, *17* (4), 1383–1394.

(25) Borchmann, D. E.; Ten Brummelhuis, N.; Weck, M. *Macromolecules* **2013**, *46* (11), 4426–4431.

(26) Leemhuis, M.; Akeroyd, N.; Kruijtzer, J. A. W.; van Nostrum, C. F.; Hennink, W. E. *Eur. Polym. J.* **2008**, *44* (2), 308–317.

(27) Zou, J.; Hew, C. C.; Themistou, E.; Li, Y.; Chen, C. K.; Alexandridis, P.; Cheng, C. *Adv. Mater.* **2011**, *23* (37), 4274–4277.

(28) Kalelkar, P. P.; Alas, G. R.; Collard, D. M. *Macromolecules* **2016**, *49* (7), 2609–2617.

(29) Vert, M.; Dos Santos, I.; Ponsart, S.; Alauzet, N.; Morgat, J. L.; Coudane, J.; Garreau, H. *Polym. Int.* **2002**, *51* (10), 840–844.

(30) Hamlet, C. G.; Sadd, P. A.; Crews, C.; Velíšek, J.; Baxter, D. E. *Food Addit. Contam.* **2002**, *19* (7), 619–631.

(31) Hope, D. B.; Wålti, M. *J. Chem. Soc. C Org.* **1970**, No. 18, 2475–2478.

(32) Ovitt, T. M.; Coates, G. W. *J. Am. Chem. Soc.* **2002**, *124* (7), 1316–1326.

(33) Holysz, R. P. *J. Am. Chem. Soc.* **1953**, *75* (18), 4432–4437.

(34) Tonelli, A. E.; Schilling, F. C. *Acc. Chem. Res.* **1981**, *14* (8), 233–238.

(35) Duda, A.; Biela, T.; Libiszowski, J.; Penczek, S.; Dubois, P.; Mecerreyes, D.; Jéroˆme, R. *Polym. Degrad. Stab.* **1998**, *59* (1), 215–222.

(36) Frazer, R. Q.; Byron, R. T.; Osborne, P. B.; West, K. P. *J. Long. Term. Eff. Med. Implants* **2005**, *15* (6), 629–639.

(37) Timmer, M. D.; Ambrose, C. G.; Mikos, A. G. *J. Biomed. Mater. Res.* **2003**, *66A* (4), 811–818.

(38) Miki, D.; Dastgheib, K.; Kim, T.; Pfister-Serres, A.; Smeds, K. A.; Inoue, M.; Hatchell, D. L.; Grinstaff, M. W. *Cornea* **2002**, *21* (4), 393–399.

(39) Amsden, B. *Soft Matter* **2007**, *3* (11), 1335–1348.

(40) Jia, X.; Burdick, J. A.; Kobler, J.; Clifton, R. J.; Rosowski, J. J.; Zeitels, S. M.; Langer,

R. *Macromolecules* **2004**, *37* (9), 3239–3248.

(41) Sanabria-DeLong, N.; Crosby, A. J.; Tew, G. N. *Biomacromolecules* **2008**, *9* (10), 2784–2791.

(42) Metters, A. T.; Anseth, K. S.; Bowman, C. N. *Polymer (Guildf).* **2000**, *41* (11), 3993–4004.

(43) Gao, H.; Li, W.; Matyjaszewski, K. *Macromolecules* **2008**, *41* (7), 2335–2340.

(44) Wagner, H. L. *Journal of physical and chemical reference data*. 1987, pp 165–173.

(45) Pounder, R. J.; Dove, A. P. *Biomacromolecules* **2010**, *11* (8), 1930–1939.

(46) Du Boullay, O. T.; Saffon, N.; Diehl, J. P.; Martin-Vaca, B.; Bourissou, D. *Biomacromolecules* **2010**, *11* (8), 1921–1929.

(47) Niu, Y.; Li, Y.; Lu, Y.; Xu, W.; Xia, X. N.; Lu, Y. B.; Ji, J.; Cheng, J. J.; Ren, J.; Cheng, J. J. *RSC Adv.* **2014**, *4* (102), 58432–58439.

(48) Matthes, D.; Richter, L.; Muïler, J.; Denisiuk, A.; Feifel, S. C.; Xu, Y.; Espinosa-Artiles, P.; Susmuth, R. D.; Molna, I. *Chem. Commun.* **2012**, *48* (48), 5674–5676.

(49) Du Boullay, O. T.; Bonduelle, C.; Martin-Vaca, B.; Bourissou, D. *Chem. Commun.* **2008**, *12* (15), 1786–1788.

(50) Pounder, R. J.; Fox, D. J.; Barker, I. A.; Bennison, M. J.; Dove, A. P.; Jerome, R.; Jerome, C.; Dubois, P. *Polym. Chem.* **2011**, *2* (10), 2204–2212.

Chapter 5. Conclusions

In Chapter 2, the polymerisation of monomer **M45** was investigated. It was firstly found that when using a literature procedure, which describes the synthesis of a polyesteracetal, a polyester, **P3**, was formed. The polymerisation was conducted at a high concentration, high temperature and over 24 h. After a brief catalyst screening process, catalyst **C13** was found to be the optimal catalyst to polymerise **M2** and **M45**. Catalyst **C13** was used to synthesise **P3** with moderate to high conversions (67 – 99 %) in under 7 hours at a reduced temperature of 40 °C. The chemical composition of the copolymer was varied and increased ratios of **M2** to **M45** were observed to produce less disperse polymer products. Higher molecular weight polymer **P3** was synthesised up to a M_n of 43600 g/mol by increasing the monomer feedstock, however it was necessary to conduct these polymerisations at 70 °C to achieve good conversions.

The compatibility of polymerising monomer **M45** with two other ROP monomers was also tested in Chapter 2. Copolymerisations of **M45** and **M47** with **C13** were conducted at ambient temperatures and with moderate to good control over the dispersity of the product (Đ = 1.78 – 1.25). Analysis of the **P11** copolymers by ^{1}H NMR spectroscopy revealed the copolymers had differing caprolactone diad concentrations. The diad concentrations were used to calculate the average length of caprolactone and glycolic acid chains within the copolymer and by comparing these values to the expected random values the degree of randomness was calculated. The various feedstocks used to synthesise **P11** copolymers were found to have each produced different degrees of randomness. A third and novel copolymer was made from monomer **M45** when it was copolymerised with monomer **M3**. Like **P3** and **P11**, the chemical composition of **P12** was varied by adjusting the ratio of **M3** to **M45** in the initial monomer feedstock.

To bridge the gap between synthesising a homopolymer *vs*. a copolymer from 1,3-dioxolan-4-one type monomers additional substitution to the monomer was necessary, due to **P10** being insoluble. In Chapter 3, a methyl substituted 1,3-dioxolan-4-one, **M46**, was used to synthesise the homopolymer **P1**. This outlined the potential scope of this new synthetic route for improving upon the current methods used to make a polymer that has become one of the biggest growing focuses in polymer chemistry. Screening a variety of MeAl(salen) catalysts for the promotion of the polymerisation of **M46** did not lead to any significant increases in overall polymerisation performance. However, it did provide the evidence which enabled us to identify the Tishchenko reaction as a major competing side reaction and the cause of

polymer products' decreased MWs. Using the optimised catalyst and polymerisation conditions monomer **M49** was polymerised to form a phenyl substituted PAHA. The polymer which had previously been shown to have a significantly increased T_g over other common polyesters formed by ROP, had proven difficult to obtain in an isotactic form as it had only ever been synthesised from **M43**, an OCA monomer. ROP of monomer **M49** proved capable of forming isotactic **P5**. Despite, requiring prolonged reaction times in comparison to the phenyl substituted OCA, it alleviated the cost and toxicity issues associated with OCA monomers. Despite best attempts, higher molecular weight polymer **P5** were produced as atactic. Alterations to the reaction set-up were used to try and remove the polymerisation product paraformaldehyde, however, no improvements were made. Paraformaldehyde was eliminated by using a ketone, acetone, as the ring-closing reagent. It was used to synthesise monomers **M50** and **M51**. The increased substitution of the monomer meant longer reaction times were necessary for the polymerisation of **M50** and increased reaction temperatures were required for the polymerisation of **M51**. Despite this, the polymer **P5** produced from the ROP of **M51** had an M_n more closely aligned with its $M_{n,th}$ than previously realised when using **M49**.

Finally, Chapter 5 explored the use of a diverse range of substituted 1,3-dioxolan-4-ones to synthesise a host of different PAHA. 1,3-Dioxolan-4-one type monomers provided a key opportunity which allowed us to improve upon the yields of the previous cyclic diesters. Simple alkyl substituted monomers were polymerised to access PAHAs with a wide range of glass transition temperatures. The substituents' range of steric bulk provided a key insight into the mechanism, as increased steric bulk led to drastic decreases in the monomer's rate of polymerisation. This was suggestive of a coordination-insertion type mechanism. A propargyl substituted monomer, **M58**, was homopolymerised to form PAHA containing pendant alkyne groups. However, the M_n values at high conversions were far from the $M_{n,th}$.values. These discrepancies were nullified when the monomer was used to form a copolymer, which primarily consisted of **P3**, and also contained a functional group Raman active in the cell silent region. The project in collaboration with Ms Sally Vanden-Hehir and Prof. Alison Hulme is ongoing and its goal will be to image the uptake of nanoparticles into cells by Raman spectroscopy. A beta-chloro substituted monomer was used to form a copolymer with **M2**, and provided the opportunity to form an olefin functionality directly onto the backbone of a PAHA *via* post-polymerisation modification. The polymer was then used to form a networked copolymer with methyl methacrylate in a free radical polymerisation, initiated by either heat or UV irradiation. The networked was synthesised with a varying degree of crosslinking, as indicated by the Mark-Houwink parameters of the polymer, which could be controlled simply by altering the initial feedstock. Other monomers substituted with an ester and benzyl ether

were synthesised, however, were found to be a non-viable option for the synthesis of hydroxyl or carboxylic acid substituted PAHAs.

The work of this thesis has demonstrated that 1,3-dioxolan-4-one compounds can be polymerised to form a variety of 15 different homopolymers and copolymers with good control over properties such as M_n, $Đ$. The new synthetic method is of significance as it provides a pathway which both improves upon yields of cyclic diester monomers and avoids the use of phosgene, diphosgene or triphosgene. The continued research and development into biodegradable polymers from renewable resources will play a big role in the drive towards a more sustainable future. Research will need to continue in the ongoing pursuit of diversifying the properties available from polyesters in order to provide replacements for the world's ever-growing need and use of plastic materials. The likelihood PAHAs and other polyesters meeting these requirements and the world becoming more sustainable looks brighter with each academic publication in this field.

Chapter 6. Experimental Procedures

6.1 Materials

Commercial reagents were purchased from Acros Organics, Alfa, Fisher or Sigma Aldrich and used as received unless otherwise stated. *Rac*-lactide and L-lactide were purchased from Corbion and were purified by three vacuum sublimations prior to polymerisations. Chloroform-d, chlorobenzene was purified by stirring over CaH_2, and distilled under an inert atmosphere. Benzyl alcohol, 2-(benzyloxy)ethanol, β-butyrolactone, ε-caprolactone, and 1,8-diazabicyclo[5.4.0]undec-7-ene (DBU), methyl methacrylate were purified by stirring over CaH_2, and distilled under vacuum. Tetrahydrofuran, benzene-d_6 and toluene-d_8 were dried over sodium/benzophenone and distilled under an inert atmosphere. Toluene, dichloromethane, hexane and diethyl ether were obtained from an Innovative Technologies purification system, consisting of alumina and copper catalyst. The solvents were degassed by three freeze-pump-thaw cycles prior to use. α-Hydroxy acids for monomer synthesis were purchased from various vendors unless otherwise stated.

6.2 General Considerations

All air-sensitive manipulations were performed in an MBraun LABmaster sp glovebox equipped with a -35°C freezer, [O_2] and [H_2O] were <0.1ppm according to built-in analysers or n a dual manifold Schlenk line using standard Schlenk techniques. All ^{1}H, $^{13}C\{1H\}$, NMR spectra were obtained on Bruker Avance III 400, and 500 MHz spectrometers or on a Bruker Avance I 600 MHz spectrometer. $^{13}C\{^{1}H\}$ denotes proton decoupled 13C spectra. All spectra were obtained at ambient temperature unless otherwise stated. The chemical shifts (δ) and coupling constants (J) were recorded in parts per million (ppm) and Hertz (Hz) respectively. ^{1}H, $^{13}C\{^{1}H\}$ multiplicities and coupling constants are reported where applicable. The residual solvent peak of the deuterated solvent was used as a reference and spectra were recording relative to it. Mass spectra were recorded on a Bruker micrOTOF II spectrometer. Mass spectrometry was performed on a Bruker UltraflexExtreme MALDI-ToF spectrometer. MALDI-ToF samples were prepared using the following matrices; 2,5-dihydroxybenzoic acid for poly(lactic acid) and poly(hexahydromandelic acid), dithranol for poly(mandelic acid) and sodium or potassium trifluoroacetate was used as the ionisation source. Differential scanning calorimetry (DSC) was carried out using a DSC 404 F3 Pegasus® DSC instrument using a heat (25–200 °C)/cool (200–25 °C)/heat (25–500 °C) cycle at a rate of 10 °C min−1 or on a

TA DSC2500 equipped with a TA refrigerated cooling system RCS 90. Gel permeation chromatography (GPC) was carried out in THF at a flow rate of 1 mL min^{-1} at 35 °C on a Malvern Instruments Viscotek 270 GPC Max triple detection system with 2×mixed bed styrene/DVB columns (300 × 7.5 mm). PLA, PHB, PCL dn/dc values used were 0.050,[1] 0.065,[2] 0.072. Infrared spectroscopy was carried out on a Shimadzu IRAffinity-1S Fourier transform spectrophotometer.

6.3 Synthesis of Monomers

Synthesis of 1,3-dioxolan-4-one (**M45**).[3]

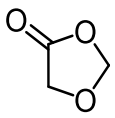

Glycolic acid (22.80 g, 300 mmol) and paraformaldehyde (12.90 g, 360 mmol) and p-TsOH·H_2O (2.42 g, 14.0 mmol) were dissolved in benzene (800 mL). The reaction mixture was refluxed and water was removed from the mixture *via* azeotropic distillation for 6 h using a Dean-Stark apparatus. The mixture was cooled, washed with saturated aqueous $NaHCO_3$ solution (400 mL), deionized water (400 mL) and saturated aqueous NaCl solution (400 mL), and dried with magnesium sulfate. The evaporation of the solvent led to obtaining the crude product. The product was purified and dried by stirring over CaH_2 for 16 h at ambient temperature followed by distillation under vacuum at 25 °C 0.1 mmHg to yield 7.39 g, 23% as a colourless oil. ^{1}H NMR (500 MHz, Chloroform-d) δ 5.50 (s, 2H, OCH_2O), 4.20 (s, 2H, CCH_2O). ^{13}C NMR (126 MHz, Chloroform-d) δ 171.20, 96.10, 62.45 ppm.

Synthesis of *S*-5-methyl-1,3-dioxolan-4-one (**M46**).[4]

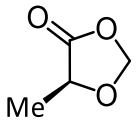

Synthesised as per **M45** using *L*-lactic acid (80% w/w H_2O solution) (29.2 g, 0.32 mol), and paraformaldehyde (12 g, 0.4 mol) benzene (1600 mL). p-TsOH·H_2O (4.94 g, 26 mmol) and distilled at 25 °C at 0.1 mmHg to yield 25.6 g, 80% as a colourless oil. ^{1}H NMR (500 MHz, Chloroform-d) δ 5.56 (s, 1H, OCH_2O), 5.32 (s, 1H, OCH_2O), 4.27 (q, JHH = 7, 1H, CH_3CH), 1.47 (d, JHH = 7, 3H, CH_3CH). ^{13}C NMR (126 MHz, Chloroform-d) δ 173.58, 93.88, 69.57, 15.76 ppm.

Synthesis of *S*-5-phenyl-1,3-dioxolan-4-one (***S-M49***), *rac*-5-Phenyl-1,3-dioxolan-4-one (*rac*- **M49**) and *R*-5-Phenyl-1,3-dioxolan-4-one (*R*- **M49**).[5]

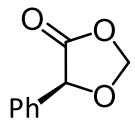
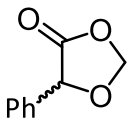
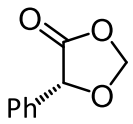

Synthesised as per **M45** using mandelic acid (11.9 g, 78 mmol), and paraformaldehyde (3.2 g, 100 mmol) benzene (400 mL). p-TsOH·H_2O (1.23 g, 6.5 mmol) and distilled at 90 °C at 0.1 mmHg to yield 12.3 g, 96 % as a colourless oil.

^{1}H NMR (500 MHz, Chloroform-d) δ 7.52 – 7.37 (m, 5H, Ar), 5.65 (s, 1H, C*H*$_2$), 5.47 (s, 1H, C*H*$_2$), 5.23 (s, 1H, C*H*) ppm. ^{13}C NMR (126 MHz, Chloroform-d) δ 171.38, 133.30, 129.24, 128.90, 126.52, 94.57, 74.49 ppm.

Synthesis of 2,2,5-trimethyl-1,3-dioxolan-4-one (Me_3DOX) (**M50**).[6]

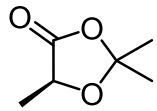

L-lactic acid (80% w/w H_2O solution) (0.7 g, 7.53 mmol), and p-TsOH·H_2O (0.13 g, 0.75 mmol) were dissolved in a mixture of acetone and benzene (1:1, 50mL). The reaction mixture was refluxed and water was removed from the mixture *via* azeotropic distillation for 6 h using a Dean-Stark apparatus. The mixture was cooled, washed with saturated aqueous $NaHCO_3$ solution (25 mL), deionized water (25 mL) and saturated aqueous NaCl solution (25 mL), and dried with magnesium sulfate. The evaporation of the solvent led to obtaining the crude product. The product was purified and dried by stirring over CaH_2 for 16 h at ambient temperature followed by distillation under vacuum at 40 °C 0.1 mmHg to yield 0.52 g, 60% as a colourless oil. ^{1}H NMR (500 MHz, Chloroform-d) δ 4.43 (q, *JHH*= 6.8 Hz, 1H, C*H*CH_3), 1.56 (s, 3H, OOCC*H*$_3$), 1.49 (s, 3H, OOCC*H*$_3$), 1.42 (d, *JHH*= 6.8 Hz, 3H, CHC*H*$_3$). ^{13}C NMR (126 MHz, Chloroform-d) δ 173.78, 110.36, 110.29, 110.06, 70.40, 27.41, 25.56, 17.36.

2,2-Dimethyl-5-phenyl-1,3-dioxolan-4-one (Me_2PhDOX) (**M51**).[6]

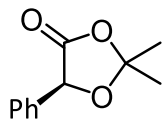

Synthesised as per **M50** using *R*-mandelic acid (1.15 g, 7.53 mmol) and p-TsOH·H_2O (0.13 g, 0.75 mmol) were dissolved in a mixture of acetone and benzene (1:1, 50mL). The product was recrystallised from toluene three times to give a white crystalline solid, 95% yield. Melting point = 71 °C. ^{1}H NMR (500 MHz, Chloroform-d) δ 7.52 – 7.46 (m, 2H, Ar), 7.48 – 7.36 (m, 3H, Ar), 5.42 (s, 1H, OOCC*H*), 1.75 (s, 3H, OOCC*H*$_3$), 1.70 (s, 3H, OOCC*H*$_3$). ^{13}C NMR (126 MHz, Chloroform-d) δ 171.42, 134.45, 128.95, 128.73, 126.42, 110.94, 75.89, 27.26, 26.19.

Synthesis of *S*-i-propyl-1,3-dioxolan-4-one (**M52**).[5]

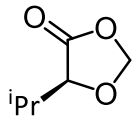

The parent α-hydroxy acid valic acid was first prepared by the diazotisation of valine.[7]

Synthesised as per **M45** using valic acid (17.97g, 150 mmol), and paraformaldehyde (6.45 g, 200 mmol) benzene (800 mL). p-TsOH·H_2O (2.46 g, 13 mmol) and distilled at 40 °C at 0.1 mmHg to yield 22 g, 90 % as a colourless oil.

^{1}H NMR (500 MHz, Chloroform-d) δ 5.56 (s, 1H, OC*H*$_2$O), 5.38 (s, 1H, OC*H*$_2$O), 4.04 (dt, JHH= 4.4, 0.7 Hz, 1H, OCC*H*O), 2.18 (heptd, JHH= 6.8, 4.2 Hz, 1H, $(CH_3)_2$C*H*, 1.05 (dd, JHH= 45, 6.9 Hz, 6H, C*H*$_3$). ^{13}C NMR (126 MHz, Chloroform-d) δ 172.35, 94.48, 29.88, 18.26, 16.65.

Synthesis of 5-cyclohexyl-1,3-dioxolan-4-one (**M53**).

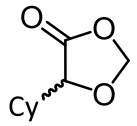

Synthesised as per **M45** using hexahydromandelic acid (1.192 g, 7.53 mmol), and paraformaldehyde (0.36 g, 12 mmol) benzene (40 mL). p-TsOH·H_2O (0.13 g, 0.7 mmol) and distilled at 60 °C at 0.1 mmHg to yield 1.2 g, 93 % yield. ^{1}H NMR (500 MHz, Chloroform-d) δ 5.50 (s, 1H, OC*H*$_2$O), 5.42 (s, 1H, OC*H*$_2$O), 4.03 (d, JHH= 4.0 Hz, 1H, C*H*), 1.91 – 1.73 (m, 3H), 1.72 – 1.58 (m, 2H, CyH), 1.34 – 1.09 (m, 6H, CyH). ^{13}C NMR (126 MHz, Chloroform-d) δ 172.59, 94.74, 39.43, 26.92, 26.08, 26.02, 25.87. HRMS: $C_9H_{14}O_3$ Theoretical mass: 170.09326, m/z: 170.09375.

Synthesis of 5-n-butyl-1,3-dioxolan-4-one (**M54**).[5]

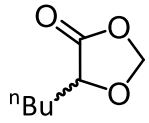

Synthesised as per **M45** using α-hydroxyhexanoic acid (6.38 g, 48.3 mmol), and paraformaldehyde (1.04 g, 58 mmol) benzene (300 mL). p-TsOH·H_2O (0.93 g, 4.8 mmol) and distilled three times at 50 °C at 0.1 mmHg to yield 4.2 g, 60 % yield. ^{1}H NMR (500 MHz, Chloroform-d) δ 5.53 (s, 1H, OC*H*$_2$O), 5.33 (s, 1H, OC*H*$_2$O), 4.16 (m, 1H, OCC*H*O), 1.85 (m, 1H, CHC*H*$_2$), 1.77 - 1.65 (m, 1H, $CH_2CH_2CH_2CH_3$), 1.52 – 1.27 (m, 4H, C*H*$_2$C*H*$_2$CH$_3$), 0.89 (t, JHH= 7.2 Hz, 3H, C*H*$_3$). ^{13}C NMR (126 MHz, Chloroform-d) δ 172.98, 94.03, 73.02, 29.92, 26.88, 22.12, 13.66.

Synthesis of 5-i-butyl-1,3-dioxolan-4-one (**M55**).[5]

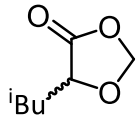

The parent α-hydroxy acid α-hydroxyisocaproic acid was first prepared by the diazotisation of i-leucine.[8]

Synthesised as per **M45** using α-hydroxyisocaproic acid (6.38 g, 48.3 mmol), and paraformaldehyde (1.04 g, 58 mmol) benzene (300 mL). p-TsOH·H_2O (0.93 g, 4.8 mmol) and distilled three times at 55 °C at 0.1 mmHg to yield 4.2 g, 60 % yield. ^{1}H NMR (500 MHz, Chloroform-d) δ 5.55 (s, 1H OC*H*$_2$O), 5.35 (s, 1H OC*H*$_2$O), 4.20 (ddd, *JHH*= 9.3, 3.9, 0.9 Hz, 1H, OCC*H*O), 1.87 (dh, *JHH*= 8.1, 6.6 Hz, 1H, C*H*(CH_3)), 1.75 – 1.59 (m, 2H, C*H*$_2$CH(CH_3)), 0.96 (dd, *JHH*= 6.8, 5.5 Hz, 6H, C*H*$_3$). ^{13}C NMR (126 MHz, Chloroform-d) δ 173.43, 93.93, 71.83, 38.95, 25.03, 22.79, 21.63.

Synthesis of 5-t-butyl-1,3-dioxolan-4-one (**M56**).

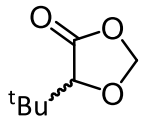

The parent α-hydroxy acid α-hydroxy-3,3-dimethylbutyric acid was first prepared by the diazotisation of t-leucine.[9]

Synthesised as per **M45** using α-hydroxy-3,3-dimethylbutyric acid (6.38 g, 48.3 mmol), and paraformaldehyde (1.04 g, 58 mmol) benzene (300 mL). p-TsOH·H_2O (0.93 g, 4.8 mmol) and distilled three times at 55 °C at 0.1 mmHg to yield 4.2 g, 60 % yield. ^{1}H NMR (601 MHz, Chloroform-d) δ 5.48 (s, 1H, OC*H*$_2$O), 5.38 (s, 1H, OC*H*$_2$O), 3.82 (s, 1H, C*H*(CH_3)$_3$, 1.05 (s, 9H, C*H*$_3$) ^{13}C NMR (151 MHz, Chloroform-d) δ 171.55, 93.90,79.98, 25.28. HRMS: $C_7H_{12}O_3$ Theoretical mass: 144.07810, m/z: 144.07752.

5-Propynyl-1,3-dioxolan-4-one (**M58**)

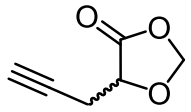

The parent α-hydroxy acid 2-Hydroxy-4-pentynoic acid was first prepared reacting ethyl glyoxalate and propargyl bromide in a Barbier reaction, followed by the hydrolysis of the ethyl ester.[10]

Synthesised as per **M45** using 2-Hydroxy-4-pentynoic acid (5.6 g, 49 mmol), and paraformaldehyde (1.8 g, 60 mmol) benzene (400 mL). p-TsOH·H_2O (0.95 g, 4.8 mmol) and distilled at 70 °C at 0.1 mmHg to yield 4.66 g, 66 % yield. ^{1}H NMR (500 MHz, Chloroform-d) δ 5.65 (d, *JHH*= 0.7 Hz, 1H), 5.49 (d, *JHH*= 0.7 Hz, 1H), 4.42 – 4.35 (m, 1H), 2.82 (ddd, *JHH*= 17.4, 4.4, 2.7 Hz, 1H), 2.71 (ddd, *JHH*= 17.3, 5.6, 2.6 Hz, 1H), 2.09 (t, *JHH*= 2.7 Hz, 1H).

5-(Chloromethyl)-1,3-dioxolan-4-one (**M59**)

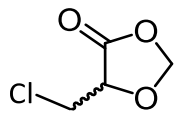

The parent α-hydroxy carboxylic acid 3-chloro-2-hydroxypropanoic acid was prepared by the oxidation of 3-Chloropropane-1,2-diol following a literature procedure.[11]

M59 was synthesised as per **M45** using 3-chloro-2-hydroxypropanoic acid (80 % H_2O (19.79 g, 0.127 mol), and paraformaldehyde (3.15 g, 0.175 mol) benzene (800 mL). p-TsOH·H_2O (2.76 g, 16 mmol) and distilled at 70 °C at 0.1 mmHg to yield 8.03 g, 46 % yield. ^{1}H NMR (500 MHz, chloroform-d) δ 5.69 (d, JHH= 1.0 Hz, 1H, OC*H*$_2$O), 5.56 (s, 1H, OC*H*$_2$O), 4.63 – 4.58 (m, 1H, C*H*), 3.92 (dd, JHH= 12.3, 3.1 Hz, 1H, ClC*H*$_2$), 3.88 (dd, JHH= 12.3, 3.8 Hz, 1H, ClC*H*$_2$).

Attempted synthesis of parent α-hydroxy ester ethyl 2-hydroxy-3-butenoate 1:

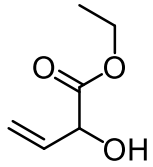

To a flask containing Zn (1.4g) in anhydrous THF (3 mL) and diethyl ether (10 mL) vinyl bromide 1M THF (3 mL, 2.9 mmol) was added under an inert atmosphere. The mixture was stirred at room temperature for 30 min and then cooled in an ice bath. A solution of ethyl glyoxylate (50 %w/w in toluene) and vinyl bromide 1M THF (9 mL, 8.7 mmol) in anhydrous diethyl ether (15 mL) was added dropwise to the Zn slurry at 0 °C. After the addition was complete, the mixture was stirred at 0 °C overnight. The reaction mixture was then poured into a conical flask containing ice-cold HCl 3M aq. (50 mL). After separation of the organic layer, the aqueous layer was extracted with ether (3 × 300 mL), and the combined organic layers were dried over $MgSO_4$. Filtration and removal of the solvent did no lead to the desired product.

Attempted synthesis of parent α-hydroxy ester ethyl 2-hydroxy-3-butenoate 2:

Various adaptations of this synthesis were carried out. A dried 50 %W/W solution of ethyl glyoxylate in toluene (0.6, 3.0 mmol) was dissolved in anhydrous THF (3 mL). The solution was cooled to -78 °C, before a solution of vinyl magnesium bromide in THF 1M (3.0 mL, 3.0 mmol) was added dropwise. The reaction was stirred at -78 °C for 1 hours before being allowed to reach room temperature, and stirred for a further 22 hours. An aliquot was taken and NMR was used to confirm that the target ethyl 2-hydroxy-3-butenoate had been synthesised. Methanol (0.2 mL) was added to the reaction mixture, which was then transferred dropwise into ice cold HCl 3M (10 mL) to extinguish the Grignard reagent. The organic layer was separated and the aqueous layer was washed with Diethyl ether (3 x 2.0 ± 0.5 ml). The combined organic extracts were dried over anhydrous $MgSO_4$, filtered and the solvent was removed under reduced pressure to yield the crude product of 2-hydroxy-3-butenoic acid ethyl ester, a viscous dark brown oil. ^{1}H-NMR (500 MHz; Chloroform-d); 1a signals δH / ppm = 1.28 (t, 3H, CH_3), 4.28 (q, 2H, O-CH_2-CH_3), 4.76 (m, 1H, CHO), 5.25-5.30 (m, 1H, CH_2=CH),

5.49-5.53 (m, 1H, CH_2=CH), 5.85-6.09 (m, 1H, CH_2=CH) and additional non-solvent signals δH / ppm = 1.39 (t) 1.42 (s), 2.86 (t), 3.32 (s), 3.52 (s), 3.94 (m), 4.12-4.17 (m), 4.39 (q), 4.87 (s), 4.92 (s), 4.94 (s), 5.55-5.57 (m), 9.4 (s).

5-(Benzyloxymethyl)-1,3-dioxolan-4-one (**M61**)

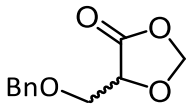

The parent α-hydroxy carboxylic acid 3-benzyloxy-2-hydroxypropanoic acid was prepared by the diazotisation of BnOserine following a literature procedure.[12]

M61 was synthesised as per **M45** using BnOserine (3.9 g, 20 mol), and paraformaldehyde (0.9 g, 32 mmol) benzene (150 mL). p-TsOH·H_2O (0.4 g, 16 mmol) and distilled at 70 °C at 0.1 mmHg to yield 7.9 g, 99 % yield.

Synthesis of 5-(*S*)-[(benzyloxycarbonyl)methyl]-2,2-dimethyl-1,3-dioxolan-4-one (**M62**).[13]

Attempted ring closing method 1 to form **M62a**:

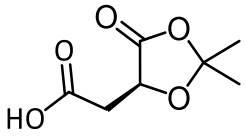

M62a

Synthesised as per 11: *L*-Malic acid (1.01 g, 7.53 mmol) and p-TsOH·H_2O (0.13 g, 0.75 mmol) were dissolved in a mixture of acetone and benzene (1:1, 50mL) and were reluxed in a Deans-Stark apparatus for 6 hours. Starting material was recovered and product formation was not observed.

Attempted ring closing method 2 to form **M62a**:

L-Malic acid (1.01 g, 7.53 mmol) and p-TsOH·H_2O (0.13 g, 0.75 mmol) were dissolved and refluxed in acetone (100 mL). Starting material was recovered and product formation was not observed.

Synthesised following a modified literature procedure to form **M62a**:[14]

L-Malic acid (1.01 g, 7.53 mmol) and p-TsOH·H_2O (0.13 g, 0.75 mmol) were dissolved in 2,2-dimethoxypropane (3.7 mL, 30 mmol) and stirred at room temperature for 3.5 hours. The solution was diluted with water (5 mL) and $NaHCO_3$ (0.06 g, 0.75 mmol) was added. The reaction mixture was extracted with DCM (5 x 5 mL), the organic layers were collected, dried with $NaSO_4$, and the evaporation of the solvent led to obtaining the product. The crude product was used directly without further purification.

Benzyl protection of **M62a** to form **M62**:[14]

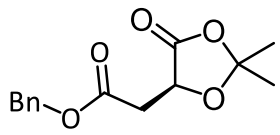

Dry triethylamine (2.8 mL, 2 mmol) was added to a solution of 13a (3 g, 17 mmol) in anhydrous acetone (15 mL) under an inert atmosphere. Benzyl bromide (8.9 mL, 75 mmol) was charged to the reaction vessel and the solution was refluxed for 60 h at 50 °C before being cooled to room temperature. The reaction mixture was isolated by filtration and the solids washed with additional acetone. The evaporation of the solvent led to obtaining the crude product and was dissolved in ethyl acetate (100 mL) and H_2O (50 mL). The aqueous layer was further extracted with ethyl acetate (2 × 40 mL) before the combined organic layers were dried with $MgSO_4$, filtered, and the evaporation of the solvent led to obtaining the crude product. The product was recrystallised from Diethyl ether to yield white crystals (12.14 g, 46 mmol, 80%). Data were in accordance with that previously reported.[14] ^{1}H NMR (500 MHz, Chloroform-d) δ 7.39 – 7.29 (m, 5H, Ar), 5.18 (d, *JHH*= 3.3 Hz, 2H, ArCH_2), 4.74 (dd, *JHH*= 6.5, 3.9 Hz, 1H, C*H*), 2.98 (dd, *JHH*= 17.0, 3.9 Hz, 1H, CHCH_2), 2.85 (dd, *JHH*= 17.0, 6.5 Hz, 2H, CHCH_2), 1.57 (dd, *JHH*= 9.6, 0.8 Hz, 6H, CH_3). ^{13}C NMR (Chloroform-d, 126.0 MHz): δ169.14, 135.35, 128.66, 128.55, 128.47, 111.25, 70.77, 67.06, 36.32, 26.75, 25.96.

6.4 Synthesis of Proligands

Synthesis of *N,N'*-bis(3,5-di-*tert*-butylsalicylidene)-1,3-propanediamine.[15]

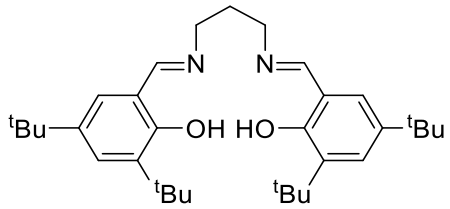

1,3-diaminopropane (0.73 g, 9.79 mmol) was added rapidly to a stirring solution of 3,5-di-*tert*-butylsalicylaldehyde (4.59 g, 19.57 mmol) in ethanol (50 mL). After refluxing for 4 hours at 78 °C the precipitated solid was filtered, washed with cold ethanol and dried under vacuum to yield the product at 85 %.

^{1}H NMR (500 MHz, Chloroform-*d*) δ 13.82 (s, 2H, O*H*), 8.40 (d, *JHH*= 1.3 Hz, 2H, NC*H*), 7.40 (d, *JHH*= 2.5 Hz, 2H, *Ar*), 7.10 (d, *JHH*= 2.5 Hz, 2H, *Ar*), 3.72 (td, *JHH*= 6.6, 1.2 Hz, 4H, NC$H_{2,}$), 2.14 (p, *JHH*= 6.6 Hz, 2H, $CH_2CH_2CH_2$), 1.47 (s, 18H, $(CH_3)_3$), 1.32 (s, 18H). ^{13}C NMR (126 MHz, Chloroform-*d*) δ 166.62, 158.26, 140.19, 136.84, 127.03, 125.98, 118.00, 56.90, 35.20, 34.29, 31.89, 31.66, 29.60.

Synthesis of *N,N'*-bis(3,5-di-*tert*-butylsalicylidene)ethylenediamine.[15]

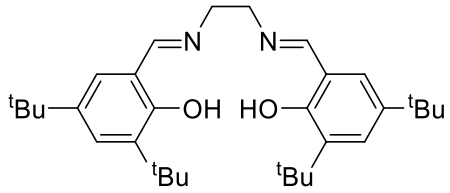

Synthesised as per 16 using ethylenediamine (0.59 g, 9.79 mmol) 3,5-di-*tert*-butylsalicylaldehyde (4.59 g, 19.57 mmol) in ethanol (50 mL).

^{1}H NMR (500 MHz, Chloroform-*d*) δ 13.63 (s, 2H, O*H*), 8.38 (s, 2H, NC*H*), 7.36 (d, *JHH*= 2.4 Hz, 2H, *Ar*), 7.11 – 7.04 (m, 2H, *Ar*), 3.92 (s, 4H, CH_2), 1.43 (s, 18H, $(CH_3)_3$), 1.28 (S, 18H, $(CH_3)_3$). ^{13}C NMR (126 MHz, Chloroform-*d*) δ 167.72, 158.17, 140.20, 136.74, 127.16, 126.19, 117.96, 59.77, 35.17, 34.26, 31.62, 29.58.

Synthesis of *N,N'*-bis(3,5-di-*tert*-butylsalicylidene)-2,2-dimethyl-1,3-propanediamine. [15]

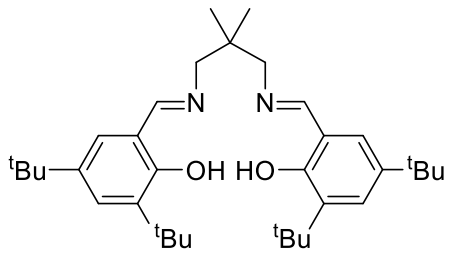

Synthesised as per 16 using 2,2-dimethyl-1,3-propanediamine (1.0 g, 9.79 mmol) 3,5-di-*tert*-butylsalicylaldehyde (4.59 g, 19.57 mmol) in ethanol (50 mL).

^{1}H NMR (500 MHz, Chloroform-*d*) δ 13.85 (s, 2H, O*H*), 8.38 (s, 1H, NC*H*), 7.40 (d, *JHH*= 2.5 Hz, 2H, *Ar*), 7.11 (d, *JHH*= 2.5 Hz, 2H, *Ar*),

3.49 (d, *JHH*= 1.2 Hz, 4H, CH_2), 1.48 (s, 18H, (CH_3)$_3$), 1.32 (s, 18H, (CH_3)$_3$), 1.21 (s, 6H, (CH_3)$_2$). ^{13}C NMR (126 MHz, Chloroform-*d*) δ 166.89, 158.34, 140.13, 136.81, 127.04, 126.07, 118.02, 68.43, 36.49, 35.22, 34.28, 31.66, 29.60, 24.72.

Synthesis of *N*,*N'*-bis(3,5-di-*tert*-butylsalicylidene)*o*-phenylenediamine.[16]

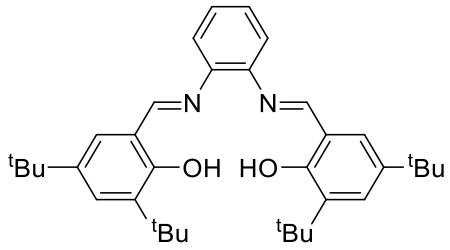

Synthesised as per 16 using *o*-phenylenediamine (1.08 g, 10 mmol) 3,5-di-*tert*-butylsalicylaldehyde (4.87 g, 20 mmol) in ethanol (45 mL).

^{1}H NMR (500 MHz, Chloroform-*d*) δ 13.52 (d, *JHH*= 1.2 Hz, 2H, O*H*), 8.66 (d, *JHH*= 1.0 Hz, 2H, NC*H*), 7.44 (d, *JHH*= 2.1 Hz, 2H, *Ar*), 7.35 – 7.29 (m, 2H, *Ar*), 7.28 – 7.18 (m, 4H, *Ar*), 1.46 – 1.41 (m, 18H, (CH_3)$_3$), 1.34 – 1.30 (m, 18H, (CH_3)$_3$). ^{13}C NMR (126 MHz, Chloroform-*d*) δ 164.87, 158.72, 142.91, 140.46, 137.34, 128.31, 127.43, 126.91, 119.96, 118.50, 35.27, 34.32, 31.62, 29.59.

Synthesis of *N*,*N'*-bis(3,5-di-chlorosalicylidene)-1,3-propanediamine.[15]

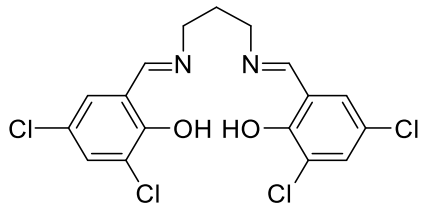

Synthesised as per 16 using 1,3-diaminopropane (0.73 g, 9.79 mmol) and 3,5-dichlorosalicylaldehyde (3.82 g, 19.57 mmol) in ethanol (50 mL).

^{1}H NMR (500 MHz, Chloroform-*d*) δ 14.32 (s, 2H, O*H*), 8.31 (s, 2H, NC*H*), 7.44 – 7.39 (m, 2H, *Ar*), 7.18 – 7.14 (m, 2H, *Ar*), 3.78 (m, 4H, NCH_2), 2.20 – 2.10 (m, 2H, $CH_2CH_2CH_2$). ^{13}C NMR (126 MHz, Chloroform-*d*) δ 164.32, 156.81, 132.51, 129.14, 123.03, 122.94, 119.50, 56.10, 31.37.

Synthesis of *N*,*N'*-bis(3,5-di-chlorosalicylidene)ethylenediamine.[15]

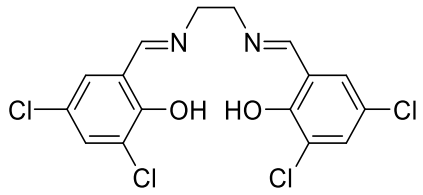

Synthesised as per 16 using ethylenediamine (0.59 g, 9.79 mmol) and 3,5-dichlorosalicylaldehyde (3.82 g, 19.57 mmol) in ethanol (50 mL).

^{1}H NMR (500 MHz, Chloroform-*d*) δ 13.63 (s, 2H, O*H*), 8.38 (s, 2H, NC*H*), 7.36 (d, *JHH*= 2.4 Hz, 2H, *Ar*), 7.06 (d, *JHH*= 2.3 Hz, 2H, *Ar*), 3.92 (s, 4H, CH_2). ^{13}C NMR (126 MHz, Chloroform-*d*) δ 167.72, 158.17, 140.20, 136.74, 127.16, 126.19, 117.96, 59.77, 35.17, 34.26, 31.62, 29.58.

Synthesis of *N*,*N'*-bis(3,5-di-chlorosalicylidene)-2,2-dimethyl-1,3-propanediamine.[15]

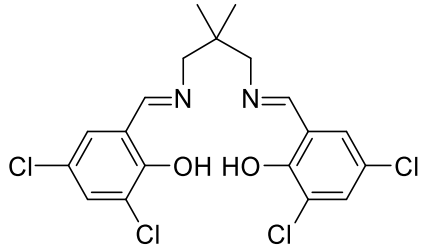

Synthesised as per 16 using 2,2-dimethyl-1,3-propanediamine (1.0 g, 9.79 mmol) 3,5-di-chlorosalicylaldehyde (3.82 g, 19.57 mmol) in ethanol (50 mL).

^{1}H NMR (500 MHz, Chloroform-*d*) δ 14.41 (s, 2H, O*H*), 8.27 (d, *JHH*= 1.3 Hz, 2H, NC*H*), 7.42 (d, *JHH*= 2.5 Hz, 2H, *Ar*), 7.17 (d, *JHH*= 2.5 Hz, 2H, *Ar*), 3.54 (d, *JHH*= 1.3 Hz, 4H, CH_2), 1.08 (s, 6H, (CH_3)$_2$). ^{13}C NMR (126 MHz, Chloroform-*d*) δ 164.61, 156.95, 132.55, 129.24, 123.00, 122.91, 119.45, 67.33, 36.40, 24.33.

6.5 Synthesis of Catalysts

In the glovebox, one equivalent of trimethyl aluminium 2M toluene solution was added dropwise to a vigorously stirring toluene solution of the respective proligand, in a Schlenk flask. After bubbling had subsided, the Schlenk flask was sealed and removed from the glovebox. The reaction vessel was immersed in a preheated oil bath at 110 °C. Upon heating and stirring for 16 h, the reaction was allowed to cool to room temperature. It is at this stage variations between synthesises are observed. If the product was observed to crystallise from solution, the remainder of the solution was removed by cannula filtration and the product washed with hexane three times before being dried under vacuum. If no product was observed, *ca*. three quarters the solvent was removed before being replaced with hexane and being cooled to 0 °C. The product was then isolated in the same fashion as described above.

Synthesis of *N,N'*-bis(3,5-di-chlorosalicylidene)ethylenediamine (**C9**).[15]

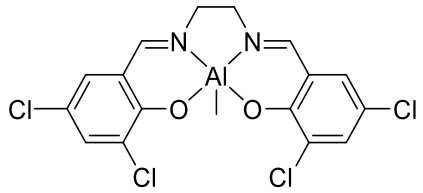

^{1}H NMR (500 MHz, THF-d_8) δ 8.38 (s, 2H, NC*H*), 7.51 (d, *JHH*= 2.7 Hz, 2H, *Ar*), 7.17 (d, *JHH*= 2.7 Hz, 2H), *Ar*, 4.07 (m, 2H, CH_2), 3.89 (m, 2H, CH_2), -1.12 (s, 3H, AlCH_3). ^{13}C NMR (126 MHz, THF-d_8) δ 169.03, 167.60, 160.79, 135.08, 134.20, 131.46, 129.83, 129.19, 129.07, 128.02, 127.15, 126.20, 121.35, 120.29, 119.76, 55.47.

Synthesis of *N,N'*-bis(3,5-di-*tert*-butylsalicylidene)ethylenediamine (**C10**).[15]

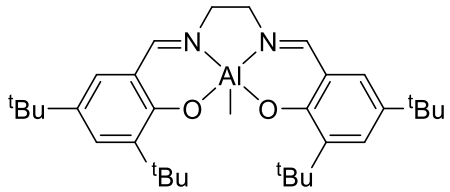

^{1}H NMR (500 MHz, Benzene-d_6) δ 8.80 (s, 2H, NC*H*), 7.77 (d, *JHH*= 2.7 Hz, 2H, Ar), 7.38 (s, 2H, Ar), 6.89 (d, *JHH*= 2.7 Hz, 2H, Ar), 3.24 – 2.82 (m, 2H, CH_2), 2.69 – 2.48 (m, 2H, CH_2), 1.86 (s, 18H, (CH_3))$_3$), 1.39 (s, 18H, (CH_3)$_3$), -0.53 (s, 3H, AlCH_3). ^{13}C NMR (126 MHz, Benzene-d_6) δ 169.08, 164.30, 141.74, 137.61, 130.62, 118.97, 54.79, 36.16, 34.20, 31.77, 30.27.

Synthesis of *N*,*N'*-bis(3,5-di-chlorosalicylidene)-1,3-propanediamine (**C12**).[15]

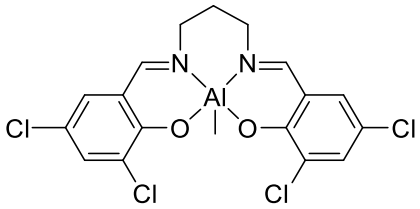

^{1}H NMR (400 MHz, CD_2Cl_2) δ 8.12 (s, 2H, NC*H*), 7.45 (d, JHH = 2.6, 2H, Ar), 7.11 (d, JHH = 2.6, 2H, Ar), 4.24-4.17 (m, 2H, NCH_2), 3.67-3.72 (m, 2H, NCH_2), 2.24-1.99 (m, 2H, $CH_2CH_2CH_2$, -0.66 (s, 3H, AlCH_3).^{13}C NMR (126 MHz, CD_2Cl_2)*:* δ 167.60, 159.78, 141.36, 134.65, 130.42, 127.09, 120.26, 120.17, 60.60, 30.60, -9.46.

Synthesis of *N*,*N'*-bis(3,5-di-*tert*-butylsalicylidene)-1,3-propanediamine (**C13**).[17]

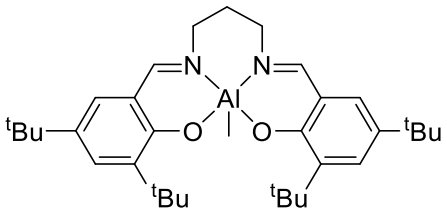

^{1}H NMR (500 MHz, Benzene-d_6) δ 8.75 (s, 2H, NC*H*), 7.75 (d, *JHH*= 2.7 Hz, 2H, Ar), 7.34 (s, 2H, Ar), 6.89 (d, *JHH*= 2.7 Hz, 2H, Ar), 3.07 – 2.79 (m, 2H, NCH_2), 2.75 – 2.38 (m, 2H, NCH_2), 1.86 (s, 18H, (CH_3))$_3$), 1.57-1.43 (m, 2H, $CH_2CH_2CH_2$) 1.39 (s, 18H, (CH_3)$_3$), -0.53 (s, 3H, AlCH_3). ^{13}C NMR (126 MHz, Benzene-d_6) δ 170.15, 164.12, 141.29, 137.48, 130.25, 127.45, 118.89, 54.94, 35.94, 34.16, 31.68, 30.18, 27.38.

Synthesis of *N*,*N'*-bis(3,5-di-chlorosalicylidene)-2,2-dimethyl-1,3-propanediamine (**C15**) [15]

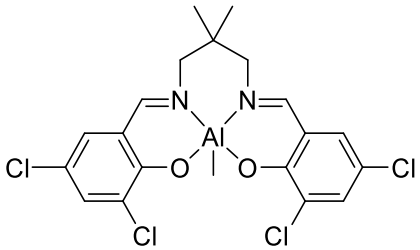

^{1}H NMR (500 MHz, THF-d_8) δ 8.23 (d, *JHH* = 1.6 Hz, 2H, NC*H*), 7.46 (d, *JHH* = 2.7 Hz, 1H, *Ar*), 7.21 (s, 1H, *Ar*), 4.19 (d, *JHH* = 11.9 Hz, 2H), 3.34 (d, *JHH* = 11.8 Hz, 2H, CH_2), 1.15 (s, 3H, (CH_3)$_2$), 0.88 (s, 3H, (CH_3)$_2$), -0.71 (s, 3H, AlCH_3). ^{13}C NMR (126 MHz, Chloroform-*d*) δ 167.50, 159.96, 134.86, 129.97, 127.70, 120.42, 119.68, 71.93, 36.68, 26.15, 22.33, 1.18.

Synthesis of *N*,*N'*-bis(3,5-di-*tert*-butylsalicylidene)-2,2-dimethyl-1,3-propanediamine (**C16**).[15]

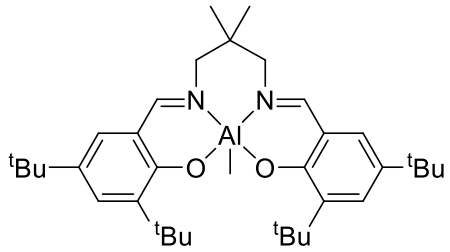

^{1}H NMR (500 MHz, Benzene-d_6) δ 8.80 (s, 2H, NC*H*), 7.76 (d, *JHH*= 2.7 Hz, 2H, *Ar*), 7.52 (s, 2H, *Ar*), 7.00 (d, *JHH*= 2.6 Hz, 2H, *Ar*), 2.89 (dd, *JHH*= 12.1, 1.1 Hz, 2H, CH_2), 2.63 (dd, *JHH*= 12.1, 0.9 Hz, 2H, CH_2), 1.84 (s, 18H, (CH_3)$_3$), 1.37 (s, 19H, (CH_3)$_3$), 0.58 (s, 3H, (CH_3)$_2$), 0.41 (s, 3H, (CH_3)$_2$), -0.43 (s, 3H, AlCH_3). ^{13}C NMR (126 MHz, Benzene-d_6) δ 170.10, 164.10, 141.63, 137.73, 130.54, 119.15, 67.02, 36.09, 35.82, 34.21, 31.74, 30.17, 25.52, 25.06.

Synthesis of *N*,*N'*-bis(3,5-di-*tert*-butylsalicylidene)*o*-phenylenediamine (**C23**).[16]

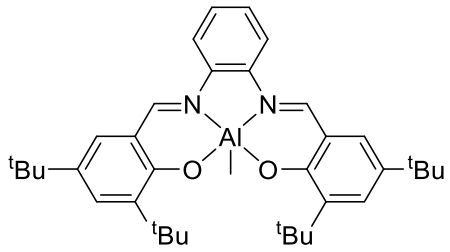

^{1}H NMR (500 MHz, Chloroform-*d*) δ 8.80 (s, 2H, NC*H*), 7.70 (dd, *JHH*= 6.1, 3.4 Hz, 2H, *Ar*), 7.60 (d, *JHH*= 2.6 Hz, 2H), *Ar*, 7.39 (dd, *JHH*= 6.1, 3.3 Hz, 2H, *Ar*), 7.16 (d, *JHH*= 2.6 Hz, 2H, *Ar*), 1.57 (s, 18H, (CH_3)$_3$), 1.35 (s, 18H, (CH_3)$_3$), -1.19 (s, 3H, AlCH_3). ^{13}C NMR (126 MHz, Chloroform-*d*) δ 165.08, 162.01, 141.58, 139.06, 138.44, 132.15, 128.09, 127.97, 118.74, 115.82, 35.82, 34.21, 31.48, 29.96, 1.19.

6.6 Polymerisations

6.6.1 General Polymerisation Conditions

All polymerisations were carried out in an identical manner unless otherwise stated. In a nitrogen filled glovebox, catalyst and benzyl alcohol was dissolved in solvent and subsequently added to monomer(s). The mixture was then charged to an ampoule. The ampoule was then sealed, removed from the glovebox and placed in a preheated oil bath at T °C for Xh. After Xh, the ampoule was cooled and 3-4 drops of methanol was added to quench the polymerization. The polymer was then dissolved in dichloromethane and a sample was taken for conducting ^{1}H NMR spectroscopy on a crude sample. The polymer was then precipitated from cold methanol and cooled overnight at -35 °C. The white precipitate was filtered, dried under vacuum to constant weight and a sample of this was used for GPC analysis.

This procedure is modified when organocatalysts TBD and DBU were used, by quenching with 3-4 drops of formic acid rather than methanol.

6.6.2 Reaction monitoring by NMR spectroscopy

Procedure for kinetics monitored by NMR spectroscopy

In a nitrogen filled glovebox, 0.01 mmol of catalyst and 1µL (0.01 mmol) of benzyl alcohol were dissolved in 1mL of toluene-d8. 1 mmol of monomer was then added and the solution was transferred to a Young's NMR tube. The NMR tube was removed from the glovebox and immediately placed into an NMR spectrometer.

6.6.3 Polymerisation of *rac*-lactide and glycolide

C1 (81 mg, 0.2 mmol), lauryl alcohol (37 mg, 0.2 mmol) were placed in a round bottom flask and heated to 120 °C. rac-**M2** (2.02 g, 14 mmol) was added to the reaction vessel and was stirred for two hours. In 10-minute intervals 10 portions of **M1** (0.07 g, 0.6 mmol) were added to the reaction vessel. After the two reactions had been completed the mixture was cooled to room temperature. The resultant solid was dissolved in dichloromethane and a sample was taken for a crude ^{1}H NMR spectroscopy. The polymer was then precipitated from 250 mL of cold methanol and cooled overnight at -35^{o}C. The solvent was decanted from the

precipitated sold, and the solid was dried under vacuum to constant weight and a sample of this was used for GPC analysis.

6.6.4 PLGA used as a macroinitiator for the polymerisation of **M58**

In a nitrogen filled glovebox, **C1** (0.4 mg, 0.01 mmol), **P3** (57 mg, 0.01 mmol) and **M58** (11.9 mg, 0.094 mmol) were dissolved in toluene (0.5 mL) and the solution was charged to an ampoule. The ampoule was then sealed, removed from the glovebox and placed in a preheated oil bath at 120 ^{o}C for 24 h. After 24 h, the ampoule was cooled and 3-4 drops of methanol was added to quench the polymerization. The polymer was then dissolved in dichloromethane and a sample was taken for a crude ^{1}H NMR spectroscopy. The polymer was then precipitated from 20mL of cold methanol and cooled overnight at -35^{o}C. The white precipitate was filtered, dried under vacuum to constant weight and a sample of this was used for GPC analysis.

6.6.5 Modification of Poly(lactic acid-co-3-chlorolactic acid) to form Poly(lactic acid-co- hydroxy acrylic acid)

Under an inert atmosphere polymer **P17** (1 g) was dissolved in anhydrous acetonitrile (50 mL). 1.5 equivalents of *N*,*N*-diisopropylethylamine was charged to the Schlenk flask and the resulting solution was stirred at 40 °C for 16 hours. The solvent was removed under vacuum and the resulting solid was dissolved in DCM and then added dropwise to cold methanol. The precipitated polymer was then filtered and dried to constant weight. The products were attained in various yields 10 – 95 %.

6.6.6 UV Initiated Free Radical Polymerisation

Polymer **P18** and initiator 1-hydroxycyclohexyl phenyl ketone were dissolved in monomer bulk (**M60**) and charged to a vial to make a cylinder of 1-2 mm in height and 20 mm in diameter. The vial was placed 5 cm beneath an arc lamp (Dymax Bluewave 75, 280–450 nm, > 19 W/cm^{2}) and irradiated continuously for 15 minutes.

Poly(lactic acid-co-glycolic acid) (**P3**):

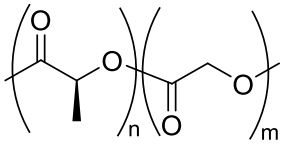

^{1}H NMR (601 MHz, Chloroform-d) δ 5.16 (q, *JHH* = 7 Hz, 1H, C*H*), 4.90 – 4.57 (m, 2H, CH_2), 1.58 (d, *JHH* = 7 Hz, 3H, CH_3). ^{13}C NMR (126 MHz, Chloroform-d) δ 169.58, 166.49, 69.01, 60.79, 16.64.

Poly(caprolactone-co-glycolic acid) (**P11**):

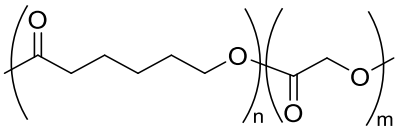

^{1}H NMR (500 MHz, Chloroform-d) δ 4.82 – 4.54 (m, 2H), 4.20– 4.00 (m, 2H), 2.44– 2.24 (m, 2H), 1.73 – 1.58 (m, 4H), 1.47 – 1.30 (m, 2H). ^{13}C NMR (126 MHz, Chloroform-d) δ 172.69, 167.85, 65.08, 60.55, 33.54, 28.15, 25.22, 24.34.

Poly(3-hyroxybutyrate-co-glycolic acid) (**P12**):

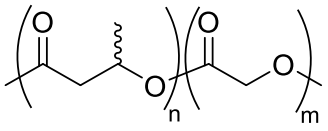

^{1}H NMR (500 MHz, Chloroform-d) δ 5.47 – 5.26 (m, 2H, OCCH_2C), 4.83 – 4.49 (m, 2H, OCCH_2O), 2.82 – 2.47 (m, 1H, CH_3C*H*O), 1.41 – 1.18 (m, 3H, CH_3). ^{13}C NMR (126 MHz, Chloroform-d) δ 169.30, 166.91, 68.66, 61.00, 40.27, 19.86.

Poly(lactic acid) (**P3**):

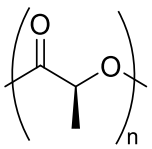

^{1}H NMR (500 MHz, Chloroform-d) δ 5.16 (q, *JHH* = 7 Hz, 1H, C*H*), 1.58 (d, *JHH* = 7 Hz, 3H, CH_3). ^{13}C NMR (126 MHz, Chloroform-d) δ 169.59, 69.01, 16.65

Poly(mandelic acid) (**P5**):

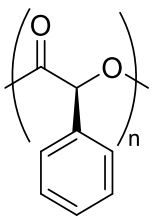

^{1}H NMR (601 MHz, Chloroform-d) δ 7.48 – 7.01 (m, 5H, Ar), 6.15 – 5.92 (m, 1H, C*H*). ^{13}C NMR (151 MHz, Chloroform-d) δ 166.76, 132.33, 129.34, 128.64, 127.80, 74.75.

Poly(vandelic acid) (**P6**):

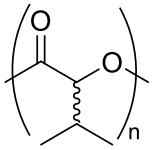

^{1}H NMR (500 MHz, Chloroform-d) δ: 5.08 - 4.83 (m, 1H, OC*H*), 2.3 (m, 1H, C*H*(CH3)$_2$), 1.05 (m, 6H, CH_3). ^{13}C NMR (125 MHz, Chloroform-d) δ: 168.86, 68.52, 31.13, 12.38.

Poly(hexahydromandelic acid) (**P9**):

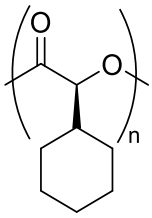

^{1}H NMR (500 MHz, Chloroform-d) δ 5.05 – 4.87 (m, 1H, C*H*), 2.32 – 0.68 (m, 11H, Cy). ^{13}C NMR (126 MHz, Chloroform-d) δ 168.70, 39.51, 28.69, 27.18, 25.89.

Poly(2-^{n}Butylhexanoic acid):

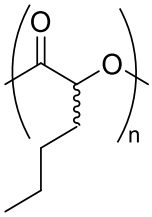

^{1}H NMR (601 MHz, Chloroform-d) δ 5.21 – 5.03 (m, 1H, C*H*), 2.03 – 1.85 (m, 2H, CHCH_2), 1.45 – 1.30 (m, 2H, CHCH$_2$CH_2), 0.98 – 0.82 (m, 4H, CH_2CH_3). ^{13}C NMR (126 MHz, Chloroform-d) δ 169.17, 72.49, 33.66, 27.03, 22.36, 13.78.

Poly(2-^{i}Butylhexanoic acid) (**P7**):

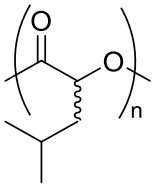

^{1}H NMR (601 MHz, Chloroform-d) δ 5.14-5.04 (dd, *JHH* = 9.4, 4.2 Hz, 1H, OC*H*), 1.85 – 1.73 (m, 3H, CH_2C*H*(CH$_3$)$_2$), 0.94 (dd, *JHH* = 20.2, 6.4 Hz, 6H, (CH_3)$_2$). ^{13}C NMR (126 MHz, Chloroform-d) δ 169.70, 71.34, 39.31, 24.50, 22.96, 21.41

Poly(pentynoic acid) (**P15**)

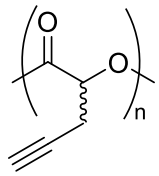

^{1}H NMR (500 MHz, Chloroform-d) δ 5.43 – 5.31 (m, 1H, OC*H*), 2.99 – 2.77 (m, 2H, CH_2), 2.14 – 2.03 (m, 1H, CH_2CCH). ^{13}C NMR (126 MHz, Chloroform-d) δ 169.81, 72.05, 61.67, 21.98.

Poly(glycolic acid-co-lactic acid-co-pentynoic acid) (**P16**):

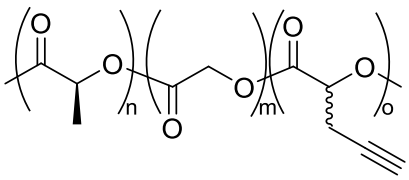

^{1}H NMR (500 MHz, Chloroform-d) δ 5.43 – 5.11 (m, 9H), 4.97 – 4.58 (m, 7H), 2.99 – 2.77 (m, 2H), 2.14 – 2.03 (br s, 1H), 1.64 – 1.49 (m, 23H). ^{13}C NMR (126 MHz, Chloroform-d) δ 169.81 – 169.21 (m), 166.56, 72.05 – 71.36 (m), 71.84, 71.14 – 70.32 (m), 69.64 – 68.64 (m), 61.67 – 60.21 (m), 21.98 – 21.45 (m), 17.11 – 16.43 (m).

Poly(L-lactic acid-co-3-chlorolactic acid) (**P17**):

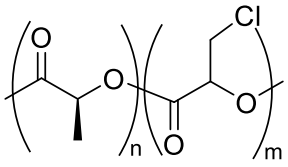

^{1}H NMR (400 MHz, Chloroform-*d*) δ 5.42 (ddd, *JHH*= 25.8, 6.6, 3.3 Hz, 1H, C*H*CH_2), 5.16 (q, *JHH*= 7.2 Hz, 23H, C*H*CH_3), 4.05 – 3.84 (m, 2H, CH_2), 1.58 (d, *JHH*= 7.2 Hz, 69H, CH_3). ^{13}C NMR (126 MHz, Chloroform-*d*) δ 169.72, 165.88, 72.41, 69.15, 42.31, 16.79.

Poly(lactic acid-co- hydroxy acrylic acid) (**P18**):

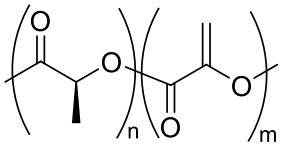

^{1}H NMR (601 MHz, Chloroform-d) δ 6.20 (m, 1H, CH_2), 5.61 (dd, JHH= 9.1, 2.1 Hz, 1H, CH_2), 5.31 – 5.12 (m, 23H, CH_3), 1.67 – 1.49 (m, 69H). ^{13}C NMR (151 MHz, Chloroform-d) δ 169.39, 160.15, 143.22, 115.89, 68.95, 16.63.

Poly(2-hydroxy-3- (phenylmethoxy)-propanoic acid) (**P14**):

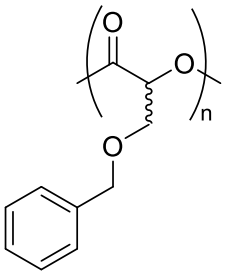

^{1}H-NMR (500 MHz; $CDCl_3$) δ 7.21-7.62 (m, 5H, Ar), 5.37-5.54 (m, 1H, OC*H*), 4.65-4.90 (m, 2H, CHCH_2O), 3.83-4.01 (m, 2H, C$H_2C_6H_5$). ^{13}C-NMR (500 MHz; $CDCl_3$) δ 166.76, 137.6, 128.56, 127.82, 73.56, 72.92, 68.65.

6.7 References

(1) Fiore, G. L.; Klinkenberg, J. L.; Fraser, C. L. *Macromolecules* **2008**, *41* (23), 9397–9405.

(2) Hori, Y.; Hagiwara, T. *Int. J. Biol. Macromol.* **1999**, *25* (1–3), 237–245.

(3) Martin, R. T.; Camargo, L. P.; Miller, S. A. *Green Chem.* **2014**, *16* (4), 1768–1773.

(4) Salomaa, P.; Laiho, S.; Cyvin, S. J.; Kvande, P. C.; Meisingseth, E. *Acta Chem. Scand.* **1963**, *17*, 103–110.

(5) Vidyasagar Reddy, G.; Sreevani, V.; Iyengar, D. . *Tetrahedron Lett.* **2001**, *42* (3), 531–532.

(6) Połoński, T. *Tetrahedron* **1983**, *39* (19), 3139–3143.

(7) Nitsch, D.; Huber, S. M.; Pöthig, A.; Narayanan, A.; Olah, G. A.; Prakash, G. K. S.; Bach, T. *J. Am. Chem. Soc.* **2014**, *136* (7), 2851–2857.

(8) Yang, D.; Li, B.; Ng, F. F.; Yan, Y. L.; Qu, J.; Wu, Y. D. *J. Org. Chem.* **2001**, *66* (22), 7303–7312.

(9) Quast, H.; Leybach, H. *Chem. Ber.* **1991**, *124* (4), 849–859.

(10) Jiang, X.; Vogel, E. B.; Smith, M. R.; Baker, G. L. *Macromolecules* **2008**, *41* (6), 1937–1944.

(11) Hope, D. B.; Wålti, M. *J. Chem. Soc. C Org.* **1970**, No. 18, 2475–2478.

(12) Okrasa, K.; Levy, C.; Wilding, M.; Goodall, M.; Baudendistel, N.; Hauer, B.; Leys, D.; Micklefield, J. *Angew. Chemie - Int. Ed.* **2009**, *48* (41), 7691–7694.

(13) Denmark, S. E.; Yang, S. M. *J. Am. Chem. Soc.* **2004**, *126* (39), 12432–12440.

(14) Pounder, R. J.; Fox, D. J.; Barker, I. A.; Bennison, M. J.; Dove, A. P.; Jerome, R.; Jerome, C.; Dubois, P. *Polym. Chem.* **2011**, *2* (10), 2204–2212.

(15) Hormnirun, P.; Marshall, E. L.; Gibson, V. C.; Pugh, R. I.; White, A. J. P. *Proc. Natl. Acad. Sci. U. S. A.* **2006**, *103* (42), 15343–15348.

(16) Atwood, D. a.; Hill, M. S.; Jegier, J. a.; Rutherford, D. *Organometallics* **1997**, *16* (12), 2659–2664.

(17) Hormnirun, P.; Marshall, E. L.; Gibson, V. C.; White, A. J. P.; Williams, D. J. *J. Am. Chem. Soc.* **2004**, *126* (9), 2688–2689.